Enhancing Cardiac Repair

targeting I/R injury and adverse remodeling

Fatih Arslan

ISBN: 9789461081926
Cover photo: Tomb of Sesi at Sakkara
Lay-out: Wendy Schoneveld, www.wenziD.nl
Printed by: Gildeprint drukkerijen, Enschede

Enhancing Cardiac Repair

targeting I/R injury and adverse remodeling

Het bevorderen van cardiaal herstel
ischemie/reperfusie schade en averechts remodelleren als aangrijpingspunten
(met een samenvatting in het Nederlands)

Kalbin Onarımını Pekiştirmek
iskemi/reperfüzyon hasarını ve kalbin tersine yeniden biçimlenmesini esas alarak
(Türkçe özeti ile)

PROEFSCHRIFT

ter verkrijging van de graad van doctor aan de Universiteit Utrecht op gezag van de rector magnificus, prof. dr. G.J. van der Zwaan, ingevolge het besluit van het college voor promoties in het openbaar te verdedigen op dinsdag 6 september 2011 des middags te 2.30 uur

door

Fatih Arslan

geboren op 5 februari 1982 te Arnhem

Promotoren
Prof. dr. D.P.V. de Kleijn
Prof. dr. G. Pasterkamp

Financial support by the Dutch Heart Foundation for the publication of this thesis is gratefully acknowledged. Part of the research described in this thesis was supported by a grant of the Dutch Heart Foundation (DHF-2010T001).

Financial support by the Heart & Long Foundation Utrecht for the publication of this thesis is gratefully acknowledged.

Publication of this thesis was additionally supported by:
Stichting Cardiovasculaire Biologie, Boehringer Ingelheim BV, Merck Sharp & Dohme BV, Novartis Pharma BV, Servier Nederland Farma BV.

Voor mijn ouders,

mijn grootouders,

en Fatma

CONTENTS

PART I

Myocardial Ischemia/Reperfusion Injury

CHAPTER 1

This chapter describes the interaction between the injured myocardium and cells involved in cardiac repair

Fatih Arslan, Dominique P. de Kleijn & Gerard Pasterkamp

Innate immune signaling in cardiac ischemia

Despite advances in treatment of patients who suffer from ischemic heart disease, morbidity related to myocardial infarction is increasing in Western societies. Acute and chronic immune responses elicited by myocardial ischemia have an important role in the functional deterioration of the heart. Research on modulation of the inflammatory responses was focused on effector mediators such as leukocytes. However, increasing evidence indicates that various endogenous ligands that act as 'danger signals', also called danger-associated molecular patterns (DAMPs), are released upon injury and modulate inflammation. Originally described as part of the first-line defense against invading microorganisms, several Toll-like receptors (TLRs) on leukocytes and parenchymal cells have now been shown to respond to such signals and to have a pivotal role in noninfectious pathological cardiovascular conditions, such as ischemia-reperfusion injury and heart failure. From a therapeutic perspective, DAMPs are attractive targets owing to their specific induction after injury. In this Review, we will discuss innate immune activation through TLRs in cardiac ischemia mediated by DAMPs.

Nat Rev Cardiol. 2011;8(5):292-300

The role of the immune system in the development of cardiovascular disease first became evident in the 1880s, when the German pathologist Rudolf Virchow (1821-1902) suggested the driving mechanism behind atherosclerosis to be an inflammatory process.[1] He recognized that "irritants" enable the affected vasculature to attract substances out of the blood and retain them.[2] More specifically, these irritants were thought to attract leukocytes to atherosclerotic lesions. In retrospect, this notion was probably the first recognition of nonpathogenic factors that could affect leukocyte behavior and organ function. Not until the late 1960s was a substantial influence of a myocardial depressant factor first described in the context of hemorrhagic shock.[3-5]

Blood flow blockage in a coronary artery leads to myocardial infarction (MI) with ischemic death of cardiomyocytes. Restoring flow is a prerequisite for cardiomyocyte salvage, but injury to both endothelial cells and cardiomyocytes occurs during reperfusion. The innate immune system has a crucial role in both initiation and progression of the subsequent repair response, which involves immune cells such as neutrophils and macrophages. Whether these repair mechanisms are favorable or harmful to cardiac function is partly dependent on the amount of tissue damage that is caused by inflammatory cells early after ischemia.6 Furthermore, signals triggered by the endangered myocardium and by inflammatory cells influence the behavior of nonimmune cells (such as endothelial cells or myofibroblasts) via receptors of the innate immune system.[6-8]

Toll-like receptors (TLRs) form an important part of the innate immune system and are able to recognize a variety of peptides, proteins and nucleotide fragments. The activation of the transcription factor nuclear factor kappa B (NFκB) is well-recognized as a hallmark of innate immunity activation after cardiac ischemia.[6, 9, 10] As the signaling cascade triggered by TLRs also involves NFκB, a new paradigm of noninfectious activation of the innate immune system following cardiac ischemia can be postulated. In this Review, we focus on innate immune responses in cardiac ischemia induced by endogenous mediators, and discuss both experimental and clinical studies highlighting the critical role of endogenous TLR ligands in myocardial ischemia-reperfusion (I/R) injury and postinfarction cardiac remodeling.

Inflammatory responses after ischemia

Leukocyte activation and recruitment, and cytokine production characterize the initial phase of the inflammatory repair response after an ischemic insult to the myocardium.[11] Within seconds after I/R injury, blood flow in the affected vessel is disturbed because of microembolism, platelet activation, neutrophil plugging, and endothelial cell dysfunction, a situation referred to as the 'no-reflow' phenomenon.[12] In parallel, a cardiac cytokine burst is initiated and followed by neutrophil activation that causes direct injury to endothelial cells via production of reactive oxygen species (ROS), proteases, cytokines and lipids.[13] As a consequence, endothelial cells increase expression of adhesion molecules, which facilitates leukocyte binding. In addition, intercellular tight junctions are compromised, which increases vascular permeability. This effect promotes migration of cells such as leukocytes into the myocardium, which, in close proximity to cardiomyocytes and endothelial cells, can generate ROS and proteases once oxygen supply is restored. ROS are known to cause cell death via oxidative stress,6 while excessive protease activity leads to increased degradation of the extracellular matrix.[14] Excessive cell death and matrix degradation can compromise the structural integrity of the infarcted myocardium and result in maladaptive remodeling thereafter.[15]

Over the past decade, a great deal of evidence has emerged demonstrating that the inflammatory immune response in cardiac ischemia is a well-orchestrated process. We now know that this response is triggered by the injured myocardium. Cytokines released from stressed myocardial cells, de novo

expression of proteins upon injury, and hydrophobic portions of proteins or lipids are all part of so-called danger-associated molecular patterns (DAMPs) that activate leukocytes-a key concept of the 'danger model' of immunity.

The 'danger model'

The 'danger model' was first described by Polly Matzinger in 2002 and provided a theoretical framework that explained immune responses after tissue injury.[16, 17] In the classic model of immunity, the system was described to function by discriminating between 'self' and 'nonself' after priming early in life. However, this model failed to explain why the immune system remains silent with changes to 'self' later in life, for example during puberty, pregnancy or if cancer develops. According to the 'danger model', rather than acting upon the discrimination of 'self' and 'nonself' (for example cardiomyocytes versus bacteria), leukocytes react to alarm signals released by stressed cells such as infected or ischemic cardiomyocytes. The 'danger model' triggered the search for such endogenous activators of the immune response and their receptors.

TLRs are known to recognize ligands released as a result of injury. These molecules have gained much attention in DAMP-mediated activation of the innate immune system and subsequent inflammation after cardiac ischemia.[18] The mechanisms by which DAMPs activate and control leukocyte behavior and whether DAMPs can be used as therapeutic targets in order to modulate detrimental inflammatory responses remains unknown. Before we discuss specific DAMPs related to cardiac ischemia, we provide an overview of TLR signaling in general and in cardiac ischemia.

TLR signaling pathways

TLRs are evolutionary conserved transmembrane receptors that recognize so-called 'pathogen-associated molecular patterns', enabling host defense against invading pathogens. In addition, TLRs can also detect DAMPs[16, 17] and the subsequent induction of the immune response is thought to mediate repair mechanisms of injured tissue.[18]

The intracellular TLRs (TLR3, TLR7, TLR8, TLR9 and TLR13) detect nucleic acids, particularly viral and bacterial DNA.[19] The level of cell surface expression of TLRs can be modulated by receptor activation, thus enabling a TLR-mediated positive and negative feedback loop in immune responses.[20]

A key component of TLR activation is the recruitment of adaptor proteins, such as myeloid-differentiation primary response protein MyD88, after ligand-receptor interaction. MyD88 is crucial for the subsequent transcription of proinflammatory genes initiated by NFκB.[21] Members of the NFκB family consist of several subunits (for example p52 and p65) and are maintained in an inactive state within the cytoplasm through binding to inhibitors of NFκB (IκBs). After TLR activation, IκBs are phosphorylated, ubiquitinated, and then degraded via proteolysis. The detachment from IκBs enables nuclear translocation of NFκB subunits and subsequent transcription of proinflammatory genes.[21] Alternatively, after TLR2 activation, MyD88 can also promote induction of apoptosis via activation of Jun N-terminal kinases (JNKs; Figure 1).[21]

Our current understanding of TLR signaling provides evidence for the role of nonpathogenic inflammatory mediators in several cardiovascular disorders. Early observations that inflammation had a pivotal role in I/R injury,6 cardiomyocyte apoptosis,[7] heart failure,[9, 10] atherosclerosis,[22] and myocarditis,[23] can now be partly attributed to detrimental TLR activation.[6, 7, 24-26] Currently, seven parenchymal TLRs have been identified as key mediators of noninfectious cardiac disorders (Table 1).

Table 1. TLRs and their association with cardiovascular disease

TLRs	DAMPs	Disorders
TLR2	necrotic cells, oxidized LDL, serum amyloid A, ApoCIII, heat shock proteins, HMGB1, hyaluronic acid, fibronectin-EDA, biglycan	I/R injury[20, 32]; adverse remodeling[35]; contractile dysfunction[31, 32, 108]; atherosclerosis[103, 109, 110]
TLR3	mRNA	viral cardiomyopathy/myocarditis[111, 112]
TLR4	heat shock proteins, HMGB1, tenascin C, fibrinogen, fibronectin-EDA, oxidized LDL, minimally-modified LDL	I/R injury[113]; adverse remodeling[36]; contractile dysfunction[31]; viral cardiomyopathy/myocarditis[114]; atherosclerosis[103, 110, 115]
TLR5	unknown	contractile dysfunction[31]
TLR7/8	cardiac myosin	viral cardiomyopathy/myocarditis[116, 117]
TLR9	nucleic acid-containing immune complexes, endogenous DNA	adverse remodeling[117]; contractile dysfunction[118, 119]; acute allograft rejection[120]

Adapted from Cole JE *et al*.[121]; Apo, apolipoprotein; EDA, exon encoding type III repeat extra domain A; HMGB1, high mobility group box protein B1; I/R, ischemia-reperfusion; TLR, Toll-like receptor.

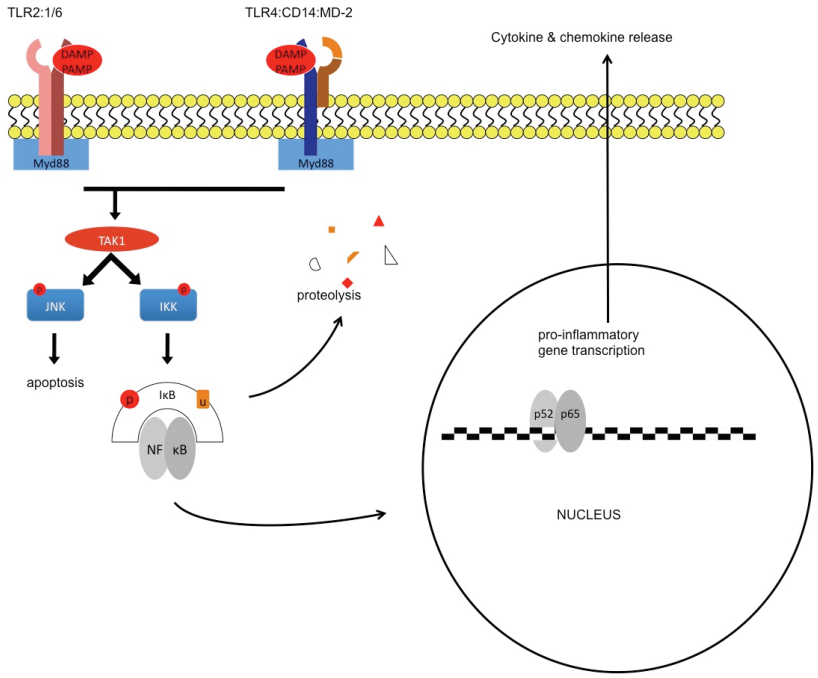

Figure 1. TLR signaling. *TLR2 can form a dimer with TLR1 or TLR6. TLR4 might require co-receptors, such as CD14 and MD2 for signal activation. MyD88 is recruited to the intracellular domain of TLRs, which in turn recruits TAK1. TAK1 phosphorylates JNK and IKK. JNK can lead to apoptosis-mediated cell dysfunction and death. Activated IKK phosphorylates the inhibitory complex IκB. Subsequently, IκB is ubiquitinated and degraded via proteolysis. NFκB can then translocate to the nucleus and initiate transcription of proinflammatory genes. Abbreviations: CD14, monocyte differentiation antigen CD14; IκB, inhibitor of nuclear factor kappa B; IKK, inhibitor of nuclear factor kappa B kinase; JNK, mitogen-activated protein kinases; NFκB, nuclear factor kappa B; MD2, lymphocyte antigen 96; MyD88, myeloid differentiation primary response protein MyD88; TAK1, Transforming growth factor-beta-activated kinase 1 (also known as mitogen-activated protein kinase kinase kinase 7); TLR, Toll-like receptor; Ub, ubiquitin.*

TLR signaling in cardiac ischemia

In cardiac ischemia, ligand binding to TLRs induces an inflammatory cascade via nuclear translocation of NFκB and subsequent proinflammatory gene transcription (Figure 1).[6, 27, 28] The expression of TLRs by circulating blood cells and parenchymal cells has implications in myocardial I/R injury and postinfarction remodeling. Parenchymal TLR signaling contributes to changes in cellular function and viability of cardiomyocytes and endothelial cells after ischemia. In addition, TLR signaling in circulating cells that have migrated into the myocardium mediates repair mechanisms involved in postinfarction remodeling. We discuss the divergent roles of TLR signaling in the circulatory and parenchymal compartments for myocardial I/R injury and remodeling separately.

TLR signaling in myocardial I/R injury

To understand the functional consequences of TLR activation in the blood and parenchymal compartment, one needs to acknowledge the various cellular events during myocardial I/R injury that influence myocardial viability and function: Firstly, ischemic-reperfused endothelial cells express adhesion molecules that promote leukocyte plugging and decrease blood flow through the culprit coronary artery (the 'no-reflow' phenomenon). Secondly, despite successful reperfusion, the myocardium can exhibit reversible contractile dysfunction, also known as 'stunning'. Thirdly, the ischemic-reperfused myocardium is known to be arrhythmogenic. Fourthly, additional cell death can occur during reperfusion, which increases infarct size (so-called lethal reperfusion injury). These four events do not occur chronologically and can happen independently from each other.[28]

In mice, endothelial dysfunction after myocardial I/R injury was shown to be mediated by both parenchymal and circulating TLR2.[29] In order to investigate the differential contribution of parenchymal versus circulating cells, perfused hearts can be studied in a Langendorff apparatus, which eliminates the effects brought about by blood cells. Using this technique, Knuefermann et al. demonstrated that hearts from TLR2−/− mice challenged with Staphylococcus aureus are protected against contractile deterioration compared with wild-type (WT) hearts.[30] Although this model demonstrates the cardiac-depressant properties of pathogens, this report and others show that parenchymal TLR activation affects myocardial contractility.[30, 31] Sakata et al. showed that Langendorff-perfused TLR2−/− mouse hearts have better contractile performance after I/R injury than hearts from WT animals, but that both exhibit similar infarct size.[32] Blockage of tumor necrosis factor (TNF), which reduces contractile dysfunction, led to a substantial improvement in contractile performance in perfused WT hearts that reached the same level as in TLR2−/− hearts.[32] These results show that TLR2 activation in cardiac cells leads to deterioration of myocardial function after I/R injury. In addition, the findings indicate that parenchymal TLR2 activation does not mediate lethal reperfusion injury, since infarct size in TLR2−/− hearts was similar to that in WT hearts. Findings from our own group showed that, indeed, circulating TLR2 signaling mediates lethal reperfusion injury in vivo,[20] thus providing direct support for the observation by Sakata and colleagues.[32] Bone-marrow transplantation experiments revealed that WT mice with TLR2−/− bone marrow were protected against lethal reperfusion injury to the same extent as mice with total TLR2 knockout, whereas TLR2−/− mice with WT bone marrow showed no protection at all.[20] Further analysis of blood cells after myocardial I/R injury showed that surface expression of the activation marker integrin alpha-M (CD11b) is increased in circulating monocytes during the first hour of reperfusion as well as the surface expression of TLR2. The upregulation of TLR2 and CD11b was prevented in vivo by TLR2 inhibition.[20]

These studies indicate that TLR2 signaling outside the myocardium mediates lethal myocardial I/R injury and that contractile disturbance after myocardial I/R injury depends on parenchymal TLR2 signaling (Figure 2). In addition, they show that cytokines such as TNF are part of the vicious circle in myocardial I/R injury and can act as endogenous mediators of TLR-induced injury.

TLR signaling in postischemic remodeling

Immediately after cardiomyocyte death, processes are initiated to repair and maintain the structural integrity of the heart. The functional consequences of cardiac remodeling, in addition to infarct size, are an important determinant of prognosis.[33, 34] TLR signaling has a crucial role in cardiac remodeling after MI. Remodeling of the central scar and peri-infarct zone is a dynamic process in which three chronological phases can be distinguished that determine the structural integrity of the infarcted heart. The first is the inflammatory phase, which is characterized by an increase of cytokine production and leukocyte influx. The second is the proliferative phase, which is marked by fibroblast transdifferentiation and matrix protein deposition. The third is the maturation phase, in which a mature collagen-based scar is formed.[14] The continuous alterations in matrix content after infarction can trigger recruitment of circulating cells via the release of DAMPs (Figure 3).

We and others have shown that expression of TLR2 and TLR4 mediates adverse ventricular remodeling in mice via enhanced inflammation and fibrosis[35, 36] and that TLR4 activation in monocytes is associated with the development of heart failure in patients after MI.[37] Using NFκB-p50 knockout mice, we showed that bone-marrow-derived cells were involved in postinfarct dilatation and functional deterioration of the myocardium through accentuated inflammation, increased activity of matrixmetalloproteases (MMP) 2 and MMP9 and impaired collagen deposition in the scar area.[38] From these data, we postulate that TLR and downstream NFκB activation in cells that migrate into the infarcted myocardium aggravate

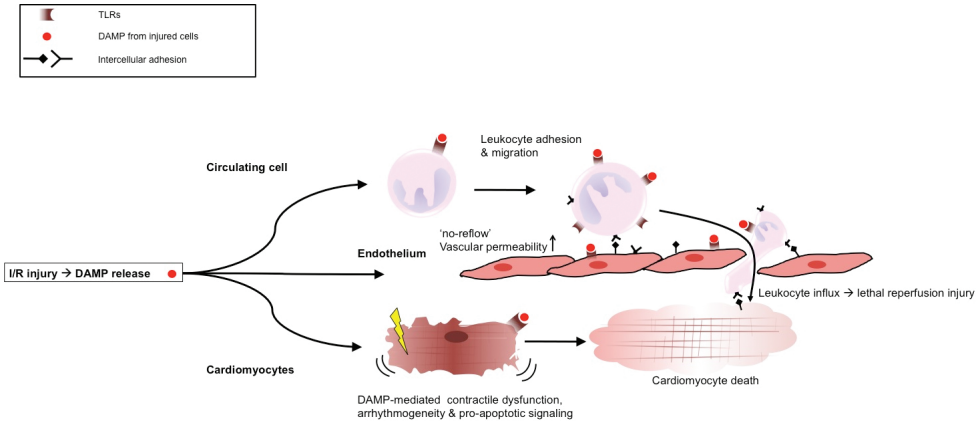

Figure 2. The role of DAMPs in myocardial ischemia-reperfusion injury. *'Danger signals', or DAMPs, are released after ischemia-reperfusion injury from apoptotic and/or necrotic endothelial cells and cardiomyocytes. In turn, these 'danger signals' activate the TLRs of adjacent and circulating cells. TLR activation by DAMPs of adjacent viable cardiomyocytes can result in deteriorating contractility or even apoptosis. Endothelial dysfunction during the first few minutes after reperfusion results in vasoconstriction and impaired blood flow owing to leukocyte adhesion, which can further impair endothelial cell function. In addition, leukocytes can directly cause cell death of cardiomyocytes and endothelial cells as a result of production of reactive oxygen species. Abbreviations: DAMP, danger-associated molecular pattern; TLR, Toll-like receptor.*

adverse inflammatory responses, matrix breakdown and fibrotic processes and lead to maladaptive remodeling. Although the abovementioned studies cannot explain why distant cells exert adverse effects in the postischemic myocardium, data on extra domain A (EDA) of fibronectin, which are discussed below, provide evidence for the pivotal role of DAMPs in this process.

DAMPs in cardiac ischemia

The postischemic reperfused myocardium is characterized by a rapid series of detrimental events at cellular level. Within minutes of ischemic injury, intracellular Ca2+ concentration rises owing to sarcoplasmic/endoplasmic reticulum calcium ATPase 2 dysfunction, mitochondrial permeability transition pores open and proapoptotic signaling is initiated. These pathological changes lead to lethal hypercontracture, Ca2+-dependent apoptosis, and the release of proapoptotic proteins such as cytochrome c or Diablo homolog (also known as Smac). Subsequently, DNA fragmentation occurs, eventually leading to cell-membrane swelling and necrosis.[39-42] In contrast to the fast acute events in I/R injury, postinfarct ventricular remodeling is a chronic process in which consecutive events result in inflammation and subsequent extracellular matrix (ECM) degradation. Products related to cell death and ECM degradation can all serve as DAMPs to adjacent myocardial cells and migrating cells after cardiac ischemia. DAMPs secreted by ischemic cells (either actively or passively) have been shown to activate TLRs and initiate a proinflammatory response. Early reports of this process showed that heat shock protein (HSP) 60, released from apoptotic cells,[43] activates TLR4+/CD14+ leukocytes.[44, 45]

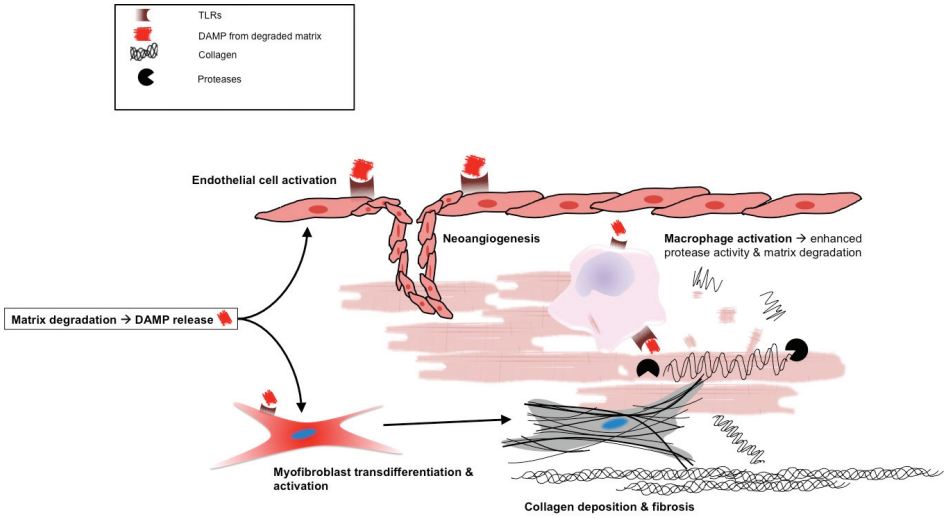

Figure 3. The role of DAMPs in cardiac remodeling. *Dead cardiomyocytes and matrix degradation products are potent activators of macrophages and fibroblasts. Macrophages degrade the matrix by secreting metalloproteinases and clearing cell debris, resulting in more degradation products. Degradation products are involved in myofibroblast transdifferentiation. In turn, myofibroblasts are the primary source for deposition of collagen and other matrix products to mature the scar and finalize the wound healing process. DAMPs also activate endothelial cells with subsequent increase in angiogenesis that is beneficial for cardiac remodeling. The balance between matrix breakdown and deposition determines the fate of cardiac remodeling and subsequent function. Abbreviations: DAMP, danger-associated molecular pattern; TLR, Toll-like receptor.*

These findings led to the identification of other endogenous TLR ligands that were expressed following cardiac ischemia. One might hypothesize that DAMPs facilitate recruitment and differentiation of cells involved in the reparative processes after infarction. In the following sections, we discuss the known DAMPs involved in cardiac ischemia and their role in cardiac repair responses. Importantly, we should point out that several previous candidates for endogenous TLR ligands were wrongly identified owing to contamination in in vitro experiments.[46-48]

Heat shock proteins

HSPs are members of the stress protein family that were initially described as proteins synthesized in response to heat shock.[49] HSPs are abundantly present in the cytosol under physiological conditions but their expression is further induced after cell stress. HSPs are molecular chaperones that recognize hydrophobic portions of proteins, through which they inhibit protein aggregation and subsequently promote correct protein folding.[50, 51] Currie and colleagues were the first to document the upregulation of cardiac HSP70 (initially identified as HSP71) synthesis under ischemic conditions.[52, 53] Animal experiments and clinical observations show that divergent responses and differential expression of HSPs in pathological cardiac conditions can occur. Overexpression of HSP20 or HSP70 protects the heart of rodents against I/R injury,[54-56] while both proteins have little or no role in adverse remodeling.[57, 58] Although cardiac protection was observed after heat-shock treatment,[59] several experiments illustrate the limitations of both early models of MI and the protective window of opportunity for HSPs. In vivo, 45 min of ischemia followed by 3 h of reperfusion after heat shock resulted in a statistically nonsignificant increase of infarct size in rabbits compared with animals without heat shock, while HSP72 expression was increased.[59] In rats that underwent heat shock before permanent coronary occlusion, heat shock neither decreased infarct size nor improved cardiac function, although more neutrophils accumulated in the heart than in animals not subjected to heat shock.[60] Neutrophil influx is associated with increased injury after cardiac ischemia,[13] which suggests that heat shock before MI might do more harm than good. In line with this notion, HSP60 is well known for its detrimental effects in cardiac ischemia. In contrast to HSP20 and HSP70, HSP60 is strongly associated with the development of ischemic heart failure[57, 58] and is a leukocyte-activating factor and mediator of cell death.[59, 60] In addition, T-lymphocytes from patients suffering from an acute coronary syndrome (ACS) are reactive to HSP60, whereas leukocytes from patients with chronic stable angina are not.[61] This finding suggests that the enhanced leukocyte reactivity to HSP60 in patients with ACS could be caused by increased plasma-membrane TLR expression, in view of the fact that HSP60 is a TLR4 ligand.[45, 62] Lin et al. have provided support for this theory by showing that HSP60 from mitochondria and cytosol of cardiomyocytes in culture translocates to the plasma membrane and is detectable in plasma of rats with heart failure. Furthermore, cell-surface HSP60 was associated with increased apoptosis of cardiomyocytes in the failing heart.[63] An early report described TLR4 to be upregulated in failing human myocardium.[64] In 2009, Kim et al. showed that HSP60 induces apoptosis in rat cardiomyocytes partly via TLR4.[62]

On the basis of these findings, we postulate that in the setting of heart failure HSP60 translocates to the cell membrane, is secreted by the failing cardiomyocyte and directly induces apoptosis. This supposition is in line with observations in the failing myocardium of increased apoptosis of myocytes and nonmyocytes.[65-68] In addition, we propose that HSP60 is detected by circulating monocytes, leading to the initiation of adverse ventricular remodeling via TLR4.[36, 45]

High mobility group protein B1

The highly conserved high mobility group protein B1 (HMGB1) is a highly conserved nuclear protein-mouse and human HMGB1 proteins only differ in two amino acids. Besides its role in nucleic-acid stabilization and transcription,[69] HMGB1 also induces deleterious immune responses. HMGB1 passively enters the extracellular environment from necrotic cells and serves as a DAMP for leukocytes.[70, 71] In addition, leukocytes actively secrete HMGB1 upon activation by immunogenic ligands,[72-74] which results in a positive feedback loop. Leukocytes and endothelial cells stimulated with HMGB1 secrete potent cytokines and adhesion molecules.[75] The receptors for advanced glycation end products (RAGE), TLR2, TLR4 and TLR9, were identified as effector receptors for HMGB1.[76-78] These HMGB1-mediated processes have been studied mainly in vitro and the findings from these investigations suggest that HMGB1 is proinflammatory and deleterious after MI. Results from in vivo studies, however, have yielded apparently contradictory results regarding role of HMGB1 in cardiac I/R injury.[75, 79, 80]

The rise in HMGB1 levels in response to ischemic injury of the human heart is well-documented.[80, 81] Kohno et al. showed that peak serum levels of HMGB1 were higher in patients with pump failure and cardiac rupture than in those without, and patients with increased peak HMGB1 levels were more likely to die from cardiac causes. Furthermore, HMGB1 levels were directly proportional to brain natriuretic peptide levels 6 months after MI.[80] These results suggest that HMGB1 exerts deleterious actions on the myocardium after infarction. However, two independent research groups have documented that increased availability of local HMGB1 actually prevents adverse ventricular remodeling after experimental MI.[79, 82] Takahashi et al. have nicely demonstrated that rats injected with HMGB1 in the peri-infarct area 21 days after MI had higher left ventricular ejection fractions within a week. The main mechanisms behind this effect were decreased fibrosis and inflammation.[79] Furthermore, Kitahara et al. showed, using transgenic mice, that cardiac-specific overexpression of HMGB1 improved cardiac function and increased survival rate after MI.[82] The researchers attributed the protective effect of HMGB1 to neovascularization in the border zone, resulting in smaller infarct size 28 days after infarction. In another study, mouse hearts injected with HMGB1 in the peri-infarct zone (4 h after MI) showed attenuated ventricular dilatation and enhanced cardiac function.[83] The study investigators suggested that the therapeutic effect of HMGB1 was related to increased cardiac regeneration. HMGB1 injection induced proliferation of cardiac progenitor cells expressing the surface marker c-kit and their differentiation into cardiomyocytes.[83] Further exploration of this mechanism in vitro revealed that HMGB1 might act as a paracrine factor that stimulates secretion of growth factors, cytokines and chemokines from cardiac fibroblasts. HMGB1 also stimulated c-kit-expressing cells to differentiate into an endothelial lineage,[84] supporting the findings by Kitahara et al. Added support for the findings of these studies was provided by Kohno and collaborators, who showed that neutralizing endogenous HMGB1 by injecting anti-HMGB1 antibodies increased left ventricular dimensions and worsened both systolic and diastolic performance after experimental MI in rats.[80]

In contrast to these apparently beneficial therapeutic effects of increased local HMGB1 availability in experimental models of chronic ischemia, systemic increase of HMGB1 before myocardial I/R injury has been shown to be deleterious. In HMGB1-pretreated mice, infarct size increased by 30% after myocardial I/R injury compared with control mice.[85] This detrimental effect was mediated by RAGE and characterized by increased NFκB activity and TNF and interleukin 6 production. Furthermore, in cardiomyocytes stimulated with HMGB1 in culture, contractility decreased in a protein kinase C-dependent manner.[86] HMGB1 also has a key role in sepsis-related lethality and distant organ failure.[87, 88] Cardiac dysfunction is often observed in patients with sepsis[89] and, therefore, we suggest that HMGB1 serves as a myocardial-depressant factor.

One possible explanation for discrepancies in the abovementioned studies might lie in the application of different MI models. In a nonreperfused infarction model, neoangiogenesis is a dominant mediator of cardiac remodeling and improves cardiac repair.[10] In I/R models, however, inflammation is accelerated and is detrimental to cardiac function and viability.[10] Neoangiogenesis can be considered as an inflammatory process;[90, 91] therefore, enhanced inflammation by local HMGB1 delivery in a nonreperfused ischemic heart model will enhance neoangiogenesis and cardiac repair. By contrast, enhanced inflammation by HMGB1 delivery in an I/R model further increases inflammation and leads to deterioration in cardiac function (Figure 4). In both models, HMGB1 enhances inflammation, but the outcome differs, as inflammation has negative effects in I/R injury but is favorable in the angiogenic response after chronic ischemia. For this reason, careful evaluation of HMGB1 as a therapeutic target after cardiac ischemia is required. Special care should be taken in patients with a high risk of malignant cell formation, such as those with a history of cancer, since HMGBs have carcinogenic properties and can induce angiogenesis in tumors.[92, 93]

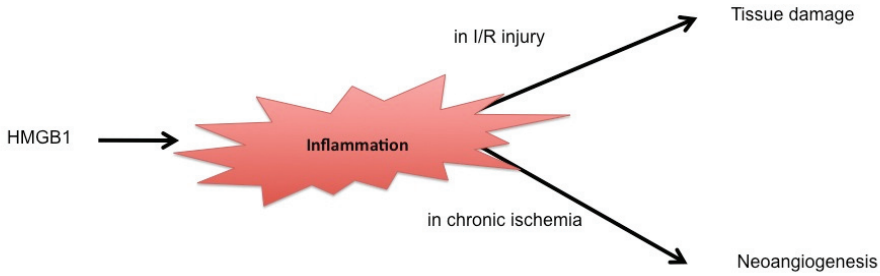

Figure 4. Divergent HMGB1-mediated responses after ischemia. HMGB1 enhances inflammation. In the setting of myocardial ischemia-reperfusion injury, this enhancement in inflammation further increases tissue damage. However, enhanced inflammation in the setting of chronic ischemia stimulates neoangiogenesis and thus has protective effects after infarction. Abbreviation: HMGB1, high mobility group protein B1.

Hyaluronic acid and fibronectin-EDA

HSPs and HMGB1 are considered to be DAMPs released from apoptotic or necrotic cells caused by ischemia and reperfusion. However, the dynamic alterations of the ECM during cardiac repair also have a great impact on the immune responses after an episode of severe cardiac ischemia. ECM degradation products as well as de novo synthesized matrix molecules might act as endogenous DAMPs.

Hyaluronic acid is a large polysaccharide that acts as a shock-absorbent molecule for matrices such as cartilage. Hyaluronic acid is part of the ECM in normal hearts. After MI, however, hyaluronic acid is fragmented into soluble low molecular weight (LMW) hyaluronic acid and its deposition in the myocardium is substantially increased.[94] Hyaluronic acid has the ability to bind water and resist flow,[95] thereby contributing to interstitial edema in the infarcted myocardium.[96] Both LMW and high molecular weight (HMW) hyaluronic-acid fragments are ligands for TLR2 and TLR4. However, whereas LMW hyaluronic acid is proinflammatory, HMW hyaluronic acid exerts antiapoptotic and anti-inflammatory actions. The exact role of hyaluronic-acid fragments after infarction remains to be studied. Although both LMW and HMW hyaluronic acid are ligands for TLR2 and TLR4, one cannot exclude the possibility that the anti-inflammatory effect of HMW hyaluronic acid is due to binding to a yet unrecognized receptor.[90, 97-101]

Fibronectin is a multifunctional adhesive ECM glycoprotein, which contains an alternatively spliced exon encoding type III repeat extra domain A (EDA), an exon that is transcribed only during embryogenesis and after tissue injury in tissue and circulating cells. EDA serves as a ligand for integrin α4β1 and induces cell adhesion within the newly formed matrix.[102] In addition, EDA acts as an endogenous ligand for both TLR2 and TLR4.[103] In vitro, EDA induces proinflammatory gene expression and activates monocytes.[103] We have shown that, in mice, EDA is indeed upregulated after MI and returns to baseline levels 4 weeks thereafter. More importantly, fibronectin-EDA$^{-/-}$ mice exhibited improved survival and cardiac function and reduced expansive remodeling of the left ventricle after experimental MI. Furthermore, fibronectin-EDA expression within the myocardium triggered adverse remodeling after bone-marrow transplantation.[104] These findings support the hypothesis that fibronectin-EDA serves as an endogenous ligand for TLR and is released after cardiac injury to activate circulating cells after MI. In vivo, the lack of fibronectin-EDA led to suppressed inflammation in the postinfarction myocardium, decreased TLR2 expression on peripheral blood monocytes, and reduced fibrosis via altered myofibroblast transdifferentiation without affecting proper scar formation.[104]

Cardiac myosin

Chronic inflammation of the myocardium and subsequent dilated cardiomyopathy were described as consequences of autoantibodies against cardiac myosin.[105, 106] Zhang et al. demonstrated that cardiac myosin acts as an endogenous ligand for TLR2 and TLR8.[107] At the present time, however, whether cardiac myosin has a role in reperfusion injury or adverse remodeling after MI is unknown. We can speculate that myosin released after infarction could exert detrimental effects via binding to and activation of TLR2 in leukocytes, resulting in increased infarct size after reperfusion. Future studies are mandatory to elucidate the potential role of cardiac myosin as a DAMP in MI.

CONCLUSIONS

Detrimental inflammatory responses in cardiac ischemia have been consistently observed over several decades. Despite our detailed understanding of inflammation in heart failure or after acute MI, novel therapeutic strategies from the preclinical arena have not yet been introduced into the clinical setting. TLRs are ideal candidates to bridge the gap between cardiac-related injury and circulating mediators of inflammation, because TLRs can recognize injury-related molecules.

Evidence exists that TLRs are indeed crucial for postinfarct healing processes but are also mediators of reperfusion injury. They can be activated by molecules released after cell stress, cell death, or both. Endogenous activators of TLRs are interesting as therapeutic targets and are likely to be safe because most of them are only released after tissue injury and might not have a systemic biological function under physiological conditions. Some endogenous ligands enhance viability and cardiac repair, whereas others have deleterious actions. Purification of beneficial DAMPs for therapeutic applications is an attractive idea, but it is also very challenging. Contamination of endogenous TLR-activator isolations with endotoxins or other material can not only alter study results, but also hamper clinical application.

In theory, every single molecule that normally resides within the cell is a potential DAMP when released after cell death. The relative contribution of these signals to postischemic injury can differ, thereby making it possible to identify several candidate molecules with a major impact in postischemic

inflammation. In addition, genetic variations can influence the responsiveness of the immune system to certain DAMPs and, therefore, be of great importance to cardiac repair mechanisms. For this reason, future studies should address genetic determinants of processes associated with DAMP signaling. Furthermore, the research conducted so far has focused on leukocyte/lymphocyte and cardiomyocyte function after altering innate immune activity. However, fibroblast transdifferentiation is crucial in postinfarct repair responses. TLRs could also exert their action by affecting myofibroblast function and differentiation after cardiac ischemia, although this possibility remains to be studied.
Our current body of knowledge about the role of DAMPs in the infarcted myocardium does not explain why local enhancement of several candidates-as opposed to their systemic elevation-improves cardiac function. A better understanding of both spatial and temporal functions of endogenous ligands will be of utmost importance to the development of successful therapies for cardiac ischemia.

OVERVIEW OF THE THESIS

The main topic of the thesis is to study novel approaches that may enhance cardiac repair after MI. We have taken the 'danger model' as a theoretical framework to design our animal experiments. In **Part I**, **Chapter 2** demonstrates that circulating cells expressing TLR2 are involved in reperfusion-induced injury after cardiac ischemia. Using a mouse I/R injury model, we show that systemic TLR2 inhibition reduces infarct size and improves cardiac function. In **Chapter 3**, we established a successful translation of murine results into a porcine model, which is physiologically and anatomically more relevant to the human situation. We showed that a novel humanized anti-TLR2 antibody reduces infarct size and improves cardiac function in pigs after myocardial I/R injury. While previous chapters discussed interventions that targeted circulating cells to reduce cardiac injury, **Chapters 4-7** introduce exosomes as a novel therapeutic to directly enhance myocardial viability. **Chapter 4** describes the purification of exosomes from mesenchymal stem cell (MSC) secretion and infarct size reduction after exosome administration in mice. In **Chapter 5**, we investigated fetal tissue as an alternative source for MSC derivation due to restricted access to clinical grade human embryonic stem cells. In addition, we studied whether immortalization would be an option to have access to infinite supply of MSCs and higher production rate of exosomes (**Chapter 6**). In **Chapter 7** we explored the molecular mechanisms and physiological consequences of infarct size reduction exerted by exosomes.
In **Part II**, we used a chronic coronary artery ligation model to study left ventricular remodeling independent from infarct size. **Chapter 8** reports that chronic inhibition of TLR2 signaling in circulating cells prevents adverse remodeling after MI. In **Chapter 9**, we show that fibronectin-EDA may serve as a DAMP and mediates post-infarct inflammation and ventricular remodeling. In **Chapter 10**, we demonstrate that haptoglobin is crucial for scavenging oxidative stress in the infarcted heart, thereby reducing the DAMP-burden after MI. The experiment shows that in the absence of haptoglobin early repair mechanisms and long-term remodeling are severely impaired.
Part III (**Chapter 11-15**) provides a general discussion, summary of the thesis and additional information.

REFERENCES

1 Virchow R. Cellular pathology. As based upon physiological and pathological histology. Lecture XVI--Atheromatous affection of arteries. 1858. Nutr Rev. 1989;47:23-25.

2 Van AW. I. Landerer's Mechanical Theory of Inflammation. Ann Surg. 1885;2:479-485.

3 Brand ED, Lefer AM. Myocardial depressant factor in plasma from cats in irreversible post-oligemic shock. Proc Soc Exp Biol Med. 1966;122:200-203.

4 Lefer AM, Cowgill R, Marshall FF, Hall LM, Brand ED. Characterization of a myocardial depressant factor present in hemorrhagic shock. Am J Physiol. 1967;213:492-498.

5 Lefer AM, Rovetto MJ. Influence of a myocardial depressant factor on physiologic properties of cardiac muscle. Proc Soc Exp Biol Med. 1970;134:269-273.

6 Arslan F, de Kleijn DP, Timmers L, Doevendans PA, Pasterkamp G. Bridging innate immunity and myocardial ischemia/reperfusion injury: the search for therapeutic targets. Curr Pharm Des. 2008;14:1205-1216.

7 Chao W. Toll-like receptor signaling: a critical modulator of cell survival and ischemic injury in the heart. Am J Physiol Heart Circ Physiol. 2009;296:H1-12.

8 Frangogiannis NG. Chemokines in the ischemic myocardium: from inflammation to fibrosis. Inflamm Res. 2004;53:585-595.

9 Kelly RA, Smith TW. Cytokines and cardiac contractile function. Circulation. 1997;95:778-781.

10 Mann DL. Inflammatory mediators and the failing heart: past, present, and the foreseeable future. Circ Res. 2002;91:988-998.

11 Frangogiannis NG. The immune system and cardiac repair. Pharmacol Res. 2008;58:88-111.

12 Rezkalla SH, Kloner RA. Coronary no-reflow phenomenon: from the experimental laboratory to the cardiac catheterization laboratory. Catheter Cardiovasc Interv. 2008;72:950-957.

13 Vinten-Johansen J. Involvement of neutrophils in the pathogenesis of lethal myocardial reperfusion injury. Cardiovasc Res. 2004;61:481-497.

14 Dobaczewski M, Gonzalez-Quesada C, Frangogiannis NG. The extracellular matrix as a modulator of the inflammatory and reparative response following myocardial infarction. J Mol Cell Cardiol. 2009.

15 Spinale FG. Myocardial matrix remodeling and the matrix metalloproteinases: influence on cardiac form and function. Physiol Rev. 2007;87:1285-1342.

16 Matzinger P. The danger model: a renewed sense of self. Science. 2002;296:301-305.

17 Seong SY, Matzinger P. Hydrophobicity: an ancient damage-associated molecular pattern that initiates innate immune responses. Nat Rev Immunol. 2004;4:469-478.

18 Ionita MG, Arslan F, de Kleijn DP, Pasterkamp G. Endogenous inflammatory molecules engage Toll-like receptors in cardiovascular disease. J Innate Immun. 2010;2:307-315.

19 Blasius AL, Beutler B. Intracellular toll-like receptors. Immunity. 2010;32:305-315.

20 Arslan F, Smeets MB, O'Neill LA, Keogh B, McGuirk P, Timmers L, Tersteeg C, Hoefer IE, Doevendans PA, Pasterkamp G, de Kleijn DP. Myocardial ischemia/reperfusion injury is mediated by leukocytic toll-like receptor-2 and reduced by systemic administration of a novel anti-toll-like receptor-2 antibody. Circulation. 2010;121:80-90.

21 Akira S, Takeda K. Toll-like receptor signalling. Nat Rev Immunol. 2004;4:499-511.

22 Hansson GK. Immune and inflammatory mechanisms in the development of atherosclerosis. Br Heart J. 1993;69:S38-S41.

23 Brodison A, Swann JW. Myocarditis: a review. J Infect. 1998;37:99-103.

24 Hansson GK, Edfeldt K. Toll to be paid at the gateway to the vessel wall. Arterioscler Thromb Vasc Biol. 2005;25:1085-1087.

25 Frantz S, Ertl G, Bauersachs J. Toll-like receptor signaling in the ischemic heart. Front Biosci. 2008;13:5772-5779.

26 Li M, Zhou Y, Feng G, Su SB. The critical role of Toll-like receptor signaling pathways in the induction and progression of autoimmune diseases. Curr Mol Med. 2009;9:365-374.

27 Kumar H, Kawai T, Akira S. Toll-like receptors and innate immunity. Biochem Biophys Res Commun. 2009;388:621-625.

28 Arslan F, Keogh B, McGuirk P, Parker AE. TLR2 and TLR4 in ischemia reperfusion injury. Mediators Inflamm. 2010;2010:704202.

29 Favre J, Musette P, Douin-Echinard V, Laude K, Henry JP, Arnal JF, Thuillez C, Richard V. Toll-like receptors 2-deficient mice are protected against postischemic coronary endothelial dysfunction. Arterioscler Thromb Vasc Biol. 2007;27:1064-1071.

30 Knuefermann P, Sakata Y, Baker JS, Huang CH, Sekiguchi K, Hardarson HS, Takeuchi O, Akira S, Vallejo JG. Toll-like receptor 2 mediates Staphylococcus aureus-induced myocardial dysfunction and cytokine production in the heart. Circulation. 2004;110:3693-3698.

31 Boyd JH, Mathur S, Wang Y, Bateman RM, Walley KR. Toll-like receptor stimulation in cardiomyoctes decreases contractility and initiates an NF-kappaB dependent inflammatory response. Cardiovasc Res. 2006;72:384-393.

32 Sakata Y, Dong JW, Vallejo JG, Huang CH, Baker JS, Tracey KJ, Tacheuchi O, Akira S, Mann DL. Toll-like receptor 2 modulates left ventricular function following ischemia-reperfusion injury. Am J Physiol Heart Circ Physiol. 2007;292:H503-H509.

33 Cohn JN, Ferrari R, Sharpe N. Cardiac remodeling--concepts and clinical implications: a consensus paper from an international forum on cardiac remodeling. Behalf of an International Forum on Cardiac Remodeling. J Am Coll Cardiol. 2000;35:569-582.

34 Landmesser U, Wollert KC, Drexler H. Potential novel pharmacological therapies for myocardial remodelling. Cardiovasc Res. 2009;81:519-527.

35 Shishido T, Nozaki N, Yamaguchi S, Shibata Y, Nitobe J, Miyamoto T, Takahashi H, Arimoto T, Maeda K, Yamakawa M, Takeuchi O, Akira S, Takeishi Y, Kubota I. Toll-like receptor-2 modulates ventricular remodeling after myocardial infarction. Circulation. 2003;108:2905-2910.

36 Timmers L, Sluijter JP, van Keulen JK, Hoefer IE, Nederhoff MG, Goumans MJ, Doevendans PA, van Echteld CJ, Joles JA, Quax PH, Piek JJ, Pasterkamp G, de Kleijn DP. Toll-like receptor 4 mediates maladaptive left ventricular remodeling and impairs cardiac function after myocardial infarction. Circ Res. 2008;102:257-264.

37 Satoh M, Shimoda Y, Maesawa C, Akatsu T, Ishikawa Y, Minami Y, Hiramori K, Nakamura M. Activated toll-like receptor 4 in monocytes is associated with heart failure after acute myocardial infarction. Int J Cardiol. 2006;109:226-234.

38 Timmers L, van Keulen JK, Hoefer IE, Meijs MF, van MB, den OK, van Echteld CJ, Pasterkamp G, de Kleijn DP. Targeted deletion of nuclear factor kappaB p50 enhances cardiac remodeling and dysfunction following myocardial infarction. Circ Res. 2009;104:699-706.

39 Eefting F, Rensing B, Wigman J, Pannekoek WJ, Liu WM, Cramer MJ, Lips DJ, Doevendans PA. Role of apoptosis in reperfusion injury. Cardiovasc Res. 2004;61:414-426.

40 Piper HM, Abdallah Y, Schafer C. The first minutes of reperfusion: a window of opportunity for cardioprotection. Cardiovasc Res. 2004;61:365-371.

41 Gustafsson AB, Gottlieb RA. Heart mitochondria: gates of life and death. Cardiovasc Res. 2008;77:334-343.

42 Inserte J, Barrabes JA, Hernando V, Garcia-Dorado D. Orphan targets for reperfusion injury. Cardiovasc Res. 2009;83:169-178.

43 Garrido C, Gurbuxani S, Ravagnan L, Kroemer G. Heat shock proteins: endogenous modulators of apoptotic cell death. Biochem Biophys Res Commun. 2001;286:433-442.

44 Kol A, Lichtman AH, Finberg RW, Libby P, Kurt-Jones EA. Cutting edge: heat shock protein (HSP) 60 activates the innate immune response: CD14 is an essential receptor for HSP60 activation of mononuclear cells. J Immunol. 2000;164:13-17.

45 Ohashi K, Burkart V, Flohe S, Kolb H. Cutting edge: heat shock protein 60 is a putative endogenous ligand of the toll-like receptor-4 complex. J Immunol. 2000;164:558-561.

46 Tsan MF, Gao B. Endogenous ligands of Toll-like receptors. J Leukoc Biol. 2004;76:514-519.

47 Tsan MF, Baochong G. Pathogen-associated molecular pattern contamination as putative endogenous ligands of Toll-like receptors. J Endotoxin Res. 2007;13:6-14.

48 Erridge C, Samani NJ. Saturated fatty acids do not directly stimulate Toll-like receptor signaling. Arterioscler Thromb Vasc Biol. 2009;29:1944-1949.

49 Tissieres A, Mitchell HK, Tracy UM. Protein synthesis in salivary glands of Drosophila melanogaster: relation to chromosome puffs. J Mol Biol. 1974;84:389-398.

50 Daugaard M, Rohde M, Jaattela M. The heat shock protein 70 family: Highly homologous proteins with overlapping and distinct functions. FEBS Lett. 2007;581:3702-3710.

51 Young JC. Mechanisms of the Hsp70 chaperone system. Biochem Cell Biol. 2010;88:291-300.

52 Currie RW, White FP. Trauma-induced protein in rat tissues: a physiological role for a “heat shock” protein? Science. 1981;214:72-73.

53 Currie RW. Effects of ischemia and perfusion temperature on the synthesis of stress-induced (heat shock) proteins in isolated and perfused rat hearts. J Mol Cell Cardiol. 1987;19:795-808.

54 Yellon DM, Latchman DS. Stress proteins and myocardial protection. J Mol Cell Cardiol. 1992;24:113-124.

55 Gupta M, Vavasis C, Frishman WH. Heat shock proteins in cardiovascular disease a new therapeutic target. Cardiol Rev. 2004;12:26-30.

56 Fan GC, Chu G, Kranias EG. Hsp20 and its cardioprotection. Trends Cardiovasc Med. 2005;15:138-141.

57 Knowlton AA, Kapadia S, Torre-Amione G, Durand JB, Bies R, Young J, Mann DL. Differential expression of heat shock proteins in normal and failing human hearts. J Mol Cell Cardiol. 1998;30:811-818.

58 Tanonaka K, Yoshida H, Toga W, Furuhama K, Takeo S. Myocardial heat shock proteins during the development of heart failure. Biochem Biophys Res Commun. 2001;283:520-525.

59 Yellon DM, Iliodromitis E, Latchman DS, Van Winkle DM, Downey JM, Williams FM, Williams TJ. Whole body heat stress fails to limit infarct size in the reperfused rabbit heart. Cardiovasc Res. 1992;26:342-346.

60 Legare JF, Oxner A, Heimrath O, Myers T, Currie RW. Heat shock treatment results in increased recruitment of labeled PMN following myocardial infarction. Am J Physiol Heart Circ Physiol. 2007;293:H3210-H3215.

61 Zal B, Kaski JC, Arno G, Akiyu JP, Xu Q, Cole D, Whelan M, Russell N, Madrigal JA, Dodi IA, Baboonian C. Heat-shock protein 60-reactive CD4+CD28null T cells in patients with acute coronary syndromes. Circulation. 2004;109:1230-1235.

62 Kim SC, Stice JP, Chen L, Jung JS, Gupta S, Wang Y, Baumgarten G, Trial J, Knowlton AA. Extracellular Heat Shock Protein 60, Cardiac Myocytes, and Apoptosis. Circ Res. 2009.

63 Lin L, Kim SC, Wang Y, Gupta S, Davis B, Simon SI, Torre-Amione G, Knowlton AA. HSP60 in heart failure: abnormal distribution and role in cardiac myocyte apoptosis. Am J Physiol Heart Circ Physiol. 2007;293:H2238-H2247.

64 Frantz S, Kobzik L, Kim YD, Fukazawa R, Medzhitov R, Lee RT, Kelly RA. Toll4 (TLR4) expression in cardiac myocytes in normal and failing myocardium. J Clin Invest. 1999;104:271-280.

65 Olivetti G, Abbi R, Quaini F, Kajstura J, Cheng W, Nitahara JA, Quaini E, Di LC, Beltrami CA, Krajewski S, Reed JC, Anversa P. Apoptosis in the failing human heart. N Engl J Med. 1997;336:1131-1141.

66 Sharma AK, Dhingra S, Khaper N, Singal PK. Activation of apoptotic processes during transition from hypertrophy to heart failure in guinea pigs. Am J Physiol Heart Circ Physiol. 2007;293:H1384-H1390.

67 Dorn GW. Apoptotic and non-apoptotic programmed cardiomyocyte death in ventricular remodelling. Cardiovasc Res. 2009;81:465-473.

68 Park M, Shen YT, Gaussin V, Heyndrickx GR, Bartunek J, Resuello RR, Natividad FF, Kitsis RN, Vatner DE, Vatner SF. Apoptosis predominates in nonmyocytes in heart failure. Am J Physiol Heart Circ Physiol. 2009;297:H785-H791.

69 Muller S, Ronfani L, Bianchi ME. Regulated expression and subcellular localization of HMGB1, a chromatin protein with a cytokine function. J Intern Med. 2004;255:332-343.

70 Scaffidi P, Misteli T, Bianchi ME. Release of chromatin protein HMGB1 by necrotic cells triggers inflammation. Nature. 2002;418:191-195.

71 Lotze MT, Tracey KJ. High-mobility group box 1 protein (HMGB1): nuclear weapon in the immune arsenal. Nat Rev Immunol. 2005;5:331-342.

72 Bonaldi T, Talamo F, Scaffidi P, Ferrera D, Porto A, Bachi A, Rubartelli A, Agresti A, Bianchi ME. Monocytic cells hyperacetylate chromatin protein HMGB1 to redirect it towards secretion. EMBO J. 2003;22:5551-5560.

73 Rendon-Mitchell B, Ochani M, Li J, Han J, Wang H, Yang H, Susarla S, Czura C, Mitchell RA, Chen G, Sama AE, Tracey KJ, Wang H. IFN-gamma induces high mobility group box 1 protein release partly through a TNF-dependent mechanism. J Immunol. 2003;170:3890-3897.

74 Chen G, Li J, Ochani M, Rendon-Mitchell B, Qiang X, Susarla S, Ulloa L, Yang H, Fan S, Goyert SM, Wang P, Tracey KJ, Sama AE, Wang H. Bacterial endotoxin stimulates macrophages to release HMGB1 partly through. J Leukoc Biol. 2004;76:994-1001.

75 Li W, Sama AE, Wang H. Role of HMGB1 in cardiovascular diseases. Curr Opin Pharmacol. 2006;6:130-135.

76 Park JS, Svetkauskaite D, He Q, Kim JY, Strassheim D, Ishizaka A, Abraham E. Involvement of toll-like receptors 2 and 4 in cellular activation by high mobility group box 1 protein. J Biol Chem. 2004;279:7370-7377.

77 Ivanov S, Dragoi AM, Wang X, Dallacosta C, Louten J, Musco G, Sitia G, Yap GS, Wan Y, Biron CA, Bianchi ME, Wang H, Chu WM. A novel role for HMGB1 in TLR9-mediated inflammatory responses to CpG-DNA. Blood. 2007;110:1970-1981.

78 Tian J, Avalos AM, Mao SY, Chen B, Senthil K, Wu H, Parroche P, Drabic S, Golenbock D, Sirois C, Hua J, An LL, Audoly L, La RG, Bierhaus A, Naworth P, Marshak-Rothstein A, Crow MK, Fitzgerald KA, Latz E, Kiener PA, Coyle AJ. Toll-like receptor 9-dependent activation by DNA-containing immune complexes is mediated by HMGB1 and RAGE. Nat Immunol. 2007;8:487-496.

79 Takahashi K, Fukushima S, Yamahara K, Yashiro K, Shintani Y, Coppen SR, Salem HK, Brouilette SW, Yacoub MH, Suzuki K. Modulated inflammation by injection of high-mobility group box 1 recovers post-infarction chronically failing heart. Circulation. 2008;118:S106-S114.

80 Kohno T, Anzai T, Naito K, Miyasho T, Okamoto M, Yokota H, Yamada S, Maekawa Y, Takahashi T, Yoshikawa T, Ishizaka A, Ogawa S. Role of high-mobility group box 1 protein in post-infarction healing process and left ventricular remodelling. Cardiovasc Res. 2009;81:565-573.

81 Goldstein RS, Gallowitsch-Puerta M, Yang L, Rosas-Ballina M, Huston JM, Czura CJ, Lee DC, Ward MF, Bruchfeld AN, Wang H, Lesser ML, Church AL, Litroff AH, Sama AE, Tracey KJ. Elevated high-mobility group box 1 levels in patients with cerebral and myocardial ischemia. Shock. 2006;25:571-574.

82 Kitahara T, Takeishi Y, Harada M, Niizeki T, Suzuki S, Sasaki T, Ishino M, Bilim O, Nakajima O, Kubota I. High-mobility group box 1 restores cardiac function after myocardial infarction in transgenic mice. Cardiovasc Res. 2008;80:40-46.

83 Limana F, Germani A, Zacheo A, Kajstura J, Di CA, Borsellino G, Leoni O, Palumbo R, Battistini L, Rastaldo R, Muller S, Pompilio G, Anversa P, Bianchi ME, Capogrossi MC. Exogenous high-mobility group box 1 protein induces myocardial regeneration after infarction via enhanced cardiac C-kit+ cell proliferation and differentiation. Circ Res. 2005;97:e73-e83.

84 Rossini A, Zacheo A, Mocini D, Totta P, Facchiano A, Castoldi R, Sordini P, Pompilio G, Abeni D, Capogrossi MC, Germani A. HMGB1-stimulated human primary cardiac fibroblasts exert a paracrine action on human and murine cardiac stem cells. J Mol Cell Cardiol. 2008;44:683-693.

85 Andrassy M, Volz HC, Igwe JC, Funke B, Eichberger SN, Kaya Z, Buss S, Autschbach F, Pleger ST, Lukic IK, Bea F, Hardt SE, Humpert PM, Bianchi ME, Mairbaurl H, Nawroth PP, Remppis A, Katus HA, Bierhaus A. High-mobility group box-1 in ischemia-reperfusion injury of the heart. Circulation. 2008;117:3216-3226.

86 Tzeng HP, Fan J, Vallejo JG, Dong JW, Chen X, Houser SR, Mann DL. Negative inotropic effects of high-mobility group box 1 protein in isolated contracting cardiac myocytes. Am J Physiol Heart Circ Physiol. 2008;294:H1490-H1496.

87 Wang H, Bloom O, Zhang M, Vishnubhakat JM, Ombrellino M, Che J, Frazier A, Yang H, Ivanova S, Borovikova L, Manogue KR, Faist E, Abraham E, Andersson J, Andersson U, Molina PE, Abumrad NN, Sama A, Tracey KJ. HMG-1 as a late mediator of endotoxin lethality in mice. Science. 1999;285:248-251.

88 Yang H, Ochani M, Li J, Qiang X, Tanovic M, Harris HE, Susarla SM, Ulloa L, Wang H, DiRaimo R, Czura CJ, Wang H, Roth J, Warren HS, Fink MP, Fenton MJ, Andersson U, Tracey KJ. Reversing established sepsis with antagonists of endogenous high-mobility group box 1. Proc Natl Acad Sci U S A. 2004;101:296-301.

89 Natanson C, Danner RL, Elin RJ, Hosseini JM, Peart KW, Banks SM, MacVittie TJ, Walker RI, Parrillo JE. Role of endotoxemia in cardiovascular dysfunction and mortality. Escherichia coli and Staphylococcus aureus challenges in a canine model of human septic shock. J Clin Invest. 1989;83:243-251.

90 Ono M. Molecular links between tumor angiogenesis and inflammation: inflammatory stimuli of macrophages and cancer cells as targets for therapeutic strategy. Cancer Sci. 2008;99:1501-1506.

91 vid Dong ZM, Aplin AC, Nicosia RF. Regulation of angiogenesis by macrophages, dendritic cells, and circulating myelomonocytic cells. Curr Pharm Des. 2009;15:365-379.

92 Sharma A, Ray R, Rajeswari MR. Overexpression of high mobility group (HMG) B1 and B2 proteins directly correlates with the progression of squamous cell carcinoma in skin. Cancer Invest. 2008;26:843-851.

93 Srikrishna G, Freeze HH. Endogenous damage-associated molecular pattern molecules at the crossroads of inflammation and cancer. Neoplasia. 2009;11:615-628.

94 Dobaczewski M, Bujak M, Zymek P, Ren G, Entman ML, Frangogiannis NG. Extracellular matrix remodeling in canine and mouse myocardial infarcts. Cell Tissue Res. 2006;324:475-488.

95 Comper WD, Laurent TC. Physiological function of connective tissue polysaccharides. Physiol Rev. 1978;58:255-315.

96 Waldenstrom A, Martinussen HJ, Gerdin B, Hallgren R. Accumulation of hyaluronan and tissue edema in experimental myocardial infarction. J Clin Invest. 1991;88:1622-1628.

97 Termeer C, Benedix F, Sleeman J, Fieber C, Voith U, Ahrens T, Miyake K, Freudenberg M, Galanos C, Simon JC. Oligosaccharides of Hyaluronan activate dendritic cells via toll-like receptor 4. J Exp Med. 2002;195:99-111.

98 Jiang D, Liang J, Fan J, Yu S, Chen S, Luo Y, Prestwich GD, Mascarenhas MM, Garg HG, Quinn DA, Homer RJ, Goldstein DR, Bucala R, Lee PJ, Medzhitov R, Noble PW. Regulation of lung injury and repair by Toll-like receptors and hyaluronan. Nat Med. 2005;11:1173-1179.

99 Scheibner KA, Lutz MA, Boodoo S, Fenton MJ, Powell JD, Horton MR. Hyaluronan fragments act as an endogenous danger signal by engaging TLR2. J Immunol. 2006;177:1272-1281.

100 Gariboldi S, Palazzo M, Zanobbio L, Selleri S, Sommariva M, Sfondrini L, Cavicchini S, Balsari A, Rumio C. Low molecular weight hyaluronic acid increases the self-defense of skin epithelium by induction of beta-defensin 2 via TLR2 and TLR4. J Immunol. 2008;181:2103-2110.

101 Zheng L, Riehl TE, Stenson WF. Regulation of colonic epithelial repair in mice by Toll-like receptors and hyaluronic acid. Gastroenterology. 2009;137:2041-2051.

102 Liao YF, Gotwals PJ, Koteliansky VE, Sheppard D, Van De WL. The EIIIA segment of fibronectin is a ligand for integrins alpha 9beta 1 and alpha 4beta 1 providing a novel mechanism for regulating cell adhesion by alternative splicing. J Biol Chem. 2002;277:14467-14474.

103 Schoneveld AH, Hoefer I, Sluijter JP, Laman JD, de Kleijn DP, Pasterkamp G. Atherosclerotic lesion development and Toll like receptor 2 and 4 responsiveness. Atherosclerosis. 2008;197:95-104.

104 Arslan F, Smeets MB, Riem Vis PW, Karper JC, Quax PH, Bongartz LG, Peters JH, Hoefer IE, Doevendans PA, Pasterkamp G, de Kleijn DP. Lack of fibronectin-EDA promotes survival and prevents adverse remodeling and heart function deterioration after myocardial infarction. Circ Res. 2011;108:582-592.

105 Fairweather D, Frisancho-Kiss S, Njoku DB, Nyland JF, Kaya Z, Yusung SA, Davis SE, Frisancho JA, Barrett MA, Rose NR. Complement receptor 1 and 2 deficiency increases coxsackievirus B3-induced myocarditis, dilated cardiomyopathy, and heart failure by increasing macrophages, IL-1beta, and immune complex deposition in the heart. J Immunol. 2006;176:3516-3524.

106 Li Y, Heuser JS, Cunningham LC, Kosanke SD, Cunningham MW. Mimicry and antibody-mediated cell signaling in autoimmune myocarditis. J Immunol. 2006;177:8234-8240.

107 Zhang P, Cox CJ, Alvarez KM, Cunningham MW. Cutting edge: cardiac myosin activates innate immune responses through TLRs. J Immunol. 2009;183:27-31.

108 Zhu X, Bagchi A, Zhao H, Kirschning CJ, Hajjar RJ, Chao W, Hellman J, Schmidt U. Toll-like receptor 2 activation by bacterial peptidoglycan-associated lipoprotein activates cardiomyocyte inflammation and contractile dysfunction. Crit Care Med. 2007;35:886-892.

109 Schoneveld AH, Oude Nijhuis MM, van MB, Laman JD, de Kleijn DP, Pasterkamp G. Toll-like receptor 2 stimulation induces intimal hyperplasia and atherosclerotic lesion development. Cardiovasc Res. 2005;66:162-169.

110 Bjorkbacka H. Multiple roles of Toll-like receptor signaling in atherosclerosis. Curr Opin Lipidol. 2006;17:527-533.

111 Hardarson HS, Baker JS, Yang Z, Purevjav E, Huang CH, Alexopoulou L, Li N, Flavell RA, Bowles NE, Vallejo JG. Toll-like receptor 3 is an essential component of the innate stress response in virus-induced cardiac injury. Am J Physiol Heart Circ Physiol. 2007;292:H251-H258.

112 Richer MJ, Lavallee DJ, Shanina I, Horwitz MS. Toll-like receptor 3 signaling on macrophages is required for survival following coxsackievirus B4 infection. PLoS One. 2009;4:e4127.

113 Oyama J, Blais C, Jr., Liu X, Pu M, Kobzik L, Kelly RA, Bourcier T. Reduced myocardial ischemia-reperfusion injury in toll-like receptor 4-deficient mice. Circulation. 2004;109:784-789.

114 Fairweather D, Yusung S, Frisancho S, Barrett M, Gatewood S, Steele R, Rose NR. IL-12 receptor beta 1 and Toll-like receptor 4 increase IL-1 beta- and IL-18-associated myocarditis and coxsackievirus replication. J Immunol. 2003;170:4731-4737.

115 Vink A, Schoneveld AH, van der Meer JJ, van Middelaar BJ, Sluijter JP, Smeets MB, Quax PH, Lim SK, Borst C, Pasterkamp G, de Kleijn DP. In vivo evidence for a role of toll-like receptor 4 in the development of intimal lesions. Circulation. 2002;106:1985-1990.

116 Triantafilou K, Orthopoulos G, Vakakis E, Ahmed MA, Golenbock DT, Lepper PM, Triantafilou M. Human cardiac inflammatory responses triggered by Coxsackie B viruses are mainly Toll-like receptor (TLR) 8-dependent. Cell Microbiol. 2005;7:1117-1126.

117 Yu Q, Vazquez R, Khojeini EV, Patel C, Venkataramani R, Larson DF. IL-18 induction of osteopontin mediates cardiac fibrosis and diastolic dysfunction in mice. Am J Physiol Heart Circ Physiol. 2009;297:H76-H85.

118 Bulicheva N, Fidelina O, Mkrtumova N, Neverova M, Bogush A, Bogush M, Roginko O, Veiko N. Effect of cell-free DNA of patients with cardiomyopathy and rDNA on the frequency of contraction of electrically paced neonatal rat ventricular myocytes in culture. Ann N Y Acad Sci. 2008;1137:273-277.

119 Knuefermann P, Schwederski M, Velten M, Krings P, Ehrentraut H, Rudiger M, Boehm O, Fink K, Dreiner U, Grohe C, Hoeft A, Baumgarten G, Koch A, Zacharowski K, Meyer R. Bacterial DNA induces myocardial inflammation and reduces cardiomyocyte contractility: role of toll-like receptor 9. Cardiovasc Res. 2008;78:26-35.

120 Chen L, Ahmed E, Wang T, Wang Y, Ochando J, Chong AS, Alegre ML. TLR signals promote IL-6/IL-17-dependent transplant rejection. J Immunol. 2009;182:6217-6225.

121 Cole JE, Georgiou E, Monaco C. The expression and functions of toll-like receptors in atherosclerosis. Mediators Inflamm. 2010;2010:393946.

CHAPTER 2

This chapter describes that systemic inhibition of Toll-like receptor 2 reduces infarct size and improves cardiac function after I/R injury in mice

Fatih Arslan, Mirjam B. Smeets, Luke A.J. O'Neill, Brian Keogh, Peter McGuirk, Leo Timmers, Claudia Tersteeg, Imo E. Hoefer, Pieter A. Doevendans, Gerard Pasterkamp & Dominique P. de Kleijn

Myocardial ischemia/reperfusion injury is mediated by leukocytic TLR2 and reduced by systemic administration of a novel anti-TLR2 antibody

Background

Reperfusion therapy for myocardial infarction is hampered by detrimental inflammatory responses partly via Toll-like receptor (TLR) activation. Targeting TLR signaling may optimize reperfusion therapy and enhance cell survival and heart function after myocardial infarction. Here we evaluated the role of TLR2 as a therapeutic target using a novel monoclonal anti-TLR2 antibody.

Methods and Results

Mice underwent 30 minutes ischemia, followed by reperfusion. Compounds were administered 5 minutes prior to reperfusion. Cardiac function and dimensions were assessed at baseline and 28 days post-infarction, using 9.4T mouse-MRI. Saline and IgG isotype treatment resulted in 34.5±3.3% and 31.4±2.7% infarction, respectively. Bone marrow transplantation experiments between wild-type and TLR2null mice revealed that final infarct size is determined by circulating TLR2 expression. A single intravenous bolus injection of anti-TLR2 antibody reduced infarct size to 18.9±2.2% (p=0.001). Compared to saline, anti-TLR2 treated mice exhibited less expansive remodeling (end-diastolic volume: 68.2±2.5 µL versus 76.8±3.5 µL; p=0.046), and preserved systolic performance (ejection fraction: 51.0±2.1% vs. 39.9±2.2%, p=0.009; systolic wall thickening: 3.3±6.0 versus 22.0±4.4%, p=0.038). Anti-TLR2 treatment significantly reduced neutrophil, macrophage and T-lymphocyte infiltration. Furthermore, TNFα, IL1α, GM-CSF and IL-10 were significantly reduced as were phosphorylated-c-JNK, phosphorylated-p38-MAPK and Caspase 3/7 activity levels.

Conclusions

Circulating TLR2 expression mediates myocardial I/R injury. Antagonizing TLR2 5 minutes prior to reperfusion reduces infarct size and preserves cardiac function and geometry. Anti-TLR2 therapy exerts its action by reducing leukocyte influx, cytokine production and pro-apoptotic signaling. Hence, monoclonal anti-TLR2 antibody is a potential candidate as an adjunctive for reperfusion therapy in patients with myocardial infarction.

Circulation. 2010;121(1):80-90

Early restoration of blood flow through the occluded coronary artery is currently the most effective therapy to limit infarct size and preserve cardiac function and geometry after acute myocardial infarction (MI)[1]. Nevertheless, reperfusion alone is insufficient to save endangered myocardium, since complications due to loss of viable myocardium are still common after MI even after restoration of blood flow. Furthermore, studies have clearly demonstrated that reperfusion following ischemia causes additional cell death and increase of infarct size, termed myocardial ischemia/reperfusion (I/R) injury. Many interventions aiming at reducing myocardial I/R injury have proven to be successful in experimental studies, but fail in clinical settings[2]. Administration of experimental compounds prior to the ischemic period, rather than in the late ischemic period prior to reperfusion, is one reason for the failure of successful translation in the clinic[3, 4].

Myocardial I/R injury is characterized by a rapid increase of cytokines and chemokines and influx of leukocytes into the endangered myocardial region[3]. Inflammatory responses after myocardial I/R injury are detrimental for cell survival and extra cellular matrix integrity via enhanced activation of pro-apoptotic signaling pathways. The extent of cardiomyocyte apoptosis determines infarct size and subsequent heart function. Mitogen activated protein kinases c-Jun N-terminal kinase (c-JNK) and p38 mitogen-activated protein kinase (p38-MAPK) are well documented as pro-apoptotic mediators of myocardial I/R injury[5]. Indeed, cardiac infarct healing and post-MI remodeling are also processes, in which leukocytes, cytokines and chemokines play both a beneficial and detrimental role6. For example, administration of methylprednisolone results in more frequent cardiac ruptures7 despite infarct size reduction in animal models[8, 9]. Hence, the challenge lies in ameliorating the detrimental inflammatory response, while leaving the tissue repair response unaffected.

Modulating Toll-like receptor (TLR) activation may enhance the 'good' and blunt the 'bad' of the inflammatory response after myocardial I/R injury. TLRs are expressed by leukocytes and recognize pathogen associated molecular patterns in order to defend the host from invading microorganisms. TLRs are also capable of recognizing endogenous 'danger signals' released during cell death[10]. More intriguing is the fact that TLRs are also expressed on cells with no direct role in host innate immune responses, like endothelial[11] cells and cardiomyocytes[12]. Upon activation, TLRs exert their inflammatory response through NF-κB translocation to the nucleus[13]. Therefore, inhibition of TLRs may provide new therapeutic options after myocardial infarction. This view is supported by recent observations in TLR knock-out mice. For example, *ex vivo* experiments show that $TLR2^{-/-}$ hearts perform better compared to wild type (WT) after myocardial I/R injury[14]. $TLR2^{-/-}$ mice are protected against endothelial dysfunction after myocardial I/R injury[15], whereas TLR2 stimulation impairs cardiomyocyte contractility via NF-κB[16]. Furthermore, deficient TLR2 or 4 signaling in mice prevents adverse cardiac remodeling resulting in preserved cardiac function and geometry after MI[17, 18]. This evidence suggests that preventing TLR activation may be beneficial after MI, through prevention of myocardial I/R injury and enhancement of tissue repair responses. In this study we show, *in vivo*, the relative contribution of TLR2 in parenchymal and circulating blood cells to myocardial I/R injury. In addition, we have demonstrated that treatment with a novel anti-TLR2 monoclonal antibody reduces myocardial I/R injury and preserves cardiac function and geometry.

RESULTS

TLR2 on hematopoietic cells mediates myocardial I/R injury

Using an *in vivo* mouse model of myocardial I/R injury (30 min. ischemia followed by reperfusion), saline treatment results in 34.5±3.3% IS/AAR (Figure 1). TLR2$^{-/-}$ mice show an infarcted area of 23±2.9% (~33% reduction, p=0.029). Final infarct size is determined by hematopoietic derived TLR2. TLR2$^{-/-}$/WT BM are not protected against myocardial I/R injury, as shown by similar infarct size to saline treated WT mice (33.9±3.2% vs. 34.5±3.3%; p=1.0). WT/TLR2$^{-/-}$ BM are protected against myocardial I/R injury to the same extent as complete TLR2$^{-/-}$ mice, resulting in approximately 34% reduction of infarct size (22.9±2.7% vs. 34.5±3.3%; p=0.024). The extent of endangered myocardium was similar in all animals. The mean AAR/LV is approximately 41% (Figure 1 in the online data supplement). Bone marrow transplantation itself after radiation does not affect final infarct size, since no significant difference in infarct size occurs in WT/WT BM and in TLR2$^{-/-}$/ TLR2$^{-/-}$ BM.

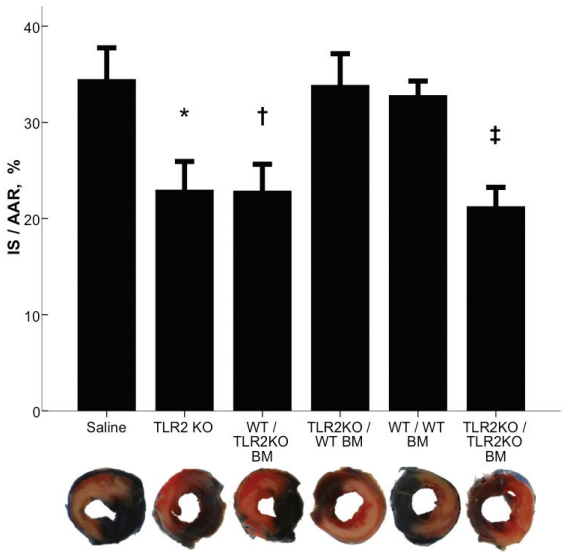

Figure 1. Circulating TLR2 expression mediates MI/R injury. *Infarct size (IS) as a percentage of the area at risk (AAR). Representative cross-sections after TTC staining are shown below corresponding bars. Each bar represents Mean±SEM; n=10/group; *p=0.019, †p=0.014, ‡p=0.013 compared to saline. TLR2 KO=Toll-like receptor 2 knock-out; WT/TLR2KO BM=wild-type mice with TLR2 KO bone marrow; TLR2 KO/WT BM=TLR2 KO mice with WT bone marrow; WT/WT BM=wild-type mice with wild-type bone marrow; TLR2 KO/TLR2 KO BM=TLR2 knock-out mice with TLR2 knock-out bone marrow.*

OPN-301 selectively inhibits human mononuclear TLR2, reduces infarct size and preserves heart function *in vivo*

Systemic inhibition of TLR2 could prevent myocardial I/R injury, since TLR2 on circulating cells mediates myocardial I/R injury. Hence, we studied the therapeutic potential of OPN-301, a novel monoclonal antibody against TLR2. OPN-301 is a mouse IgG1 antibody that inhibits TLR2 mediated responses in mouse, pig, monkey and human (data not shown), indicating that it is specific for a critical epitope.

The IC_{50} for OPN-301 in human peripheral blood monocytes ranges from 50-100 ng/ml for TNFα, and is slightly lower for both IL-1α and IL-6 (approximately 25ng/ml). NF-κB activation is inhibited in human mononuclear THP-1 cells pretreated with OPN-301, after Pam-3-CSK4 (P3C) stimulation (selective ligand for TLR2) (Figure 2a). However, NF-κB activation does occur after lipopolysaccharide (LPS) stimulation pretreated with OPN-301 (Figure 2b). These results demonstrate that OPN-301 selectively inhibits TLR2 signaling. Furthermore, OPN-301 prevents NF-κB activation in a dose dependent manner (Figure 2a). TNFα production after P3C stimulation in a mouse macrophage cell line was also highly inhibited in cells pretreated with OPN-301, compared to IgG1 isotype control (Figure 2c). *In vivo*, a single dose of OPN-301 administered 5 minutes prior to reperfusion reduces infarct size to 18.9±2.2% (~45% reduction, p=0.001 compared to saline; Figure 3a). Also the infarct size reduction reveals a dose dependent correlation (Figure 3b). Both IgG isotype and SB239063 treatments do not reduce infarct size, resulting in 31.4±2.7% (p=0.931 compared to saline) and 31.7±2.4% (p=0.956 compared to saline) infarction within the area at risk, respectively (Figure 3a). AAR/LV was similar between the treatment groups (p>0.937 compared to saline treatment; Figure 1 in the online data supplement). Both TLR2 and CD11b expression in monocytes decrease till the end of the 30 minutes of ischemia, whereas 1 hour reperfusion causes an increase of TLR2 and CD11b expression. Post-reperfusion TLR2 and CD11b expression in monocytes is inhibited upon anti-TLR2 treatment (Figure 3c and d).

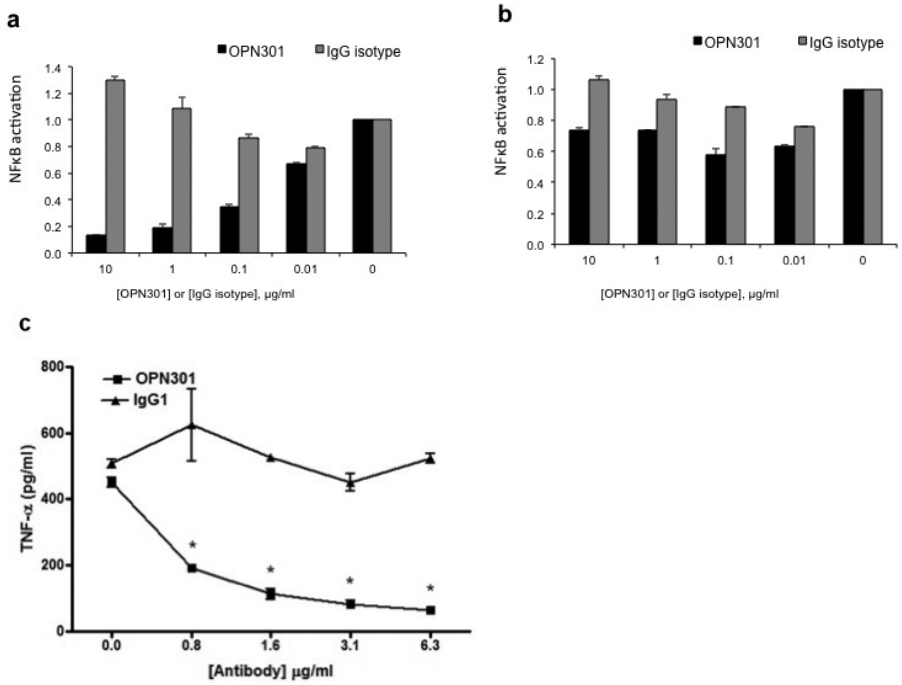

Figure 2. OPN-301 prevents NF-κB activation and TNFα production though selective inhibition of TLR2. *(**A**) NF-κB activity after P3C (100 ng/ml) stimulation in OPN-301 and IgG isotype (ranging from 0 to 10 μg/ml) treated THP-1 blue cells. Note the dose response in OPN-301 treated cells. (**B**) NF-κB activity in treated cells (OPN-301 and IgG isotype) after LPS (1 ng/ml) stimulation. Control NF-κB activity in ligand-treated cells without antibody (OPN-301 or IgG isotype) was set as 1. All differences are significant at p<0.01 level. (**C**) TNFα production in J774 cells. Note the dose response in OPN-301 treated J774 cells; *p<0.001, unpaired students T test. Each bar represents Mean±SEM, three independent experiments performed in duplicate.*

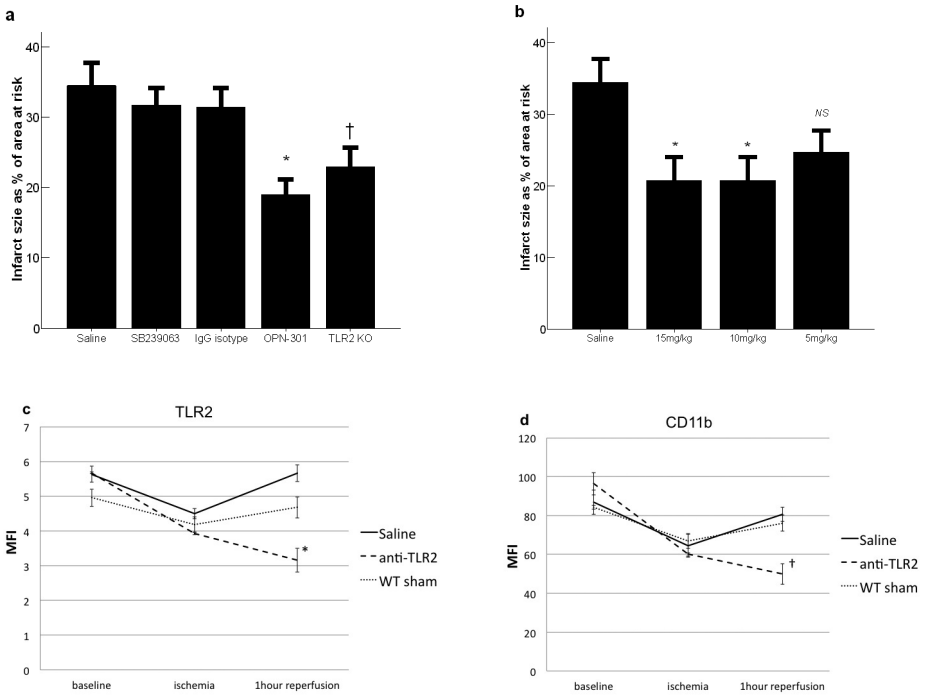

Figure 3. anti-TLR2 treatment reduces infarct size. *(**A**) Infarct size (IS) as a percentage of area at risk (AAR) upon treatment with SB239063, IgG isotype and OPN-301. TLR2 KO serves as an illustrative control; n=10/group, *p=0.001, †p=0.016. (**B**) Dose response of OPN-301 in infarct size reduction; n=6/group, *p=0.028; NS=non significant (**C**) TLR2 and (**D**) CD11b expression levels in monocytes. No differences are observed at baseline and after 30 minutes of ischemia. After 1 hour reperfusion, OPN-301 treatment inhibits both TLR2 (*p=0.001) and CD11b (†p<0.001 compared to saline) expression in monocytes n=5/group; Each bar represents Mean±SEM; MFI=mean fluorescence intensity*

In concordance with the extensive infarct development, saline treatment significantly deteriorates LV volumes and ejection fraction (Figure 4a; movie 1 in the online data supplement). In contrast, OPN-301 treated animals show preserved LV volumes and cardiac performance, as shown by significant smaller end-systolic (p=0.021) and end-diastolic volumes (p=0.046) and higher ejection fraction (p=0.009) compared to saline treatment (Figure 4a; movie 2 in the online data supplement). Furthermore, OPN-301 treated animals show preserved regional LV function. SWT in both remote and infarct area and EF are significantly higher in OPN-301 treated animals (Table 1). In line with the prevention of reperfusion injury (Figure 3), mice treated with anti-TLR2 antibody exhibit reduced scar formation after 28 days infarction (Figure 4b and c). No difference is observed in any of the hemodynamic parameters measured (i.e. heart rate, blood pressure) between the animals (data not shown).

Anti-TLR2 treatment reduces inflammation after myocardial I/R injury *in vivo*

To further elucidate the role of leukocytes in our treated animals, we studied the influx of neutrophils and macrophages after myocardial I/R injury. OPN-301 treatment results in reduced neutrophil influx after 1 hour, 1 day and 3 days post-reperfusion compared to both saline and IgG isotype treatment (Figure 5a).

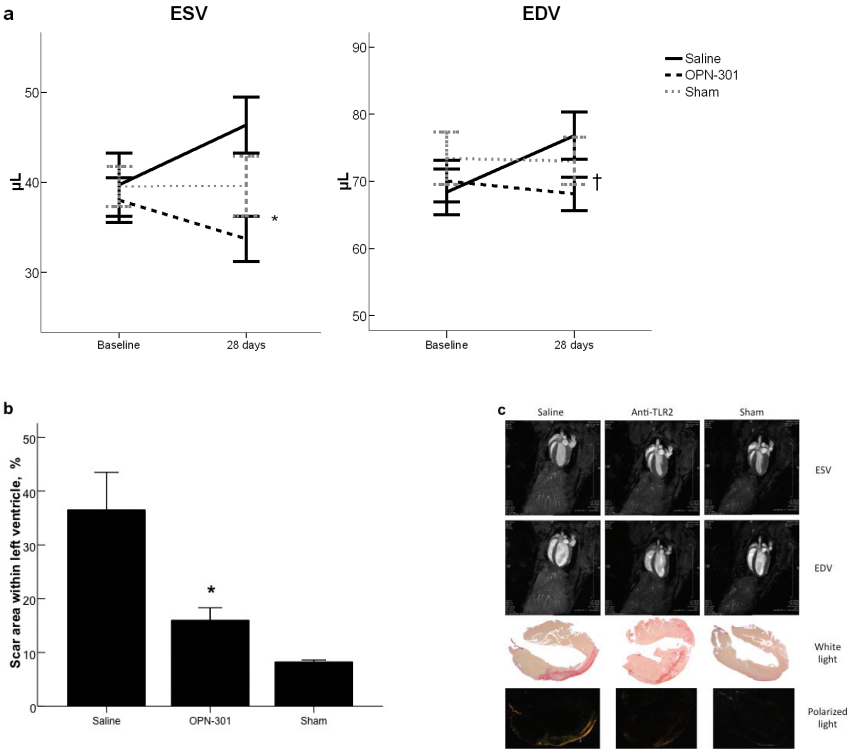

Figure 4. Cardiac function and geometry at baseline and 28 days post-infarction. *(**A**) Saline treatment results in 22.8±12.3% increase in end-systolic volume (ESV) and 13.9±6.9% increase in end-diastolic volume (EDV). However, OPN-301 treatment preserves ESV and EDV. Sham operation does not affect cardiac function and geometry; n=8/group; *p=0.021, †p=0.046 compared to saline treatment. (**B**) Scar area as a percentage of the left ventricle in mice after 28 days infarction; *p=0.003 compared to saline treatment. (**C**) Representative 4-chamber MR images and scarred tissue (Picrosirius Red staining) 28 days post MI/R injury. Each bar represents Mean±SEM;*

Table 1. Wall thickness (WT), systolic wall thickening (SWT) and ejection fraction (EF) 28 days post-reperfusion injury.

	Baseline	28 days	Baseline	28 days
WT septum (remote, mm)	0.79±0.02	0.81±0.02	0.76±0.01	0.81±0.02
WT free wall (infarct, mm)	0.83±0.01	0.92±0.05	0.86±0.03	0.90±0.03
SWT septum (remote, %)	43.7±4.4	33.3±3.2	48.5±3.3	49.0±4.8†
SWT free wall (infarct, %)	54.8±1.4	3.3±6.0*	50.2±3.9	22.0±4.4*‡
EF (%)	42.6±2.1	39.9±2.2	45.8±2.4	51.0±2.1§

Mann-Whitney U test: *p<0.001 compared to baseline; †p=0.021, ‡ p=0.038 and §p=0.009 compared to saline treatment; Data are represented as Mean±SEM, n=8/group.

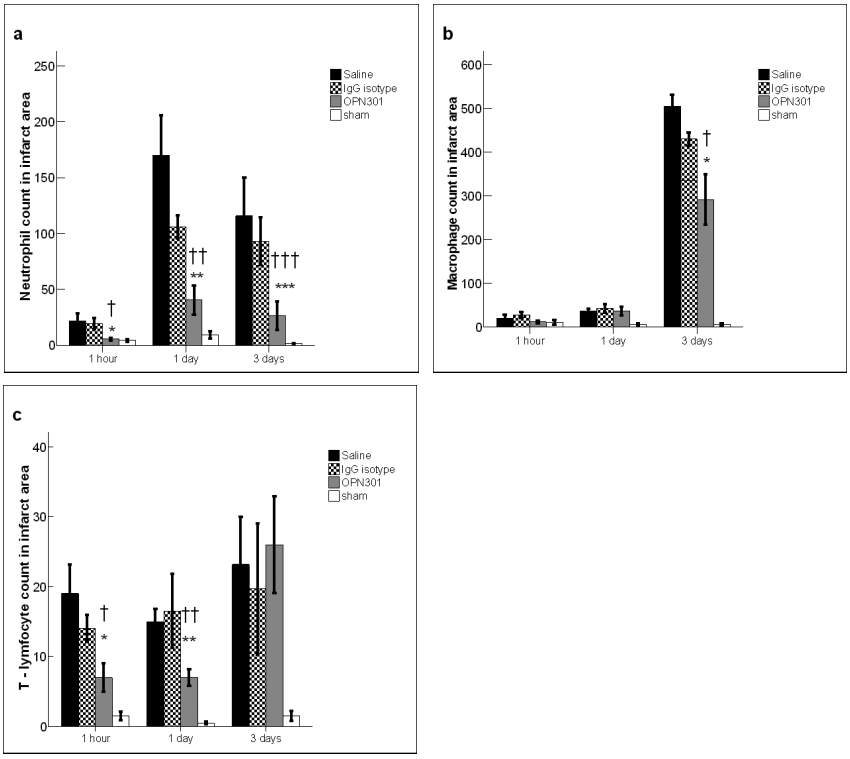

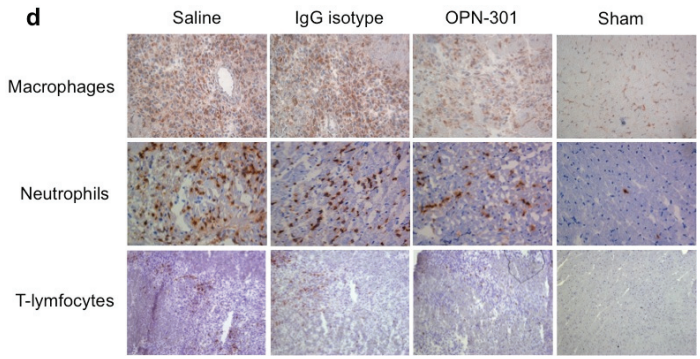

Figure 5. anti-TLR2 treatment reduces leukocyte influx after MI/R injury. *(**A**) Number of neutrophils in the infarcted area in treated animals after 1 hour, 1 day and 3 days reperfusion; *p=0.006, **p<0.001, ***p=0.008 compared to saline; †p=0.018, ††p=0.04, †††p=0.04 compared to IgG isotype treatment. (**B**) Number of macrophages after MI/R injury. *p<0.001 compared to saline, †p=0.004 compared to IgG isotype treatment. (**C**) Number of T-lymphocytes after MI/R injury, *p=0.002, **p=0.08 compared to saline; †p=0.046, ††p=0.041 compared to IgG isotype treatment. (**D**) Representative sections of neutrophil (1 day post MI/R injury), macrophage (3 days post MI/R injury) and T-lymphocyte (1 day post MI/R injury) influx. Each bar represents Mean±SEM, n=6/group per time point.*

After 1 day, macrophages enter the myocardium to remove necrotic cells (e.g. neutrophils, myocytes) and debris, contributing to post-MI extracellular matrix remodeling[19]. OPN-301 treated animals show a reduction of macrophage influx, consistent with our previous observation (Figure 5b). T-lymphocyte influx was also highly reduced in OPN-301 treated animals after 1 hour and 1 day reperfusion (Figure 5c and d; remaining representative sections are in Figure 2 through 4 in the online data supplement). The reduced influx of leukocytes after OPN-301 treatment may be caused by changes in peripheral blood composition upon treatment. Whole blood analyses revealed no differences between saline and OPN-301 treatment after 1 and 3 days reperfusion (Figure 5 in the online data supplement).
In addition, we studied cytokine and chemokine expression levels in ischemic/reperfused hearts. Mice treated with OPN-301 show diminished tissue TNFα levels at all time points, whereas saline and IgG isotype treatment results in increased levels of TNFα (Figure 6a). Significant reduction upon OPN-301 treatment is also seen in the levels of IL-1α (at 1 day reperfusion; Figure 6b), IL-10 (at all time points; Figure 6c) and GM-CSF levels (responsible for monocyte maturation and activation) at all time points (Figure 6d). We performed quantitative PCR to investigate if the highly reduced inflammation at tissue level depends on changes in chemotactic and adhesive factors in the heart. At the mRNA level, monocyte

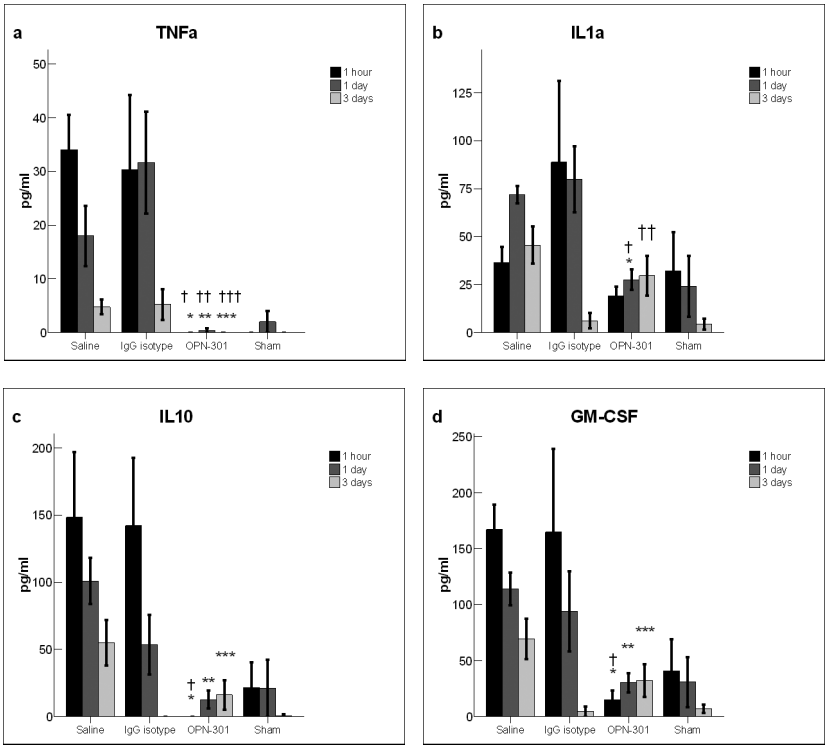

Figure 6. Anti-TLR2 treatment reduces tissue levels of inflammatory cytokines. *(**A**) TNFα levels are almost diminished upon OPN-301 treatment after MI/R injury. *p=0.016, **p=0.039, ***p=0.047 compared to saline; †p=0.036, ††p=0.001, †††p=0.031 compared to IgG isotype treatment. (**B**) IL1α levels, *p=0.018 compared to saline, †p=0.007, ††p=0.038 compared to IgG isotype treatment. (**C**) IL10 levels are almost diminished upon OPN-301 treatment, *p=0.034, **p=0.002, ***p=0.013 compared to saline, †p=0.05 compared to IgG isotype treatment. (**D**) Reduced GM-CSF levels upon OPN-301 treatment, *p=0.033, **p=0.017, ***p=0.041 compared to saline, †p=0.042 compared to IgG isotype treatment. Each bar represents Mean±SEM, n=6/group/time point.*

chemotactic protein (MCP)-1, intercellular adhesion molecule (ICAM)-1 and vascular cell adhesion molecule (VCAM)-1 expression do not correlate with the observed decrease in leukocyte infiltration. While expression levels are the same at 1 hour reperfusion, MCP-1 and ICAM-1 are significantly decreased upon OPN-301 treatment after 1 day reperfusion (p=0.008 and p=0.059 respectively compared to saline; Table 1 in the online data supplement).

Anti-TLR2 treatment inhibits pro-apoptotic signaling pathways after myocardial I/R injury *in vivo*

Having established that anti-TLR2 treatment with OPN-301 is a potent suppressor of key markers of inflammation, we next sought to examine the effects of OPN-301 on critical signaling pathways involved in cardiac function and remodeling. Anti-TLR2 treated mice exhibit less activation of pro-apoptotic signaling pathways compared to saline treatment. At all time points after reperfusion, the levels of

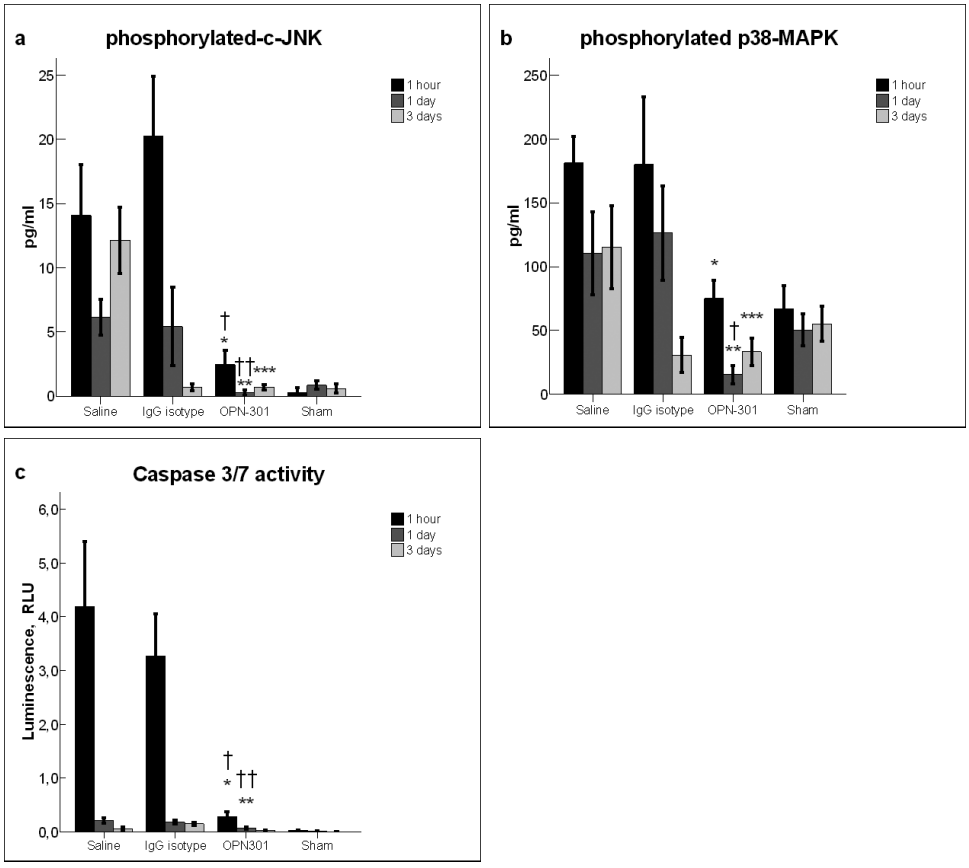

Figure 7. Pro-apoptotic signaling in hearts after MI/R injury. *(**A**) Phosphorylated c-JNK levels are decreased upon OPN-301 treatment, *p=0.049, **p=0.024, ***p<0.001 compared to saline; †p=0.005, ††p=0.045 compared to IgG isotype treatment. (**B**) Phosphorylated p38-MAPK levels, *p=0.044, **p=0.016, ***p=0.008 compared to saline, †p=0.006 compared to IgG isotype treatment. (**C**) Caspase 3/7 levels, *p=0.005, **p=0.005 compared to saline; †p=0.03, ††p=0.024 compared to IgG isotype treatment. Each bar represents Mean±SEM, n=6/group/time point. Phosphoprotein levels are expressed as pg/ml and Caspase 3/7 activity is expressed as relative light units (RLU). Both assessments are corrected for total protein concentration.*

phosphorylated c-JNK (Figure 7a) and phosphorylated p38-MAPK are significantly decreased (Figure 7b). In line with this observation, OPN-301 treated animals show highly reduced Caspase 3/7 activity levels after 1 hour and 1 day reperfusion (Fig 7c).

DISCUSSION

Many advances in clinical cardiology for the treatment of acute myocardial infarction have aimed at restoring epicardial flow in the occluded coronary artery. Indeed, restored epicardial flow is a prerequisite for cardiomyocyte salvage, however, injury to both endothelial cells and cardiomyocytes occur due to reperfusion therapy. As a consequence of restored flow, both myocardial perfusion and cardiomyocyte survival is hampered, causing a paradoxical increase in cell death and deterioration in cardiac function. Since the phenomenon of myocardial I/R injury was first described by Jennings et al.[20] in 1960, a significant amount of research has been conducted to elucidate the mechanisms that underlie myocardial I/R injury and investigate cardioprotective interventions. Despite the increased knowledge about underlying mechanisms, none of the experimental interventions has proven to be effective in the clinic. Only a few have been shown to reduce surrogate markers of myocardial I/R injury[21] or to have an effect in secondary end-points[22]. This highlights the fact that myocardial I/R injury is a complex pathological condition[23], to which a clinical therapy remains a great challenge. The discovery of Toll-like receptors (TLRs) in the cardiovascular system has greatly contributed to our current knowledge on how the inflammatory reaction initiates and enhances myocardial I/R injury and post-infarct remodeling[24]. Furthermore, previous studies using TLR knock-out animals provide evidence for TLRs as novel therapeutic targets in the cardiovascular system.

We have shown that TLR2-dependent circulating blood components mediate myocardial I/R injury. Interestingly, our study is supported by earlier observations in which *ex vivo* Langendorff-perfused hearts showed similar infarct size after myocardial I/R injury[25, 26]. Feng et al.[27] and Sakata et al.[28] showed similar infarct size after global myocardial I/R injury in MyD88$^{-/-}$ (downstream of both TLR2 and TLR4) and TLR2$^{-/-}$ hearts compared to wild-type littermates. Our study shows that circulating and not parenchymal TLR2 determines final infarct size, which explains the negative observations in Langendorff perfused heart experiments.

Our experiments demonstrate that anti-TLR2 treatment could potentially be applied successfully in human patients with acute myocardial infarction. First, we used a novel anti-TLR2 monoclonal antibody treatment to inhibit TLR signaling *in vivo*, which can potentially be used in humans. Secondly, we chose a clinically applicable time point for drug administration in the setting of acute myocardial infarction. Finally, 28 day survival experiments demonstrate long-term efficacy of an anti-TLR2 treatment. We have demonstrated that treatment of mice with OPN-301 reduces infarct size by approximately 45% and prevents subsequent deterioration of cardiac function and geometry, after a single intravenous bolus just 5 min prior to reperfusion. Hence, it has the potential to be effective when it is administered to patients with AMI in the ambulance or emergency room, before reperfusion therapy through primary percutaneous transluminal coronary angioplasty (PTCA). Our model also showed that the p38-MAPK inhibitor SB239063 did not reduce infarct size, when given in the late ischemic period prior to reperfusion. We chose this compound as positive control based on experimental data in which it was effective when administered before ischemia[29]. Our study emphasizes the importance of a clinically relevant model (i.e. in which compounds are given in the late ischemic period) to test therapeutic drugs in the pre-clinical stage.

OPN-301 exerts its action through selectively inhibiting TLR2 signaling in leukocytes. It suppresses leukocyte infiltration in the post-ischemic/reperfused myocardium partly via CD11b downregulation, without affecting peripheral blood composition. Levels of highly potent inflammatory cytokines involved in cardiomyocyte injury and cardiac dysfunction (reviewed in ref. 6) are substantially decreased or even diminished. The decreased levels of cytokines are consistent with the reduction in infarct size and preserved heart function. In addition, decreased neutrophil, macrophage and T-lymphocyte infiltration occurs upon OPN-301 treatment and is not likely due to decreased chemotaxis and adhesion, but rather decreased activation of these leukocyte subsets. Only the expression of MCP-1 is significantly decreased at day 1 after myocardial I/R injury. Decreased infiltration, however, is already seen after 1 hour reperfusion and infarct size increase does not occur beyond the first day. This is in accordance with our notion that circulating TLR2 plays a crucial role in myocardial I/R injury and not parenchymal TLR2. The exact mechanism by which TLR2 inhibition leads to decreased leukocyte infiltration remains to be addressed. One possible mechanism is that TLR2 inhibition prevents activation of circulating cells by endogenous 'danger signals'. Endogenous ligands released during cardiomyocyte necrosis (e.g. HMGB1) may act as an activating ligand for TLRs[30].

Our study also demonstrates that IgG isotype antibody, used as a negative control in our experiments, has several non-significant anti-inflammatory effects. It does not reduce infarct size, however, when compared to saline treatment we do observe a slightly decreased neutrophil influx (Figure 5a) and slightly reduced IL-1α (at 3 days) IL-10 (at 1 and 3 days) and GM-CSF levels (at 3 days; Figure 6). These observations point towards binding of IgG isotype antibodies to membrane bound Fc-receptor. This notion must be considered when isotype controls are used, especially in in vitro assays using single cells (lacking total organ functional assessments) with inflammatory markers as a read-out.

In summary, our study shows that myocardial I/R injury is mediated by TLR2 dependent blood components. Inhibition of TLR2 with OPN301 reduces myocardial I/R injury, preserves cardiac function and geometry *in vivo*. The main mode of action of OPN301 is preventing the detrimental NF-κB mediated inflammation: reduction of leukocyte infiltration, reducing cytokine production, and reducing pro-apoptotic signaling and apoptosis. Moreover, our study demonstrates that OPN-301 is a good candidate as an adjunctive therapeutic for patients undergoing PTCA, since it has shown to be effective when administered at a clinically applicable time point.

Acknowledgements

We would like to thank the following persons for their assistance: Ben J. van Middelaar, Krista den Ouden, Chaylendra Strijder, Petra Holmut, Arjan Schoneveld, Gert-Jan Rood (all from the University Medical Center Utrecht, The Netherlands); dr. Christopher Locher (currently Vertex Pharmaceuticals), Mrs. Mary Reilly and dr. Mark Heffernan (all from Opsona Therapeutics Ltd.). We thank S. Akira (Osaka University, Japan) & T. van de Poll (AMC Amsterdam, the Netherlands) for providing us with the TLR2$^{-/-}$ mouse

Funding Sources

This work is supported by research grants from the European Community's 6th Framework Program (contract LSHMCT-2006-037400, IMMUNATH) and Utrecht University & NWO Mozaïek grant (017.004.004 to F.A.).

METHODS

Animals and experimental design

TLR2$^{-/-}$ animals were backcrossed for 6 generations into a C57Bl6 background. Male C57Bl6/J and C57Bl6-TLR2$^{-/-}$ mice (10-12 wks, 25-30 g) received standard diet and water *ad libitum*. Experimental compounds were administered via the tail vein, 5 minutes prior to reperfusion. Mice were given 250 µl of stock with either PBS, IgG isotype 10 mg/kg as a negative control (R&D systems), SB239063 0.5 mg/kg (a p38-MAPK inhibitor) as a positive control (Alexis Corp.) and OPN-301 10 mg/kg (kindly provided by Opsona Therapeutics Ltd.). Where possible, recommendations from the National Heart Lung and Blood Institute (NHLBI) Working Group on the Translation of Therapies for Protecting the Heart from Ischemia[31] were applied; the surgeon was blind to the treatment. Digital photos of infarcts were encrypted before being analyzed by the researcher. Heart function and geometry assessment was done by a technician blinded to treatment. All animal experiments are performed in accordance with the national guidelines on animal care and with prior approval by the Animal Experimentation Committee of Utrecht University.

Myocardial ischemia/reperfusion injury *in vivo*

Mice were anesthetized with a mixture of Fentanyl® 0.05 mg/kg, Dormicum® 5 mg/kg and Domitor® 0.5 mg/kg through an intraperitoneal injection. Atropine 0.05 mg/kg was subcutaneously administered after coronary ligation. Core body temperature was maintained around 37°C during surgery by continuous monitoring with a rectal thermometer and automatic heating blanket. Mice were intubated and ventilated (Harvard Apparatus Inc.) with 100% oxygen. The left coronary artery (LCA) was ligated for 30 minutes using an 8-0 vicryl suture with a section of polyethylene-10 tubing placed over the LCA. Ischemia was confirmed by bleaching of the myocardium and ventricular tachyarrhythmia. Reperfusion was initiated by releasing the ligature and removing the polyethylene-10 tubing. In sham operated animals the suture was placed beneath the LCA without ligating. Reperfusion of the endangered myocardium was characterized by typical hyperemia in the first few minutes. A piece of the loosened suture was left in place in order to determine ischemic area during termination. The chest wall was closed and the animals received subcutaneously Antisedan® 2.5 mg/kg, Anexate® 0.5 mg/kg and Temgesic® 0.1 mg/kg.

Generation of chimeric mice

We generated chimeric mice to study the relative contribution of TLR2 expression in blood and parenchymal cells to myocardial I/R injury. Donor bone marrow (BM) cells were collected from wild-type (WT) C57Bl6 and TLR2 knock-out (TLR2$^{-/-}$) mice by flushing humerus, femurs and tibiae with RPMI-1640 medium. Recipient mice received 5x10^6 BM cells after receiving a single dose of 7 Gy. Mice recovered for 6 weeks to ensure stable engraftment of the donor bone marrow cells. Hereafter, chimerization was confirmed by phenotyping TLR2 expression on peripheral blood samples with Cytomics FC500 (Beckman Coulter) analysis. Successful chimerization (>95% circulating donor cells) was achieved in all mice (data not shown). Irradiated WT mice with TLR2$^{-/-}$ bone marrow are referred as WT/TLR2$^{-/-}$BM, and TLR2$^{-/-}$ mice with WT bone marrow as TLR2$^{-/-}$/WT BM.

Infarct size

Infarct size (IS) was determined 24 hours after myocardial I/R, and expressed as a percentage of the Area-At-Risk (AAR). The ratio AAR/LV is a measure for the extent of myocardial tissue that underwent ischemia and reperfusion (i.e. endangered area). The ratio IS/AAR is an accurate measure to determine infarct size within endangered myocardium and is the primary endpoint from which the efficacy of treatment is assessed. To determine the AAR, the LCA was ligated once again (at the level marked by the suture left in place) and 4% Evans blue dye was injected via the thoracic aorta in a retrograde fashion. Hearts were rapidly explanted, rinsed in 0.9% saline and put in -20ºC freezer for 1 hour. Hereafter, hearts were mechanically sliced into five 1-mm cross sections. Heart sections were incubated in 1% triphenyltetrazolium chloride (Sigma-Aldrich) at 37ºC for 15 minutes before placing them in formaldehyde for another 15 minutes. Viable tissue stains red and infarcted tissue appears white. Heart sections were digitally photographed (Canon EOS 400D) under a microscope (Carl Zeiss®). IS, AAR and total LV area were measured using ImageJ software (version 1.34).

Magnetic resonance imaging

Twenty-four mice (n=8/group) underwent serial assessment of cardiac dimensions and function by high resolution magnetic resonance imaging (MRI, 9.4 T, Bruker, Rheinstetten, Germany) under isoflurane anesthesia before and 28 days after myocardial I/R injury. Long axis and short axis images with 1.0 mm interval between the slices were obtained and used to compute end-diastolic volume (EDV, largest volume) and end-systolic volume (ESV, smallest volume). The ejection fraction (EF) was calculated as 100*(EDV-ESV)/EDV. All MRI data are analyzed using Qmass digital imaging software (Medis, Leiden, The Netherlands).

NF-κB activation assay

THP1-Blue™-CD14 cells (Invivogen, San Diego, USA) were used for *in vitro* efficacy assessment of OPN-301. Detailed information on THP-1-Blue-CD14 cells is found in the online Data supplement at http://circ.ahajournals.org/cgi/content/full/CIRCULATIONAHA.109.880187/DC1. The THP1-Blue-CD14 cells were incubated for 30 minutes with OPN-301 or IgG isotype, followed by 18 hours incubation at 37°C with Pam-3-CSK4 (P3C; 100 ng/ml) or Lipopolysaccharide (LPS; 1 ng/ml). Quantification of NF-κB activity was done according to the manufacturers' protocol.

Murine TNFα production assay

Mouse macrophage J774 cells (1x10^6/ml) were used for *in vitro* efficacy assessment of OPN-301. Cells were co-incubated with Pam3Csk4 (100 ng/ml) in the presence of a dose range of OPN301 and IgG1 isotype control. Six hours post incubation at 37oC/5% CO_2, supernatants were removed and TNFα was assayed by ELISA (Duoset, RnD Systems, UK).

Immunohistochemistry

Upon termination, hearts were excised and snap frozen in liquid nitrogen. Frozen sections were stained for Ly-6G (for neutrophils; rat anti-mouse Ly-6G 1:200, Abcam, Cambridge, United Kingdom), MAC-3 (for macrophages; rat anti-mouse MAC-3 1:50, BD Pharmingen, Breda, the Netherlands) and CD3 (for T-lymphocytes; rabbit anti-human CD3 1:100, Dako, Heverlee, Belgium) by overnight incubation with the first antibody at 4°C for MAC-3 or by 1 hour incubation at RT for Ly-6G and CD3. Detailed information on secondary antibodies and incubation time is found in the online Data Supplement at http://circ.ahajournals.org/cgi/content/full/CIRCULATIONAHA.109.880187/DC1.

Quantification of scar area after 28 days infarction was performed using Picrosirius Red staining of 4% formalin fixated and paraffin embedded heart sections. Analysis was done with circularly polarized light and digital image microscopy. Total scar area was determined as the percentage positive staining of the left ventricular wall.

Protein and RNA isolation

Total RNA and protein were isolated from snap frozen infarcted heart sections using 1 ml TripureTM Isolation Reagent (Roche) according to the manufacturers' protocol.

Caspase 3/7 activity

The level of apoptosis after treatment was assessed using the Caspase-Glo® 3/7 assay kit (G8090; Promega, Madison, USA). One microliter protein sample was diluted 24 µl assay buffer, and the protocol is further followed according to the manufacturer's instructions.

Flow Cytometry

TLR2 and CD11b expression on circulating monocytes of EDTA anticoagulated blood was analyzed by flow cytometry (Cytomics FC500, Beckman Coulter). Whole blood was stained for TLR2 (fluorescein isothiocyanate (FITC); eBioscience, San Diego, USA), CD11b (FITC; Serotec, Oxford, UK) and F4/80 for monocytes (Alexa fluor 647; Serotec, Oxford, UK).

Peripheral blood composition was determined using fluorescent antibodies for monocytes (CD14-FITC; BioLegend, San Diego, USA), neutrophils (Ly6G-APC; RnD systems, Abingdon, UK) and lymphocytes (CD3-FITC; eBioscience, San Diego, USA).

Tumor necrosis factor (TNF)-α, interleukin (IL)1α, IL10 and granulocyte macrophage-colony stimulating factor (GM-CSF) levels in isolated protein samples were measured using the Th1/Th2 multiplex (Bender MedSystems, Vienna, Austria). The protein samples were diluted 1:1 in assay buffer, and the protocol is further followed according to the manufacturer's instructions.

Phosphorylated target protein for p38-mitogen activated protein kinase (MAPK; Thr^{180}/Tyr^{182}), c-Jun N-terminal kinase (c-JNK; Thr183/Tyr185) were measured using the Bio-Plex Multiplex Assay (Bio-Rad Laboratories) according to the instructions of the manufacturer, after 1:8 dilution in assay buffer.

Polymerase chain reaction

Gene expression levels of Monocyte Chemotactic Protein (MCP)-1, Inter Cellular Adhesion Molecule (ICAM-)1 and Vascular Cell Adhesion Molecule (VCAM-)1 were quantified using quantitative polymerase chain reaction (qPCR). Further information is found in the online Data Supplement at http://circ.ahajournals.org/cgi/content/full/CIRCULATIONAHA.109.880187/DC1.

Statistical analysis

Data are represented as Mean±SEM. One-way ANOVA with post-hoc 2-sided Dunnet-t test adjustment (saline was set as control) was used to compare infarct size between groups. Non-parametric t-test for TLR2 expression data analysis and one-way ANOVA post-hoc LSD test was used for comparison of cytokine and protein levels between the groups and one-way ANOVA post-hoc Dunnett's T3 test for mRNA data. All statistical analyses were performed using SPSS 15.1.1. and $p < 0.05$ was considered significant.

REFERENCES

1 Cannon CP, Gibson CM, Lambrew CT, Shoultz DA, Levy D, French WJ, Gore JM, Weaver WD, Rogers WJ, Tiefenbrunn AJ. Relationship of symptom-onset-to-balloon time and door-to-balloon time with mortality in patients undergoing angioplasty for acute myocardial infarction. JAMA 2000 June 14;283(22):2941-7.

2 Yellon DM, Hausenloy DJ. Myocardial reperfusion injury. N Engl J Med 2007 September 13;357(11):1121-35.

3 Arslan F, de Kleijn DP, Timmers L, Doevendans PA, Pasterkamp G. Bridging innate immunity and myocardial ischemia/reperfusion injury: the search for therapeutic targets. Curr Pharm Des 2008;14(12):1205-16.

4 Bolli R, Becker L, Gross G, Mentzer R, Jr., Balshaw D, Lathrop DA. Myocardial protection at a crossroads: the need for translation into clinical therapy. Circ Res 2004 July 23;95(2):125-34.

5 Sugden PH, Clerk A. "Stress-responsive" mitogen-activated protein kinases (c-Jun N-terminal kinases and p38 mitogen-activated protein kinases) in the myocardium. Circ Res 1998 August 24;83(4):345-52.

6 Frangogiannis NG. The immune system and cardiac repair. Pharmacol Res 2008 August;58(2):88-111.

7 Roberts R, DeMello V, Sobel BE. Deleterious effects of methylprednisolone in patients with myocardial infarction. Circulation 1976 March;53(3 Suppl):I204-I206.

8 Libby P, Maroko PR, Bloor CM, Sobel BE, Braunwald E. Reduction of experimental myocardial infarct size by corticosteroid administration. J Clin Invest 1973 March;52(3):599-607.

9 Spath JA, Jr., Lane DL, Lefer AM. Protective action of methylprednisolone on the myocardium during experimental myocardial ischemia in the cat. Circ Res 1974 July;35(1):44-51.

10 Matzinger P. The danger model: a renewed sense of self. Science 2002 April 12;296(5566):301-5.

11 Faure E, Equils O, Sieling PA, Thomas L, Zhang FX, Kirschning CJ, Polentarutti N, Muzio M, Arditi M. Bacterial lipopolysaccharide activates NF-kappaB through toll-like receptor 4 (TLR-4) in cultured human dermal endothelial cells. Differential expression of TLR-4 and TLR-2 in endothelial cells. J Biol Chem 2000 April 14;275(15):11058-63.

12 Frantz S, Kobzik L, Kim YD, Fukazawa R, Medzhitov R, Lee RT, Kelly RA. Toll4 (TLR4) expression in cardiac myocytes in normal and failing myocardium. J Clin Invest 1999 August;104(3):271-80.

13 Brikos C, O'Neill LA. Signalling of toll-like receptors. Handb Exp Pharmacol 2008;(183):21-50.

14 Sakata Y, Dong JW, Vallejo JG, Huang CH, Baker JS, Tracey KJ, Tacheuchi O, Akira S, Mann DL. Toll-like receptor 2 modulates left ventricular function following ischemia-reperfusion injury. Am J Physiol Heart Circ Physiol 2007 January;292(1):H503-H509.

15 Favre J, Musette P, Douin-Echinard V, Laude K, Henry JP, Arnal JF, Thuillez C, Richard V. Toll-like receptors 2-deficient mice are protected against postischemic coronary endothelial dysfunction. Arterioscler Thromb Vasc Biol 2007 May;27(5):1064-71.

16 Boyd JH, Mathur S, Wang Y, Bateman RM, Walley KR. Toll-like receptor stimulation in cardiomyoctes decreases contractility and initiates an NF-kappaB dependent inflammatory response. Cardiovasc Res 2006 December 1;72(3):384-93.

17 Shishido T, Nozaki N, Yamaguchi S, Shibata Y, Nitobe J, Miyamoto T, Takahashi H, Arimoto T, Maeda K, Yamakawa M, Takeuchi O, Akira S, Takeishi Y, Kubota I. Toll-like receptor-2 modulates ventricular remodeling after myocardial infarction. Circulation 2003 December 9;108(23):2905-10.

18 Timmers L, Sluijter JP, van Keulen JK, Hoefer IE, Nederhoff MG, Goumans MJ, Doevendans PA, van Echteld CJ, Joles JA, Quax PH, Piek JJ, Pasterkamp G, de Kleijn DP. Toll-like receptor 4 mediates maladaptive left ventricular remodeling and impairs cardiac function after myocardial infarction. Circ Res 2008 February 1;102(2):257-64.

19 Frangogiannis NG. The immune system and cardiac repair. Pharmacol Res 2008 August;58(2):88-111.

20 Jennings Rb, Sommers Hm, Smyth Ga, Flack Ha, Linn H. Myocardial Necrosis induced by temporary occlusion of a coronary artery in the dog. Arch Pathol 1960 July;70:68-78.

21 Piot C, Croisille P, Staat P, Thibault H, Rioufol G, Mewton N, Elbelghiti R, Cung TT, Bonnefoy E, Angoulvant D, Macia C, Raczka F, Sportouch C, Gahide G, Finet G, ndre-Fouet X, Revel D, Kirkorian G, Monassier JP, Derumeaux G, Ovize M. Effect of cyclosporine on reperfusion injury in acute myocardial infarction. N Engl J Med 2008 July 31;359(5):473-81.

22 Ross AM, Gibbons RJ, Stone GW, Kloner RA, Alexander RW. A randomized, double-blinded, placebo-controlled multicenter trial of adenosine as an adjunct to reperfusion in the treatment of acute myocardial infarction (AMISTAD-II). J Am Coll Cardiol 2005 June 7;45(11):1775-80.

23 Murphy E, Steenbergen C. Mechanisms underlying acute protection from cardiac ischemia-reperfusion injury. Physiol Rev 2008 April;88(2):581-609.

24 Chao W. Toll-like Receptor Signaling: A Critical Modulator of Cell Survival and Ischemic Injury in the Heart. Am J Physiol Heart Circ Physiol 2008 November 14.

25 Sakata Y, Dong JW, Vallejo JG, Huang CH, Baker JS, Tracey KJ, Tacheuchi O, Akira S, Mann DL. Toll-like receptor 2 modulates left ventricular function following ischemia-reperfusion injury. Am J Physiol Heart Circ Physiol 2007 January;292(1):H503-H509.

26 Feng Y, Zhao H, Xu X, Buys ES, Raher MJ, Bopassa JC, Thibault H, Scherrer-Crosbie M, Schmidt U, Chao W. Innate immune adaptor MyD88 mediates neutrophil recruitment and myocardial injury after ischemia-reperfusion in mice. Am J Physiol Heart Circ Physiol 2008 September;295(3):H1311-H1318.

27 Feng Y, Zhao H, Xu X, Buys ES, Raher MJ, Bopassa JC, Thibault H, Scherrer-Crosbie M, Schmidt U, Chao W. Innate immune adaptor MyD88 mediates neutrophil recruitment and myocardial injury after ischemia-reperfusion in mice. Am J Physiol Heart Circ Physiol 2008 September;295(3):H1311-H1318.

28 Sakata Y, Dong JW, Vallejo JG, Huang CH, Baker JS, Tracey KJ, Tacheuchi O, Akira S, Mann DL. Toll-like receptor 2 modulates left ventricular function following ischemia-reperfusion injury. Am J Physiol Heart Circ Physiol 2007 January;292(1):H503-H509.

29 Gao F, Yue TL, Shi DW, Christopher TA, Lopez BL, Ohlstein EH, Barone FC, Ma XL. p38 MAPK inhibition reduces myocardial reperfusion injury via inhibition of endothelial adhesion molecule expression and blockade of PMN accumulation. Cardiovasc Res 2002 February 1;53(2):414-22.

30 Klune JR, Billiar TR, Tsung A. HMGB1 preconditioning: therapeutic application for a danger signal? J Leukoc Biol 2008 March;83(3):558-63.

31 Bolli R, Becker L, Gross G, Mentzer R, Jr., Balshaw D, Lathrop DA. Myocardial protection at a crossroads: the need for translation into clinical therapy. Circ Res 2004 July 23;95(2):125-34.

CHAPTER 3

This chapter demonstrates that a humanized anti-TLR2 antibody reduces infarct size and improves systolic function in pigs. Moreover, the study provides evidence that TLR2 inhibition is effective in a large animal model that resembles the human anatomy and physiology.

Fatih Arslan, Jaco H. Houtgraaf, Brian Keogh, Kushan Kazemi, William J. McCormack, Luke A.J. O'Neill, Renate de Jong, Leo Timmers, Mirjam B. Smeets, Lars Akeroyd, Mary Reilly, Gerard Pasterkamp & Dominique P. de Kleijn

Treatment with OPN-305, a humanized anti-Toll-like receptor-2 antibody, reduces myocardial ischemia/reperfusion injury in pigs

Background

Toll-like receptor (TLR)-2 is an important mediator of innate immunity and ischemia/reperfusion-induced cardiac injury. We have previously shown that TLR2 inhibition reduces infarct size and improves cardiac function in mice. However, the therapeutic efficacy of a clinical grade humanized anti-TLR2 antibody, OPN-305, in a large animal model remained to be addressed.

Methods and Results

Pigs (n=10/group) underwent 75 minutes ischemia, followed by 24 hours reperfusion. Saline or OPN-305 (25, 12.5 or 6.25 mg/kg) was infused intravenously 15 minutes before reperfusion. Cardiac function and geometry were assessed by echocardiography. Infarct size was calculated as the percentage of the area-at-risk (IS/AAR). Flow cytometry analysis revealed specific binding of OPN-305 to porcine TLR2. *In vivo*, OPN-305 exhibited a half-life of 8±2 days. Intravenous administration of OPN-305 prior to reperfusion resulted in smaller infarct size (47% reduction, p=0.024) compared to saline treatment. Pigs treated with all three doses of OPN-305 showed a significant preservation of systolic performance, whereas saline treatment completely diminished the contractile capacity of the infarct area.

Conclusions

OPN-305 significantly reduced infarct size and preserves cardiac function in pigs after I/R injury. Hence, OPN-305 is a promising adjunctive therapeutic for patients with acute MI.

Under revision

Blood flow restoration through the culprit coronary artery is necessary to save endangered myocardium after acute myocardial infarction (MI). It is well established that early reperfusion limits infarct size (IS) and improves clinical outcome of patients suffering from acute MI.[1] Nevertheless, current reperfusion therapy remains suboptimal since complications after MI are an increasing burden to society. Furthermore, additional cell death occurs during the reperfusion phase caused by detrimental inflammatory responses.[2, 3] Innate immune responses are major contributors to cell death via deleterious pro-inflammatory cytokine release and cell-to-cell interactions between leukocytes and cardiomyocytes. Previous experiments clearly show a 'window of opportunity' for adjunctive therapeutic strategies targeting innate immune responses to increase myocardial viability and survival.[4] Unfortunately, most immune modulating interventions that have proven to be effective in experimental studies failed in the clinical setting.[5] Drug administration before the ischemic period and lack of large animal testing are key reasons for the failure of successful translation in the clinic. In order to achieve clinical relevance, experimental compounds need to be administered in the late ischemic period or during reperfusion, while large animals have greater physiological relevance to human compared to murine models of myocardial infarction.[6, 7]

Reperfusion triggers the activation of innate immunity and accelerates inflammation in the heart.[8] Blood flow restoration after ischemia results in infarct size increase, therefore hampering the true potential of reperfusion therapy.[2] Adjunctive therapies inhibiting innate immunity have shown to further limit infarct size after myocardial ischemia/reperfusion (I/R). However, a completely abolished inflammatory response is detrimental for repair responses, since inflammation is critical for proper wound healing.[9, 10] For example, corticosteroid administration reduces infarct size but results in aneurysm formation and rupture of the myocardium after infarction.[11, 12]

The discovery of Toll-like receptors (TLRs) have increased the therapeutic value of innate immune modulating interventions[13]. Originally known as pathogen recognition receptors that mediate innate immunity, TLRs have also been shown to recognize endogenous molecules released after tissue injury, also referred to as "danger signals".[14] These "danger signals" released after cell death are thought to engage with TLRs to induce innate immune signaling.[15-18] TLR and subsequent Nuclear Factor-kappa B (NF-κB) activation are key mediators of innate immunity in I/R injury. Innate immune activation after reperfusion results in a positive feedback loop characterized by an accelerated cytokine and chemokine release and subsequent leukocyte infiltration to the ischemic/reperfused myocardium. In turn, the enhanced inflammatory status in the heart depresses cardiomyocyte function and cell viability.[4, 19] In addition, excessive inflammation is detrimental for extracellular matrix (ECM) integrity and structure due to enhanced protease activity and pro-fibrotic changes in the remote myocardium.[20] Inhibition of TLR signaling has the potential to dampen inflammation, intervening at the level of immune activation by endogenous danger signals. Lack of TLR2 signaling has been shown to be protective against cardiomyocyte and endothelial cell dysfunction after I/R injury.[21-23] We have previously shown that OPN-301, a murine monoclonal anti-TLR2 antibody against human TLR2 that cross reacts with murine TLR2, reduces infarct size and improves cardiac function in mice.[24] OPN-301 significantly reduced inflammation and pro-apoptotic signaling in the heart. Prior to this study, it was unclear if TLR2 inhibition would be effective in a large animal model with physiological and anatomical relevance to humans. In the present study, we demonstrate in a clinically relevant model, that TLR2 inhibition prior to reperfusion reduces infarct size and improves systolic performance in pigs using a clinical grade humanized TLR2 antagonist, OPN-305.

RESULTS

Specificity and half-life determination of OPN-305

As shown in Figure 1, the humanized anti-TLR2 antibody OPN-305 binds specifically to porcine TLR2. Hereafter, we characterized the pharmacokinetics of OPN-305 by intravenous administration at 3 different doses (n=4/group) in pigs: 25, 12.5 and 6.25 mg/kg. An OPN-305 specific ELISA was developed at Opsona Therapeutics Ltd. in the presence of pooled pig plasma, in order to determine the half-life of OPN-305. As shown in Figure 1, there is a dose-dependent C_{max}, as expected, and that all three doses exhibit a half-life of 8±2 days.

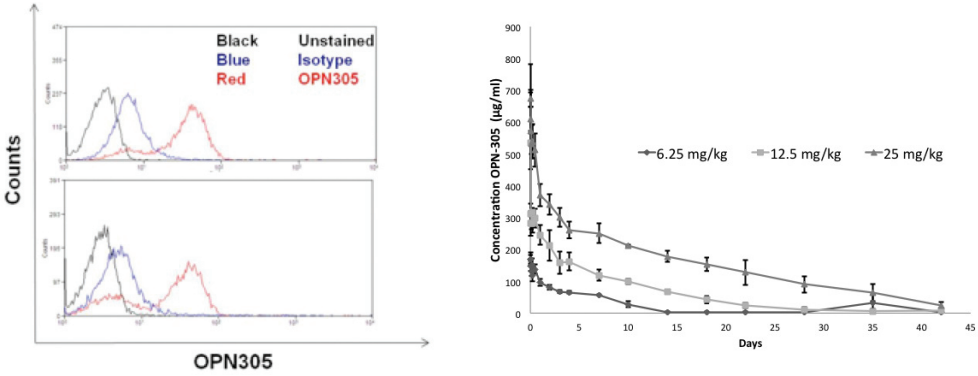

Figure 1. Binding and half-life of OPN-305. *OPN-305, detected by FACS, binds to porcine PBMCs (2 individual porcine samples). Plasma concentration of OPN-305 at 25, 12.5 and 6.25 mg/kg doses after single bolus administration. Each bar represents Mean±SEM, n=4/group for in vivo experiments.*

OPN-305 Treatment Prior To Reperfusion Reduces Infarct Size

Having established the pharmacokinetics and binding capacity of OPN-305 to porcine cells, we investigated the therapeutic efficacy of inhibiting TLR2-mediated myocardial I/R injury in pigs. Forty pigs underwent myocardial I/R injury (n=10/group). Two pigs (6.25 and 25 mg/kg treated) died after surgery due to post-infarct ventricular fibrillation. Seven animals met the exclusion criteria and were excluded from all analyses (4 pigs with <20% AAR; 3 pigs >95% infarction). Intravenous OPN-305 administration 15 minutes prior to reperfusion reduced infarct size in all treated groups (IS/AAR; Figure 2A). However, only 12.5 mg/kg reached statistical significance (47% reduction compared to saline treatment; p=0.024). The extent of endangered myocardium during ischemia (AAR/LV) did not differ between the groups (Figure 2B).

OPN-305 Improves Systolic Function After Myocardial I/R Injury

Transthoracal 2-dimensional echocardiographic analyses revealed no differences between the groups in cardiac function and geometry at baseline. One day after reperfusion, there was no difference in global ejection fraction (EF) between the groups (Figure 3A). However, fractional shortening (FS) was higher in OPN-305 treated animals (Figure 3B). In line with decreased infarct size and improved FS, local systolic function (systolic wall thickening (SWT)) of the infarct area was significantly enhanced in OPN-305 treated animals (Figure 3C). Whereas saline treatment resulted in complete loss of contraction of

the infarct area (as shown by a negative SWT index), OPN-305 treatment at all doses significantly preserved systolic performance. There was no difference in the amount of reperfusion-induced edema after 24 hours (wall thickness (WT); Figure 3D). The increased systolic performance in OPN-305 treated animals was also supported by a trend towards a decrease in end-systolic volume (ESV) in a dose dependent manner, whereas end-diastolic volume (EDV) did not differ between the groups 1 day after reperfusion (Figure 3E).

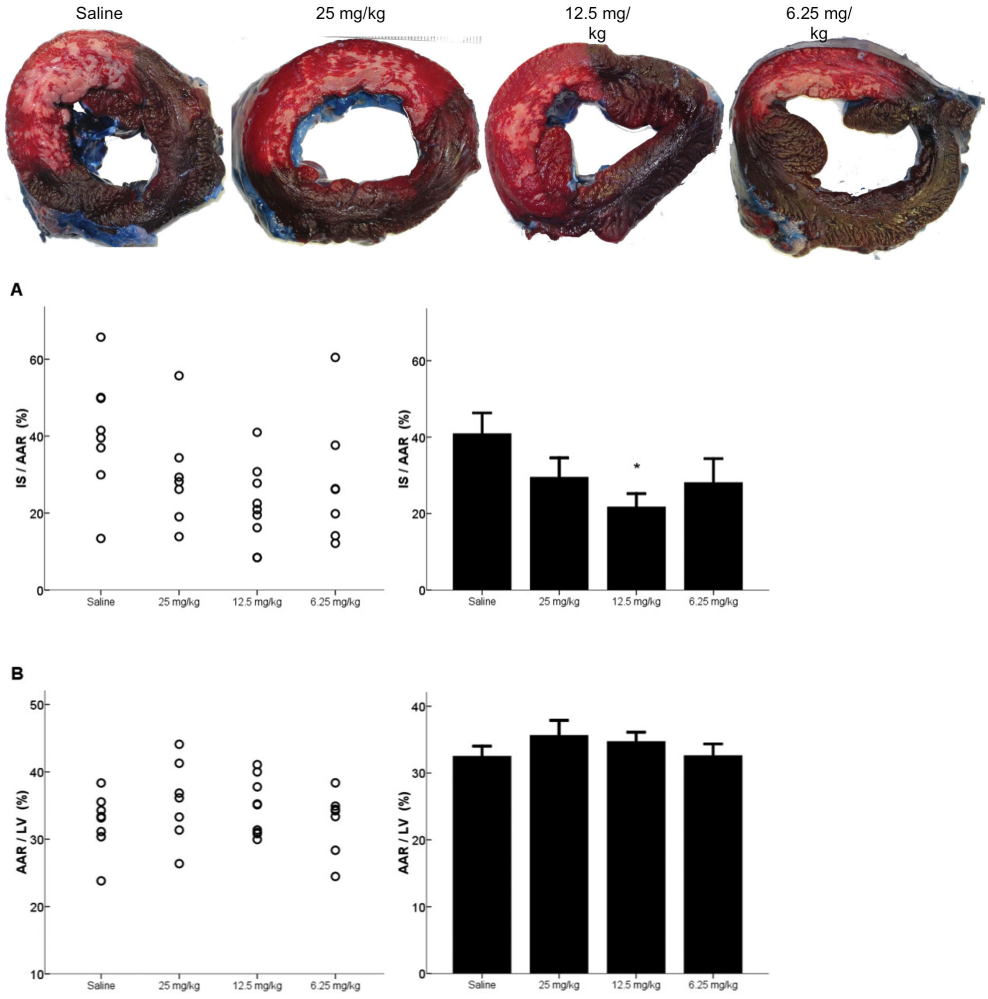

Figure 2. OPN-305 reduces infarct size. *(**A**) Infarct size as a percentage of the area at risk (IS/LV); *p=0.024 compared to saline treatment. (**B**) The extent of ischemic/reperfused myocardium as percentage of the left ventricle (AAR/LV). Each bar represents Mean±SEM, n=8 for saline, n=7 for 25 mg/kg, n=9 for 12.5 mg/kg and n=7 for 6.25 mg/kg treated groups. Representative TTC-stained cross-section of hearts are shown for each group.*

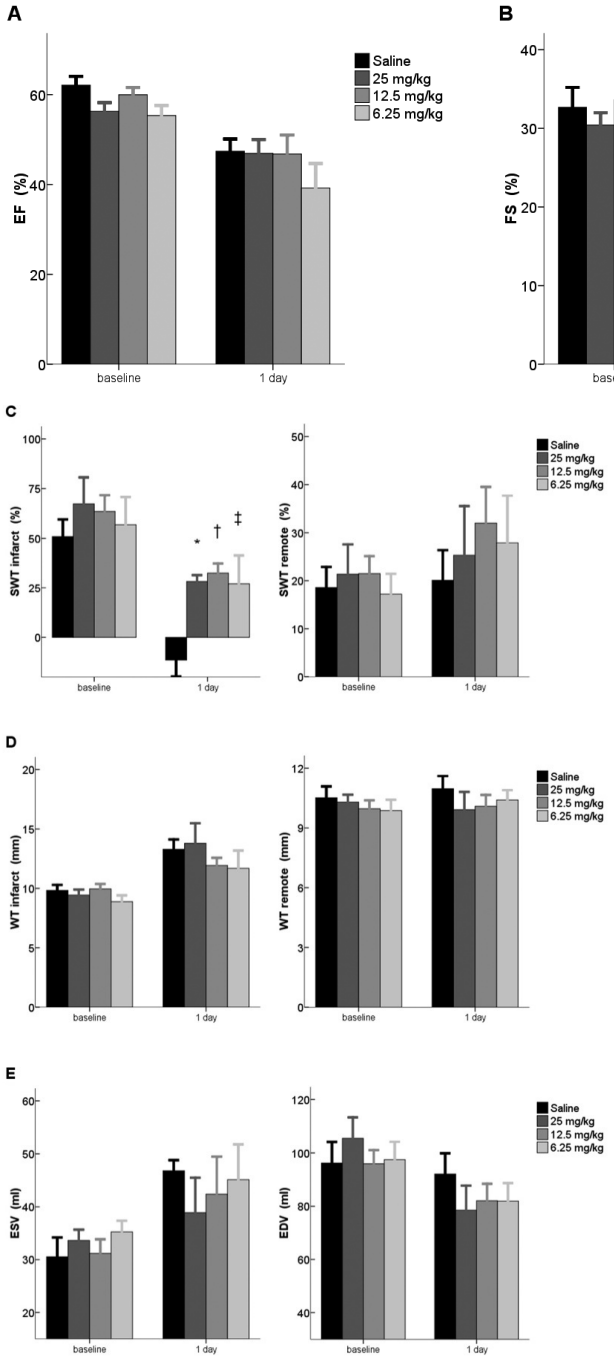

Figure 3. OPN-305 improves systolic performance after I/R injury. *Baseline and post-infarct (**A**) Global ejection fraction (EF). (**B**) Fractional shortening (FS); *p=0.011 compared to saline treatment. (**C**) Systolic wall thickening (SWT) of infarct and remote area; *p=0.031, †p=0.006 ‡p=0.019 compared to saline treatment. (**D**) Wall thickness (WT) of infarct and remote area. (**E**) End-systolic and end-diastolic volume (ESV and EDV, respectively). Each bar represents Mean±SEM.*

DISCUSSION

Current therapy for patients suffering from acute MI is early reperfusion of the ischemic myocardium. Recent technical (e.g. stents) and pharmacological (e.g. glycoprotein IIaIIIb inhibitors) advances have resulted in a significant decline of infarct-related deaths over the past decade. However, increased survival after acute MI also led to increased morbidity due to excessive tissue loss in the surviving patients. Fortunately, experimental and clinical studies have clearly demonstrated that adjunctive therapeutics to reperfusion offer the potential to further enhance myocardial viability after infarction. One of the potential therapeutic options is to reduce detrimental activation of innate immunity after myocardial I/R injury. TLRs have shown to be a critical mediator of innate immunity as a first-line defense against pathogens as well as ischemia-induced cardiac injury.[4, 13, 19] Injury-related endogenous activators, referred to as "danger signals", released after cell death are thought to activate TLRs and initiate deleterious inflammatory responses.[15-18] There is a great amount of evidence that shows the pivotal role of TLR2 in I/R injury of various organs.[8] Previous studies have clearly demonstrated that TLR2 mediates I/R injury of the myocardium and endothelial cells.[22, 23] Recently, we have shown that myocardial I/R injury is mediated by expression of TLR2 on circulating cells. More importantly, OPN-301 (a mouse anti-TLR2 antibody) administration just prior to reperfusion reduced infarct size and improved cardiac function in mice.[24] These data provided a rationale to assess the therapeutic efficacy of a humanized anti-TLR2 antibody, OPN-305. In the present study, we determined the therapeutic potential of TLR2 inhibition using a porcine myocardial I/R model that is more physiologically relevant to the human situation compared to mice.

First, we confirmed that OPN-305 binds specifically to porcine TLR2. *In vivo*, OPN-305 exhibited a half-life of 8-9 days. The relatively short half-life reduces long-term inhibition of TLR2, thereby decreasing the risk for a potential unfavorable effect of chronic TLR2 inhibition.

Secondly, we assessed the therapeutic efficacy of OPN-305 using a porcine myocardial I/R injury model. In line with our previous studies,[24] we observed a significant reduction in infarct size of approximately 45% in 12.5 mg/kg OPN-305 treated animals compared to saline treated pigs. Although the highest and lowest dose of OPN-305 also reduced infarct size, it did not reach statistical significance. There is 1 pig in both groups with a relative large infarct size that impairs the statistical power in the 25 and 6.25 mg/kg groups. We also did not observe a dose response in our study. One possible explanation may be that all three doses were already above the least required dose to achieve a therapeutic effect. In our previous mouse study, we observed that 5 mg/kg resulted in a non-significant infarct size reduction.[24] Based on *in vitro* data, the IC50 in blood assays is approximately 1-2 μg/ml. A rough estimate of the blood volume in a 70 kg pig is 5 liters, giving an approximate liquid fraction of 2.5 liters. At a dose of 6.25mg/kg, the total amount of antibody administered is 437.5mg. Based on estimated blood volume and amount administered, the highest theoretical blood concentration of OPN-305 is 175μg/ml. This is already several fold higher than the required concentration to achieve IC50. As such, any dose above 6.25mg/kg should be as efficacious. The dose of 25mg/kg in the current study was chosen based on an *in vivo* pilot study (data not shown), and lower doses were chosen on a serial dilution basis.

We excluded 7 animals for 2 reasons: too small area at risk (AAR) and failure to reperfuse the ischemic myocardium. AAR is one of the most important determinants of final infarct size: the greater the AAR, the larger the infarct within the left ventricle. The size of the AAR is determined by the extent of

myocardium perfused by a) the culprit coronary artery and b) collateral flow. In our study, ischemia was induced by ligating the proximal LCx coronary artery. Previous experiments showed that coronary ligation at this site results in approximately 33% of endangered myocardium within the left ventricle.[25] The relatively small AAR in 4 pigs is probably due to anatomical variation seen in outbreed animals.[7] Despite the coronary occlusion at the very proximal level, collateral flow may have caused for sufficient perfusion behind the ligation. This notion is supported by the fact that 3 excluded pigs had no infarction at all, despite 75 minutes of coronary occlusion. The 4th pig showed 100% infarction within the small AAR (6%), which resembles a non-perfused ischemia model. For this reason, we excluded 3 pigs with >95% infarction. In addition to AAR, the ischemic duration is another important determinant of final infarct size. We used 75 minutes ischemia followed by 24 hours reperfusion, since damage to the myocardium using this model does not result in transmural infarctions. Infarctions caused by 75 minutes ischemia and reperfusion are characterized by patchy, endocardial and midmyocardial infarctions. The fact that almost the entire AAR was infarcted in 3 pigs suggests that reperfusion did not occur after releasing the coronary ligation. It is very likely that this is caused by thrombus formation, despite an intensive anti-coagulant regime. Pigs are known for their hypercoagulability.[26] For this reason we used acetylisalicylic acid, clopidogrel (both loaded prior to surgery) and heparin prior to ischemia to target 3 different pathways involved in coagulation: Tromboxane-A_2 and ADP-receptor mediated platelet aggregation, and Thrombin/FXa mediated coagulation, respectively. Nevertheless, the individual coagulability in these 3 outbreed pigs may have varied and thus may have caused thrombus formation despite 3 different anti-coagulants.

Finally, OPN-305 significantly improved systolic performance within the infarct area. The systolic wall thickening (the percentage increase of myocardial thickening during contraction) within the infarct region was significantly higher in OPN-305 treated pigs compared to saline treatment. Moreover, saline treatment resulted in a complete loss of contractile performance (bulging; as shown by a negative SWT index), whereas all OPN-305 treated animals still showed some residual contractility within the infarct area. These findings are in line with the higher myocardial viability seen in OPN-305 treated animals as shown by the TTC staining. Although not statistically significant, these results were supported by a trend towards smaller ESVs. Smaller ESVs suggests that OPN-305 treated animals were able to pump more blood out of the left ventricle. In addition, FS (measured by the percentage change in left ventricular diameter perpendicular to the infarct and remote region) was also significantly improved in OPN-305 treated animals. The fact that saline treatment resulted in similar global EF is likely attributable to compensatory actions of adjacent non-ischemic regions in these animals. In the current study, only the center of the AAR and the remote myocardium (septal wall) were used to assess local function.

In conclusion, administration of OPN-305 15 minutes prior to reperfusion results in a significant reduction of infarct size and improves systolic performance in a porcine I/R model. The efficacy in this large animal model indicates that it has great clinical potential. Our study provides a solid rationale to assess the therapeutic efficacy of OPN-305 in patients suffering from acute MI.

Acknowledgements

We would like to thank the following persons for their biotechnical assistance: Cees Verlaan, Marlijn Jansen, Joyce Visser, Maringa Emons, Merel Schurink, Hester de Bruin and Evelyn Velema.

Funding Sources

This work is supported by research grants from the Netherlands Organisation for Scientific Research (NWO) & Utrecht University Mozaïek grant (contract 017.004.004 to F.A.) and Netherlands Heart Foundation (contract 2010.T001 to F.A.).

Disclosures

Professor O'Neill is co-founder and shareholder of Opsona Therapeutics Ltd. Dr. Keogh, Mary Reilly and William J. McCormack are employees of Opsona Therapeutics Ltd. The other authors report no conflict of interests.

METHODS

Animals and Experimental Design

Forty (n=10/group) female Topigs 20 (van Beek SPF pig farm B.V., Lelystad, the Netherlands; 65-70 kg of weight; 4-5 months of age) underwent 75 minutes of ischemia followed by 24 hours of reperfusion.

Experimental compounds were intravenously administered 15 minutes prior to reperfusion (infusion rate 200 ml/hour). Pigs were given 50 ml of stock with either saline, 25, 12.5 or 6.25 mg/kg. Where possible, recommendations from the National Heart, Lung and Blood Institute (NHLBI) Working Group on the Translation of Therapies for Protecting the Heart from Ischemia were applied.[5] Analysis of infarct size and functional data was done by researchers blinded for the treatment. All animal experiments were performed in accordance with the national guidelines on animal care and with prior approval by the Animal Experimentation Committee of Utrecht University.

Administration of OPN-305 to Determine Half-Life

OPN-305 was administered intravenously to a separate group of 12 pigs (4/group) at the following doses: 6.25mg/kg, 12.5mg/kg and 25mg/kg. The pigs were bled via an indwelling central venous catheter at the following time points; pre-administration and at 5, 30 min., 1, 2, 4, 6, 12, 24 hours, 2, 3, 4, 7, 10, 14, 18, 22, 28, 35 and 42 days after OPN-305 injection. Plasma was derived from the samples, aliquoted and frozen at -20˚C. Determination of OPN305 in plasma was achieved using a quantitative ELISA based approach.

Premedication & Anesthesia

All animals were pretreated with amiodarone (400 mg/day; start 10 days prior to surgery), clopidogrel (75 mg/day; start 3 days prior to surgery) and acetylsalicylic acid (80 mg/day; start 10 days prior to surgery). To treat post-surgical pain, pigs were given fentanil patches (25 µg/hr; Durogesic® Janssen-Cilag, the Netherlands) 1 day before surgery. Pigs were sedated with intramuscular injection with ketamin (10 mg/kg), midazolam (0.5 mg/kg) and atropine (0.04 mg/kg). Hereafter, sodium thiopental (5 mg/kg) was given intravenously, prior to intubation. Intravenous administration of amoxicillin/clavulanic acid (1000/100 mg) was given before surgery.

Prior to ventilation (tidal volume 10 ml/kg; respiration rate 12/minute; oxygen/air mixture), a bolus injection of midazolam (0.5 mg/kg) and sufentanil citrate (6 µg/kg) was given intravenously. Metoprolol (5 mg) was administered before and after infarction. Amiodarone (300 mg) was given intravenously prior

to incision. Pigs were kept under anesthesia during the surgical procedure using intravenous infusions of midazolam (1 mg/kg/hr), sufentanil citrate (6 µg/kg/hr) and pancronium bromide (0.1 mg/kg/hr).

Surgical Procedures

For the pharmacokinetic studies, percutaneous tunneled sterile silicone central venous catheters (right external jugular vein) were inserted and flushed daily with 250 IE heparin diluted in 5 ml saline. The tip of the catheter was placed 10 cm through the external jugular vein in the *vena cava superior*, while the syringe fitting end was placed dorsally in the neck for easy conscious blood drawing.

For the induction of infarctions, pigs were anesthetized and electrocardiogram, arterial blood pressure and capnogram were continuously monitored. Core body temperature was kept constant at 37°C. A midsternotomy was performed to open the mediastinal cavity. The pericardium was opened and a 2-0 prolene suture was placed beneath the proximal left circumflex (LCx) coronary artery. Heparin (15.000 IE) was given to prevent thrombus formation in the LCx during and after ischemia. Ischemia was induced by ligating the LCx between the suture and a polyethylene tube. Ischemia was confirmed by electrocardiogram. Reperfusion was initiated by releasing the ligature and removing the polyethylene tubing. A piece of the loosened suture was left in place to determine the ischemic area upon termination. Thoracic drains were placed to remove excessive fluid and air from the thoracic cavity and the sternum was closed. Weaning from mechanical ventilation and subsequent extubation occured after unassisted breathing for several times.

Echocardiography

End-diastolic and -systolic volume (EDV, ESV), ejection fraction (EF), wall thickness (WT), systolic wall thickening (SWT) and fractional shortening (FS) were determined using short- and long-axis transthoracic ultrasound image acquisition. Echocardiography was performed at baseline and 24 hours after reperfusion. Short- and long-axis images were obtained for EF calculation. WT, SWT and FS were calculated at basal level on short-axis images. EF = 100*(EDV - ESV)/EDV; SWT = 100*(wall thickness ED - wall thickness ES)/wall thickness ED; FS = 100*(ED diameter - ES diameter)/ED diameter.

Infarct Size

Infarct Size (IS) is expressed as a percentage of the Area-At-Risk (AAR). The ratio AAR/LV is a measure for the extent of myocardial tissue that underwent ischemia and reperfusion (i.e. endangered area). The ratio IS/AAR is an accurate measure to determine infarct size within the endangered myocardium and is the primary endpoint from which the efficacy of treatment is addressed.

To determine the AAR, the LCx was ligated again (at the level marked by the suture left in place) and 50 ml 4% Evans' blue dye was injected via the apex in the left ventricular cavity. Hearts were rapidly explanted, rinsed in 0.9% saline and mechanically sliced into 4-5 cross-sections. Heart sections were weighed and incubated in 1% triphenyltetrazolium chloride (Sigma-Aldrich) at 37ºC for 10 minutes. Viable tissue stains red and infarcted tissue appears white. Heart sections were digitally photographed (Canon EOS 400D) under a microscope (Carl Zeiss®). IS, AAR and total LV area were measured using ImageJ software (version 1.43) and corrected for the weight of the corresponding slice.

Exclusion Criteria

Operated pigs were excluded for all analysis based on a small AAR (AAR/LV<20%) and failure to reperfuse the ischemic myocardium (IS/AAR>95%).

FACS Staining of Cells

Porcine PBMCs were purified using Polymorphprep (Axis-Shield) as per manufacturer's instructions. Cells were washed and resuspended in 1% BSA in PBS. Cells were counted and $1x10^6$ cells were used per tube. OPN-305 was used to stain porcine cells and a polyclonal preparation of human IgG4 (Sigma) was used as the isotype control staining as there was no monoclonal IgG4 isotype available. Binding was detected with PE conjugated anti-human IgG4 (Southern Biotech). All incubations were carried out on ice for 25 minutes with 3x washing in 1% BSA between each antibody step. Cells were fixed with 1% paraformaldehyde and acquired using a Dako Cyan prior to analysis using Summit version 4.3.

OPN-305 ELISA

In brief, the ELISA format uses His-tagged TLR2 (50ng/ml) bound to nickel coated plates. After blocking with 1% BSA/0.05% Tween 20 in PBS, a standard curve of OPN-305 and quality control samples were added to the plate. Bound OPN-305 was detected using biotinylated anti-human IgG4 (1/5000) followed by conjugation of streptavidin HRP (1/5000). The signal was visualized using TMB and the reaction was stopped using sulphuric acid.

For each assay run to pass, it must reach the following criteria: (I) At least 75% of the calibration points to be within ±20% of the nominal concentration (%RE of the back-calculated values). Duplicate measurements of individual calibration points to have a CV of ≤20%. (II) Mean intra-batch precision of within ≤20% CV for the validation QC samples. (III) Mean intra-batch accuracy for validation QC samples to be within ±20% of the nominal concentration (%RE of the back-calculated values). (IV)At least 67% of the QC samples should be within 20% of their respective nominal (theoretical) values: 33% of the QC samples can be outside the +/- 20% nominal value. (V) During the PK analysis, samples were diluted to ensure that they fall in the range of the curve. In the instance, for example, where a sample when diluted 1/100 and 1/1000 falls on the standard curve, the reading that has the a) lowest %CV and b) is falling on the linear part of the curve (not at the very top or very bottom of the curve) was taken as the concentration of the sample.

Statistical Analysis

All data are expressed as Mean ± SEM. To correct for multiple comparisons, One-way ANOVA with post-hoc Dunnett t-test (saline treatment was set as control) was used to compare infarct size between groups. All statistical analyses were performed using SPSS 15.1.1. for Windows and $p < 0.05$ was considered significant.

REFERENCES

1 Cannon CP, Gibson CM, Lambrew CT, Shoultz DA, Levy D, French WJ, Gore JM, Weaver WD, Rogers WJ, Tiefenbrunn AJ. Relationship of symptom-onset-to-balloon time and door-to-balloon time with mortality in patients undergoing angioplasty for acute myocardial infarction. JAMA. 2000;283:2941-2947.

2 Braunwald E, Kloner RA. Myocardial reperfusion: a double-edged sword? J Clin Invest. 1985;76:1713-1719.

3 Fliss H, Gattinger D. Apoptosis in ischemic and reperfused rat myocardium. Circ Res. 1996;79:949-956.

4 Arslan F, de Kleijn DP, Timmers L, Doevendans PA, Pasterkamp G. Bridging innate immunity and myocardial ischemia/reperfusion injury: the search for therapeutic targets. Curr Pharm Des. 2008;14:1205-1216.

5 Bolli R, Becker L, Gross G, Mentzer R, Jr., Balshaw D, Lathrop DA. Myocardial protection at a crossroads: the need for translation into clinical therapy. Circ Res. 2004;95:125-134.

6 Weaver ME, Pantely GA, Bristow JD, Ladley HD. A quantitative study of the anatomy and distribution of coronary arteries in swine in comparison with other animals and man. Cardiovasc Res. 1986;20:907-917.

7 Klocke R, Tian W, Kuhlmann MT, Nikol S. Surgical animal models of heart failure related to coronary heart disease. Cardiovasc Res. 2007;74:29-38.

8 Arslan F, Keogh B, McGuirk P, Parker AE. TLR2 and TLR4 in ischemia reperfusion injury. Mediators Inflamm. 2010;2010:704202.

9 Kloner RA, Fishbein MC, Lew H, Maroko PR, Braunwald E. Mummification of the infarcted myocardium by high dose corticosteroids. Circulation. 1978;57:56-63.

10 Jugdutt BI, Joljart MJ, Khan MI. Rate of collagen deposition during healing and ventricular remodeling after myocardial infarction in rat and dog models. Circulation. 1996;94:94-101.

11 Libby P, Maroko PR, Bloor CM, Sobel BE, Braunwald E. Reduction of experimental myocardial infarct size by corticosteroid administration. J Clin Invest. 1973;52:599-607.

12 Roberts R, DeMello V, Sobel BE. Deleterious effects of methylprednisolone in patients with myocardial infarction. Circulation. 1976;53:I204-I206.

13 Hennessy EJ, Parker AE, O'Neill LA. Targeting Toll-like receptors: emerging therapeutics? Nat Rev Drug Discov. 2010;9:293-307.

14 Ionita MG, Arslan F, de Kleijn DP, Pasterkamp G. Endogenous inflammatory molecules engage Toll-like receptors in cardiovascular disease. J Innate Immun. 2010;2:307-315.

15 Matzinger P. The danger model: a renewed sense of self. Science. 2002;296:301-305.

16 Seong SY, Matzinger P. Hydrophobicity: an ancient damage-associated molecular pattern that initiates innate immune responses. Nat Rev Immunol. 2004;4:469-478.

17 Arslan F, de Kleijn DP, Pasterkamp G. Innate immune signaling in cardiac ischemia. Nat Rev Cardiol. 2011.

18 Arslan F, Smeets MB, Riem Vis PW, Karper JC, Quax PH, Bongartz LG, Peters JH, Hoefer IE, Doevendans PA, Pasterkamp G, de Kleijn DP. Lack of Fibronectin-EDA Promotes Survival and Prevents Adverse Remodeling and Heart Function Deterioration After Myocardial Infarction. Circ Res. 2011;108:582-592.

19 Chao W. Toll-like receptor signaling: a critical modulator of cell survival and ischemic injury in the heart. Am J Physiol Heart Circ Physiol. 2009;296:H1-12.

20 Frangogiannis NG. The immune system and cardiac repair. Pharmacol Res. 2008;58:88-111.

21 Boyd JH, Mathur S, Wang Y, Bateman RM, Walley KR. Toll-like receptor stimulation in cardiomyoctes decreases contractility and initiates an NF-kappaB dependent inflammatory response. Cardiovasc Res. 2006;72:384-393.

22 Sakata Y, Dong JW, Vallejo JG, Huang CH, Baker JS, Tracey KJ, Tacheuchi O, Akira S, Mann DL. Toll-like receptor 2 modulates left ventricular function following ischemia-reperfusion injury. Am J Physiol Heart Circ Physiol. 2007;292:H503-H509.

23 Favre J, Musette P, Douin-Echinard V, Laude K, Henry JP, Arnal JF, Thuillez C, Richard V. Toll-like receptors 2-deficient mice are protected against postischemic coronary endothelial dysfunction. Arterioscler Thromb Vasc Biol. 2007;27:1064-1071.

24 Arslan F, Smeets MB, O'Neill LA, Keogh B, McGuirk P, Timmers L, Tersteeg C, Hoefer IE, Doevendans PA, Pasterkamp G, de Kleijn DP. Myocardial ischemia/reperfusion injury is mediated by leukocytic toll-like receptor-2 and reduced by systemic administration of a novel anti-toll-like receptor-2 antibody. Circulation. 2010;121:80-90.

25 Timmers L, Lim SK, Arslan F, Armstrong JS, Hoefer IE, Doevendans PA, Piek JJ, El Oakley RM, Choo A, Lee CN, Pasterkamp G, de Kleijn DP. Reduction of myocardial infarct size by human mesenchymal stem cell conditioned medium. Stem Cell Res. 2007;1:129-137.

26 Roussi J, Andre P, Samama M, Pignaud G, Bonneau M, Laporte A, Drouet L. Platelet functions and haemostasis parameters in pigs: absence of side effects of a procedure of general anaesthesia. Thromb Res. 1996;81:297-305.

CHAPTER 4

In this chapter we purified a homogenous population of microparticles, referred to as exosomes, which mediated the cardioprotective actions of mesenchymal stem cell secretion

Fatih Arslan*, Ruenn Chai Lai*, May May Lee, Newman Siu Kwan Sze, Andre Choo, Tian Sheng Chen, Manuel Salto-Tellez, Leo Timmers, Chuen Neng Lee, Reida Menshawe El Oakley, Gerard Pasterkamp, Dominique P. de Kleijn, Sai Kiang Lim

* Co-first authors

Exosome secreted by MSC reduces myocardial ischemia/reperfusion injury

Background

Human ESC-derived mesenchymal stem cell (MSC)-conditioned medium (CM) was previously shown to mediate cardioprotection during myocardial ischemia/reperfusion injury through large complexes of 50-100 ηm.

Methods and Results

Here we show that these MSCs secreted 50- to 100-ηm particles. These particles could be visualized by electron microscopy and were shown to be phospholipid vesicles consisting of cholesterol, sphingomyelin, and phosphatidylcholine. They contained coimmunoprecipitating exosome-associated proteins, e.g., CD81, CD9, and Alix. These particles were purified as a homogeneous population of particles with a hydrodynamic radius of 55-65 nm by size-exclusion fractionation on a HPLC. Together these observations indicated that these particles are exosomes. These purified exosomes reduced infarct size in a mouse model of myocardial ischemia/reperfusion injury.

Conclusions

MSC mediated its cardioprotective paracrine effect by secreting exosomes. This novel role of exosomes highlights a new perspective into intercellular mediation of tissue injury and repair, and engenders novel approaches to the development of biologics for tissue repair.

Stem Cell Res. 2010;4(3):214-22

Mesenchymal stem cells (MSCs) derived from adult bone marrow have emerged as one of the most promising stem cell types for treating cardiovascular disease.[1] Although the therapeutic effect of MSCs has been attributed to their differentiation into reparative or replacement cell types (e.g., cardiomyocytes, endothelial cells, and vascular smooth cells)[2, 3], it remains to be established if the number of differentiated cell types generated is therapeutically relevant. Recent reports have suggested that some of these reparative effects are mediated by paracrine factors secreted by MSCs.[4-7] In support of this paracrine hypothesis, many studies have observed that MSCs secrete cytokines, chemokines, and growth factors that could potentially repair injured cardiac tissue mainly through cardiac and vascular tissue growth and regeneration.[8, 9] This paracrine hypothesis could potentially provide for a non-cell-based alternative for using MSCs in treatment of cardiovascular disease.[1] Non-cell-based therapies as opposed to cell-based therapies are generally easier to manufacture and are safer as they are nonviable.

We have previously performed an unbiased proteomic analysis of a chemically defined medium conditioned by highly expandable human ESC-derived MSC cultures.[10, 11] We identified > 200 proteins in the secretion of these MSCs. Computational analysis of the secretome predicted that collectively, the secretome has the potential to repair injured tissue such as in myocardial ischemia/reperfusion (MI/R) injury. MI/R injury refers to cell death and functional deterioration that occurs during reperfusion therapy to restore blood flow and salvage cardiomyocytes at risk of dying from ischemia in an acute MI (AMI).[12, 13] Therefore, the effectiveness of reperfusion therapy can be greatly enhanced by preventing reperfusion injury for which there is currently no treatment.[14] We tested the computational prediction of tissue salvage during reperfusion injury in a pig and mouse models of MI/R injury. An intravenous bolus administration of MSC-CM just before reperfusion substantially reduced infarct size in both pig and mouse models of MI/R injury by ~ 60 and ~ 50%, respectively.[15] There was also a significant preservation of cardiac function and reduction of oxidative stress as early as 4 h after reperfusion. However, the active component in the secretion and the mechanism by which it mediates this fast-acting effect on MI/R injury have not been elucidated.

It is obvious that the immediacy of this protective effect precludes the relatively lengthy process of gene transcription and tissue regeneration as part of the mechanism. Also, many of the secreted proteins are membrane and intracellular proteins, and are not known to cross plasma membranes readily. This suggests that if these proteins mediate the cardioprotective effect, the mechanism underlying the therapeutic effect of MSC secretion must involve a vehicle that facilitates crossing of membranes, thus representing a radical shift from our present understanding of MSC paracrine secretion which is limited to extracellular signaling by cytokines, chemokines, and growth factors. To better understand the cardioprotective paracrine effects of MSCs, we then systematically fractionated the MSC-CM using membranes with different molecular weight cut off (MWCO). Based on these fractionations, we demonstrated that the cardioprotective activity was in a > 1000-kDa MW fraction.[15] This suggested that the cardioprotective effect was mediated by large complexes with a diameter of 50-100 nm.

Here we demonstrate that these large complexes are exosomes. By improving our proteomic analysis, we extended our previously reported list of 201 secreted proteins to 739 proteins and observed the presence of many exosome-associated proteins. Some of these proteins were in detergent-sensitive complexes. These proteins can be sedimented by ultracentrifugation together with the membrane phospholipids. Size-exclusion fractionation by HPLC and dynamic light scattering analysis revealed the presence of a population of particles with a hydrodynamic radius (Rh) of 55-65 nm. More importantly, this HPLC fraction reduced infarct size in a mouse model of MI/R injury.

RESULTS

Cardioprotective secretion contains exosome-associated proteins that form multiprotein complexes

To identify the active component, we had previously fractionated the CM by ultrafiltration through membranes with different MWCO. It was shown that CM filtered through a membrane with MWCO of 1000 kDa was not protective in a mouse model of MI/R injury.[15] However, CM concentrated by 125 times against a similar membrane was protective. We observed that after filtration through filters with a MWCO smaller than 0.2 mm such as 100, 300, 500, or 1000 kDa, the filtered CM was not cardioprotective (Figure 1A). In contrast, CM concentrated against a 1000-kDa membrane or a 100-kDa membrane to retain particles > 1000 or 100 kDa, respectively, was cardioprotective (Figure 1). These observations suggested that the active fraction consisted of large complexes of > 1000 kDa or had a predicted diameter of 50-100 nm. Consistent with this, visualization of the CM by electron microscopy revealed the presence of spherical structures with a diameter of 50-100 nm and the morphology of a lipid vesicle (Figure 1B). Based on this size range and morphology, we postulated that the likely candidate was a secreted phospholipid vesicle known as exosome.[16, 17]

To test this, we first determined if the CM contained the subset of proteins that are commonly found in exosomes such as CD9, CD81, and Alix.[18] These proteins were not present in our previous proteomic profiling of the secretion.[11] By making modifications to our proteomics methodology, we extended our list of proteins found in the MSC secretion from 201 to 739 proteins (Online Supplementary Table 1).

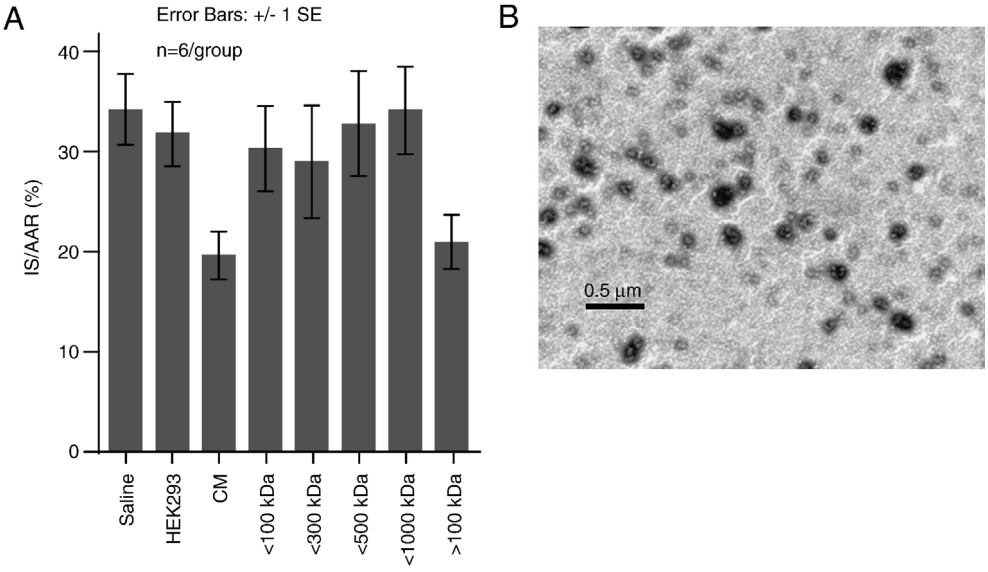

Figure 1. Cardioprotective properties of CM fractions. *(**A**) Saline, HEK293 CM, or different preparations of hESC-MSC CM were administered to a mouse model of MI/R injury as described under Materials and methods. The < 1000, < 500, < 300, and < 100 kDa represented CM filtered sequentially with membranes that had MWCO of 1000, 500, 300, and 100 kDa, respectively. The > 100 kDa represented CM concentrated 50 times against a TFF membrane with MWCO of 100 kDa. The infarct size (IS) was expressed as a fraction of the area at risk (AAR) in the left ventricle. (**B**) Transmission electron microscopic picture of CM; scale bar represents 500 nm.*

The computationally predicted biological activities of this proteome suggested that the secretion will have significant biological effects on cardiac tissue injury and repair (Figure S1). The subsets of exosome-associated proteins CD9, CD81, and Alix were confirmed to be present in the secretion by Western blot analysis (lane 1, Figure 2A). The MW of CD9 and CD81 was the expected 25 and 22-26 kDa, respectively. Consistent with our hypothesis that the large complexes are exosomes, we observed that CD9 and Alix coimmunoprecipitated with CD81, suggesting that these proteins were in a single complex (Figure 2A).

A 24-kDa CD9 sediments at 200 000 g and is retained by membrane with 500-kDa MWCO

As exosomes are routinely purified by ultracentrifugation[19], we next determined if CD9 was associated with a large complex that can be precipitated by ultracentrifugation. The CM was first fractionated

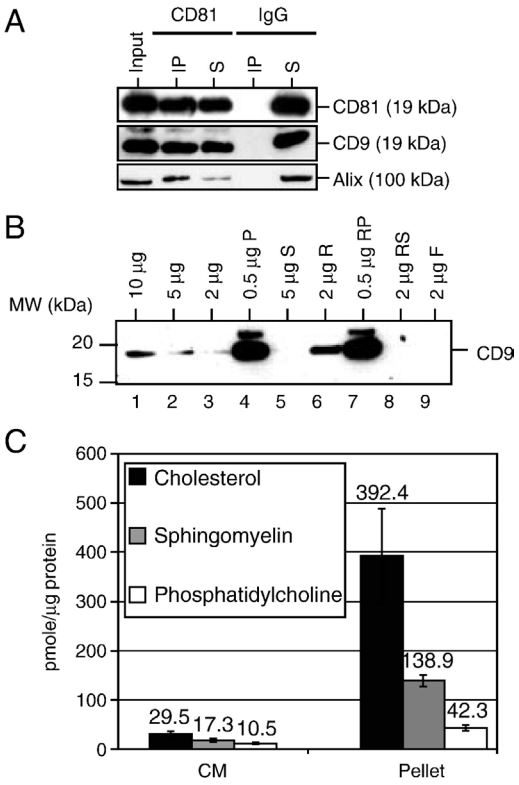

Figure 2. Presence of large lipid complexes in CM. *(**A**) Coimmunoprecipitation of CD81, CD9, and Alix. After immunoprecipitation of hESC-MSC CM with anti-CD81 or mouse IgG, the immunoprecipitate (IP) and supernatant (S) were analyzed by Western blot hybridization using antibody against CD9 and Alix. (**B**) Size fractionation by ultrafiltration and ultracentrifugation. CM was concentrated 5X using a membrane with MWCO of 500 kDa. The retentate and the unfiltered CM were then ultracentrifuged at 200 000 g for 2 h. The supernatant and the pellet were analyzed by Western blotting for the presence of CD9. Lanes 1-3: Different protein amount of CM. Lanes 4 and 5: The pellet (P) and supernatant (S) after ultracentrifugation of unfiltered CM. Lane 6: Retentate (R) after filtration of CM through a membrane with MWCO of 500 kDa. Lanes 7 and 8: The pellet (RP) and supernatant (RS) after ultracentrifugation of retentate. Lane 9: Filtrate (F) after filtration of CM through a membrane with MWCO of 500 kDa. (**C**) Amount of cholesterol, spingomyelin, and phosphatidylcholine in CM and in the pellet after 200 000 g ultracentrifugation of the CM was assayed and quantitated as picomole per microgram protein.*

through a membrane (MWCO = 500 kDa) into a > 500-kDa retentate fraction and a < 500-kDa filtrate fraction followed by ultracentrifugation of both fractions. The 24-kDa CD9 was found in the > 500-kDa retentate fraction and could be precipitated by ultracentrifugation (Figure 2B). CD9 was not detected in the < 500-kDa filtrate fraction. Consistent with our exosome hypothesis, major plasma membrane phospholipids such as cholesterol, sphingomyelin, and phosphatidylcholine were also precipitated by ultracentrifugation at 200 000 g for 2 h as evidenced by their enrichment in the precipitate (Figure 2C).

Proteins in the CM are associated with phospholipid membrane

As exosomes are phospholipid vesicles, they are known to have a typical density range of 1.10 to 1.18 g ml−1 that could be resolved on sucrose gradients.[19, 20] We therefore postulated that the flotation densities of the putative exosome-associated proteins would be different before and after release from such vesicles by a detergent-based buffer. Therefore, CM or CM pretreated with a detergent-based lysis buffer was fractionated on a sucrose density gradient by equilibrium ultracentrifugation. The fractions were analyzed for the distribution of CD9 and CD81. Both CD9 and CD81 which coimmunoprecipitated (Figure 2A) had a similar flotation density that was heavier than that expected of proteins in their MW range (Figure 3). Pretreatment with a detergent-based cell lysis buffer decreased the apparent flotation densities of CD9 and CD81 to that of proteins in a similar MW range (Figure 3). Our observations demonstrated that the detergent-sensitive flotation densities of proteins were consistent with their location in lipid vesicles.

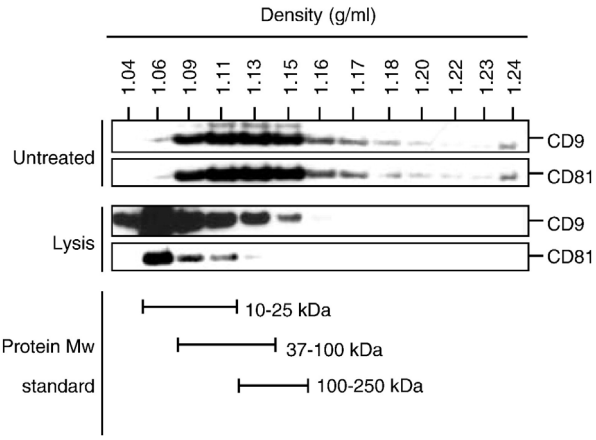

Figure 3. Protein analysis of CM fractionated on a sucrose gradient density. *CM or CM pretreated with lysis buffer was loaded on a sucrose density gradient prepared by layering 14 sucrose solutions of concentrations from 22.8 to 60% (w/v) in a SW60Ti centrifuge tube and then ultracentrifuged for 16.5 h at 200 000 g, 4°C, in a SW60Ti rotor. The gradients were removed from the top and the density of each fraction was calculated by weighing a fixed volume of each fraction. The fractions were analyzed by Western blot analysis for CD9 and CD81 in CM (upper panel) and pretreated CM (lower panel). The distribution of a protein standard molecular weight marker set after fractionation in a similar gradient is denoted at the bottom of the figure.*

Exosomal proteins are either membrane bound or encapsulated

As many of the secreted proteins in the CM are known membrane or cytosolic proteins, we investigated if these proteins in the CM were also membrane bound or localized within the lumen of the putative exosomes by limited trypsinization. Membrane-bound proteins would expected to be partially resistant whereas luminal proteins are expected to be resistant to trypsinization. Treatment with a detergent-based lysis buffer would abrogate this resistance. As expected, CD9, a membrane-bound protein was susceptible to trypsin digestion and generated two detectable tryptic peptide intermediates (Figure 4). In contrast, SOD-1, a cytosolic protein was resistant to trypsin digestion. Pretreatment of CM with a detergent-based cell lysis buffer abolished the resistance of CD9 and SOD-1 to trypsin digestion. The detergent-sensitive partial susceptibility of CD9 and resistance of SOD-1 to trypsin digestion were consistent with their localization in a lipid membrane and lumen of an exosome, respectively.

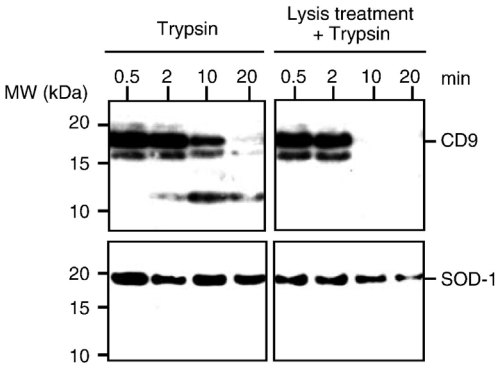

Figure 4. Trypsinization of CM. *CM treated with either PBS or lysis buffer was digested with trypsin and an aliquot was removed at 0.5, 2, 10, and 20 min. A trypsin inhibitor, PMSF, was then added to terminate the trypsinization reaction and the aliquots were analyzed for the presence of CD9 and SOD-1 by Western blot hybridization.*

Purification of a homogeneous population of exosomes by HPLC fractionation

To demonstrate directly that the active cardioprotective component in the secretion is an exosome, CM and nonconditioned medium (NCM) were first fractionated by size exclusion on a HPLC column (Figure 5A). The eluent was monitored by absorbance at 220 nm and then examined by dynamic light scattering which has a hydrodynamic radius (Rh) detection range of 1 to 1000 nm. The first four eluting fractions in CM (F1-F4) were not present in the NCM and therefore represented secretion from the hESC-MSCs. F1, the fastest eluting fraction with a retention time of 12 min, represented the fraction containing the largest particles in the CM. The particles in F1 were sufficiently homogeneous in size such that they could be determined by dynamic light scattering to have a hydrodynamic radius (Rh) of 55-65 nm. All other peaks contained particles that were too heterogeneous in size to be estimated by dynamic light scattering. F1 contained 4% of total protein input but contained 50% of the CD9 in the input (Figure 5B). Proteins were distributed among F2, F3, and F4 fractions according to the principle of size-exclusion fractionation such that larger proteins were eluted first in F2 followed by the smaller proteins in F3 and the smallest in F4 (Figure 5C). In contrast, proteins in the F1 fraction had a MW distribution that spanned the entire MW spectrum of F2, F3, and F4 (Figure 5C). The proteins in the F1 fraction despite having a MW range of 20 to 250 kDa sedimented at a similar flotation density of 1.11-

1.16 g/ml (Figure 6B) that was similar to that of CD9 in the CM (Figure 3). These features of the F1 fraction, i.e., the presence of proteins with a wide spectrum of MW sizes and identical flotation density, the exclusive presence of CD9, and a homogeneous size, indicated that a homogeneous exosome population was purified from the CM by HPLC fractionation. When 0.4 µg of F1 protein was administered to a mouse model of MI/R injury 5 min prior to reperfusion, the F1 fraction reduced infarct size to the same extent as 3 µg CM protein (Figure 7A). All animals in this study had the same degree of endangered myocardium, as illustrated by similar area at risk within the left ventricle (Figure 7B).

Paracrine effect was mediated through heart tissues

For elucidating the mechanism of this paracrine effect, an important prerequisite is the identification of the target tissues. Here we determine that the paracrine effect on MR/I injury was a heart autonomous effect and was independent of circulating cells including immune cells. Using an ex vivo mouse Langendorff heart model of ischemia/reperfusion injury, we observed that conditioned medium reduced relative infarct size to the same extent as in a mouse model (Figure 8).

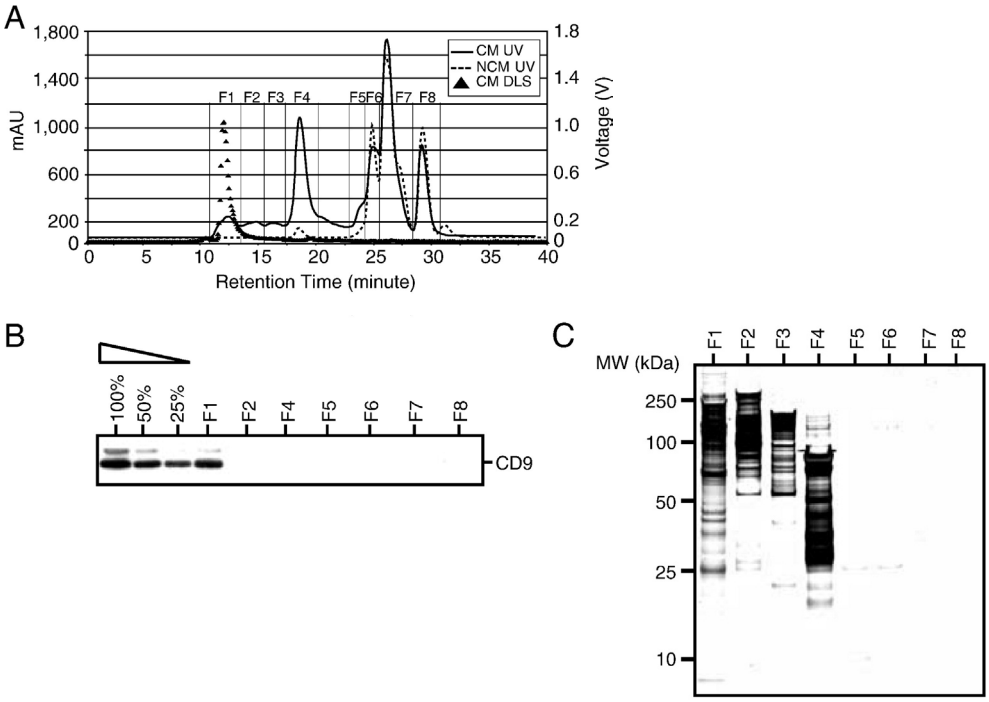

Figure 5. HPLC fractionation of CM. *(**A**) HPLC fractionation and dynamic light scattering of CM and NCM. CM and NCM were fractionated on a HPLC using a BioSep S4000, 7.8 mm × 30 cm column. The components in CM or NCM were eluted with 20 mM phosphate buffer with 150 mM NaCl at pH 7.2. The elution mode was isocratic and the run time was 40 min. The eluent was monitored for UV absorbance at 220 nm. Each eluting peak was then analyzed by light scattering and signals as measured in voltage are represented by solid triangles. The eluted fractions, F1 to F8, were collected, their volumes were adjusted to 50% of the input volume of CM, and an equal volume of each fraction was analyzed for (**B**) the presence of CD9 by Western blot hybridization. Lanes 1-3 were CM loaded at 2X, 1X, or 0.5X of the volume loaded used for each of the fractions, F1 to F8 (lanes 4-11), and therefore represented the equivalent of 100, 50, and 25% input CM. (**C**) Equal volumes of F1-F8 were separated on a SDS-PAGE and then stained with silver.*

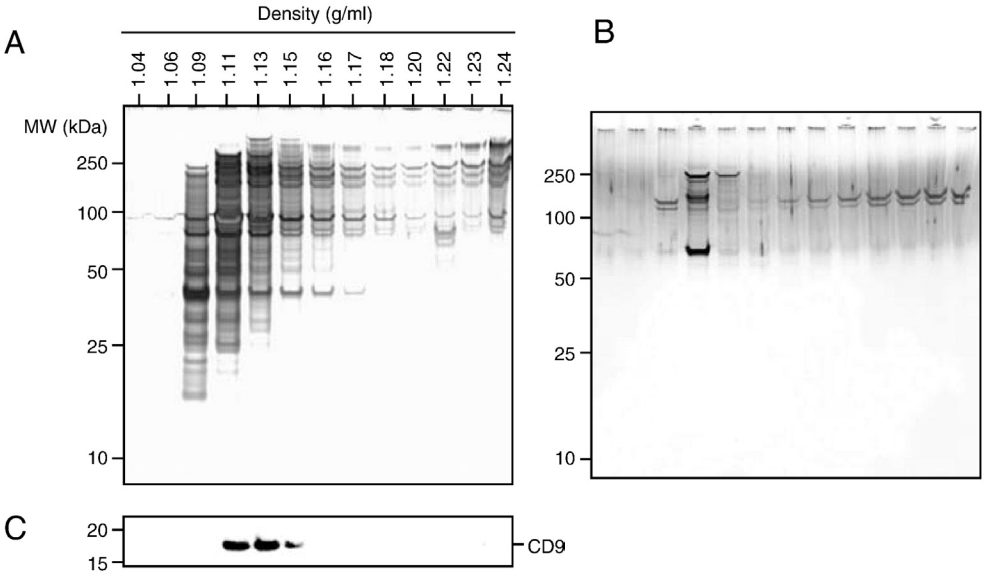

Figure 6. Flotation densities. *Flotation densities of proteins in CM and HPLC-purified F1 fraction were determined by fractionating CM and F1 onto a sucrose gradient density as described above. The 13 fractions for (**A**) CM and (**B**) F1 were separated on a SDS-PAGE and then stained with silver. (**C**) To evaluate the distribution of smaller proteins, the F1 was also assayed for CD9 (20 kDa) by Western blot hybridization. Proteins in the > 1.20 g/ml density fractions were denatured proteins.*

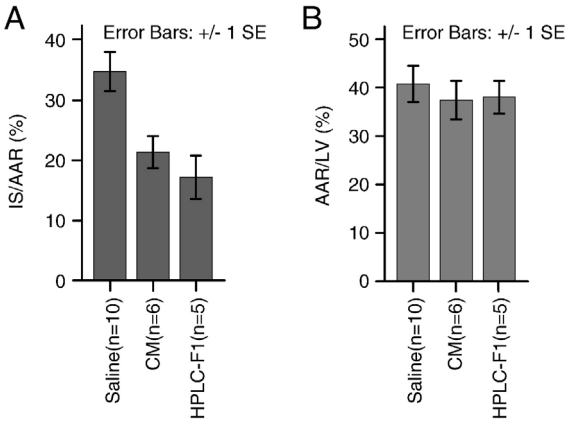

Figure 7. Cardioprotective exosomes. *(**A**) 0.4 µg F1 protein was administered intravenously to a mouse model of MI/R injury 5 min before reperfusion. Infarct sizes (IS) as a percentage of the area at risk (AAR) on treatment with saline (n=10), conditioned medium from hESC-MSCs (n=6), and HPLC fraction (n=5) were measured. Saline treatment resulted in 34.5 ± 3.3% infarction. CM treatment resulted in 21.2 ± 2.6% infarction (p=0.022 compared to saline) and F1 fraction treatment resulted in 17.0 ± 3.6% infarction (p=0.004 compared to saline). (**B**) AAR as a percentage of the left ventricle (LV), showing the amount of endangered myocardium after MI/R injury. All animals were affected to the same extent by the operative procedure, resulting in 39.1 ± 2.2% of AAR among the groups. Each bar represents mean ± SEM.*

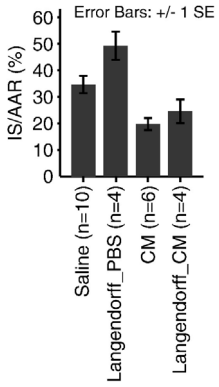

Figure 8. Secretion reduced myocardial ischemia-reperfusion injury ex vivo. *Perfusion buffer containing 3.5 µg/ml CM was used to perfuse mouse heart in an ex vivo mouse Langendorff heart model of MI/R injury 5 min before reperfusion. Infarct sizes (IS) as a percentage of the area at risk (AAR) on treatment with PBS (n=4) and CM (n=4) were measured after 3 h reperfusion. Langendorff_PBS treatment resulted in 49.3 ± 5.3% infarction. Langendorff_CM treatment resulted in 24.6 ± 4.4% infarction (p< 0.001 compared to Langendorff_PBS). As a reference for comparison, the in vivo effects of saline and CM on IS/AAR as described in Figure 7 are also included.*

DISCUSSION

The trophic effects of MSC transplantation on ameliorating the deleterious consequences of myocardial ischemia have been implicated in several studies.[4] Transplantation of MSCs into ischemic myocardium has been shown to induce several tissue responses such as an increased production of angiogenic factors and decreased apoptosis.[21] It was postulated that these responses were better explained by secretion of paracrine factors than by differentiation of MSCs. In this context, MSCs were shown to secrete many growth factors and cytokines that have effects on cells in their vicinity. To date, many of these studies have focused exclusively on proteins that are known to be secreted. These proteins generally included cytokines, chemokines, and other growth factors.[4] However, our unbiased proteomic profiling of proteins in the secretion of MSCs revealed an abundance of membrane and cytosolic proteins.[11] This suggests that the trophic effects of MSCs may not be mediated by soluble growth factors and cytokines alone. This was underscored by our observation that the cardioprotective effects of CM were mediated by 50- to 100-nm complexes of > 1000 kDa and not small soluble proteins.

Based on the size of the complex, we postulated that the cardioprotective complex in the CM was likely to be an exosome. Exosomes are formed from multivesicular bodies with a bilipid membrane. They have a diameter of 40-100 nm and are known to be secreted by many cell types.[16, 17] Electron microscopy confirmed that the CM contained lipid-like vesicles of about 50-100 nm in diameter. The functions of exosomes are not known but they are thought to be important in intercellular communications. Although exosomes are known to have a cell-type-specific protein composition, most carry a common subset of proteins that included CD9, CD81, Alix, TSP-1, SOD-1, and pyruvate kinase.[18] CD9 and CD81 are tetrapannin membrane proteins that are also localized in the membrane of exosomes. Consistent with the presence of exosomes, CM contained coimmunoprecipitating complexes of CD81, CD9, and Alix. Ultracentrifugation precipitated CD9 with phospholipids and cholesterol, suggesting that the CD81,

CD9, and Alix complex was associated with a phospholipid vesicle. This was confirmed by the detergent-sensitive flotation densities of these proteins where we demonstrated that the flotation densities of these proteins in the CM were that of phospholipid vesicles and that detergent treatment which dissolved phospholipid membrane altered the flotation densities of the proteins. We further demonstrated that CD9 in the CM was a membrane-bound protein while SOD-1 was localized within a lipid vesicle by their respective partial and complete resistance to trypsin degradation and the abrogation of this resistance by detergent. Taken together, our observations demonstrated that exosomes with a diameter of 50-100 nm are present in the CM and are therefore the likely candidate for the cardioprotective component in the CM. This was confirmed when a HLPC-purified homogeneous population of particles that had an enrichment of CD9 and a Rh of 55-65 nm substantially reduced infarct size in a mouse model of MI/R injury at a reduced protein dosage equivalent to 10% of the CM dosage. We further demonstrated using an ex vivo mouse Langendorff heart model of MI/R injury that this paracrine effect was a heart autonomous effect, and was independent of circulating cells, such as immune cells or platelets.

In summary, we have identified exosome as the cardioprotective component in MSC paracrine secretion. This involvement of exosomes represents a radical shift in our current understanding of the paracrine effect of MSC transplantation on tissue repair which hitherto has been limited to cytokine, chemokine, or growth factor-mediated extracellular signaling. It also highlights for the first time the role of exosome as mediator of tissue repair. As lipid vesicles, exosomes represent an ideal vehicle to effect an immediate physiological response to repair and recover from injury through the rapid intracellular delivery of functional proteins. Recently, it was demonstrated that in addition to proteins, microvesicles have the potential to mediate intercellular transfer of genetic material.[22] Several tumor cell types[23, 24], peripheral blood cells[25, 26], endothelial progenitor cells[27], and embryonic stem cells[28] have been shown to secrete RNA-containing microvesicles. More importantly, these microvesicular RNA could be transferred to other cells and translated in the recipient cells.[26-28] We also recently demonstrated that the MSC-derived exosomes described here also contained miRNAs and these miRNAs were predominantly in the precursor form.[8] For ischemic/reperfused myocardium, this feature of rapid initiation of cellular repair through the intracellular delivery of functional proteins and possibly RNA is particularly critical as the time window for therapeutic intervention is very narrow. We speculate that the involvement of exosomes in cardioprotection may represent a general function of exosomes in tissue repair. It is possible that different cell types produce exosomes that are specific for certain type of cells or injuries. If true, this novel tissue-repair function of exosomes could potentially engender new approaches to the development of biologics.

Acknowledgments

We gratefully acknowledge Kong Meng Hoi and Eddy Tan at the Bioprocessing Technology Institute (BTI) for helping in the purification of the exosomes and Jayanthi Padmanabhan and Jeremy Lee (BTI) for the preparation and concentration of the conditioned medium.

Appendix A. Supplementary Data

Supplementary data associated with this article can be found in the online version, at doi:10.1016/j.scr.2009.12.003.

METHODS

Preparation of CM

The culture of HuES9.E1 cells and preparation of HuES9.E1 CM were performed as described previously ([Lian et al., 2007] and [Sze et al., 2007]). For the < 100-, < 300-, < 500-, or < 1000-kDa preparations in Figure 1, the CM was first concentrated 25X by tangential flow filtration (TFF) using a membrane with a 10-kDa MWCO (Sartorius, Goettingen, Germany) and then filtered sequentially through membranes with MWCO of 1000 kDa (Sartorius), 500 kDa (Millipore, Billerica, MA), 300 kDa (Sartorius), and finally 100 kDa (Sartorius). All other CM and NCM used were concentrated 25X or 50X by TFF using a membrane with 10- or 100-kDa MWCO (Sartorius). The CM and NCM preparations were filtered with a 0.2-µm filter before storage or use.

Electron microscopy, antibody array assay, protein analysis

Electron microscopy, antibody array assay, and protein analysis were done using standard protocols; for details please refer to Online Supplementary Materials and Methods.

LC MS/MS analysis

Proteins in 2 ml of dialyzed CM or NCM were analysis by LC MS/MS using standard protocols with some modifications; for details please refer to Online Supplementary Materials and Methods.

Immunoprecipitation of exosome-associated proteins

Dynabead M-280 sheep anti-mouse IgG (Invitrogen Corporation, Carlsbad, CA) was washed using 0.1% BSA/PBS before incubation with mouse anti-human CD81 antibody for 2 h with gentle shaking at room temperature. The dynabeads were washed twice and incubated with CM with gentle shaking for 2 h at room temperature. The supernatant was then collected, and the dynabeads were gently washed twice before PBS was added. The supernatant and the dynabeads were denatured, resolved on 4-12% SDS-PAGE, and analyzed by Western blotting.

Sucrose gradient density equilibrium centrifugation

To generate the sucrose gradient density for centrifugation, 14 sucrose solutions with concentrations from 22.8 to 60% were prepared and layered sequentially in an ultracentrifuge tube (Beckman Coulter Inc., CA) starting with the most concentrated solution. CM was loaded on top before ultracentrifugation for 16.5 h at 200 000 g, 4°C in a SW60Ti rotor (Beckman Coulter Inc.). After centrifugation, 13 fractions were collected starting from the top of the gradient. The densities of each were determined by weighing a fixed volume. For pretreatment with detergent-based lysis buffer (Cell Extraction Buffer, Biovision, Mountain View, CA), CM was incubated with an equal volume of the lysis buffer containing protease inhibitors (Halt Protease Inhibitor Cocktail, Thermo Fisher Scientific Inc., Waltham, MA) for 30 min at room temperature with gentle shaking. The protein concentration of CM was quantified using the NanoOrange Protein Quantification kit (Invitrogen Corporation) according to the manufacturer's instructions.

Sphingomyelin, phosphatidylcholine, and cholesterol assay

Cholesterol, sphingomyelin, and phosphatidylcholine concentration in CM and pellet from the ultracentrifugation of CM at 200 000 g for 2 h at 4°C was determined using commercially available assay kits. Cholesterol was measured using the Amplex Red Cholesterol Assay kit (Invitrogen Corporation),

sphingomyelin, and phosphatidylcholine were measured using the Sphingomyelin Assay Kit and Phosphatidylcholine Assay Kit (Cayman Chemical Company, Ann Arbor, MI) respectively.

Limited trypsinization of CM

CM was incubated with equal volumes of either PBS or lysis buffer (Cell Extraction Buffer, Biovision, Mountain View, CA) for 45 min at 4°C with gentle shaking. Then 16 µl of 10× trypsin (Invitrogen Corporation) was added and incubated at 37°C with gentle shaking. An aliquot was removed at 30 s, 1 min, 5 min, and 20 min, and 1 µl of a 100 mM trypsin inhibitor, PMSF (Sigma-Aldrich, St. Louis, MO), was added. The mixture was denatured and analyzed by Western blot analysis.

HPLC dynamic light scattering

The instrument setup consisted of a liquid chromatography system with a binary pump, an auto injector, a thermostated column oven and a UV-visible detector operated by the Class VP software from Shimadzu Corporation (Kyoto, Japan). The Chromatography columns used were TSK Guard column SWXL, 6 × 40 mm and TSK gel G4000 SWXL, 7.8 × 300 mm from Tosoh Corporation (Tokyo, Japan).The following detectors, Dawn 8 (light scattering), Optilab (refractive index), and QELS (dynamic light scattering), were connected in series following the UV-visible detector. The last three detectors were from Wyatt Technology Corporation (CA, USA) and were operated by the ASTRA software. For details please refer to Supplementary Materials and Methods.

MI and surgical procedure

All experiments were performed in accordance with the Guide for the Care and Use of Laboratory Pigs prepared by the Institute of Laboratory Animal Resources and with prior approval by the Animal Experimentation Committee of the Faculty of Medicine, Utrecht University, the Netherlands. The CM and the HPLC fraction 1 (F1) were tested in a mouse model of MI/R injury. MI was induced by 30 min left coronary artery (LCA) occlusion and subsequent reperfusion. Five minutes before reperfusion, mice were intravenously infused with 200 µl saline-diluted CM containing 3 µg protein or HPLC F1 containing 0.4 µg protein via the tail vein. Control animals were infused with 200 µl saline. After 24 h reperfusion, infarct size (IS) as a percentage of the area at risk (AAR) was assessed using Evans' blue dye injection and TTC staining as described previously (Arslan et al., 2010).

Mouse Langendorff heart model of ischemia/reperfusion injury

For the mouse Langendorff heart model of ischemia/reperfusion injury, mice were given heparin 50 IE subcutaneously. The suture was placed in vivo without placing the knot. Hereafter, the heart was excised and aortic root was canulated and perfused in the Langendorff setup. After 10 min recovery, the suture was tightened to induce ischemia for 30 min. Just 5 min prior to reperfusion, the perfusion buffer was changed for a second buffer containing 3.5 µg/ml MSC-CM. Reperfusion was allowed for 3 h before Evans' blue dye injection and TTC staining for infarct size assessment, as described previously (Arslan et al., 2009).

REFERENCES

1 Pittenger MF, Martin BJ. Mesenchymal stem cells and their potential as cardiac therapeutics. Circ Res. 2004;95:9-20.

2 Minguell JJ, Erices A. Mesenchymal stem cells and the treatment of cardiac disease. Exp Biol Med (Maywood). 2006;231:39-49.

3 Zimmet JM, Hare JM. Emerging role for bone marrow derived mesenchymal stem cells in myocardial regenerative therapy. Basic Res Cardiol. 2005;100:471-481.

4 Caplan AI, Dennis JE. Mesenchymal stem cells as trophic mediators. J Cell Biochem. 2006;98:1076-1084.

5 Gnecchi M, He H, Liang OD, Melo LG, Morello F, Mu H, Noiseux N, Zhang L, Pratt RE, Ingwall JS, Dzau VJ. Paracrine action accounts for marked protection of ischemic heart by Akt-modified mesenchymal stem cells. Nat Med. 2005;11:367-368.

6 Gnecchi M, He H, Noiseux N, Liang OD, Zhang L, Morello F, Mu H, Melo LG, Pratt RE, Ingwall JS, Dzau VJ. Evidence supporting paracrine hypothesis for Akt-modified mesenchymal stem cell-mediated cardiac protection and functional improvement. FASEB J. 2006;20:661-669.

7 Schafer R, Northoff H. Cardioprotection and cardiac regeneration by mesenchymal stem cells. Panminerva Med. 2008;50:31-39.

8 Chen TS, Lai RC, Lee MM, Choo AB, Lee CN, Lim SK. Mesenchymal stem cell secretes microparticles enriched in pre-microRNAs. Nucleic Acids Res. 2010;38:215-224.

9 Liu CH, Hwang SM. Cytokine interactions in mesenchymal stem cells from cord blood. Cytokine. 2005;32:270-279.

10 Lian Q, Lye E, Suan YK, Khia Way TE, Salto-Tellez M, Liu TM, Palanisamy N, El Oakley RM, Lee EH, Lim B, Lim SK. Derivation of clinically compliant MSCs from CD105+. Stem Cells. 2007;25:425-436.

11 Sze SK, de Kleijn DP, Lai RC, Khia Way TE, Zhao H, Yeo KS, Low TY, Lian Q, Lee CN, Mitchell W, El Oakley RM, Lim SK. Elucidating the secretion proteome of human embryonic stem cell-derived mesenchymal stem cells. Mol Cell Proteomics. 2007;6:1680-1689.

12 Cannon CP, Gibson CM, Lambrew CT, Shoultz DA, Levy D, French WJ, Gore JM, Weaver WD, Rogers WJ, Tiefenbrunn AJ. Relationship of symptom-onset-to-balloon time and door-to-balloon time with mortality in patients undergoing angioplasty for acute myocardial infarction. JAMA. 2000;283:2941-2947.

13 Saraste A, Pulkki K, Kallajoki M, Henriksen K, Parvinen M, Voipio-Pulkki LM. Apoptosis in human acute myocardial infarction. Circulation. 1997;95:320-323.

14 Knight DR. Editorial overview: cardioprotective drugs for myocardial ischemic injury--a therapeutic area at risk. Curr Opin Investig Drugs. 2007;8:190-192.

15 Timmers L, Lim SK, Arslan F, Armstrong JS, Hoefer IE, Doevendans PA, Piek JJ, El Oakley RM, Choo A, Lee CN, Pasterkamp G, de Kleijn DP. Reduction of myocardial infarct size by human mesenchymal stem cell conditioned medium. Stem Cell Res. 2007;1:129-137.

16 Fevrier B, Raposo G. Exosomes: endosomal-derived vesicles shipping extracellular messages. Curr Opin Cell Biol. 2004;16:415-421.

17 Keller S, Sanderson MP, Stoeck A, Altevogt P. Exosomes: from biogenesis and secretion to biological function. Immunol Lett. 2006;107:102-108.

18 Olver C, Vidal M. Proteomic analysis of secreted exosomes. Subcell Biochem. 2007;43:99-131.

19 Thery C, Amigorena S, Raposo G, Clayton A. Isolation and characterization of exosomes from cell culture supernatants and biological fluids. Curr Protoc Cell Biol. 2006;Chapter 3:Unit.

20 Raposo G, Nijman HW, Stoorvogel W, Liejendekker R, Harding CV, Melief CJ, Geuze HJ. B lymphocytes secrete antigen-presenting vesicles. J Exp Med. 1996;183:1161-1172.

21 Tang YL, Zhao Q, Qin X, Shen L, Cheng L, Ge J, Phillips MI. Paracrine action enhances the effects of autologous mesenchymal stem cell transplantation on vascular regeneration in rat model of myocardial infarction. Ann Thorac Surg. 2005;80:229-236.

22 Quesenberry PJ, Aliotta JM. The paradoxical dynamism of marrow stem cells: considerations of stem cells, niches, and microvesicles. Stem Cell Rev. 2008;4:137-147.

23 Rosell R, Wei J, Taron M. Circulating MicroRNA Signatures of Tumor-Derived Exosomes for Early Diagnosis of Non-Small-Cell Lung Cancer. Clin Lung Cancer. 2009;10:8-9.

24 Taylor DD, Gercel-Taylor C. MicroRNA signatures of tumor-derived exosomes as diagnostic biomarkers of ovarian cancer. Gynecol Oncol. 2008;110:13-21.

25 Hunter MP, Ismail N, Zhang X, Aguda BD, Lee EJ, Yu L, Xiao T, Schafer J, Lee ML, Schmittgen TD, Nana-Sinkam SP, Jarjoura D, Marsh CB. Detection of microRNA expression in human peripheral blood microvesicles. PLoS One. 2008;3:e3694.

26 Valadi H, Ekstrom K, Bossios A, Sjostrand M, Lee JJ, Lotvall JO. Exosome-mediated transfer of mRNAs and microRNAs is a novel mechanism of genetic exchange between cells. Nat Cell Biol. 2007;9:654-659.

27 Deregibus MC, Cantaluppi V, Calogero R, Lo IM, Tetta C, Biancone L, Bruno S, Bussolati B, Camussi G. Endothelial progenitor cell derived microvesicles activate an angiogenic program in endothelial cells by a horizontal transfer of mRNA. Blood. 2007;110:2440-2448.

28 Ratajczak J, Miekus K, Kucia M, Zhang J, Reca R, Dvorak P, Ratajczak MZ. Embryonic stem cell-derived microvesicles reprogram hematopoietic progenitors: evidence for horizontal transfer of mRNA and protein delivery. Leukemia. 2006;20:847-856.

CHAPTER 5

In this chapter we demonstrate that MSCs from different fetal sources share similar genetic, proteomic and cardioprotective profile compared to embryonic tissue-derived MSCs

Ruenn Chai Lai, Fatih Arslan, Soon Sim Tan, Betty Tan, Andre Choo, May May Lee, Tian Sheng Chen, Bao Ju Teh, John Kun Long Eng, Harwin Sidik, Vivek Tanavde, Wei Sek Hwang, Chuen Neng Lee, Reida Menshawe El Oakley, Gerard Pasterkamp, Dominique P. de Kleijn, Kok Hian Tan and Sai Kiang Lim

Derivation and characterization of human fetal MSCs: an alternative cell source for large-scale production of cardioprotective microparticles

Background

The therapeutic effects of mesenchymal stem cells (MSCs) transplantation are thought to be mediated by MSC secretion. We have previously demonstrated that human ESC-derived MSCs (hESC-MSCs) produce cardioprotective microparticles in pig model of myocardial ischemia/reperfusion (MI/R) injury. As the safety and availability of clinical grade human ESCs remain a concern, MSCs from fetal tissue sources were evaluated as alternatives.

Methods and Results

Here we derived five MSC cultures from limb, kidney and liver tissues of three first trimester aborted fetuses and like our previously described hESC-derived MSCs; they were highly expandable and had similar telomerase activities. Each line has the potential to generate at least 1016–19 cells or 107–10 doses of cardioprotective secretion for a pig model of MI/R injury. Unlike previously described fetal MSCs, they did not express pluripotency-associated markers such as Oct4, Nanog or Tra1-60. They displayed a typical MSC surface antigen profile and differentiated into adipocytes, osteocytes and chondrocytes in vitro. Global gene expression analysis by microarray and qRT-PCR revealed a typical MSC gene expression profile that was highly correlated among the five fetal MSC cultures and with that of hESC-MSCs ($r^2 > 0.90$). Like hESC-MSCs, they produced secretion that was cardioprotective in a mouse model of MI/R injury. HPLC analysis of the secretion revealed the presence of a population of microparticles with a hydrodynamic radius of 50–65 ηm. This purified population of microparticles was cardioprotective at 1/10 dosage of the crude secretion.

Conclusions

These data demonstrate that MSCs derived from fetal tissues are a viable alternative to human ESCs as a tissue source of highly proliferative MSCs that produces cardioprotective secretion. The use fetal MSC secretion represents a viable strategy to address an urgent unmet therapeutic need for treating MI/R injury.

J Mol Cell Cardiol. 2010;48(6):1215-24

Mesenchymal stem cells (MSCs) are multipotent stem cells that have a limited but robust potential to differentiate into mesenchymal cell types, e.g. adipocytes, chondrocytes and osteocytes, with negligible risk of teratoma formation. MSC transplantation has been used to treat musculoskeletal injuries, improve cardiac function in cardiovascular disease and ameliorate the severity of graft-versus-host-disease.[1] In recent years, MSC transplantations have demonstrated therapeutic efficacy in treating different diseases but the underlying mechanism has been controversial.[2-9] Some reports have suggested that factors secreted by MSCs[10] were responsible for the therapeutic effect on arteriogenesis[11], stem cell crypt in the intestine[12], ischemic injury[5, 13-18], and hematopoiesis.[19, 20]

We have recently demonstrated that human MSCs derived from human embryonic stem cells (hESC-MSCs)[21] secrete > 200 proteins[22] and that a single bolus administration of hESC-MSCs conditioned medium (CM) 5 min prior to reperfusion significantly reduced infarct size by 60% and improved cardiac function in a pig and mouse model of myocardial ischemia/reperfusion (MI/R) injury.[23] In addition, this cardioprotection was mediated by large complexes of about 50-100 ηm in diameter. The size of these large secreted complexes suggests that they are microparticles which are broadly defined as secreted membrane particles in the size range of 0.05-1 μm.[24]

A requisite for translating cardioprotective MSC secretion into clinical applications is a clinical grade MSC source but this is currently limited by restricted access to clinical grade hESCs. Therefore, alternative tissue or cell sources that are amenable to the generation of highly expandable, clinical grade MSCs have to be developed. Here we examined fetal tissues as a candidate tissue source.

Five MSC cultures, Fllb, F1ki, F2lb, F3lb and F3li were generated from limb (lb), kidney (ki) and liver (li) tissues of three fetuses in three independent experiments. These fetal MSCs fulfilled the defining criteria of a MSC. They were highly proliferative. Each line has the potential of generating 1016-19 cells, and therefore the capacity to produce large amount of secretion. More importantly, these cells produce secretion that reduced infarct size in a mouse model of MI/R injury.[23] Like the secretion of hESC-MSCs, this cardioprotection was also mediated by large complexes. Fractionation of the secretion by size exclusion on an HPLC revealed the presence of a population of homogenously sized particles with a hydrodynamic radius of 50-65 ηm and these particles were cardioprotective in a mouse model of MI/R injury. The size of these large secreted complexes suggests that they are microparticles which are broadly defined as secreted membrane particles in the size range of 0.05-1 μm.[24]

RESULTS

Generating MSC cultures from human fetal tissues

We generated five MSC cultures from fetal limb (F1lb, F2lb, F3lb), kidney (F1ki) and liver (F3li) tissues of three fetuses in three independent experiments using feeder- and serum-free culture condition as previously described.[21] A homogenous culture of putative fibroblast-like MSCs migrated out of the tissues and adhered to the plastic culture dish, 2 days after fetal tissues were plated on gelatinized tissue culture plates. This observation was consistent with the defining characteristic of MSCs i.e. adherence to plastic. The large tissue pieces were then washed off leaving a homogenous cell culture. This procedure was performed on five different fetal tissues originating from 3 fetuses in 3 independent experiments. Each time, a homogenous culture of putative MSCs was obtained that form a typical fingerprint whorl at confluency (Figure 1A). The cultures were designated P1 when 2 × 107 cells were generated. The average population doubling time of all five cultures was between 48 and 72 h and was

most optimal at between 25% and 80% confluency or 15-50,000 cells per cm2. The cells could be maintained in continuous culture for at least 20 passages at a 1:4 split with minimal changes in population doubling time. The karyotype of all five cultures at p10-12 was normal i.e. 46 XX or 46XY as determined by G-banding (Figure 1B). At passages 14, 16 and 18, telomerase activity in all five MSC cultures was determined and the average cellular telomerase activity over three passages in each of the five cultures was equivalent to that of the previously described Hues9.E1 hESC-MSCs (Figure 2).[21] All five cultures could be expanded to at least passage 20 without obvious changes in the population doubling time. At a 1:4 split ratio and starting with 107 cells, each line would generate 1016 cells at passage 15 or 1019 cells at passage 20.

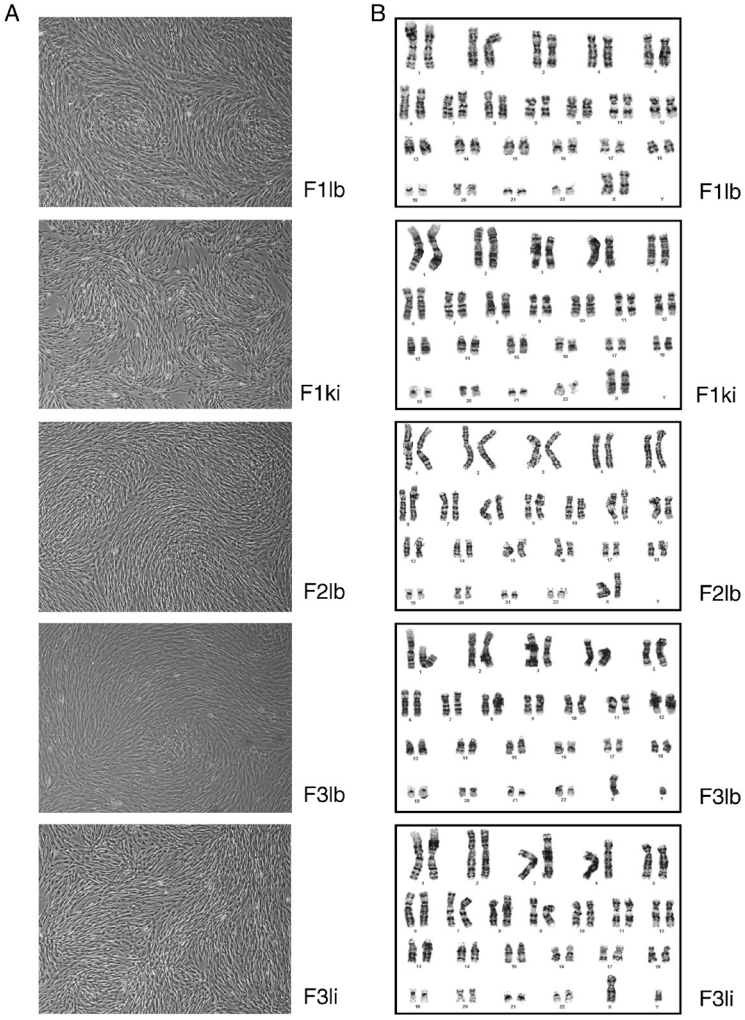

Figure 1. Characterization of fetal MSC cultures. *(**A**) Cellular morphology under phase contrast. Representative images of the five different MSCs, F1lb (p8) and F1ki (p8) derived from the limb and kidney tissues of the same fetus; F2lb (p8) derived from the limb of a second fetus; and F3lb (p8) and F3li (p8) derived from the limb and liver tissues of the same third fetus. (**B**) Karyotype analysis by G-banding was performed each of the fetal MSC cultures, F1lb (p10) F2lb (p10), F3lb (p10), F1ki (p12), and F1li (p12).*

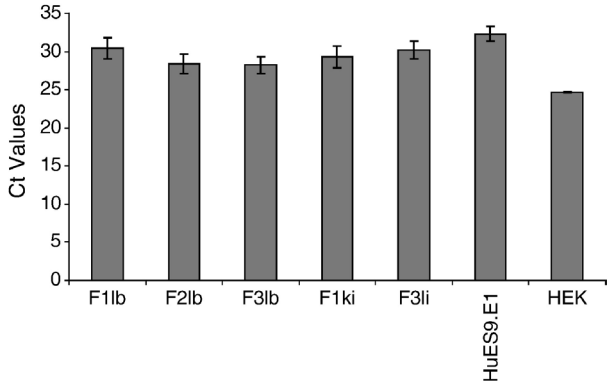

Figure 2. Telomerase activity in hESC-MSCs and fetal MSCs. *Relative telomerase activity was measured by real time quantitative telomeric repeat amplification protocol. This qPCR-based assay quantifies product generated in vitro by telomerase activity present in the samples. The relative telomerase activity which is directly proportional to the amount of telomerase products was assessed by the threshold cycle number (or Ct value) for 1 µg protein cell lysate. Hues9.E1 referred to a previously described hESC-MSCs line and HEK is a human embryonic kidney cell line. The Ct value for each fetal MSCs was the mean for three passages, P16, P18, and P20, and that for Hues9.E1 was the mean for two passages, P20 and P22. The assay was performed in triplicate for each passage.*

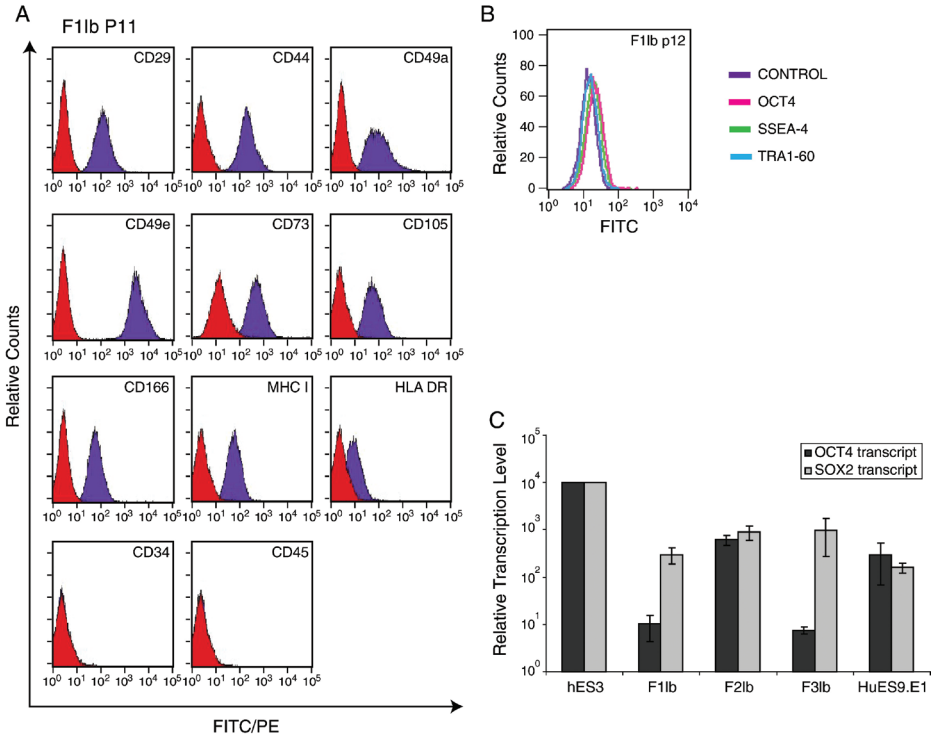

Figure 3. Marker profiling. *(**A** & **B**) F1lb MSCs at p11 or p12 were stained with a specific antibody conjugated to a fluorescent dye and analyzed by FACS. Nonspecific fluorescence was determined by incubation of similar cell aliquots with isotype-matched mouse monoclonal antibodies. (**C**) Relative transcription level of OCT4 and SOX2 was measured using quantitative RT-PCR. hES3, a human embryonic stem cells line was set as the baseline for comparison.*

Assessment of fetal cultures as MSCs

The five putative MSC cultures derived from fetal tissues were assessed according to the ISCT minimal criteria for the definition of human MSCs.[25] All five presumptive MSC cultures derived from three different fetuses were grown on plastic culture dishes as a monolayer of adherent spindle-shaped cells (Figure 1A). They were all CD29+, CD44+, CD49a+ CD49e+, CD105+, CD166+, MHC I+, CD34− and CD45− as represented by F1lb MSCs (Figure 3A). We observed that F1lb MSCs were HLA-DRlo but the remaining four cultures were HLA-DR−. In contrast to previous reports[26-35], these fetal MSCs-like hESC-MSCs did not express pluripotency-associated proteins Oct4, SSEA-4, and Tra1-60 as exemplified by F1lb MSCs (Figure 3B). However, transcripts of OCT4 and SOX2 were readily detected by real time PCR but their levels were at least ten times lower than those in hES3 human ESCs (Figure 3C). All five presumptive fetal MSC cultures could be induced to differentiate to osteoblasts, adipocytes and chondroblasts *in vitro* (Figure 4).

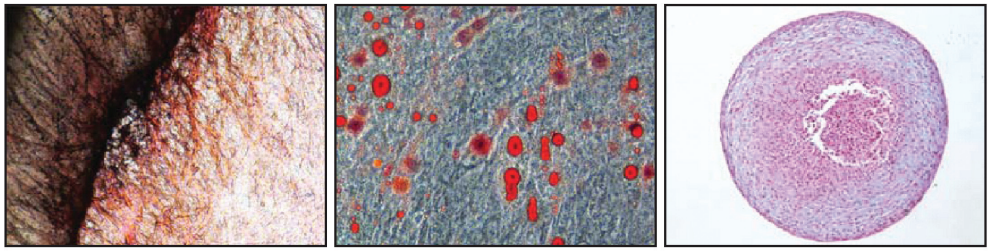

A. Osteocytes **B. Adipocytes** **C. Chrondrocytes**

Figure 4. Differentiation of fetal MSCs. *Fetal MSCs were induced to undergo osteogenesis, adipogenesis and chondrogenesis. After a) osteogenesis, b) adipogenesis and c) chondrogenesis, the differentiated cells were stained with von Kossa stain, Oil Red and Alcian blue, respectively. Images of differentiated fetal MSCs as represented by differentiated F3lb MSCs at 100× magnification.*

Gene expression profile

Genome-wide gene expression profiling of the fetal MSCs and hESC-MSCs was performed using microarray hybridization to assess 1) the relatedness among the five fetal MSC cultures derived from three different tissues and 2) the relatedness between the fetal MSC cultures and hESC-MSCs. Microarray hybridization was performed in duplicate on Sentrix Human Ref-8 Expression BeadChip version 3 (Illumina, Inc., San Diego, CA) using RNA from two or three different passages of the MSC cultures. The gene expression profile between different passages of each culture, between the five cultures or between each fetal MSC culture and hESC-MSCs was highly similar with a correlation value of > 0.9 (Figure 5).

Cardioprotective activity of secretion

Secretion by two of the fetal MSC cultures, F1lb and F1ki were tested for cardioprotective activity in a mouse model of myocardial ischemia and reperfusion injury as previously described.[36] Briefly, the cultures were grown in a chemically defined medium and the secretion harvested as we have previously described.[22] A typical culture of 109 cells yielded 100 mg protein. The gross protein composition of

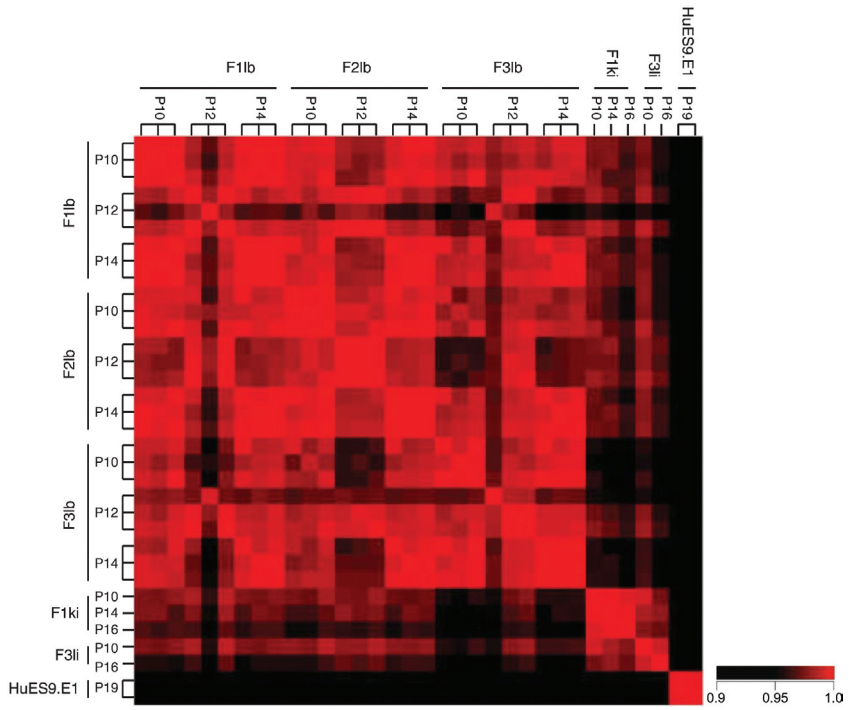

Figure 5. Gene expression analysis. *Total RNA was prepared in technical replicates from different passages of F1lb (p10, p12, p14), F1ki (p10, p14, p16), F2lb (p10, p12, p14), F3lb (p10, p12, p14) and F3li (p10, p16), and from two technical replicates of the previously described hESC-MSCs line, Hues9.E1 (p19). Seven hundred fifty nanograms of biotinylated cRNA from each sample was used for microarray analysis on the Sentrix HumanRef-8 Expression BeadChip Version 3 (Illumina, Inc., San Diego, CA). The gene expression profile of all samples was normalized by a shift to the 75th percentile, baseline transformed to median of all samples, and a heat map of correlation between pairs of array plotted.*

secretion from both F1lb and F1ki as determined by silver staining of proteins resolved on a one-D SDS-PAGE appeared similar to each other, to that of Hues9.E1 hESC-MSCs and also to that from F3lb derived from fetal limb tissues of a different sex (Figure 6A). However, the relative abundance of specific proteins such as TSP-1, SOD-1, CD81 and CD9 was different among all the secretions (Figure 6B). Nevertheless, the secretion from either F1lb or F1ki when administered to a mouse model of MI/R injury significantly reduced infarct size to the same extent as mice treated with hESC-MSC CM (Figure 6C-G). Conditioned medium from F1lb, F1ki and hESC-MSCs reduced the relative infarct size (IS) by 50%, 42% and 39% respectively ($p < 0.05$; Figure 6G). The area at risk (AAR) as a percentage of the left ventricle (LV) was similar in all the mice tested (Figure 6G).

Microparticles mediated the cardioprotection effects of the secretion

We had previously shown that the cardioprotection effects of secretion from hESC-MSCs were mediated by large complexes of 1000 kDa.[23] To determine if there were such complexes in the secretion of the fetal MSCs, the CM was fractionated by size exclusion on an HPLC column. We observed five fractions that were present in the CM but not in the non-conditioned medium (NCM) (Figure 7A).

NCM was essentially culture medium that had not been exposed to cells but was processed, concentrated

and filtered in the same manner as CM. It was previously shown to have no cardioprotective effect and was equivalent to saline in this respect. These five fractions, F1-F5 therefore represented secretion from the MSCs. In a size exclusion fractionation where larger molecules are eluted faster than smaller ones, we observed that only proteins in fraction F2 to F5 followed this principle of fractionation. Proteins in the fastest eluting F1 fraction contained proteins that spanned in entire MW spectrum of F2 to F5. This suggested that the proteins in F1 were in large aggregates (Figure 7B). To confirm this, sizes of molecules in the five fractions were determined by dynamic light scattering analysis which has a detection range of 1 to 500 ηm according to the manufacturer specification (Wyatt Technology Corporation, www.wyatt.com). The sizes of molecules in fractions F2 to F5 were too heterogeneous to

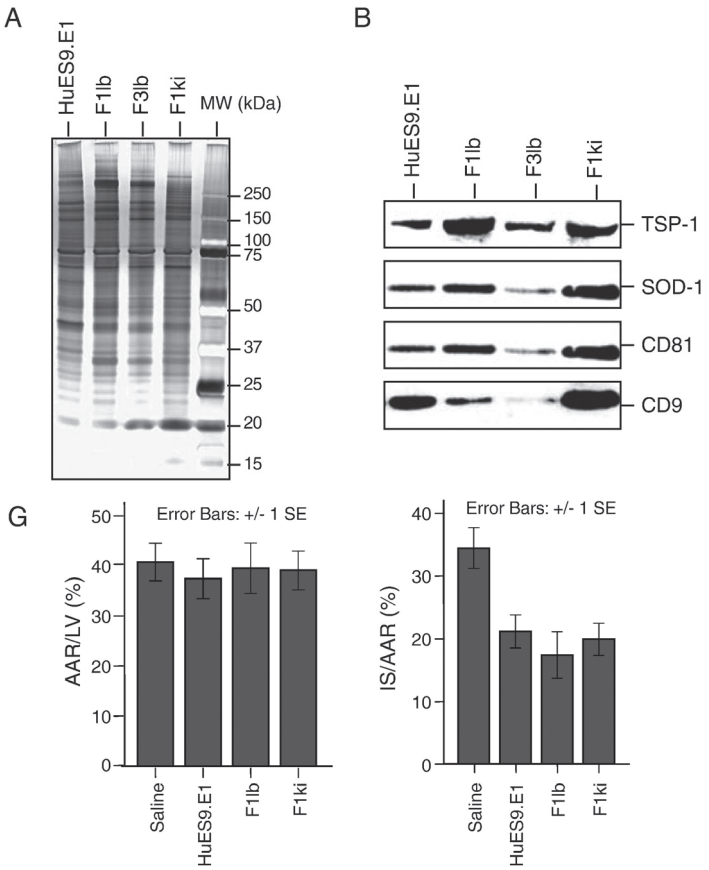

Figure 6. Cardioprotective secretion. *(**A**) Proteins in culture medium conditioned by hESC-MSCs (Hues9.E1), F1lb, F1ki or F3lb were separated on a 4%-12% SDS-PAGE gradient gel and stained with silver. Two micrograms of proteins was loaded in each lane. (**B**) Western blot analysis. CM from hESC-MSCs (Hues9.E1), F1lb, F1ki and F3lb at 4, 8, 16 and 16 µg, respectively, were resolved on an SDS-PAGE, electroblotted onto nitrocellulose membrane and probed with antibodies against TSP-1, SOD-1, CD81 and CD9. (C-F) Representative pictures of Evan blue (blue) and TTC (pink) staining on hearts of mice treated with (**C**) saline, (**D**) HuES9.E1, (**E**) F1lb, or (**F**) F1ki. (**G**) AAR as a percentage of the left ventricle (LV), showing the amount of endangered myocardium after MI/R injury. All animals were affected to the same extent by the operative procedure, resulting in 39.4 ± 2.0% of AAR among the groups. Infarct size (IS) as a percentage of the area at risk (AAR) upon treatment with saline (n=10), CM from hESC-MSCs (n=10), F1lb-MSCs (n=6) and F1ki-MSCs (n=6). Saline treatment resulted in 34.5 ± 3.3% infarction, whereas conditioned medium from hESC-MSCs, F1lb-MSCs and F1ki-MSCs resulted in 21.2 ± 3.3%, 17.4 ± 3.7% and 19.9 ± 2.6%, respectively. Each bar represents mean ± SEM.*

be determined by dynamic light scattering analysis. In spite of the wide MW spectrum of proteins in F1, the size of molecules in F1 fraction was sufficiently homogenous to be determined as having a hydrodynamic radius of 50-65 ηm by dynamic light scattering analysis. When administered to the mouse model of MI/R injury as described above, these HPLC-purified microparticles reduced infarct size at < 1/10 dosage of the secretion (Figure 7C-F).

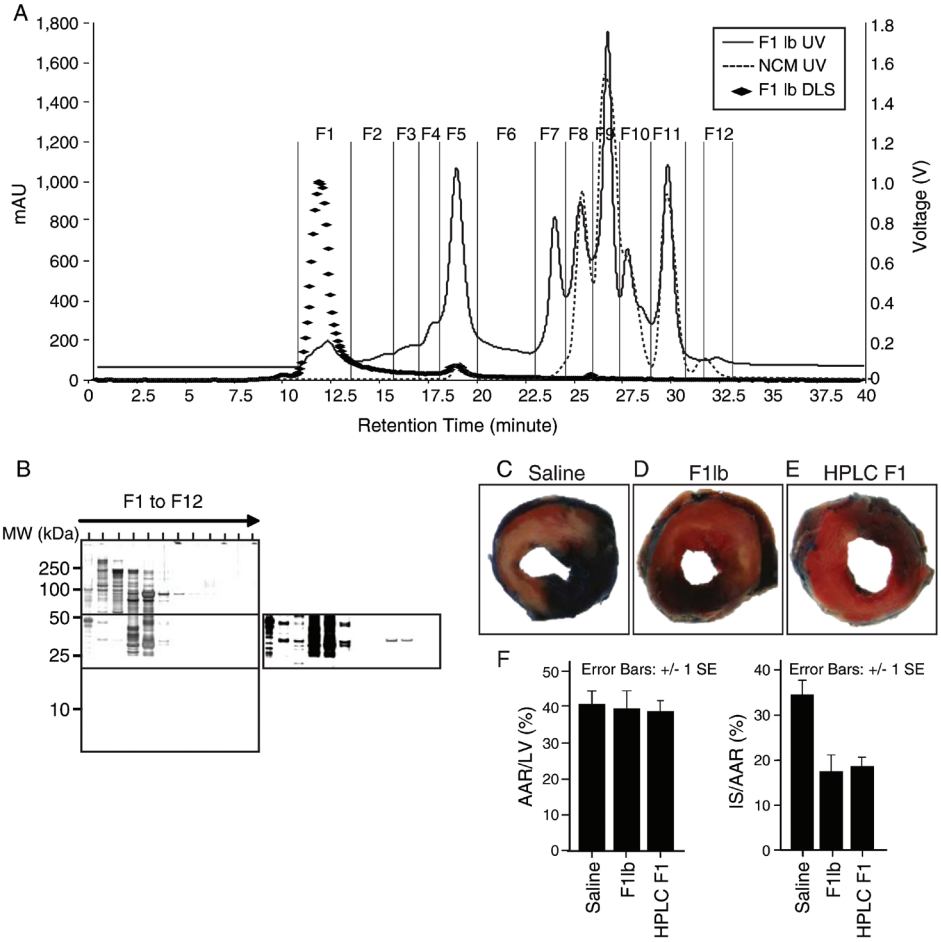

Figure 7. Cardioprotective HPLC-isolated microparticles. *(**A**) HPLC fractionation and dynamic light scattering of F1lb CM and NCM. F1lb CM and NCM were fractionated on an HPLC using BioSep S4000, 7.8 mm × 30 cm column. The components in F1lb CM or NCM were eluted with 150 mM of NaCl in 20 mM phosphate buffer, pH 7.2. The elution mode was isocratic and the run time was 40 min. The eluent was monitored with a UV-visible detector set at 220 ηm and light scattering signal was collected. The solid rhombus represented light scattering signal as measured in voltage; (**B**) The eluted fractions, F1 to F12 were collected, their volumes were adjusted to 10% of the input volume of CM and equal volume of F1-F12 was separated by gel electrophoresis and stained with silver. (**C-E**) Representative pictures of Evan blue (blue) and TTC (pink) staining on hearts of mice treated with (**C**) saline, (**D**) F1lb, or (**E**) HPLC F1. (**F**) Infarct size (IS) as a percentage of the area at risk (AAR) upon treatment with saline (n=10), F1lb CM (n=6) and HPLC F1 (n=6). Saline-treated mice had a 34.5 ± 3.3% relative infarct size while F1lb CM- and HPLC F1-treated mice had a 17.4 ± 3.7% and 18.1 ± 2.0% relative infarct size, respectively. AAR as a percentage of the left ventricle (LV), showing the amount of endangered myocardium after MI/R injury. All animals were affected to the same extent by the operative procedure, resulting in 39.4 ± 2.0% of AAR among the groups. Each bar represents mean ± SEM.*

DISCUSSION

The trophic effects of MSCs transplantation on ameliorating the deleterious consequences of myocardial ischemia have been implicated in several studies.[10] Transplantation of MSCs into ischemic myocardium has been shown to induce several tissue responses such as an increased production of angiogenic factors and decreased apoptosis that were better explained by secretion of paracrine factors than by differentiation of MSCs, the so-called paracrine hypothesis.[37]

We have recently demonstrated that hESC-MSC secretion reduces infarct size in mouse and pig MI/R injury model.[23] To translate this finding into a clinical application, an important requisite would be a safe, relatively accessible and highly proliferative source of MSCs that has the potential to generate large number of cells to minimize batch to batch variation. Although hESC-MSCs are highly proliferative and have the capacity to generate large number of cells, the number of clinical grade hESC lines and their accessibility is limited. To circumvent this limitation, we derived human MSCs directly from fetal human tissues. The traditionally used bone marrow for deriving MSCs was not an attractive alternative as a single bone marrow aspirate usually generates only 109 cells. We rationalized that fetal tissues being developmentally less mature may generate MSCs with expansion potential equivalent to that of hESC-MSCs.

The fetal MSCs-like hESC-MSCs, fulfilled the basic criteria for MSCs as defined by The International Society for Cellular Therapy.[25] They adhered to plastic, have a typical MSCs-like surface antigen profile as defined by the presence of surface antigens such as CD29, CD44, CD49a, CD49e, CD105, CD166, and MHC I and the absence of surface antigens such as HLA-DR, CD34 and CD45[38-40], and a typical MSCs differentiation potential that includes adipogenesis, chondrogenesis and osteogenesis. Irrespective of their tissue of origin, the five fetal MSC cultures derived from different tissues of three individual fetuses have a nearly identical genome-wide gene expression profile. Their gene expression profiles were also similar to that of the previously described hESC-MSCs, Hues9.E1. They were as equally proliferative as Hues9.E1 and had high levels of telomerase activity. Although the secretion by MSCs derived from different tissues, that is, limb and kidney tissues were grossly similar to that from hESC-MSCs, Hues9.E1, closer examination of specific proteins by western blot hybridization (Figure 6B) demonstrated that there were quantitative differences in the protein composition. Consistent with this observation, secretion from the fetal MSCs significantly reduced infarct size in a mouse model of MI/R injury but at a higher dosage of 150 μg instead of 3 μg per mouse. We postulate that this difference in effective dosage was due primarily to the quantitative differences in the protein composition and candidate proteins will have to be identified through systematic evaluation and validation of quantitative high throughput proteomic analysis. We further demonstrate that consistent with our previous observations[23], the cardioprotective effect of secretion from fetal MSCs was mediated by large complexes in the range of 100 to 200 ηm or possibly, microparticles.

Microparticle is a minimally defined term that encompasses a broad spectrum of secreted particles in the size range of 0.05-1 μm. Microparticles are known to be produced by numerous cell types.[41-47] Although the function of microparticles remains poorly understood, there is irrefutable evidence that microparticles have important functions. As summarized by many recent reviews, microparticles are definitively associated with many diseases such as cancer, atherosclerosis and cerebral ischemia.[42-44, 48-56] However, the specific role of microparticles in disease process and/or progress remains to be determined. As some microparticles carried biologically active materials including proteins and RNAs that can be transferred between cells, it is likely that microparticles would have

an impact either positively or negatively on a disease process and/or progress. This has led to suggestions that microparticles could be exploited as potential therapeutic vectors.[57] However, the broad definition of microparticles which encompasses all secreted membrane vesicles to include the more defined exosomes (50-100 ηm), microvesicles (100-1000 ηm), ectosomes (50-200 ηm), membrane particles (50-80 ηm), exosome-like vesicles (20-50 ηm) and apoptotic vesicles (50-500 ηm) has impeded our understanding of microparticles.[24] Other than exosomes which are the most stringently defined microparticles to date, the major distinguishing parameter for these different classes of microparticles is their size.

In this report where we not only demonstrated directly for the first time that purified microparticles in MSC secretion were cardioprotective, we also purified these microparticles by size exclusion on an HPLC which is currently one of the most precise methods for size fractionation of molecules or particles. The purified microparticles were determined by dynamic light scattering analysis to be a population of homogenously sized particles with a hydrodynamic radius of 50-65 ηm. This particle size which translated into an approximate diameter of 100-130 ηm was consistent with our previous observation that filtration through a membrane with an MW cutoff of 1000 kDa caused the filtrate to lose its cardioprotective function while that part of secretion retained by the same filter or the retentate was cardioprotective.[23] A membrane with an MW cutoff of 1000 kDa has a 100-ηm nominal pore size according to the manufacturer (Pall Corp. http://www.pall.com/). This essentially meant that the filtrate contained particles with diameter of less than 50-100 ηm and these < 50-100 ηm particles were not cardioprotective. On the other hand, the retentate containing particles >50-100 ηm was cardioprotective. Together, this study and our previous study demonstrated that cardioprotection by the secretion of hESC-MSCs and fetal MSCs was similarly mediated by microparticles with diameters of > 50-100 ηm. Our previous study also suggested that secretion devoid of the microparticles but containing all other secreted proteins as represented by the CM filtrate through a membrane with an MW cutoff of 1000 kDa was not cardioprotective. This observation of no cardioprotective activity could therefore be extrapolated to HPLC fraction 2 to 4 where there were no microparticles and the secreted proteins were eluted according to the size exclusion principle, and were therefore soluble.

The involvement of microparticles in mediating the paracrine effect of MSC transplantation on tissue repair represents a radical shift in our current understanding of the paracrine effect of MSC which hitherto has been limited to cytokine, chemokine or growth factor-mediated extracellular signaling.[10] Together our report demonstrated that MSCs derived from fetal tissues are a viable alternative to human ESCs as a tissue source of highly proliferative MSCs that produces cardioprotective secretion. A single fetal tissue could potentially generate 1016 to 1019 MSCs. A 109 cell culture secretes 100 mg protein. We have previously shown that the effective cardioprotective dose for a pig model of MI/R injury was 10 mg protein per 60-70 kg pig.[23] Therefore, a single fetal tissue could potentially generate sufficient MSCs to produce 108-11 doses. Together with the relatively simple purification of these microparticles to a population of homogenously sized microparticles, the use of secretion from fetal MSCs represents a viable strategy to address an urgent unmet therapeutic need for treating MI/R injury.[58]

Acknowledgments

We thank J.J. Chee (KKH) for her help in patient recruitment and tissue harvest, and Jayanthi Padmanabhan (BTI) for technical assistance in preparing the secretion.

METHODS

Derivation of fetal tissue derived MSCs

The collection of fetal tissue was carried out under a KK Women's and Children's Hospital (KKH) IRB approved protocol (EC200804062) in accordance with guidelines from Singapore Bioethics Advisory Committee which stated that the decision to donate the fetal tissue must be made independently from any decision to abort.[59] Only patients who have already consented to Termination of Pregnancy (TOP) in KKH Outpatient Clinic were recruited. Recruitment was carried out in strict adherence to KKH IRB's regulations to ensure patient's rights and privacy, and to provide confidential counseling for patient's fully informed consent to voluntary donation. TOP for fetal abnormalities and sexual assault cases and in minor (16 and below) were excluded. Patients with medical problems were also excluded.

The aborted specimens were collected in special sterile plastic bottles and sent to the hospital's Department of Laboratory Medicine for full pathological examinations. Appropriate pieces of fetal tissues were dissected, washed several times in sterile saline, minced, and placed in DMEM supplemented with 10% serum replacement medium, EGF (20 ηg/ml) and FGF2 (20 ηg/ml) to attach to plastic tissue culture dishes for 24-48 h. Under this condition, MSCs whose defining characteristic is adherence to plastic migrated out of the tissues and adherence to the plastic culture dish. The large tissue pieces are then washed off leaving a homogenous cell culture. The cells were maintained at 25%-80% confluency or 15-50,000 cells per cm2 and were split 1:4 at confluency by trypsinization. On reaching 2 × 107 cells usually within 2 weeks, the culture was designated P1. Master cell banks of early passage cells grown in culture medium supplemented with animal replacement medium were set up for all the lines. For all experimental work described in this study, cells at p10 were expanded in HuES Expansion medium containing 10% ES cell fetal bovine serum 1% l-glutamine, 1% non essential amino acids, and 88% DMEM (high glucose, no sodium pyruvate). All medium components were obtained from Invitrogen Corporation, Carlsbad, CA. Differentiation of the fetal MSCs to adipocytes, chondrocytes and osteocytes was performed using adipogenic, chondrogenic and osteogenic hMSC Differentiation BulletKits, respectively (Lonza, Walkersville, MD) as per manufacturer' instructions. Karyotyping by G-banding was performed at the Cytogenetics Laboratory, KKH.

Telomerase activity

Relative telomerase activity was measured by SYBR® Green real time quantitative telomeric repeat amplification protocol assay using a modified method as described by Wege et al.[60] Briefly, 3 million cells were harvested and cell lysate was prepared using a commercially available mammalian cell extraction kit (BioVision, Singapore). The composition of the reagents for the PCR amplification was 1 µg of protein cell lysate, 10 µl of 2× SYBR Green Super Mix (BioRad, Singapore) with 0.1 µg of TS primer (5'-AATCCGTCGAGCAGACTT-3'), 0.1 µg of ACX primer (5'-GCGCGG[CTTACC]3CTAACC-3') and 10 mM EGTA in a total volume of 25 µl. The reaction was first incubated at 25°C for 20 min to allow the telomerase in the cell lysate to elongate the TS primers followed by 2 min incubation at 95 °C to inactivate telomerase activity and denature the primers. The telomerase product was amplified by PCR for 40 cycles of 95°C for 30 s and 60°C for 90 s. The relative telomerase activity was assessed against that of HEK cells using the threshold cycle number (or Ct value) for 1 µg protein cell lysate.

Surface antigen analysis

Expression of cell surface antigens on fetal MSCs was analyzed using flow cytometry. The cells were trypsinized for 5 min, centrifuged, resuspended in culture media and incubated in a bacterial culture dish for 1 h in a 37°C, 5% CO2 incubator. The cells were then collected, centrifuged, and washed in 2% FBS. A total of 2.5 × 105 cells were then incubated with each of the following conjugated monoclonal antibodies: CD29-PE, CD44-FITC, CD49a-PE, CD49e-PE, CD105-FITC, CD166-PE, CD73-FITC, CD34-FITC, and CD45-FITC (PharMingen, San Diego, CA) for 60 min on ice. After incubation, cells were washed and resuspended in 2% FBS. Nonspecific fluorescence was determined by incubation of similar cell aliquots with isotype-matched mouse monoclonal antibodies (PharMingen, San Diego, CA). Data were analyzed by collecting 20,000 events on a BD FACSCalibur™ Flow Cytometer (BD Biosciences, San Jose, CA) instrument using CELLQuest software.

Quantitative RT-PCR

Total RNA was extracted from cells using TRIzol® LS Reagent (Invitrogen Corporation, Carlsbad, CA) according to manufacturer's instruction. Total RNA was converted to cDNA using the High Capacity cDNA Reverse Transcription Kit (Applied Biosystems Inc., Foster City, CA) that was based on oligo-dT primed reverse transcription. Real time PCR was performed on a StepOne™ Plus Real-Time PCR System (Applied Biosystems Inc, Foster City, CA) using 2× Fast SYBR® Green Master Mix (Applied Biosystems Inc, Foster City, CA) according to manufacturer's instruction. The primers for OCT4 were 5'-AGTGAACAGGGAATGGGTGAA-3' and 5'-AAG CGG CAG ATG GTC GT-3', and for SOX2 were 5'-TGAGAGAAAGAAGAGGAGAGA-3' and 5'-TGGGGGAAAAAAAGAGAGAGG-3'.

Illumina gene chip analysis

Total RNA was prepared in technical triplicates from different passages of F1lb (p10, p12, p14), F1ki (p12, p14, p16), F2lb (p10, p12, p14), F3lb (p10, p12, p14) and F3li (p10, p16), and from two technical replicates of the previously described hESC-MSCs line, Hues9.E1 (p19). Five hundred nanograms of RNA was converted to biotinylated cRNA using the Illumina RNA Amplification Kit (Ambion, Inc., Austin, TX) according to the manufacturer's directions. Seven hundred fifty nanograms of the biotinylated cRNA was hybridized to the Sentrix HumanRef-8 Expression BeadChip Version 3 (Illumina, Inc., San Diego, CA), and washing and scanning were performed according to the Illumina BeadStation 500× manual. The data were analyzed using Genespring GX 10. Quantile normalization was performed by a shift to 75th percentile, and the normalized data were baseline transformed to the median of all samples.

SDS-PAGE analysis and western blot hybridization

For SDS-PAGE analysis, total proteins in CM were separated on 4-12% SDS-polyacrylamide gels and stained with silver. For western blot hybridization, the proteins were electroblotted onto a nitrocellulose membrane after first separating on an SDS-PAGE. The membrane was blocked and incubated with the primary anti-human antibodies that included 1:60 dilution of mouse anti-CD9, 1:60 dilution of mouse anti-CD81, 1:56 dilution of mouse anti-Alix, 1:200 dilution of mouse anti-pyruvate kinase (PK), 1:60 dilution of mouse anti-SOD-1 or 1:60 dilution of goat anti-TSP-1. The blot was then incubated with a horseradish peroxidase-coupled secondary antibody. The secondary antibodies used were 1:1250 or 1:1364 dilution of goat anti-mouse IgG or 1:1364 dilution of donkey anti-goat IgG. All antibodies were obtained from Santa Cruz Biotechnology, Santa Cruz, CA except mouse anti-PK which is from Abcam

Inc., Cambridge, MA. The blot was then incubated with HRP-enhanced chemiluminescent substrate (Thermo Fisher Scientific Inc., Waltham, MA) and then exposed to an X-ray film.

HPLC purification of microparticles

The instrument setup consisted of a liquid chromatography system with a binary pump, an auto injector, a thermostated column oven and a UV-visible detector operated by the Class VP software from Shimadzu Corporation (Kyoto, Japan). The Chromatography columns used were TSK Guard column SWXL, 6 × 40 mm and TSK gel G4000 SWXL, 7.8 × 300 mm from Tosoh Corporation (Tokyo, Japan). The detectors Dawn 8 (light scattering), Optilab (refractive index) and QELS (dynamic light scattering) were connected in a series following the UV-visible detector. The last three detectors were from Wyatt Technology Corporation (California, USA) and were operated by the ASTRA software. The components of the sample were separated by size exclusion, that is, the larger molecules will elute before the smaller molecules. The eluent buffer used was 20 mM phosphate buffer with 150 mM of NaCl at pH 7.2. This buffer was filtered through a pore size of 0.1 µm and degassed for 15 min before use. The chromatography system was equilibrated at a flow rate of 0.5 ml/min until the signal in Dawn 8 stabilized at around 0.3 detector voltage units. The UV-visible detector was set at 220 ηm and the column was oven equilibrated to 25°C. The elution mode was isocratic and the run time was 40 min. The volume of sample injected ranged from 50 to 100 µl. The hydrodynamic radius, Rh was computed by the QELS and Dawn 8 detectors. The highest count rate (Hz) at the peak apex was taken as the Rh. Peaks of the separated components visualized at 220 ηm were collected as fractions for further characterization studies.

Testing secretion for cardioprotection

The secretion was prepared by growing the fetal MSCs in a chemically defined serum-free culture medium for 3 days as previously described.[22] Briefly, cells at p12 were first expanded in serum-containing culture medium as described above. At p15, 80% confluent cell cultures were washed three times with PBS and then incubated in a chemically defined medium consisting of DMEM without phenol red (Invitrogen Corporation, Carlsbad, CA) and supplemented with insulin, transferrin, and selenoprotein (ITS) (Invitrogen Corporation, Carlsbad, CA), 5 ηg/ml FGF2 (Invitrogen Corporation, Carlsbad, CA), 5 ng/ml PDGF AB (Peprotech, Rocky Hill, NJ), glutamine-penicillin-streptomycin, and β-mercaptoethanol overnight. The cell culture was then washed with PBS and replaced with fresh chemically defined medium for another 3 days to produce the conditioned medium. This CM was collected and clarified by centrifugation at 500 × g. The clarified CM concentrated 50 times by reducing its volume by a factor of 50 using a tangential flow filtration system with membrane MW cutoff of 100 kDa (Satorius, Goettingen, Germany). The use of a membrane MW cutoff of 100 kDa allows molecules with MW of less than 100 kDa to pass through the filter resulting a preferential loss of molecules less than 100 kDa. The concentrated CM was then sterilized by filtration through a 220 ηm filter.

The CM was tested in a mouse model of MI/R injury. MI was induced by 30 min left coronary artery (LCA) occlusion and subsequent reperfusion. Five minutes before reperfusion, mice were intravenously infused with 200 µl saline diluted CM containing 3 µg protein for Hues9.E1 (hESC-MSCs) CM or 150 µg protein for fetal MSC CM or 10 µg protein for HPLC F1 via the tail vein. Control animals were infused with 200 µl saline. After 24 h of reperfusion, infarct size (IS) as a percentage of the area at risk (AAR) was assessed using Evans' blue dye injection and TTC staining as described previously.[36]

Statistical analysis

Two-way ANOVA with post-hoc Dunnett was used to test the difference in infarct size between groups. Correlation coefficient of each pairs of array was assessed using Pearson correlation test.

REFERENCES

1 Le BK, Pittenger M. Mesenchymal stem cells: progress toward promise. Cytotherapy. 2005;7:36-45.

2 Atsma DE, Fibbe WE, Rabelink TJ. Opportunities and challenges for mesenchymal stem cell-mediated heart repair. Curr Opin Lipidol. 2007;18:645-649.

3 bdel-Latif A, Bolli R, Tleyjeh IM, Montori VM, Perin EC, Hornung CA, Zuba-Surma EK, Al-Mallah M, Dawn B. Adult bone marrow-derived cells for cardiac repair: a systematic review and meta-analysis. Arch Intern Med. 2007;167:989-997.

4 Behfar A, Terzic A. Optimizing adult mesenchymal stem cells for heart repair. J Mol Cell Cardiol. 2007;42:283-284.

5 Gnecchi M, He H, Liang OD, Melo LG, Morello F, Mu H, Noiseux N, Zhang L, Pratt RE, Ingwall JS, Dzau VJ. Paracrine action accounts for marked protection of ischemic heart by Akt-modified mesenchymal stem cells. Nat Med. 2005;11:367-368.

6 Mazhari R, Hare JM. Advances in cell-based therapy for structural heart disease. Prog Cardiovasc Dis. 2007;49:387-395.

7 Minguell JJ, Erices A. Mesenchymal stem cells and the treatment of cardiac disease. Exp Biol Med (Maywood). 2006;231:39-49.

8 Ohnishi S, Nagaya N. Prepare cells to repair the heart: mesenchymal stem cells for the treatment of heart failure. Am J Nephrol. 2007;27:301-307.

9 Schuleri KH, Boyle AJ, Hare JM. Mesenchymal stem cells for cardiac regenerative therapy. Handb Exp Pharmacol. 2007:195-218.

10 Caplan AI, Dennis JE. Mesenchymal stem cells as trophic mediators. J Cell Biochem. 2006;98:1076-1084.

11 Kinnaird T, Stabile E, Burnett MS, Shou M, Lee CW, Barr S, Fuchs S, Epstein SE. Local delivery of marrow-derived stromal cells augments collateral perfusion through paracrine mechanisms. Circulation. 2004;109:1543-1549.

12 Leedham SJ, Brittan M, McDonald SA, Wright NA. Intestinal stem cells. J Cell Mol Med. 2005;9:11-24.

13 Gnecchi M, He H, Noiseux N, Liang OD, Zhang L, Morello F, Mu H, Melo LG, Pratt RE, Ingwall JS, Dzau VJ. Evidence supporting paracrine hypothesis for Akt-modified mesenchymal stem cell-mediated cardiac protection and functional improvement. FASEB J. 2006;20:661-669.

14 Mayer H, Bertram H, Lindenmaier W, Korff T, Weber H, Weich H. Vascular endothelial growth factor (VEGF-A) expression in human mesenchymal stem cells: autocrine and paracrine role on osteoblastic and endothelial differentiation. J Cell Biochem. 2005;95:827-839.

15 Miyahara Y, Nagaya N, Kataoka M, Yanagawa B, Tanaka K, Hao H, Ishino K, Ishida H, Shimizu T, Kangawa K, Sano S, Okano T, Kitamura S, Mori H. Monolayered mesenchymal stem cells repair scarred myocardium after myocardial infarction. Nat Med. 2006;12:459-465.

16 Nakagami H, Maeda K, Morishita R, Iguchi S, Nishikawa T, Takami Y, Kikuchi Y, Saito Y, Tamai K, Ogihara T, Kaneda Y. Novel autologous cell therapy in ischemic limb disease through growth factor secretion by cultured adipose tissue-derived stromal cells. Arterioscler Thromb Vasc Biol. 2005;25:2542-2547.

17 Patschan D, Plotkin M, Goligorsky MS. Therapeutic use of stem and endothelial progenitor cells in acute renal injury: ca ira. Curr Opin Pharmacol. 2006;6:176-183.

18 Togel F, Hu Z, Weiss K, Isaac J, Lange C, Westenfelder C. Administered mesenchymal stem cells protect against ischemic acute renal failure through differentiation-independent mechanisms. Am J Physiol Renal Physiol. 2005;289:F31-F42.

19 Cheng L, Qasba P, Vanguri P, Thiede MA. Human mesenchymal stem cells support megakaryocyte and proplatelet formation from CD34(+) hematopoietic progenitor cells. J Cell Physiol. 2000;184:58-69.

20 Van Overstraeten-Schlogel N, Beguin Y, Gothot A. Role of stromal-derived factor-1 in the hematopoietic-supporting activity of human mesenchymal stem cells. Eur J Haematol. 2006;76:488-493.

21 Lian Q, Lye E, Suan YK, Khia Way TE, Salto-Tellez M, Liu TM, Palanisamy N, El Oakley RM, Lee EH, Lim B, Lim SK. Derivation of clinically compliant MSCs from CD105+. Stem Cells. 2007;25:425-436.

22 Sze SK, de Kleijn DP, Lai RC, Khia Way TE, Zhao H, Yeo KS, Low TY, Lian Q, Lee CN, Mitchell W, El Oakley RM, Lim SK. Elucidating the secretion proteome of human embryonic stem cell-derived mesenchymal stem cells. Mol Cell Proteomics. 2007;6:1680-1689.

23 Timmers L, Lim SK, Arslan F, Armstrong JS, Hoefer IE, Doevendans PA, Piek JJ, El Oakley RM, Choo A, Lee CN, Pasterkamp G, de Kleijn DP. Reduction of myocardial infarct size by human mesenchymal stem cell conditioned medium. Stem Cell Res. 2007;1:129-137.

24 Thery C, Ostrowski M, Segura E. Membrane vesicles as conveyors of immune responses. Nat Rev Immunol. 2009;9:581-593.

25 Dominici M, Le BK, Mueller I, Slaper-Cortenbach I, Marini F, Krause D, Deans R, Keating A, Prockop D, Horwitz E. Minimal criteria for defining multipotent mesenchymal stromal cells. The International Society for Cellular Therapy position statement. Cytotherapy. 2006;8:315-317.

26 Guillot PV, Gotherstrom C, Chan J, Kurata H, Fisk NM. Human first-trimester fetal MSC express pluripotency markers and grow faster and have longer telomeres than adult MSC. Stem Cells. 2007;25:646-654.

27 Jo CH, Kim OS, Park EY, Kim BJ, Lee JH, Kang SB, Lee JH, Han HS, Rhee SH, Yoon KS. Fetal mesenchymal stem cells derived from human umbilical cord sustain primitive characteristics during extensive expansion. Cell Tissue Res. 2008;334:423-433.

28 Kermani AJ, Fathi F, Mowla SJ. Characterization and genetic manipulation of human umbilical cord vein mesenchymal stem cells: potential application in cell-based gene therapy. Rejuvenation Res. 2008;11:379-386.

29 Peng HH, Wang TH, Chao AS, Chang SD. Isolation and differentiation of human mesenchymal stem cells obtained from second trimester amniotic fluid; experiments at Chang Gung Memorial Hospital. Chang Gung Med J. 2007;30:402-407.

30 Poloni A, Rosini V, Mondini E, Maurizi G, Mancini S, Discepoli G, Biasio S, Battaglini G, Berardinelli E, Serrani F, Leoni P. Characterization and expansion of mesenchymal progenitor cells from first-trimester chorionic villi of human placenta. Cytotherapy. 2008;10:690-697.

31 Roubelakis MG, Pappa KI, Bitsika V, Zagoura D, Vlahou A, Papadaki HA, Antsaklis A, Anagnou NP. Molecular and proteomic characterization of human mesenchymal stem cells derived from amniotic fluid: comparison to bone marrow mesenchymal stem cells. Stem Cells Dev. 2007;16:931-952.

32 Tsai MS, Lee JL, Chang YJ, Hwang SM. Isolation of human multipotent mesenchymal stem cells from second-trimester amniotic fluid using a novel two-stage culture protocol. Hum Reprod. 2004;19:1450-1456.

33 Wang XY, Lan Y, He WY, Zhang L, Yao HY, Hou CM, Tong Y, Liu YL, Yang G, Liu XD, Yang X, Liu B, Mao N. Identification of mesenchymal stem cells in aorta-gonad-mesonephros and yolk sac of human embryos. Blood. 2008;111:2436-2443.

34 Yen ML, Chien CC, Chiu IM, Huang HI, Chen YC, Hu HI, Yen BL. Multilineage differentiation and characterization of the human fetal osteoblastic 1.19 cell line: a possible in vitro model of human mesenchymal progenitors. Stem Cells. 2007;25:125-131.

35 Zhang ZY, Teoh SH, Chong MS, Schantz JT, Fisk NM, Choolani MA, Chan J. Superior osteogenic capacity for bone tissue engineering of fetal compared with perinatal and adult mesenchymal stem cells. Stem Cells. 2009;27:126-137.

36 Arslan F, Smeets MB, O'Neill LA, Keogh B, McGuirk P, Timmers L, Tersteeg C, Hoefer IE, Doevendans PA, Pasterkamp G, de Kleijn DP. Myocardial ischemia/reperfusion injury is mediated by leukocytic toll-like receptor-2 and reduced by systemic administration of a novel anti-toll-like receptor-2 antibody. Circulation. 2010;121:80-90.

37 Tang YL, Zhao Q, Qin X, Shen L, Cheng L, Ge J, Phillips MI. Paracrine action enhances the effects of autologous mesenchymal stem cell transplantation on vascular regeneration in rat model of myocardial infarction. Ann Thorac Surg. 2005;80:229-236.

38 Barry FP, Murphy JM. Mesenchymal stem cells: clinical applications and biological characterization. Int J Biochem Cell Biol. 2004;36:568-584.

39 Javazon EH, Beggs KJ, Flake AW. Mesenchymal stem cells: paradoxes of passaging. Exp Hematol. 2004;32:414-425.

40 Majumdar MK, Keane-Moore M, Buyaner D, Hardy WB, Moorman MA, McIntosh KR, Mosca JD. Characterization and functionality of cell surface molecules on human mesenchymal stem cells. J Biomed Sci. 2003;10:228-241.

41 Aharon A, Brenner B. Microparticles, thrombosis and cancer. Best Pract Res Clin Haematol. 2009;22:61-69.

42 Burnier L, Fontana P, Kwak BR, ngelillo-Scherrer A. Cell-derived microparticles in haemostasis and vascular medicine. Thromb Haemost. 2009;101:439-451.

43 Castellana D, Kunzelmann C, Freyssinet JM. Pathophysiologic significance of procoagulant microvesicles in cancer disease and progression. Hamostaseologie. 2009;29:51-57.

44 Chironi GN, Boulanger CM, Simon A, gnat-George F, Freyssinet JM, Tedgui A. Endothelial microparticles in diseases. Cell Tissue Res. 2009;335:143-151.

45 Meziani F, Tesse A, Andriantsitohaina R. Microparticles are vectors of paradoxical information in vascular cells including the endothelium: role in health and diseases. Pharmacol Rep. 2008;60:75-84.

46 Redman CW, Sargent IL. Circulating microparticles in normal pregnancy and pre-eclampsia. Placenta. 2008;29 Suppl A:S73-S77.

47 Zwicker JI. Tissue factor-bearing microparticles and cancer. Semin Thromb Hemost. 2008;34:195-198.

48 Al-Nedawi K, Meehan B, Rak J. Microvesicles: messengers and mediators of tumor progression. Cell Cycle. 2009;8:2014-2018.

49 Davizon P, Lopez JA. Microparticles and thrombotic disease. Curr Opin Hematol. 2009;16:334-341.

50 Doeuvre L, Plawinski L, Toti F, ngles-Cano E. Cell-derived microparticles: a new challenge in neuroscience. J Neurochem. 2009;110:457-468.

51 Esmon CT. Basic mechanisms and pathogenesis of venous thrombosis. Blood Rev. 2009;23:225-229.

52 Hartvigsen K, Chou MY, Hansen LF, Shaw PX, Tsimikas S, Binder CJ, Witztum JL. The role of innate immunity in atherogenesis. J Lipid Res. 2009;50 Suppl:S388-S393.

53 Horstman LL, Jy W, Bidot CJ, Nordberg ML, Minagar A, Alexander JS, Kelley RE, Ahn YS. Potential roles of cell-derived microparticles in ischemic brain disease. Neurol Res. 2009;31:799-806.

54 Milsom C, Rak J. Tissue factor and cancer. Pathophysiol Haemost Thromb. 2008;36:160-176.

55 Sabatier F, Camoin-Jau L, Anfosso F, Sampol J, gnat-George F. Circulating endothelial cells, microparticles and progenitors: key players towards the definition of vascular competence. J Cell Mol Med. 2009;13:454-471.

56 Stein E, McMahon B, Kwaan H, Altman JK, Frankfurt O, Tallman MS. The coagulopathy of acute promyelocytic leukaemia revisited. Best Pract Res Clin Haematol. 2009;22:153-163.

57 Benameur T, Andriantsitohaina R, Martinez MC. Therapeutic potential of plasma membrane-derived microparticles. Pharmacol Rep. 2009;61:49-57.

58 Knight DR. Editorial overview: cardioprotective drugs for myocardial ischemic injury--a therapeutic area at risk. Curr Opin Investig Drugs. 2007;8:190-192.

59 Kian CT, Leng TS. The Singapore approach to human stem cell research, therapeutic and reproductive cloning. Bioethics. 2005;19:290-303.

60 Wege H, Chui MS, Le HT, Tran JM, Zern MA. SYBR Green real-time telomeric repeat amplification protocol for the rapid quantification of telomerase activity. Nucleic Acids Res. 2003;31:E3.

CHAPTER 6

This chapter describes that immortalization of MSCs is a good option to have access to infinite supply of cells and high production rate of therapeutic exosomes

Tian Sheng Chen, Fatih Arslan, Yijun Yin, Soon Sim Tan, Ruenn Chai Lai, Andre Boon Hwa Choo, Jayanthi Padmanabhan, Chuen Neng Lee, Dominique P. de Kleijn, Sai Kiang Lim

Enabling a robust scalable manufacturing process for therapeutic exosomes through oncogenic immortalization of human ESC-derived MSCs

Background

Exosomes or secreted bi-lipid vesicles from human ESC-derived mesenchymal stem cells (hESC-MSCs) have been shown to reduce myocardial ischemia/reperfusion (I/R) injury in animal models. However, as hESC-MSCs are not infinitely expansible, large scale production of these exosomes would require replenishment of hESC-MSC through derivation from hESCs and incur recurring costs for testing and validation of each new batch. Our aim was therefore to investigate if MYC immortalization of hESC-MSC would circumvent this constraint without compromising the production of therapeutically efficacious exosomes.

Methods and Results

The hESC-MSCs were transfected by lentivirus carrying a MYC gene. The transformed cells were analyzed for MYC transgene integration, transcript and protein levels, and surface markers, rate of cell cycling, telomerase activity, karyotype, genome-wide gene expression and differentiation potential. The exosomes were isolated by HPLC fractionation and tested in a mouse model of myocardial I/R injury, and infarct sizes were further assessed by using Evans' blue dye injection and TTC staining. MYC-transformed MSCs largely resembled the parental hESC-MSCs with major differences being reduced plastic adherence, faster growth, failure to senesce, increased MYC protein expression, and loss of in vitro adipogenic potential that technically rendered the transformed cells as non-MSCs. Unexpectedly, exosomes from MYC-transformed MSCs were able to reduce relative infarct size in a mouse model of myocardial I/R injury indicating that the capacity for producing therapeutic exosomes was preserved.

Conclusions

Our results demonstrated that MYC transformation is a practical strategy in ensuring an infinite supply of cells for the production of exosomes in the milligram range as either therapeutic agents or delivery vehicles. In addition, the increased proliferative rate by MYC transformation reduces the time for cell production and thereby may reduce production costs.

J Transl Med. 2011;9(1):47

Mesenchymal stem cells (MSCs) are multipotent stem cells that have a limited but robust potential to differentiate into mesenchymal cell types, e.g. adipocytes, chondrocytes and osteocytes, with negligible risk of teratoma formation. MSC transplantation has been used in clinical trials and animal models to treat musculoskeletal injuries, improve cardiac function in cardiovascular disease and ameliorate the severity of graft-versus-host-disease.[1] In recent years, MSC transplantations have demonstrated therapeutic efficacy in treating different diseases but the underlying mechanism has been controversial.[2-9] Some reports have suggested that factors secreted by MSCs were responsible for the therapeutic effect on arteriogenesis, stem cell crypt in the intestine, ischemic injury, and hematopoiesis.[5, 10-20] In support of this paracrine hypothesis, many studies have observed that MSCs secrete cytokines, chemokines and growth factors that could potentially repair injured cardiac tissue mainly through cardiac and vascular tissue growth and regeneration.[10, 21] This paracrine hypothesis could potentially provide for a non-cell based alternative for using MSC in treatment of cardiovascular disease.[22] Non-cell based therapies as opposed to cell-based therapies are generally easier to manufacture and are safer as they are non-viable and do not elicit immune rejection.

We have previously demonstrated that culture medium conditioned by MSCs that were derived from human embryonic stem cells (HuES9.E1 MSCs) or fetal tissues could protect the heart from myocardial (I/R) injury and reduce infarct size in both pig and mouse models of myocardial I/R injury. Subsequent studies demonstrated that this cardioprotection was mediated by exosomes or microparticles of about 50-100 ηm in diameter and these microparticles carry both protein and RNA load.[23-27] These exosomes could be purified as a population of homogenously sized particles by size exclusion on HPLC and reduced infarct size in a mouse model of myocardial I/R injury at about a tenth of the dosage of the conditioned medium.[24, 25]

The identification of exosomes as the therapeutic agent in the MSC secretion could potentially provides for a biologic- rather than cell-based treatment modality. Unlike cells, exosomes do not elicit acute immune rejection and being non-viable and much smaller, they pose less safety risks such as the formation of tumor or embolism. Furthermore unlike cell-based therapies where there is a need to maintain viability, manufacture and storage of non-viable exosomes is less complex and therefore less costly. Besides being therapeutic agents, exosomes have been advocated as “natural” drug delivery vehicles.[28] These lipid vesicles could be loaded with therapeutic agents and be used to deliver the agents in a cell type specific manner. hESC- MSCs could be the ideal cellular source for the efficient production of exosomes. We have demonstrated that these cells could be grown in a chemically defined medium during the production and harvest of exosomes and these exosomes could be purified by HPLC to generate a population of homogenously sized particles.[24] Another advantage is that these cells were derived from hESCs, an infinitely expansible cell source.

While hESC-MSCs are also highly expansible in culture, they can only undergo a finite number of cell divisions. Hereafter, their growth is arrested and they senesce, unlike their parental hESC. Therefore there will be a need to constantly derive new batches of MSCs from hESCs to replenish the cell source of exosomes with each derivation necessitating recurring cost of derivation, testing and validation. To circumvent this need for re-derivation and ensure an infinite supply of identical MSCs for commercially sustainable production of exosomes as therapeutic agents or delivery vehicle, we explore the use of oncogenic transformation to bypass senescence. Oncogenic transformation could potentially alter the cell biology and affect the production or the properties of the exosomes. It was previously reported that transfection of v-MYC gene into fetal MSCs immortalized the cells but did not alter the fundament characteristics of these MSCs.[29] Here we transfected the MSCs with a lentiviral vector containing the

MYC gene which encodes for the MYC protein into the previously described hESC derived MSCs (HuES9.E1 MSC) at passage 21 (p21) and passage 16 (p16) to generate a pooled cell line and three independently derived clonal cell lines respectively.[26] We examined the transformed cells according to the ISCT minimal defining criteria for MSCs namely plastic adherence, surface antigen profile of CD29+, CD44+, CD49a+ CD49e+, CD90+, CD105+, CD166+, MHC I+, CD34−, CD45− and HLA-DR−, and potential to differentiate into adipocytes, chondrocytes and osteocytes.[30] The secretion of these cells was evaluated for the presence of exosomes and the therapeutic efficacy of these exosomes were tested in a mouse model of myocardial I/R as previously described.[24]

RESULTS

Transforming HuES9.E1 MSC cultures

HuES9.E1 MSCs at p 21 were infected with either GFP- or MYC-containing lentivirus. The infected cultures were placed under the puromycin selection for three days. Surviving cells were pooled. PCR amplification of genomic DNA demonstrated that the MYC transgene was successfully integrated in the genome (Figure 1a). Unlike the MYC-transfected cells which was pooled to form the E1-MYC 21.1 line, the GFP-transfected cells progressed into senescence with decreasing rate of proliferation and acquiring a much flattened, spreading morphology (Figure 1b) and could not be propagated more than five passages post-transfection. The MYC- transformed cells expressed a 100 fold increase in MYC transcript level relative to the GFP- transfected cells (GFP-MSCs) (Figure 1c) and higher telomerase activity (Figure 1d). To generate independently cloned lines, three HuES9.E1 MSC cultures at p16 were independently transfected and placed under puromycin drug selection. The surviving cell cultures were cloned by limiting dilution to generate three lines, E1-MYC 16.1, E1-MYC 16.2 and E1-MYC 16.3 lines, respectively. The lines were karyotyped by G-banding. The cell morphology of all three cell lines was similar to that of E1-MYC 21.1 line. Only E1-MYC 16.3 line had the parental karyotype of 46 XX with a pericentric inversion of chromosomal 9 between p11 and q13 in 20/20 metaphases, and was therefore used in all the subsequent experiments (Figure 1e).[26] In contrast to their parental cells, the MYC-transformed cells proliferated faster with a population doubling time of 13 hours versus a population doubling time of 19 hours in untransformed MSCs. The average cell cycle time as measured using CFDA cell labelling as previously described was decreased from 19 hours to 11 hours (Figure 1f).[31] The transformed cells effectively bypassed senescence and continued to maintain their proliferative rates for at least another 20 passages. The transformed cells were smaller and rounder in shape with prominent nuclei. At high cell density, these cells lose contact inhibition resulting in the formation of cell clusters (Figure 1b). Consistent with increased proliferation, the cells had higher levels of telomerase activity than GFP-transfected or non transfected cells (Figure 1d).

Assessment of MYC-MSCs

The MYC-MSC culture were assessed according to the ISCT minimal criteria for the definition of human MSCs.[30] As observed earlier (Figure 1b), the culture did not adhere to plastic culture dishes as well as their untransformed MSCs especially at confluency when the cells started to form clusters instead of adhering to the plastic dish as a monolayer. The surface antigen profile of the MYC-transformed cells was quite similar to that of their parental cells except in their negative expression of MHC I. The cells were CD29+, CD44+, CD49a+ CD49e+, CD73+ , CD90+, CD105+, CD166+, MHC I^- , HLA-DR^- , $CD34^-$ and

CD45$^-$ (Figure 2). The in vitro differentiation potential of both polyclonal E1-MYC 21.1 and monoclonal E1-MYC 16.3 cell lines was next examined (Figure 3). Both cell lines differentiated readily into chondrocytes and osteocytes (Figure 3a, b) but not adipocytes. The induction of adipogenesis in MSCs required 4 cycles of a 6-day treatment protocol consisting of 3 days' exposure to induction medium and 3 days' exposure to maintenance medium. We observed that exposure to the induction medium induced death in the MYC-transformed cells but not the untransformed parental cells (Figure 3c). These observations suggested that MYC-transformed cells cannot undergo adipogenic differentiation. Together, these observations demonstrated that unlike a previous report where MYC transformation was observed not to alter the fundamental characteristics of MSCs, we observed here that MYC transformation affected a defining property of MSCs i.e. the potential to undergo adipogenesis.[29]

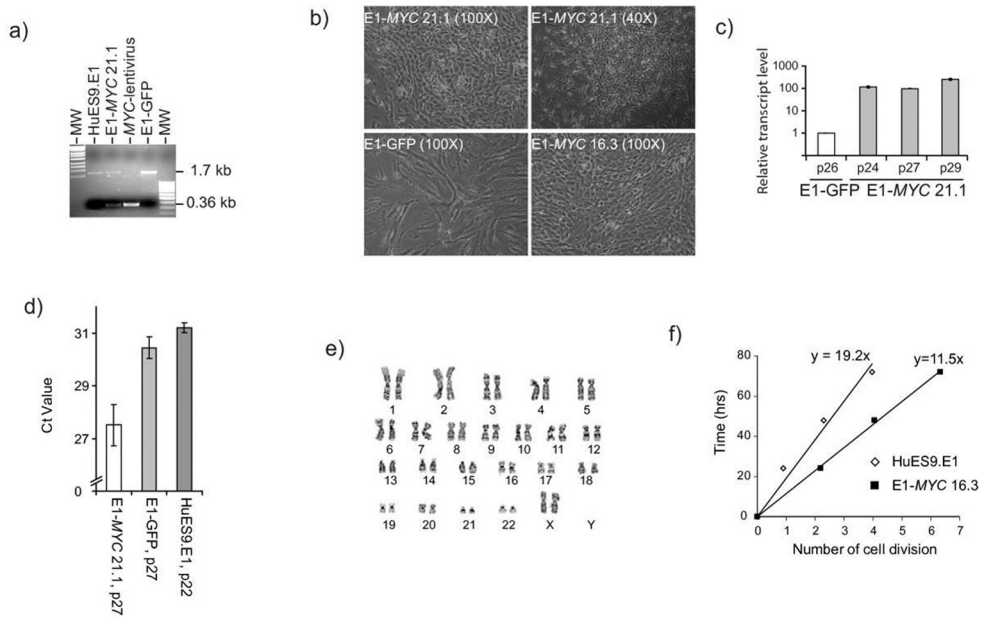

Figure 1. Transformation of hESC-MSC. *(**A**) PCR analysis of cellular DNA from MYC-transfected HuES9.E1 MSCs (E1-MYC 21.1), GFP transfected HuES9.E1 MSCs (E1-GFP) and the parental MSCs, HuES9.E1 (E1). DNA was amplified using primers specific for MYC exon 2 and exon 3, respectively. The expected PCR fragment size for the endogenous MYC gene was1.7 kb and for the transfected MYC cDNA was 0.36 kb as represented by the amplified fragment from the MYC-lentivirus. (**B**) Cell Morphology of transfected MSCs as observed under light microscopy. (**C**) Quantitative RT-PCR was performed on RNA from different passages of E1-MYC 21.1 and GFP-MSCs for the level of MYC and ACTIN mRNA. The relative MYC-transcript level was normalized to that in GFP- MSCs. (**D**) Relative telomerase activity. 1 µg of cell lysate protein was first used to extend a TS primer by telomerase activity and the telomerase product was then quantitated by real time PCR. The Ct value represented the amount of telomerase product and was therefore indirectly proportional to telomerase activity in the lysate. (**E**) Karyotpye analysis of E1-MYC 16.3 by G- banding. (**F**) Rate of cell cycling. Cells were labelled with CFDA and their fluorescence was monitored over time by flow cytometry. The loss of cellular fluorescence at each time point was used to calculate the number of cell division that the cells have undergone.*

Gene expression profile

Genome-wide gene expression profiling of MYC-transformed MSCs and their parental MSCs by microarray hybridisation was performed to assess the relatedness between the cell types. Microarray hybridization was performed in duplicate on Sentrix Human Ref-8 Expression BeadChip using RNA from E1-MYC 16.3 MSCs at p4, p7, and p8, and from the parental HuES9-E1 MSCs at p15 and p16. The gene expression profile (Accession number: GSE25296) among different passages of E1-MYC 16.3 MSCs or among different passages of the parental HuES9-E1 MSCs was highly similar with a correlation coefficient, r2 being greater than 0.98. The correlation coefficient, r2 between E1-MYC 16.1 MSCs and parental HuES9-E1 MSCs, was also relatively high at 0.92 (Figure 4a).

A total of 161 genes was upregulated and 226 genes downregulated at least 2 fold in E1-MYC 16.1 MSCs suggesting that there were changes in gene expression after MYC transformation. These differentially expressed genes were functionally clustered by PANTHER (Protein ANalysis THrough Evolutionary Relationships) in which the observed frequency of genes for each biological process in each gene set

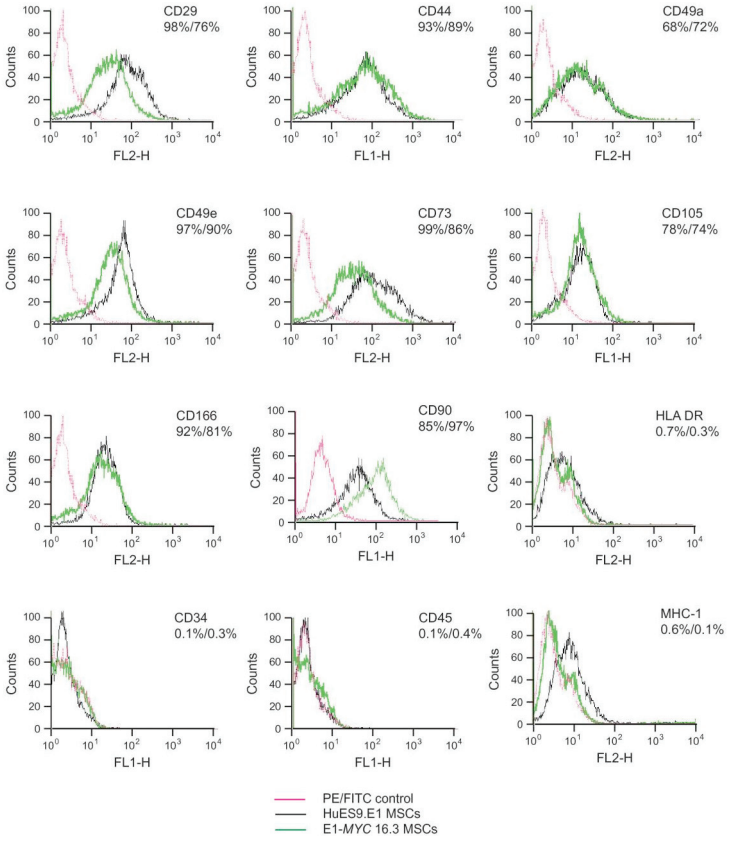

Figure 2. Surface antigen profiling. *HuES9.E1 and E1-MYC 16.3 MSCs were stained with an appropriate antibody conjugated to a fluorescent dye and analyzed by FACS. The fluorescence of HuES9.E1 or E1-MYC 16.3 was the average cellular fluorescence of cells at p16 or p6. Nonspecific fluorescence was assessed by incubating the cells with isotype-matched mouse monoclonal antibodies.*

was compared with the reference frequency which, in this case is the frequency of genes for that biological process in the NCBI database.[32, 33] There were 11 over-represented biological processes for the 161 upregulated genes namely, metabolic process, nucleobase, nucleoside, nucleotide and nucleic acid metabolic process, primary metabolic process, amino acid transport, sulfur metabolic process, organelle organization, mitochondrion organization, peroxisomal transport, cellular amino acid and derivative metabolic process, polyphosphate catabolic process and protein metabolic process. There were 4 under-represented processes: vesicle- mediated transport, exocytosis, cell surface receptor linked signal transduction, and immune system process (Figure 4b). In the 226 downregulated genes, there were 37 over- and 1 under- represented biological processes (Figure 4c). For the up-regulated genes, many of the associated over-represented processes were generally important for increasing cell mass or anabolic activity for cell division and were consistent with the observed increased cell proliferation activity. The under-represented processes, namely vesicle-mediated transport, exocytosis suggested that exosome production might not be affected. For the down-regulated genes, the 37 over-

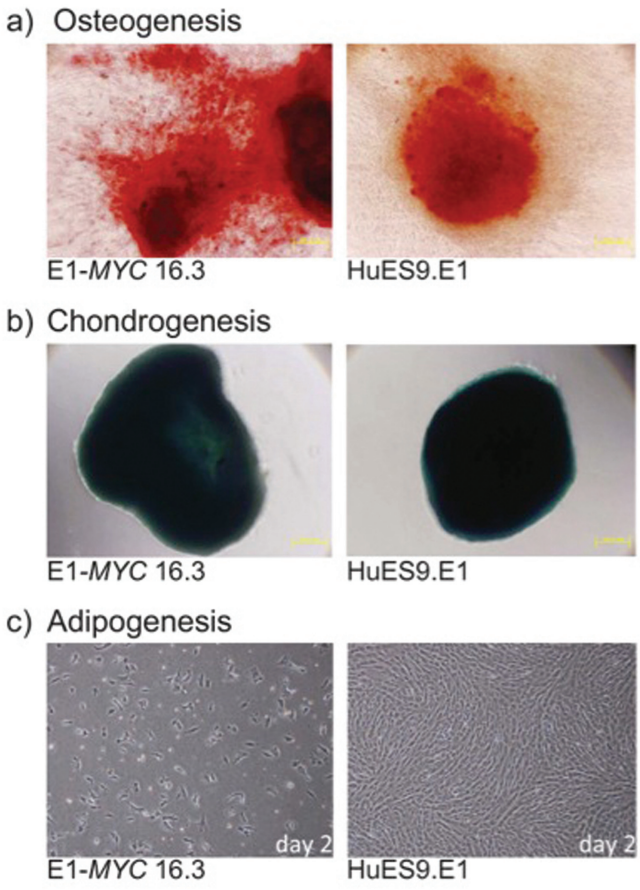

Figure 3. Differentiation of HuES9E1 and E1-MYC 16.3 MSCs*. MSCs were induced to undergo (**A**) osteogenesis and then stained with von Kossa stain; (**B**) chondrogenesis and then stained with Alcian blue; (**C**) adipogenesis where E1-MYC 16.3 and HuES9E1 MSCs were exposed to adipogenesis induction medium for two days. The cells were viewed at 100x magnification.*

represented processes could be broadly classified into processes that are associated with adhesion, differentiation, communication, immune response, cell death and metabolism. These processes were also consistent with some of our observations of the MYC-transformed MSCs, namely reduced adherence to plastic, loss of adipogenic differentiation potential and loss of MHC I expression. Cardioprotective activity of secretion The loss of adipogenic potential in MYC-transformed MSC suggested that other aspects of the characteristics of ESC-derived MSCs such as the production of therapeutic exosomes might also be compromised by the transformation. We had previously demonstrated that exosomes

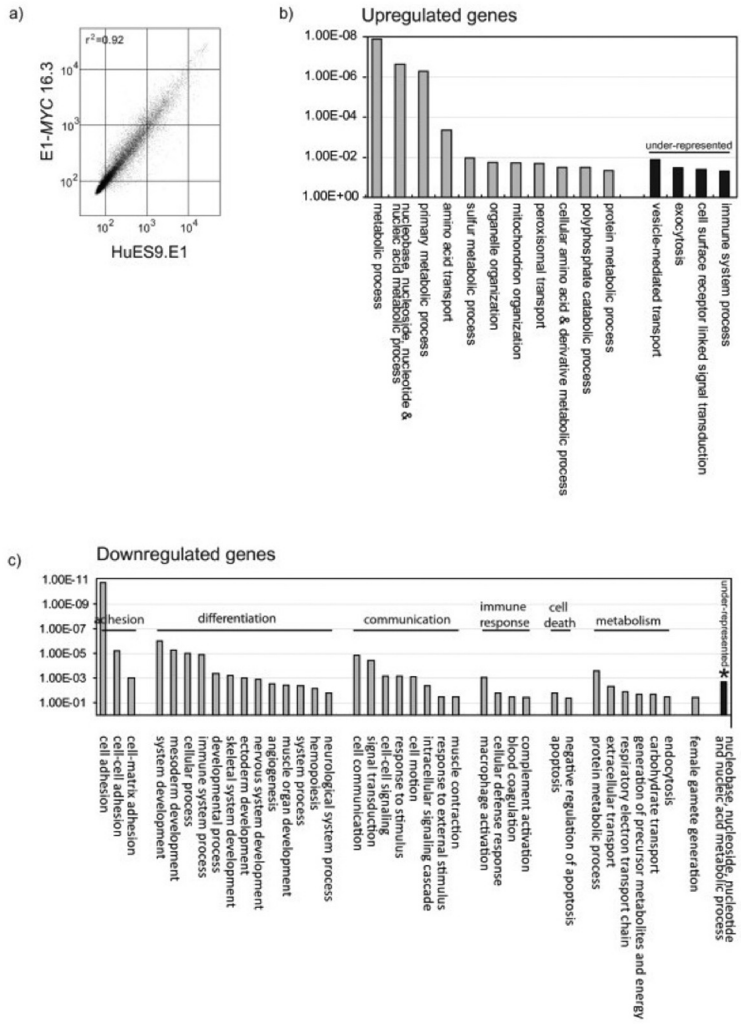

Figure 4. Gene expression analysis. *RNA from HuES9E1 and E1-MYC 16.3 MSCs were hybridized to Sentrix HumanRef-8 Expression BeadChip Version 3 and analyzed by Beadstudio and Genespring GX 10. (**A**) Pairwise comparison of gene expression between HuES9.E1 and E1-MYC 16.3 MSCs using Beadstudio analysis. (**B**), 161 genes that were over-expressed by >2-fold and (**C**) 226 genes that were under-expressed by >2-fold in E1-MYC 16.3 MSCs were analyzed using PANTHER algorithm. The observed frequency of genes for each biological process in each gene set was compared with the reference frequency which, in this case is the frequency of genes for that biological process in the NCBI database. Those biological processes whose observed frequency exceeds the reference frequency with a $p < 0.05$ are considered significant.*

secreted by ESC-derived MSCs was protective in a mouse model of myocardial I/R injury.[24] To test if this aspect was compromised, the transformed cells were grown in a chemically defined medium, the conditioned culture medium harvested and exosomes were purified as previously described.[24, 34] Despite increased MYC transcript and protein levels in the transformed cells, MYC protein was not detectable in the conditioned medium and purified exosomes (Figure 5a). The HPLC protein profile of the conditioned medium was similar to that of conditioned medium from untransformed MSCs (Figure 5b) with the fastest eluting fraction having a retention time of about 12 minutes.[24] Dynamic light scattering analysis of this peak revealed the presence of particles that were within a hydrodynamic radius range of 50-65 ηm. In a typical run, we routinely purified about 1.5 mg of exosomes per liter of conditioned medium. HPLC- purified exosomes from either E1-MYC 21.1 or E1-MYC 16.3 was administered to the mouse model of MYOCARDIAL I/R injury at a dosage of 0.3 or 0.4 µg per mouse respectively (Figure

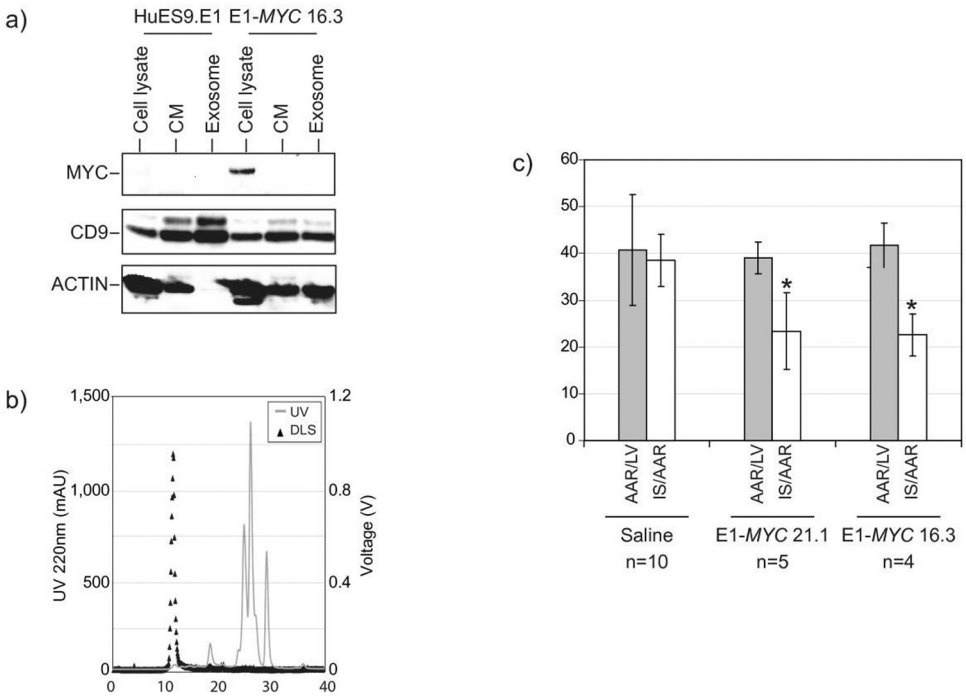

***Figure 5. Analysis of secretion**. (**A**), Western blot analysis. Proteins from cell lysate, conditioned medium (CM), and HPLC purified exosomes of E1MSCs or E1-MYC-MSCs were separated on SDS-PAGE and probed with different antibodies to detect MYC (64 kDa), ACTIN (42 kDa), and CD9 (24 kDa). (**B**) HPLC fractionation and dynamic light scattering of CM from E1-MYC-MSC. CM was fractionated on a HPLC using BioSep S4000, 7.8 mm x 30 cm column. The components in CM were eluted with 20 mM phosphate buffer with 150 mM of NaCl at pH 7.2. The elution mode was isocratic and the run time was 40 minutes. The eluent was monitored for UV absorbance at 220 ηm. Each eluting peak was then analyzed by light scattering. The fastest eluting peak (arrow) was collected for testing in a mouse model of myocardial ischemia/reperfusion injury. (**C**) 0.3 µg HPLC-purified exosomes was administered intravenously to a mouse model of myocardial I/R injury five minutes before reperfusion. Infarct size (IS) as a percentage of the area at risk (AAR) upon treatment with saline (n=10), exosomes from E1- MYC 21.1 (n=5) and exosomes from E1-MYC 16.3 (n=4) were measured. The relative infarct size (IS/AAR) in mice treated with E1-MYC 21.1 exosome or E1-MYC 16.3 exosome was 23.4 ± 8.2%, and 22.6 ± 4.5%, respectively and their relative infarct sizes were significantly lower than the relative infarct size of 38.5 ± 5.6% in saline-treated mice ($p<0.001$ and $p<0.002$, respectively).*

5c). The area at risk (AAR) as a percentage of left ventricular (LV) area in E1-MYC 21.1 exosome, E1-MYC 16.3 exosome, or the saline-treated control group was similar at 39.1 ±3.4% (n=5), 41.7±4.7% (n=4) and 40.8 ±11.8% (n=10), respectively. The relative infarct size (IS/AAR) in mice treated with E1-MYC 21.1 exosome or E1-MYC 16.3 exosome was 23.4 ± 8.2%, and 22.6 ± 4.5%, respectively and their relative infarct sizes were significantly lower than the relative infarct size of 38.5 ±5.6% in saline-treated mice ($p<0.001$ and $p<0.002$, respectively).

DISCUSSION

This report describes the transformation of human ESC-derived MSCs by over-expression of MYC gene. This transformation enabled the cells to bypass senescence, increase telomerase activity and enhance proliferation. Generally, genome-wide gene expression between the transformed cells versus their parental cells was conserved with a correlation coefficient of 0.92. The transformed cells also have the characteristic surface antigen profile: CD29+, CD44+, CD49a+, CD49e+, CD90+, CD105+, CD166+, MHC I- , HLA-DR- , CD34- and CD45- . Although the transformed cells fulfilled most of fundamental requisites in ISCT minimal criteria for the definition of human MSCs, they nevertheless have an altered MSC phenotype.[30] They exhibited reduced adherence to plastic and failed to undergo adipogenesis which ironically was reported to be most robust among the three fundamental MSC differentiation potentials in the human ESC-derived MSCs.[26] Therefore, in contrast to a previous report that observed no fundamental changes in MSC properties after MYC transformation, we observed some fundamental changes in MYC-transformed cells such that the cells no longer fulfilled the ISCT minimal criteria for the definition of human MSCs and are technically not MSCs.[29, 30] Despite the loss of a defining MSC property, the MYC-transformed cells continued to secrete exosomes that could reduce infarct size in a mouse model of myocardial I/R injury. The relative infarct size was 23.4 ± 8.2% and 22.6 ± 4.5% in mice treated with exosomes from the polyclonal and monoclonal lines, respectively. The relative infarct size in saline treated mice was 38.5 ±5.6%. These relative infarct sizes were comparable to those observed in mice treated with exosomes from the untransformed parental MSCs or fetal MSCs.[24, 25] The relative infarct sizes in mice treated with these exosomes were 17.0 ± 3.6% and 18.1 ± 2.0%, respectively against a 34.5 ± 3.3% in saline treated mice. Therefore, both independently transformed polyclonal and monoclonal lines also produced exosomes with similar therapeutic efficacy as those produced by untransformed MSCs indicating that exosome production was independent of the transformation and was consistent and reproducible. The significant reduction of infarct size by exosome treatment and the well established correlation between infarct size and subsequent adverse remodeling suggests that exosome treatment would enhance the prognostic outcome of reperfusion therapy.[35] We noted that MYC protein was present in the transformed cells but was not detectable in either the conditioned medium or exosome. As onco-protein unlike oncogene cannot be replicated or amplified, the risk of tumorigenesis by exosomes from MYC- transformed cells is further mitigated. The use of lentiviral vectors for the transformation of the cells poses another potential safety risk. Since the secreted exosome and not the transformed cells will be used as therapeutic agents, the risk from the integration of lentivirus is mitigated. Also the use of newer generation of lentiviral vector which in our case is a third generation lentiviral vector further reduces the risk of producing infectious recombinant viral particles. For the actual manufacture of therapeutic exosomes, we propose transforming the cells using some of the lentiviral vectors that are currently being tested in clinical trials.[36] This will further reduce

the risks associated with the use of lentiviral vectors for transformation.

CONCLUSION

In summary, MYC transformation represents a practical strategy in ensuring an infinite supply of cells for the production of exosomes in the milligram range as either therapeutic agents or delivery vehicles. In addition, the increased proliferative rate reduces the time for cell production and thereby reduces production costs. In conclusion, this work despite the lack of exciting novel scientific insights into biological processes provides a critical enabling technology for the development of a cost effective production process for consistent supplies of HPLC- purified therapeutic human exosomes.

Acknowledgements

We gratefully acknowledge Kong Meng Hoi and Eddy Tan at the Bioprocessing and Technology Institute for helping in the purification of the exosomes, and Bao Ju Teh at Institute of Medical Biology for technical assistance in preparing the vector and virus.

METHODS

Oncogenic transformation of HuES9.E1 MSC

The previously described human ESC-derived HuES9.E1 MSCs was infected at p21 or p16 with lentivirus carrying either a MYC gene or a GFP gene to generate two types of transfected cells, MYC-MSC and GFP-MSC, respectively. The MYC cDNA was amplified from pMXs-hc-MYC using primers PTDMYC (5' GAA TTC GAA TGC CCC TCA ACG TTA GC 3') and PTDMYCa (5' CTC GAG CGC ACA AGA GTT CCG TAG C 3') and cloned into pLVX-puro vector (Clontech, www.clontech.com).[37] Lentiviral particles were produced using Lenti-X HT Packaging System and viral titer was determined by using a Lenti-XTM qRT-PCR titration kit (Clontech, www.clontech.com). The HuES9.E1 MSCs that were infected at p21 were plated at 106 cells per 10 cm dish and infected with viruses at a MOI=5 in the presence of 4 μg/ml polybrene for overnight.[26] Cells were selected under 2 μg/ml puromycin for three days and expanded as per human ESC-derived HuES9.E1 MSCs and these cells were pooled to generate the E1-MYC 21.1 line. For the HuES9.E1 MSCs that was infected at p16, three independently clonal lines (E1-MYC 16.1, E1-MYC 16.2 and E1-MYC 16.3) were derived by limiting dilution.[26] When the cloned cells were expanded to 107 cells (or a confluent 15 cm culture dish), the passage number was designated as passage 1.

The cells were analyzed for MYC transgene integration, transcript and protein levels, surface markers, rate of cell cycling, telomerase activity, karyotype, genome-wide gene expression and differentiation potential.

HPLC purification of exosomes

The instrument setup consisted of a liquid chromatography system with a binary pump, an auto injector, a thermostated column oven and a UV-visible detector operated by the Class VP software from Shimadzu Corporation (Kyoto, Japan). The Chromatography columns used were TSK Guard column SWXL, 6 x 40 mm and TSK gel G4000 SWXL, 7.8 x 300 mm from Tosoh Corporation (Tokyo, Japan). The following detectors, Dawn 8 (light scattering), Optilab (refractive index) and QELS (dynamic light scattering) were

connected in series following the UV-visible detector. The last three detectors were from Wyatt Technology Corporation (California, USA) and were operated by the ASTRA software. The components of the sample were separated by size exclusion i.e. the larger molecules will elute before the smaller molecules. The eluent buffer used was 20 mM phosphate buffer with 150 mM of NaCl at pH 7.2. This buffer was filtered through a pore size of 0.1 µm and degassed for 15 minutes before use. The chromatography system was equilibrated at a flow rate of 0.5 ml/min until the signal in Dawn 8 stabilized at around 0.3 detector voltage units. The UV-visible detector was set at 220 ηm and the column was oven equilibrated to 25°C. The elution mode was isocratic and the run time was 40 minutes. The volume of sample injected ranged from 50 to 100 µl. The hydrodynamic radius, Rh, was computed by the QELS and Dawn 8 detectors. The highest count rate (Hz) at the peak apex was taken as the Rh. Peaks of the separated components visualized at 220 ηm were collected as fractions for further characterization studies.

Testing secretion for cardioprotection

The conditioned medium was prepared by growing the transformed MSCs in a chemically defined serum free culture medium for three days as previously described.[34] The concentrated conditioned medium was processed by HPLC fractionation to obtain the exosomes as mentioned above. The exosomes were tested in a mouse model of myocardial I/R injury. Myocardial ischemia was induced by 30 minutes left coronary artery (LCA) occlusion and subsequent reperfusion. Five minutes before reperfusion, mice were intravenously infused with 200 µl saline solution of 0.3 µg exosome protein purified from culture medium conditioned by MYC-MSCs. Control animals were infused with 200 µl saline. After 24 hours reperfusion, infarct size (IS) as a percentage of the area at risk (AAR) was assessed using Evans' blue dye injection and TTC staining as described previously.[24] All animal experiments were performed in accordance with the national guidelines on animal care and with prior approval by the Animal Experimentation Committee of Utrecht University.

Statistical analysis

Two-way ANOVA with post-hoc Dunnett was used to test the difference in infarct size between groups. Correlation coefficient of each pairs of array was assessed using Pearson correlation test.

REFERENCES

1 Le BK, Pittenger M. Mesenchymal stem cells: progress toward promise. Cytotherapy. 2005;7:36-45.

2 Atsma DE, Fibbe WE, Rabelink TJ. Opportunities and challenges for mesenchymal stem cell-mediated heart repair. Curr Opin Lipidol. 2007;18:645-649.

3 bdel-Latif A, Bolli R, Tleyjeh IM, Montori VM, Perin EC, Hornung CA, Zuba-Surma EK, Al-Mallah M, Dawn B. Adult bone marrow-derived cells for cardiac repair: a systematic review and meta-analysis. Arch Intern Med. 2007;167:989-997.

4 Behfar A, Terzic A. Optimizing adult mesenchymal stem cells for heart repair. J Mol Cell Cardiol. 2007;42:283-284.

5 Gnecchi M, He H, Liang OD, Melo LG, Morello F, Mu H, Noiseux N, Zhang L, Pratt RE, Ingwall JS, Dzau VJ. Paracrine action accounts for marked protection of ischemic heart by Akt-modified mesenchymal stem cells. Nat Med. 2005;11:367-368.

6 Mazhari R, Hare JM. Advances in cell-based therapy for structural heart disease. Prog Cardiovasc Dis. 2007;49:387-395.

7 Minguell JJ, Erices A. Mesenchymal stem cells and the treatment of cardiac disease. Exp Biol Med (Maywood). 2006;231:39-49.

8 Ohnishi S, Nagaya N. Prepare cells to repair the heart: mesenchymal stem cells for the treatment of heart failure. Am J Nephrol. 2007;27:301-307.

9 Schuleri KH, Boyle AJ, Hare JM. Mesenchymal stem cells for cardiac regenerative therapy. Handb Exp Pharmacol. 2007:195-218.

10 Caplan AI, Dennis JE. Mesenchymal stem cells as trophic mediators. J Cell Biochem. 2006;98:1076-1084.

11 Cheng L, Qasba P, Vanguri P, Thiede MA. Human mesenchymal stem cells support megakaryocyte and proplatelet formation from CD34(+) hematopoietic progenitor cells. J Cell Physiol. 2000;184:58-69.

12 Gnecchi M, He H, Noiseux N, Liang OD, Zhang L, Morello F, Mu H, Melo LG, Pratt RE, Ingwall JS, Dzau VJ. Evidence supporting paracrine hypothesis for Akt-modified mesenchymal stem cell-mediated cardiac protection and functional improvement. FASEB J. 2006;20:661-669.

13 Kinnaird T, Stabile E, Burnett MS, Shou M, Lee CW, Barr S, Fuchs S, Epstein SE. Local delivery of marrow-derived stromal cells augments collateral perfusion through paracrine mechanisms. Circulation. 2004;109:1543-1549.

14 Leedham SJ, Brittan M, McDonald SA, Wright NA. Intestinal stem cells. J Cell Mol Med. 2005;9:11-24.

15 Mayer H, Bertram H, Lindenmaier W, Korff T, Weber H, Weich H. Vascular endothelial growth factor (VEGF-A) expression in human mesenchymal stem cells: autocrine and paracrine role on osteoblastic and endothelial differentiation. J Cell Biochem. 2005;95:827-839.

16 Miyahara Y, Nagaya N, Kataoka M, Yanagawa B, Tanaka K, Hao H, Ishino K, Ishida H, Shimizu T, Kangawa K, Sano S, Okano T, Kitamura S, Mori H. Monolayered mesenchymal stem cells repair scarred myocardium after myocardial infarction. Nat Med. 2006;12:459-465.

17 Nakagami H, Maeda K, Morishita R, Iguchi S, Nishikawa T, Takami Y, Kikuchi Y, Saito Y, Tamai K, Ogihara T, Kaneda Y. Novel autologous cell therapy in ischemic limb disease through growth factor secretion by cultured adipose tissue-derived stromal cells. Arterioscler Thromb Vasc Biol. 2005;25:2542-2547.

18 Patschan D, Plotkin M, Goligorsky MS. Therapeutic use of stem and endothelial progenitor cells in acute renal injury: ca ira. Curr Opin Pharmacol. 2006;6:176-183.

19 Togel F, Hu Z, Weiss K, Isaac J, Lange C, Westenfelder C. Administered mesenchymal stem cells protect against ischemic acute renal failure through differentiation-independent mechanisms. Am J Physiol Renal Physiol. 2005;289:F31-F42.

20 Van Overstraeten-Schlogel N, Beguin Y, Gothot A. Role of stromal-derived factor-1 in the hematopoietic-supporting activity of human mesenchymal stem cells. Eur J Haematol. 2006;76:488-493.

21 Liu CH, Hwang SM. Cytokine interactions in mesenchymal stem cells from cord blood. Cytokine. 2005;32:270-279.

22 Pittenger MF, Martin BJ. Mesenchymal stem cells and their potential as cardiac therapeutics. Circ Res. 2004;95:9-20.

23 Chen TS, Lai RC, Lee MM, Choo AB, Lee CN, Lim SK. Mesenchymal stem cell secretes microparticles enriched in pre-microRNAs. Nucleic Acids Res. 2010;38:215-224.

24 Lai RC, Arslan F, Lee MM, Sze NS, Choo A, Chen TS, Salto-Tellez M, Timmers L, Lee CN, El Oakley RM, Pasterkamp G, de Kleijn DP, Lim SK. Exosome secreted by MSC reduces myocardial ischemia/reperfusion injury. Stem Cell Res. 2010;4:214-222.

25 Lai RC, Arslan F, Tan SS, Tan B, Choo A, Lee MM, Chen TS, Teh BJ, Eng JK, Sidik H, Tanavde V, Hwang WS, Lee CN, El Oakley RM, Pasterkamp G, de Kleijn DP, Tan KH, Lim SK. Derivation and characterization of human fetal MSCs: an alternative cell source for large-scale production of cardioprotective microparticles. J Mol Cell Cardiol. 2010;48:1215-1224.

26 Lian Q, Lye E, Suan YK, Khia Way TE, Salto-Tellez M, Liu TM, Palanisamy N, El Oakley RM, Lee EH, Lim B, Lim SK. Derivation of clinically compliant MSCs from CD105+. Stem Cells. 2007;25:425-436.

27 Timmers L, Lim SK, Arslan F, Armstrong JS, Hoefer IE, Doevendans PA, Piek JJ, El Oakley RM, Choo A, Lee CN, Pasterkamp G, de Kleijn DP. Reduction of myocardial infarct size by human mesenchymal stem cell conditioned medium. Stem Cell Res. 2007;1:129-137.

28 Sun D, Zhuang X, Xiang X, Liu Y, Zhang S, Liu C, Barnes S, Grizzle W, Miller D, Zhang HG. A novel nanoparticle drug delivery system: the anti-inflammatory activity of curcumin is enhanced when encapsulated in exosomes. Mol Ther. 2010;18:1606-1614.

29 Nagai A, Kim WK, Lee HJ, Jeong HS, Kim KS, Hong SH, Park IH, Kim SU. Multilineage potential of stable human mesenchymal stem cell line derived from fetal marrow. PLoS One. 2007;2:e1272.

30 Dominici M, Le BK, Mueller I, Slaper-Cortenbach I, Marini F, Krause D, Deans R, Keating A, Prockop D, Horwitz E. Minimal criteria for defining multipotent mesenchymal stromal cells. The International Society for Cellular Therapy position statement. Cytotherapy. 2006;8:315-317.

31 Que J, Lian Q, El Oakley RM, Lim B, Lim SK. PI3 K/Akt/mTOR-mediated translational control regulates proliferation and differentiation of lineage-restricted RoSH stem cell lines. J Mol Signal. 2007;2:9.

32 Thomas PD, Campbell MJ, Kejariwal A, Mi H, Karlak B, Daverman R, Diemer K, Muruganujan A, Narechania A. PANTHER: a library of protein families and subfamilies indexed by function. Genome Res. 2003;13:2129-2141.

33 Thomas PD, Kejariwal A, Guo N, Mi H, Campbell MJ, Muruganujan A, Lazareva-Ulitsky B. Applications for protein sequence-function evolution data: mRNA/protein expression analysis and coding SNP scoring tools. Nucleic Acids Res. 2006;34:W645-W650.

34 Sze SK, de Kleijn DP, Lai RC, Khia Way TE, Zhao H, Yeo KS, Low TY, Lian Q, Lee CN, Mitchell W, El Oakley RM, Lim SK. Elucidating the secretion proteome of human embryonic stem cell-derived mesenchymal stem cells. Mol Cell Proteomics. 2007;6:1680-1689.

35 Pfeffer MA, Braunwald E. Ventricular remodeling after myocardial infarction. Experimental observations and clinical implications. Circulation. 1990;81:1161-1172.

36 D'Costa J, Mansfield SG, Humeau LM. Lentiviral vectors in clinical trials: Current status. Curr Opin Mol Ther. 2009;11:554-564.

37 Kitamura T, Koshino Y, Shibata F, Oki T, Nakajima H, Nosaka T, Kumagai H. Retrovirus-mediated gene transfer and expression cloning: powerful tools in functional genomics. Exp Hematol. 2003;31:1007-1014.

CHAPTER 7

This chapter demonstrates that exosomes directly enhance viability of cardiac cells via pro-survival pathway activation and decreased apoptotic signaling

Fatih Arslan, Ruenn Chai Lai, Andre Choo, Eissa N.E. Aguor, Mirjam B. Smeets, Lars Akeroyd, Harold V. van Rijen, Leo Timmers, Pieter A. Doevendans, Gerard Pasterkamp, Sai Kiang Lim & Dominique P. de Kleijn

Exosomes target multiple mediators to reduce cardiac injury

Background

We have previously identified exosomes as the paracrine cardioprotective factor secreted by mesenchymal stem cell (MSCs). However, the mode of action, target signaling pathways and long-term physiological consequences of MSC-derived exosome treatment after myocardial infarction remain to be addressed.

Methods and Results

Mice (C57Bl6/J) underwent 30 minutes ischemia, followed by reperfusion. Purified exosomes or saline were administered 5 minutes before reperfusion. Cardiac function and geometry were assessed using 9.4T mouse-MRI and invasive PV-loop recordings. MSC-derived exosomes reduced infarct size by 45% compared to saline treatment. Ex vivo Langendorff experiments revealed that intact but not lysed exosomes enhanced viability of cardiac cells. In addition, exosome treated animals exhibited significant preservation of left ventricular geometry and contractile performance during 28 days follow-up. Within an hour after reperfusion, exosome treatment increased levels of ATP, NADH, phosphorylated-Akt and phosphorylated-GSK-3β, and reduced phosphorylated-c-JNK in ischemic/reperfused hearts. Subsequently, local and systemic inflammation was significantly reduced 24 hours after reperfusion.

Conclusions

Our study shows that intact MSC-derived exosomes restore bioenergetics, activate pro-survival signaling and inhibit pro-apoptotic signaling. Subsequently, exosomes reduce cell death and inflammation, thereby enhancing cardiac function and geometry after myocardial I/R injury. Hence, MSC-derived exosomes are a potential adjuvant to reperfusion therapy for myocardial infarction.

Submitted

Myocardial infarction (MI) and related complications (e.g. heart failure) are a great socio-economic burden to society and healthcare systems. Recent advances in (interventional) cardiology have resulted in timely and optimized coronary flow restoration through the culprit artery. Subsequently, more patients survive the initial infarction, but are susceptible to heart failure or other infarct-related comlications.[1] The increase in morbidity after MI triggered the search for adjunctive therapeutics to further limit excessive tissue loss and enhance cardiac performance. Pre-clinical studies show a great potential for engineered heart tissue for replacement therapy,[2, 3] while stem cells injections may be promising in the treatment of patients with acute MI.[4] Interestingly, there is increasing evidence showing that the observed therapeutic effects are partly mediated by stem cell secretion. This so called 'paracrine hypothesis' has gained much attention and is supported by recent experimental data.5 It has been shown that mesenchymal stem cell-conditioned medium (MSC-CM) enhance cardiomyocyte and/or progenitor survival after hypoxia-induced injury.[6-10] Furthermore, MSC-CM induce angiogenesis in the infarcted myocardium.[7, 8, 11] We have shown in both murine and porcine models of myocardial ischemia/reperfusion (I/R) injury that MSC-CM reduces infarct size.[12] High performance liquid chromatography (HPLC) and dynamic light scatter (DLS) analyses revealed that MSCs secrete cardioprotective microparticles with a hydrodynamic radius ranging from 50-65 ηm.[13] Furthermore, the therapeutic efficacy of MSC-derived exosomes was independent of the tissue source for the MSCs. For example, exosomes from human embryonic stem cell-derived MSCs were similar to those derived from other fetal tissue sources (e.g. limb, kidney). This suggests that secretion of therapeutic exosomes may be a general property of all MSCs.[14]

Exosomes are bi-lipid membrane vesicles with a diameter of 50-100 ηm. They are secreted by various cell types through the fusion of multivesicular bodies with the plasma membrane. Exosomes carry a complex cargo load of proteins and RNA with the potential to effect many cellular processes and pathways. They are involved in complex cellular interactions such as immune responses, intercellular communication and antigen presentation.[15] Multivesicular bodies store the exosomes within the cell and release them upon fusion with the plasma membrane. The identification of exosomes as the cardioprotective factor in MSC secretion makes it a potential therapeutic tool in myocardial infarction. In contrast to cell-based therapy, MSC-derived exosomes provide an 'off-the-shelf' therapeutic. Furthermore, exosomes are potentially safer as they are non-viable and will incur less manufacturing and storage costs. Although we previously described that exosomes reduce infarct size in mice,[14] the functional consequence and the mechanism for its cardioprotective actions remain unknown.
In the present study, we show that intact exosomes directly target cardiac cells to reduce infarct size after myocardial I/R injury. Furthermore, we demonstrate that exosomes exert a therapeutic effect via well-defined signaling pathways involved in survival and apoptosis of ischemic/reperfused cardiomyocytes.

RESULTS

Intact exosomes reduce myocardial I/R injury through direct interaction with myocardial cells

Thirty minutes ischemia followed by 24 hours reperfusion in saline treated animals resulted in 39±1.8% infarction within the AAR (IS/AAR; Figure 1A). A single i.v. bolus of exosomes 5 minutes prior to reperfusion reduced infarct size by 45% (21±2.2% IS/AAR; $p<0.001$), in a dose dependent manner. Infarct size reduction in myocardial I/R injury is achieved by either enhanced cardiomyocyte viability, reduced

detrimental activation of blood components or both.16-18 We performed *ex vivo* I/R experiments in the Langendorff setup, to determine the relative contribution of parenchymal and circulating cells to the cardioprotection mediated by exosomes. Three hours reperfusion with normal buffer after 30 minutes ischemia resulted in 49±5.3% IS/AAR. Exosome-containing buffer perfusion just prior to reperfusion significantly reduced infarct size to the same extent as in the *in vivo* situation (23±1.5% IS/AAR; p=0.002). This suggests that exosomes interact directly with cardiac cells to reduce infarct size. It is postulated that exosomes are internalized by target cells by endocytosis or phagocytosis in order to release their content.[19, 20] For this reason, we tested if the cardioprotection was dependent on the integrity of the exosomes as lipid microvesicles and not just their cargo. Exosomes were physically disrupted by vigorous agitation in a homogenizer before administration. The disrupted exosomes failed to reduce infarct size *in vivo* (37±3.0% IS/AAR; p=.994). In all experiments, the extent of myocardium at risk was similar in all groups (mean AAR/LV = 40±1.1%; Figure 1B).

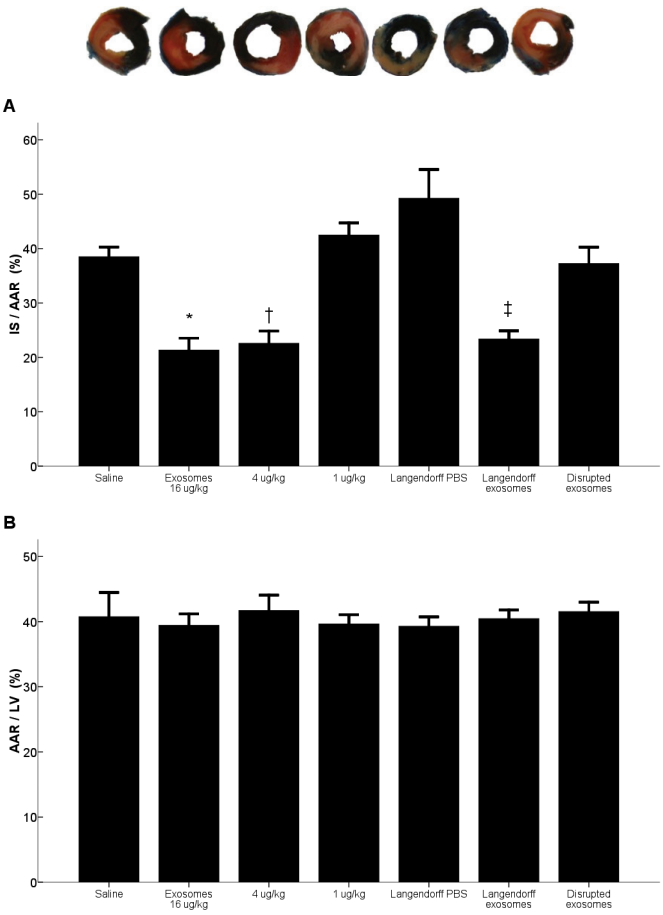

Figure 1. MSC-derived exosomes reduce myocardial I/R injury in vivo and ex vivo. *(**A**) Infarct size (IS) as a percentage of the area-at-risk (AAR) 1 day after I/R injury; *p<0.001, †p=0.001 and ‡p=0.001 compared to saline. (**B**) AAR as a percentage of the left ventricle (LV). Each bar represents Mean±SEM, n=6/group for in vivo and n=4/group for ex vivo experiments.*

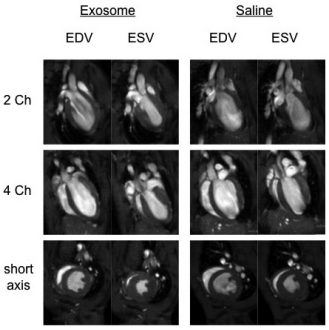
Exosome
Saline
EDV
ESV
EDV
ESV
2 Ch
4 Ch
short axis

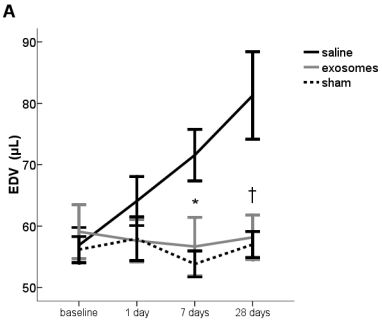
A
EDV (µL)
saline
exosomes
sham
baseline
1 day
7 days
28 days

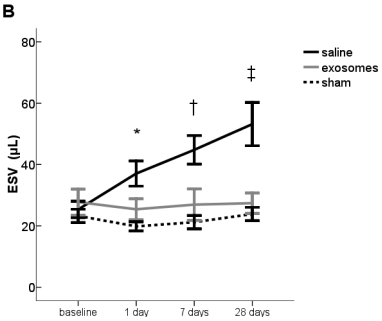
B
ESV (µL)
saline
exosomes
sham
baseline
1 day
7 days
28 days

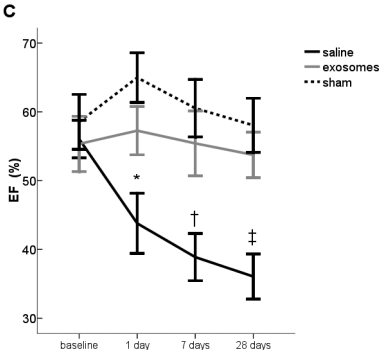
C
EF (%)
saline
exosomes
sham
baseline
1 day
7 days
28 days

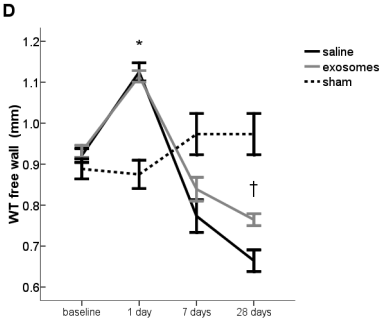
D
WT free wall (mm)
saline
exosomes
sham
baseline
1 day
7 days
28 days

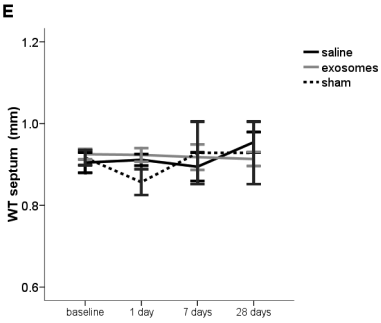
E
WT septum (mm)
saline
exosomes
sham
baseline
1 day
7 days
28 days

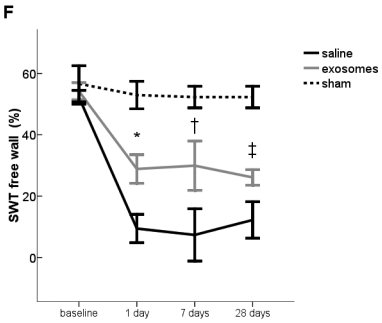
F
SWT free wall (%)
saline
exosomes
sham
baseline
1 day
7 days
28 days

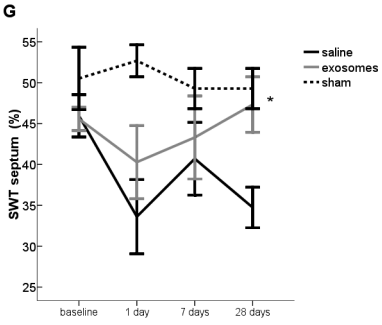
G
SWT septum (%)
saline
exosomes
sham
baseline
1 day
7 days
28 days

Exosome treatment prevents left ventricular dilatation and improves cardiac performance

We next examined the functional consequences of exosome treatment during long-term follow-up. We performed serial cardiac MRI measurements to assess both left ventricular (LV) function and geometry after I/R injury. There were no differences in LV function and dimensions at baseline. The infarct size reduction in exosome treated animals translated into significant preservation of both end-diastolic and -systolic volume (EDV, ESV) during follow-up. In addition, ejection fraction was significantly improved after exosome treatment at all time points (Figure 2A-C). Wall thickness (WT) of the infarcted area (free wall) was equally increased in saline and exosome treated animals 1 day after reperfusion (Figure 2D), presumably caused by tissue edema. Although infarct size was reduced, exosome treatment did not reduce reperfusion-induced edema as shown by equal increase in thickness of the free wall (infarct area) 1 day after reperfusion. The similar extent of tissue edema at day 1 in the MRI studies indicated that the amount of endangered myocardium did not differ between the groups. However, exosome treatment resulted in decreased thinning of the infarct area during scar maturation. This finding was in line with the infarct size reduction seen after exosome treatment. There were no differences in WT in the remote myocardium between the groups (Figure 2E). The higher extent of viable tissue after exosome treatment also significantly improved systolic thickening of the infarcted area at all time points (Figure 2F), and in the remote myocardium 28 days after infarction (Figure 2G).

At day 28, we also assessed the hemodynamic consequences using LV pressure-volume loop recordings after exosome treatment. Consistent with improved LV function and geometry, we observed higher contractility and relaxation and reduced end-diastolic pressure (EDP) in exosome treated animals (Table 1).

Table 1. Invasive left ventricular pressure measurements 28 days after infarction

	Saline	Exosomes	*p*
BPM	480±7	476±3	.60
ESP	110±2	137±10	.12
EDP	15±1	7±1	.009
dP/dT_{max}	7496±152	8951±246	.009
dP/dT_{min}	-6680±75	-8241±396	.009

Data are represented as Mean±SEM, n=5/group. BPM=beats per minute, ESP=end-systolic pressure, EDP=end-diastolic pressure.

Figure 2. MSC-derived exosomes prevent LV dilation and improve systolic function after myocardial I/R injury. *(**A**) End-diastolic volume (EDV, µL); *p=0.029 and †p=0.006 compared to saline. (**B**) End-systolic volume (ESV); *p=0.04, †p=0.017 and ‡p=0.002 compared to saline. (**C**) Ejection fraction (EF, %); *p=0.035, †p=0.015 and ‡p=0.002 compared to saline. (**D**) Wall thickness of the infarct area (WT, mm); *p<0.001 compared to baseline and †p=0.04 compared to saline. (**E**) WT of the remote myocardium. (**F**) systolic wall thickening (SWT, %); *p=0.011, †p=0.042 and ‡p=0.040 compared to saline. (**G**) SWT of the remote myocardium; *p=0.012 compared to saline. Representative MRI images are shown. Note the increased LV dimensions at systole and diastole in saline treated animals; Each bar represents Mean±SEM, n=10/group for ischemic/reperfused animals n=6/group for sham operated mice.*

Exosome treatment restores energy depletion and redox state within 30 minutes after I/R

Mitochondrial dysfunction is one of the most important determinants of viability loss after I/R injury.[21] Mitochondrial dysfunction aggravates the loss of ATP and NADH during ischemia where Kreb's cycle and oxidative phosphorylation are inhibited by the lack of oxygen. Restoring their levels will therefore be critical for the recovery of the ischemic/reperfused myocardium. We observed that within 30 minutes after reperfusion, the ATP/ADP and NADH/NAD+ ratios in the AAR of exosome-treated animals were significantly reduced (Figure 3A and B). These data demonstrate that exosome treatment is highly effective in eliciting a rapid biochemical response to restore ATP and NADH levels as reflected by reduced ATP/ADP and NADH/NAD+ ratios.

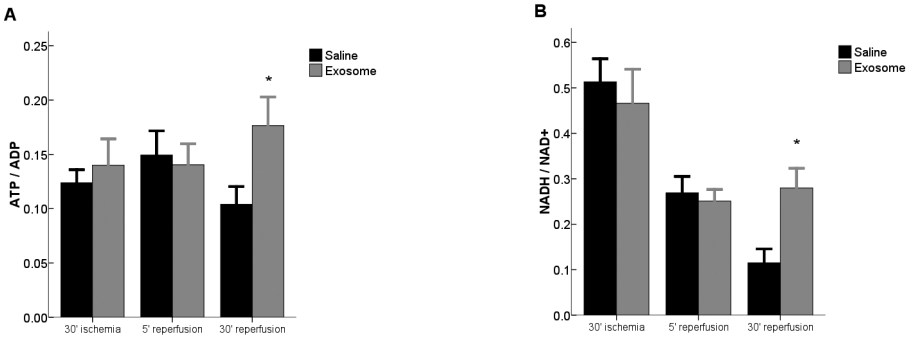

Figure 3. MSC-derived exosomes restore ATP/ADP and NADH/NAD+ levels. *Tissue levels of (**A**) ATP/ADP; *p=0.047 compared to saline. (**B**) NADH/NAD+; *p=0.027 compared to saline. Each bar represents Mean±SEM, n=6/group/time point.*

Exosome treatment phosphorylates Akt/GSK3 pathway and inhibits c-JNK signaling after I/R

Paracrine action of MSC secretion has been shown to be mediated via enhanced phosphorylation of survival pathways, especially of PI3K/Akt pathway.[5-9] In our study, exosome treatment elicited an immediate and significant increase in Akt and GSK3 phosphorylation within an hour after reperfusion, and this increase was maintained over the next 24 hours (Figure 4A and B). ERK1/2 phosphorylation has also shown to be protective in myocardial I/R injury,[21] however, was not altered by exosome treatment (Figure 4C). Phosphorylation of c-JNK, a known activator of pro-apoptotic signaling, was rapidly and significantly reduced in exosome treated animals within 1 hour reperfusion (Figure 4D).

Exosome treatment reduces inflammation after I/R

Myocardial I/R is characterized by accentuated cardiac and systemic inflammation.[16] Cardiac inflammation was assessed by neutrophil and macrophage infiltration. Exosome treatment significantly reduced neutrophil but not macrophage infiltration in the hearts at day 1 and 3 after reperfusion (Figure 5A and B). High peripheral white blood cell (WBC) count is associated with larger infarct size, worse cardiac performance and poor clinical outcome.[22-26] In line with reduced infarct size and improved cardiac performance, exosome treatment significantly reduced WBC count compared to saline treated mice after I/R injury (Figure 5C).

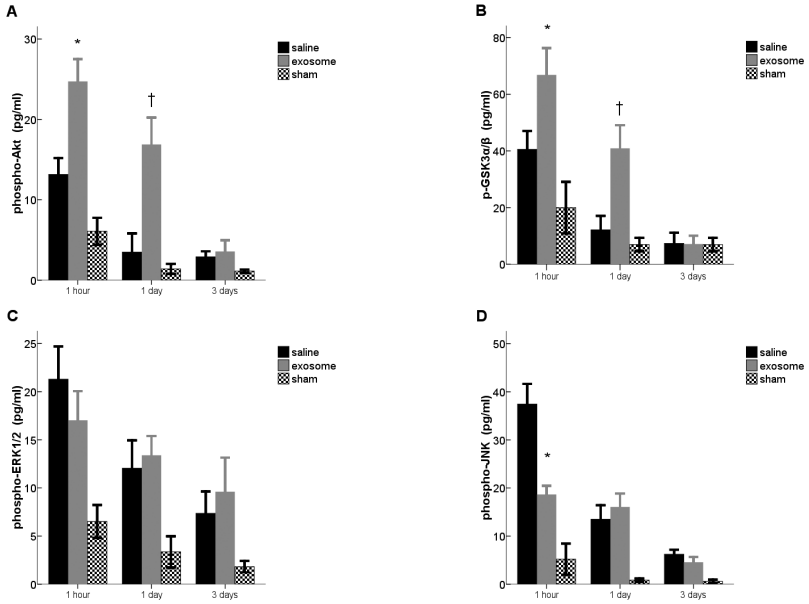

Figure 4. MSC-derived exosomes induce phosphorylation of Akt and GSK3, and reduce c-JNK phosphorylation after myocardial I/R injury. *Tissue levels of (**A**) phospho-Akt (pg/ml); *p=0.025 and †p=0.025 compared to saline. (**B**) phospho-GSK3α/ß; *p=0.025 and †p=0.016 compared to saline. (**C**) phospho-ERK1/2. (**D**) phospho-c-JNK; *p=0.045 compared to saline. Each bar represents Mean±SEM, n=6/group/time point.*

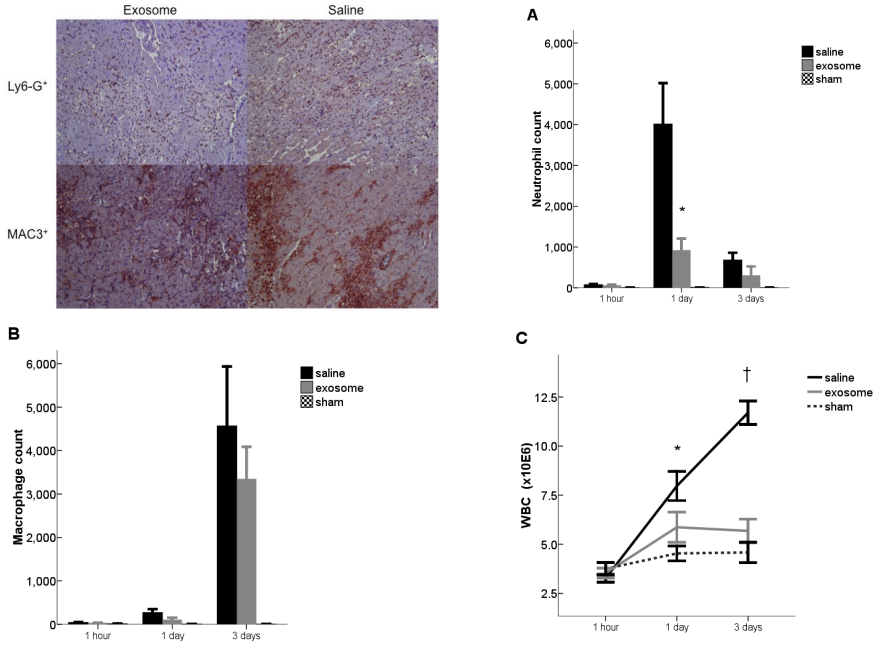

Figure 5. MSC-derived exosomes reduce inflammation after myocardial I/R injury. *(**A**) Neutrophil influx (Ly6-G^{pos} cells); *p=0.016 compared to saline. (**B**) Macrophage influx (MAC3^{pos} cells). Representative staining are shown. (**C**) Peripheral white blood cell counts after myocardial I/R injury; *p=0.045 and †p=0.009 compared to saline. Each bar represents Mean±SEM, n=6/group/time point.*

DISCUSSION

Previous studies have shown that MSC transplantation improves cardiac function after infarction. The initial hypothesis that this efficacy was mediated by the engraftment and differentiation of transplanted MSCs to replace injured tissues is increasingly untenable. Most studies suggest that MSCs mediate their therapeutic efficacy through the secretion of paracrine factors.[5-7, 27] Like others,[8-10] we have demonstrated that culture medium conditioned by MSCs reduces I/R injury in a pig and mouse model.[12] We identified the active component in this CM as an exosome, a 50-100 ηm bi-lipid membrane secreted microvesicle.[13, 14]

In this study, we demonstrated that exosomes not only reduced infarct size, but also resulted in a long-term preservation of cardiac function and reduced adverse remodeling. Interestingly, the therapeutic effect of MSC-derived exosomes was dependent on their physical integrity such that physical disruption of the bi-lipid membrane prevented cardioprotection. These observations are consistent with the reported uptake of exosomes by cells via endocytosis or phagocytosis,[19, 20]. Furthermore, *ex vivo* Langendorff experiments revealed that exosomes are able to reduce infarct size to the same extent as in the *in vivo* situation. These findings strongly indicate that exosomes exert their therapeutic effect via viability enhancement of cardiac tissue and do not require the presence of circulating blood cells. Unfortunately, we were not able to follow exosomes in vivo after administration. It appeared to be technically impossible to detect labeled exosomes ex or in vivo after administration, either fluorescent (GFP^{pos}-MSC secreted GFP^{pos}-exosomes and ex vivo protein labeling) or radioactive (^{111}In-oxinate labeling). The main issue is likely the size of the exosomes that hampers ex vivo labeling and signal intensity once taken up by ischemic/reperfused heart tissue. Novel techniques are needed to explore the dynamics of exosomes after in vivo administration.

To elucidate the underlying mechanism of cardioprotection by MSC-derived exosomes, we first determined the earliest biochemical and molecular changes in the heart. Within the first hour, exosome treatment significantly increased tissue level of ATP and NADH. This demonstrated that exosomes could elicit a rapid and efficient correction of the NADH- and ATP-deficit accumulated during ischemia when Kreb's cycle and oxidative phosphorylation are inhibited. These rapid changes were simultaneously coupled with the activation of pro-survival Akt and GSK-β3 signaling pathways and inhibition of pro-apoptotic c-JNK signaling pathway. ATP deficiency is a trigger of apoptosis and in turn apoptosis depletes ATP, causing a vicious circle of cell death.[28, 29] Therefore the rapid restoration of ATP and NADH by exosome treatment increase cellular energy supply and reductive potential to expedite the recovery of ischemic/reperfused myocardium and inhibit apoptosis. In order to result in rapid alterations of bioenergetics, exosomes need to be internalized fast. It has been shown that the internalization of MSC exosomes by H9C2 cardiomyocytes occurs within 30 minutes of exposure.[30] The simultaneous restoration of cardiac bioenergetics, rapid phosphorylation of pro-survival pathways Akt and GSK-3β and reduced phosphorylation of c-JNK probably provided an additional synergy in the amelioration of I/R injury. The importance of pro-survival kinases such as PI3 kinase-Akt and ERK1/2 in limiting reperfusion injury was recently highlighted in a position paper from the European Society of Cardiology.[31]

Finally, we observed decreased neutrophil influx in exosome treated animals. It is likely that the reduced influx is secondary to the reduced cardiac injury after exosome treatment, since leukocyte influx did

not differ between the groups at 1 hour reperfusion. In addition, we found that the reduced infarct size and improved cardiac performance were associated with low WBC counts in exosome treated animals. This finding is in line with clinical studies in which infarct size and clinical outcome is directly proportional to WBC count[22, 24-26].

The identification of exosomes as the cardioprotective factor in MSC secretion makes it a potential therapeutic tool in myocardial infarction. Exosomes will become more attractive when efficacy is shown after intracoronary injection in a large animal during the reperfusion phase. Currently, we are putting effort to test intracoronary administration of exosomes in a porcine model of myocardial I/R injury. In contrast to cell-based therapy, MSC-derived exosomes provide an 'off-the-shelf' therapeutic. Furthermore, exosomes are potentially safer as they are non-viable and will incur less manufacturing and storage costs.

CONCLUSIONS

We have shown that MSC-derived exosomes rapidly activate multiple cardioprotective pathways to reduce infarct size and prevent heart function deterioration after myocardial I/R injury. Our study demonstrates that a single intravenous administration of MSC-derived exosomes is effective when administered in the late ischemic period, just prior to reperfusion. For these reasons, MSC-derived exosomes are a potential candidate for adjunctive therapy for patients suffering from acute myocardial infarction.

Funding

This work was supported by research grants from Netherlands Organisation for Scientific Research (NWO) & Utrecht University Mozaïek grant (contract 017.004.004 to F.A.) and Bekales Foundation (P.A.D.).

Acknowledgements

We would like to thank the following persons for their assistance: Ben J. van Middelaar, Roel van der Nagel, Cees van der Kolk and Arjan Schoneveld (all from the UMC Utrecht, The Netherlands).

METHODS

Animals and Experimental Design

Male C57Bl6/J mice (10-12 wks old, 25-30 g) received standard diet and water *ad libitum*. Saline or exosomes were administered intravenously via the tail vein, 5 minutes before reperfusion. Myocardial infarction was induced by temporary left coronary artery ligation, just below the left atrial appendage as described previously.[18] Where possible, recommendations from the National Heart Lung and Blood Institute (NHLBI) Working Group on the Translation of Therapies for Protecting the Heart from Ischemia[32] were applied; the surgeon was blinded for the treatment. Digital images of the infarcts were encrypted before being analyzed by the researcher. Heart function and geometry assessments were done by a technician blinded to treatment. All animal experiments were performed in accordance with the Directive 2010/63/EU of the European Parliament, national guidelines on animal care and with prior approval by the Animal Experimentation Committee of Utrecht University.

Myocardial I/R Injury In Vivo

Mice were anesthetized with a mixture of fentanyl (Jansen-Cilag) 0.05 mg/kg, midazolam (Dormicum, Roche) 5 mg/kg and medetomidine 0.5 mg/kg through an intraperitoneal injection. The adequacy of anesthesia was monitored by checking interdigital painreflexes, righting reflexes, limb/muscle tone and spontaneous breathing frequency. Core body temperature was maintained around 37°C during surgery by continuous monitoring with a rectal thermometer and automatic heating blanket. Mice were intubated and ventilated (Harvard Apparatus Inc.) with 100% oxygen. The left coronary artery (LCA) was ligated for 30 minutes with an 8-0 Ethilon (Ethicon) with a section of polyethylene-10 tubing placed over the LCA. Ischemia was confirmed by bleaching of the myocardium and ventricular tachyarrhythmia. In sham operated animals the suture was placed beneath the LCA without ligating. Reperfusion was initiated by releasing the ligature and removing the polyethylene-10 tubing. Reperfusion of the endangered myocardium was characterized by typical hyperemia in the first few minutes. In a subgroup of mice, a piece of the loosened suture was left in place to determine the area-at-risk (AAR) during termination. The chest wall was closed and the animals received subcutaneously atipamezole (Antisedan, Pfizer) 2.5 mg/kg, flumazenil (Anexate, Roche) 0.5 mg/kg and buprenorphine (Temgesic, Schering-Plough) 0.1 mg/kg. Prior to termination, mice were anesthetized as described above before cervical dislocation. Hereafter, the hearts were rinsed with saline and subsequently explanted for further biochemical and/or histological analysis.

Exosome Purification

Exosomes were purified from huES9.E1 derived MSCs conditioned media (CM) using HPLC, as described earlier.[14, 33] Briefly, to prepare the CM, 80% confluent HuES9.E1 cell cultures were washed three times with PBS and cultured overnight in a chemically defined medium consisting of DMEM without phenol red (Invitrogen) and supplemented with insulin, transferrin, and selenoprotein (ITS; Invitrogen), 5 ng/ml FGF2 (Invitrogen), 5 ng/ml PDGF AB (Peprotech, Rocky Hill, NJ), glutamine-penicillin-streptomycin, and β-mercaptoethanol. The cultures were then rinsed three times with PBS, and fresh defined medium was added. After 3 days, the medium was collected and centrifuged at 500g, and the supernatant was filtered using a 0.2-µm filter. No Serum was used in the preparation of the CM and the cells were not stimulated. Serum-free CM collected from MSCs culture was concentrated 50x by tangential flow filtration using a membrane with a 100 kDa MWCO (Sartorius, Goettingen, Germany). Hereafter, CM

was passed through chromatography columns (TSK Guard column SWXL, 6x40 mm and TSK gel G4000 SWXL, 7.8x300 mm, Tosoh Corp., Tokyo, Japan). Exosomes were collected from the first peak of the elution, concentrated using 100 kDa MWCO filter (Sartorius). Exosomes were filtered with a 0.22 µm filter before storage -80ºC.

Infarct Size

Infarct size (IS) as a percentage of the left ventricle (LV) was determined using Evans' blue dye injection and TTC staining, 1 day after reperfusion (n=6/group).
Mice were anesthetized as described above with a mixture of fentanyl, midazolam and medetomidine. The LCA was ligated once again at the level marked by the suture left in place. Evans' blue dye (4%) was injected via the thoracic aorta in a retrograde fashion. By doing so, one can demarcate non-ischemic region in order to determine the area-at-risk (AAR); the extent of myocardial tissue that underwent ischemia (i.e. endangered myocardium). Hearts were rapidly explanted, rinsed in 0.9% saline and put in -20ºC freezer for 1 hour. Hereafter, hearts were mechanically sliced into four 1-mm cross sections. Heart sections were incubated in 1% triphenyltetrazolium-chloride (Sigma-Aldrich) at 37ºC for 15 minutes before placing them in formaldehyde for another 15 minutes. Viable tissue stains red and infarcted tissue appears white. Heart sections were digitally photographed (Canon EOS 400D) under a microscope (Carl Zeiss®). IS, AAR and total LV area were measured using ImageJ software (version 1.34). Infarct size was corrected for the weight of the corresponding heart slice.

Myocardial I/R Injury Ex Vivo

Mice (n=4/group) were given heparin 50 IE subcutaneously and were operated under general anesthesia as described above with a mixture of fentanyl, midazolam and medetomidine. The suture was placed beneath the LCA *in vivo* without ligating. Hereafter, the heart was excised and aortic root was canulated and perfused in the Langendorff setup. After 10 min recovery, the suture was tightened to induce ischemia for 30 min. Just 5 min prior to reperfusion, the perfusion buffer was changed for a second buffer containing 0.4 µg/ml MSC-derived exosomes or control. Reperfusion was initiated by releasing the suture. Following 3 hours of reperfusion, Evans' blue dye was injected after re-ligating the suture to demarcate the AAR. Subsequently, TTC staining was performed for infarct size assessment.

Cardiac Magnetic Resonance Imaging

Twenty-six mice (n=10/group in ischemic and n=6/group in sham operated mice) underwent serial assessment of cardiac dimensions and function by high resolution magnetic resonance imaging (MRI, 9.4 T, Bruker, Rheinstetten, Germany) under isoflurane anesthesia before, 1, 7 and 28 days after MI. Long axis and short axis images with 1.0 mm interval between the slices were obtained and used to compute end-diastolic volume (EDV, largest volume) and end-systolic volume (ESV, smallest volume). The ejection fraction (EF) was calculated as 100*(EDV-ESV)/EDV. Wall thickness (WT) and systolic wall thickening (SWT) were assessed from both the septum (remote myocardium) and free wall (infarct area). All MRI data are analyzed using Qmass digital imaging software (Medis, Leiden, The Netherlands).

Pressure-Volume Loop Recordings

In a subset of mice, invasive assessment of cardiac performance and LV pressure development was performed 28 days after infarction. Mice were anesthetized as described above with a mixture of

fentanyl, midazolam and medetomidine. A Millar 1.4F pressure catheter (model SPR-839) was inserted in a retrograde fashion via the right common carotid artery. Systolic function was assessed by LV end-systolic pressure and dP/dt_{max}, whereas diastolic function by LV end-diastolic pressure and dP/dt_{min}.

Immunohistochemistry

Upon termination (as described above), hearts were rinsed with saline and excised and fixated in 4% formaldehyde and embedded in paraffin. Paraffin sections were stained for Ly-6G (for neutrophils; rat anti-mouse Ly-6G 1:100, Abcam, Cambridge, United Kingdom) and MAC-3 (for macrophages; rat anti-mouse MAC-3 1:30, BD Pharmingen, Breda, the Netherlands). Sections were stained by overnight incubation with the first antibody at 4°C for MAC-3 or by 1 hour incubation at RT for Ly-6G. Before staining, sections were deparaffinized and endogenous peroxidase was blocked by 30 minutes incubation in methanol containing 1.5% H2O2. Antigen retrieval was performed by 20 minutes boiling in citrate buffer (MAC-3 and Ly-6G). For MAC-3, sections were pre-incubated with normal goat serum and incubated with the primary antibody (1:30 overnight at 4°C). Sections were then incubated for 1 hour at RT with a biotin labeled secondary antibody, followed by 1 hour incubation with streptavidin-horseradish peroxidase at RT and developed with AEC. For Ly-6G, sections were incubated with the primary antibody (1:100 for 1 hour at RT). Sections were then incubated for 30 minutes with a secondary antibody followed by 30 minutes incubation with Powervision poly-HRP anti-rabbit IgG (ImmunoVision Technologies, Daily City, USA). The staining was immediately visualized with Vector NovaRED™ substrate kit following the manufacturer's instructions (Vector Laboratories Inc., Burlingame, USA).

Protein Isolation

Total protein was isolated from snap frozen infarcted heart sections using 40 mM Tris pH 7.4.

Flow Cytometry

Phosphorylated target protein for Akt ($Ser4^{73}$), glucogen synthase kinase-3α/β (GSK-3α/β; Ser^{21}/Ser^{9}), extracellular signal-regulated kinases-1/2 (ERK1/2; Thr^{202}/Tyr^{204}), c-Jun N-terminal kinase (c-JNK; Thr^{183}/Tyr^{185}) were measured using the Bio-Plex Multiplex Assay (Bio-Rad Laboratories) according to the instructions of the manufacturer, after 1:5 dilution in assay buffer.

ATP/ADP & NADH/NAD+

ATP/ADP and NADH/NAD+ ratios were measured in the ischemic area of mice. MI was induced as described earlier. After 0 min, 5 min and 30 min of reperfusion, the ischemic area was excised and snap frozen using liquid nitrogen. Frozen tissue samples were homogenized with 1 ml extraction buffer and supernatant was collected after spinning at 14,000g for 5 minutes. Hereafter, the supernatant was passed through 10 kDa MWCO filter (Biovision) before performing the ATP/ADP and NADH/NAD+ assays according to the manufacturer's protocol (Biovision, Mountain view, CA).

Statistical Analysis

Data are represented as Mean±SEM. One-way ANOVA with post-hoc 2-sided Dunnett t-test adjustment (saline was set as control) was used for infarct size comparison between the groups. Non-parametric t-test was used for 2 group comparisons. All statistical analyses were performed using SPSS 15.1.1. and $p < 0.05$ was considered significant. The authors had full access to and take full responsibility for the integrity of the data. All authors have read and agree to the manuscript as written.

REFERENCES

1 International Cardiovascular Disease Statistics. American Heart Association 2004;Available at: URL: http://www.americanheart.org/downloadable/heart/1077185395308FS06INT4%28ebook%29.pdf.

2 Zimmermann WH, Melnychenko I, Wasmeier G, Didie M, Naito H, Nixdorff U, Hess A, Budinsky L, Brune K, Michaelis B, Dhein S, Schwoerer A, Ehmke H, Eschenhagen T. Engineered heart tissue grafts improve systolic and diastolic function in infarcted rat hearts. Nat Med. 2006;12:452-458.

3 Naito H, Melnychenko I, Didie M, Schneiderbanger K, Schubert P, Rosenkranz S, Eschenhagen T, Zimmermann WH. Optimizing engineered heart tissue for therapeutic applications as surrogate heart muscle. Circulation. 2006;114:I72-I78.

4 Martin-Rendon E, Brunskill S, Doree C, Hyde C, Watt S, Mathur A, Stanworth S. Stem cell treatment for acute myocardial infarction. Cochrane Database Syst Rev. 2008:CD006536.

5 Gnecchi M, Zhang Z, Ni A, Dzau VJ. Paracrine mechanisms in adult stem cell signaling and therapy. Circ Res. 2008;103:1204-1219.

6 Gnecchi M, He H, Noiseux N, Liang OD, Zhang L, Morello F, Mu H, Melo LG, Pratt RE, Ingwall JS, Dzau VJ. Evidence supporting paracrine hypothesis for Akt-modified mesenchymal stem cell-mediated cardiac protection and functional improvement. FASEB J. 2006;20:661-669.

7 Chimenti I, Smith RR, Li TS, Gerstenblith G, Messina E, Giacomello A, Marban E. Relative roles of direct regeneration versus paracrine effects of human cardiosphere-derived cells transplanted into infarcted mice. Circ Res. 2010;106:971-980.

8 Deuse T, Peter C, Fedak PW, Doyle T, Reichenspurner H, Zimmermann WH, Eschenhagen T, Stein W, Wu JC, Robbins RC, Schrepfer S. Hepatocyte growth factor or vascular endothelial growth factor gene transfer maximizes mesenchymal stem cell-based myocardial salvage after acute myocardial infarction. Circulation. 2009;120:S247-S254.

9 Matsuura K, Honda A, Nagai T, Fukushima N, Iwanaga K, Tokunaga M, Shimizu T, Okano T, Kasanuki H, Hagiwara N, Komuro I. Transplantation of cardiac progenitor cells ameliorates cardiac dysfunction after myocardial infarction in mice. J Clin Invest. 2009;119:2204-2217.

10 Rogers TB, Pati S, Gaa S, Riley D, Khakoo AY, Patel S, Wardlow RD, Frederick CA, Hall G, He LP, Lederer WJ. Mesenchymal stem cells stimulate protective genetic reprogramming of injured cardiac ventricular myocytes. J Mol Cell Cardiol. 2010.

11 Li H, Zuo S, He Z, Yang Y, Pasha Z, Wang Y, Xu M. Paracrine Factors Released by GATA-4 Overexpressed Mesenchymal Stem Cells Increase Angiogenesis and Cell Survival. Am J Physiol Heart Circ Physiol. 2010.

12 Timmers L, Lim SK, Arslan F, Armstrong JS, Hoefer IE, Doevendans PA, Piek JJ, El Oakley RM, Choo A, Lee CN, Pasterkamp G, de Kleijn DP. Reduction of myocardial infarct size by human mesenchymal stem cell conditioned medium. Stem Cell Res. 2007;1:129-137.

13 Lai RC, Arslan F, Tan SS, Tan B, Choo A, Lee MM, Chen TS, Teh BJ, Eng JK, Sidik H, Tanavde V, Hwang WS, Lee CN, El Oakley RM, Pasterkamp G, de Kleijn DP, Tan KH, Lim SK. Derivation and characterization of human fetal MSCs: an alternative cell source for large-scale production of cardioprotective microparticles. J Mol Cell Cardiol. 2010;48:1215-1224.

14 Lai RC, Arslan F, Lee MM, Sze NS, Choo A, Chen TS, Salto-Tellez M, Timmers L, Lee CN, El Oakley RM, Pasterkamp G, de Kleijn DP, Lim SK. Exosome secreted by MSC reduces myocardial ischemia/reperfusion injury. Stem Cell Res. 2010;4:214-222.

15 Thery C, Ostrowski M, Segura E. Membrane vesicles as conveyors of immune responses. Nat Rev Immunol. 2009;9:581-593.

16 Arslan F, de Kleijn DP, Timmers L, Doevendans PA, Pasterkamp G. Bridging innate immunity and myocardial ischemia/reperfusion injury: the search for therapeutic targets. Curr Pharm Des. 2008;14:1205-1216.

17 Yellon DM, Hausenloy DJ. Myocardial reperfusion injury. N Engl J Med. 2007;357:1121-1135.

18 Arslan F, Smeets MB, O'Neill LA, Keogh B, McGuirk P, Timmers L, Tersteeg C, Hoefer IE, Doevendans PA, Pasterkamp G, de Kleijn DP. Myocardial ischemia/reperfusion injury is mediated by leukocytic toll-like receptor-2 and reduced by systemic administration of a novel anti-toll-like receptor-2 antibody. Circulation. 2010;121:80-90.

19 Tian T, Wang Y, Wang H, Zhu Z, Xiao Z. Visualizing of the cellular uptake and intracellular trafficking of exosomes by live-cell microscopy. J Cell Biochem. 2010;111:488-496.

20 Feng D, Zhao WL, Ye YY, Bai XC, Liu RQ, Chang LF, Zhou Q, Sui SF. Cellular internalization of exosomes occurs through phagocytosis. Traffic. 2010;11:675-687.

21 Murphy E, Steenbergen C. Mechanisms underlying acute protection from cardiac ischemia-reperfusion injury. Physiol Rev. 2008;88:581-609.

22 Chia S, Nagurney JT, Brown DF, Raffel OC, Bamberg F, Senatore F, Wackers FJ, Jang IK. Association of leukocyte and neutrophil counts with infarct size, left ventricular function and outcomes after percutaneous coronary intervention for ST-elevation myocardial infarction. Am J Cardiol. 2009;103:333-337.

23 Smit JJ, Ottervanger JP, Slingerland RJ, Kolkman JJ, Suryapranata H, Hoorntje JC, Dambrink JH, Gosselink AT, de Boer MJ, Zijlstra F, van 't Hof AW. Comparison of usefulness of C-reactive protein versus white blood cell count to predict outcome after primary percutaneous coronary intervention for ST elevation myocardial infarction. Am J Cardiol. 2008;101:446-451.

24 Bauters A, Ennezat PV, Tricot O, Lallemant R, Aumegeat V, Segrestin B, Quandalle P, Lamblin N, Bauters C. Relation of admission white blood cell count to left ventricular remodeling after anterior wall acute myocardial infarction. Am J Cardiol. 2007;100:182-184.

25 Prasad A, Stone GW, Stuckey TD, Costantini CO, Mehran R, Garcia E, Tcheng JE, Cox DA, Grines CL, Lansky AJ, Gersh BJ. Relation between leucocyte count, myonecrosis, myocardial perfusion, and outcomes following primary angioplasty. Am J Cardiol. 2007;99:1067-1071.

26 Barron HV, Harr SD, Radford MJ, Wang Y, Krumholz HM. The association between white blood cell count and acute myocardial infarction mortality in patients > or =65 years of age: findings from the cooperative cardiovascular project. J Am Coll Cardiol. 2001;38:1654-1661.

27 Gnecchi M, He H, Liang OD, Melo LG, Morello F, Mu H, Noiseux N, Zhang L, Pratt RE, Ingwall JS, Dzau VJ. Paracrine action accounts for marked protection of ischemic heart by Akt-modified mesenchymal stem cells. Nat Med. 2005;11:367-368.

28 Gustafsson AB, Gottlieb RA. Heart mitochondria: gates of life and death. Cardiovasc Res. 2008;77:334-343.

29 Vander Heiden MG, Chandel NS, Schumacker PT, Thompson CB. Bcl-xL prevents cell death following growth factor withdrawal by facilitating mitochondrial ATP/ADP exchange. Mol Cell. 1999;3:159-167.

30 Chen TS, Lai RC, Lee MM, Choo AB, Lee CN, Lim SK. Mesenchymal stem cell secretes microparticles enriched in pre-microRNAs. Nucleic Acids Res. 2010;38:215-224.

31 Ovize M, Baxter GF, Di LF, Ferdinandy P, Garcia-Dorado D, Hausenloy DJ, Heusch G, Vinten-Johansen J, Yellon DM, Schulz R. Postconditioning and protection from reperfusion injury: where do we stand? Position paper from the Working Group of Cellular Biology of the Heart of the European Society of Cardiology. Cardiovasc Res. 2010;87:406-423.

32 Bolli R, Becker L, Gross G, Mentzer R, Jr., Balshaw D, Lathrop DA. Myocardial protection at a crossroads: the need for translation into clinical therapy. Circ Res. 2004;95:125-134.

33 Sze SK, de Kleijn DP, Lai RC, Khia Way TE, Zhao H, Yeo KS, Low TY, Lian Q, Lee CN, Mitchell W, El Oakley RM, Lim SK. Elucidating the secretion proteome of human embryonic stem cell-derived mesenchymal stem cells. Mol Cell Proteomics. 2007;6:1680-1689.

PART II

Adverse Remodeling

CHAPTER 8

This chapter shows that absent TLR2 signaling in bone marrow-derived cells prevents adverse remodeling after infarction

Fatih Arslan, Eissa N.E. Aguor, Mirjam B. Smeets, Pieter A. Doevendans, Gustav J. Strijkers, Gerard Pasterkamp & Dominique P. de Kleijn

Lack of circulating Toll-like receptor 2 promotes survival and prevents adverse remodeling after myocardial infarction

Background

Excessive inflammation is a known mediator of adverse cardiac remodeling after myocardial infarction. Toll-like receptors (TLRs) have been shown to play a crucial role in inflammatory responses after tissue injury. In the present study, we explored the functional and biochemical consequences of TLR2 absence in left ventricular remodeling after myocardial infarction.

Methods and Results

C57Bl6 wild-type (WT), TLR2$^{-/-}$ and chimeric mice underwent permanent ligation of the left coronary artery. Cardiac function and geometry were assessed using 9.4T mouse-MRI at baseline, 7 and 28 days after infarction. Despite similar infarct size between WT and TLR2$^{-/-}$ mice (39±1.4% vs. 42±1.5%, respectively; p=.256), the absence of TLR2 promoted survival and prevented left ventricular dilatation during 28 days follow-up. Furthermore, systolic performance of both infarcted and remote myocardium was better in TLR2$^{-/-}$ mice compared to WT animals. Chimeric mice experiments revealed that expansive remodeling after infarction was mediated by bone marrow-derived TLR2 expression. Characterization of peripheral blood cells showed that the absence of TLR2 reduced white blood cell count 7 days after infarction. Peripheral blood monocytes of TLR2$^{-/-}$ mice exhibited similar CD11b expression, but reduced CD49d levels compared to WT animals 7 days after infarction. The functional and cellular changes in TLR2$^{-/-}$ mice were preceded by significant reduction in tissue levels of TNFα, IL-1α, GM-CSF and IL-10 at 3 days after infarction.

Conclusions

Lack of TLR2 improves survival and cardiac function after myocardial infarction and is determined by leukocytic TLR2 deficiency via reduced inflammation. Hence, TLR2 is a potential therapeutic target to prevent adverse remodeling after myocardial infarction

In preparation

Optimized reperfusion strategies have resulted in improved survival of patients after myocardial infarction (MI). Unfortunately, quality of life of surviving patients is significantly decreased due to increased morbidity after infarction[1]. Heart failure is one of the most common complications after infarction and inflict an increasing socio-economic burden on Western societies. Currently, the post-infarct healing process is of increasing importance for therapeutic modulation to enhance cardiac repair and function after MI. Inflammation, proliferation and maturation are chronological processes during infarct healing that can be targeted independently from each other for therapeutic modulation[2]. Inflammation is an interesting therapeutic target, since it is initiated early and has profound effects for the later stages. Cytokine and chemokine production and subsequent leukocyte recruitment are initiated after the ischemic injury. Leukocyte migration is a critical first step in the removal of debris and matrix breakdown and subsequent scar formation[2]. The extent and type of inflammation has great impact on processes like angiogenesis and fibrosis in the (sub)chronic phase after infarction[3-5]. For this reason, modulation of the early inflammatory process may have great therapeutic value to regulate adaptive repair processes hereafter. However, inflammation is not a random binary process rather a well-orchestrated dynamic response to tissue injury. For this reason, therapeutic modulation is challenging and difficult. More importantly, inflammation has shown to have 'double-edged sword' characteristics thereby complicating therapeutic interventions[6, 7].

Recent studies have clearly demonstrated that Toll-like receptor (TLR) deficiency or inhibition enhance the 'good' and blunt the 'bad' of the inflammatory reaction in cardiac ischemia. Traditionally known as pathogen recognition receptors, TLRs have been shown to recognize endogenous activators released after cardiovascular injury[8]. TLR2 and 4 have been extensively studied in cardiac ischemia[9]. TLR4 deficiency or inhibition protects against ischemia/reperfusion (I/R) injury and adverse left ventricular remodeling[10-12]. We have recently shown that circulating TLR2 mediates myocardial I/R injury and that its inhibition is cardioprotective. TLR2 inhibition reduces monocytes activation after reperfusion, thereby inhibiting cytokine and chemokine production and subsequent reduction of apoptosis[13]. Furthermore, previous studies have shown that TLR2 deficiency prevents maladaptive remodeling[14]. However, the relative contribution of parenchymal and hematopoiesis-derived TLR2 expression to cardiac repair responses remain unknown.

In the present study, we show for the first time that circulating TLR2 expression mediates adverse remodeling after myocardial infarction. Furthermore, we investigated the functional and biochemical differences between TLR2 deficient and wild type animals during adverse remodeling after infarction.

RESULTS

Circulating TLR2 Expression Mediates Adverse Remodeling After Infarction

There were no differences between WT and TLR2$^{-/-}$ animals in cardiac function and geometry at baseline. Infarct size, determined as a percentage of the left ventricle (IS/LV), showed no differences between TLR2$^{-/-}$ and WT mice 2 days after infarction (Figure 1A). Despite similar infarct size, TLR2$^{-/-}$ animals showed improved survival compared to WT mice after infarction (Figure 1B). Most animals died between day 4 and 8 post-MI due to cardiac ruptures. Serial cardiac MRI assessments revealed a significant preservation of both function and LV dimensions during 28 days follow-up (Figure 1C and D; Table 1). TLR2$^{-/-}$ mice were relatively protected against expansive remodeling of the left ventricle when compared to WT animals. We performed bone marrow transplantation experiments from WT to irradiated knock-

out mice and vice versa, in order to dissect the relative contribution to adverse remodeling of parenchymal and circulating TLR2 expression. Chimeric mice experiments revealed that adverse remodeling is relatively prevented in WT mice with TLR2$^{-/-}$ bone marrow (WT/TLR2 KO BM). In contrast, TLR2$^{-/-}$ mice with WT bone marrow (TLR2 KO/WT BM) exhibit similar LV dilatation compared to irradiated WTs with WT bone marrow (WT/WT BM; Figure 1E).

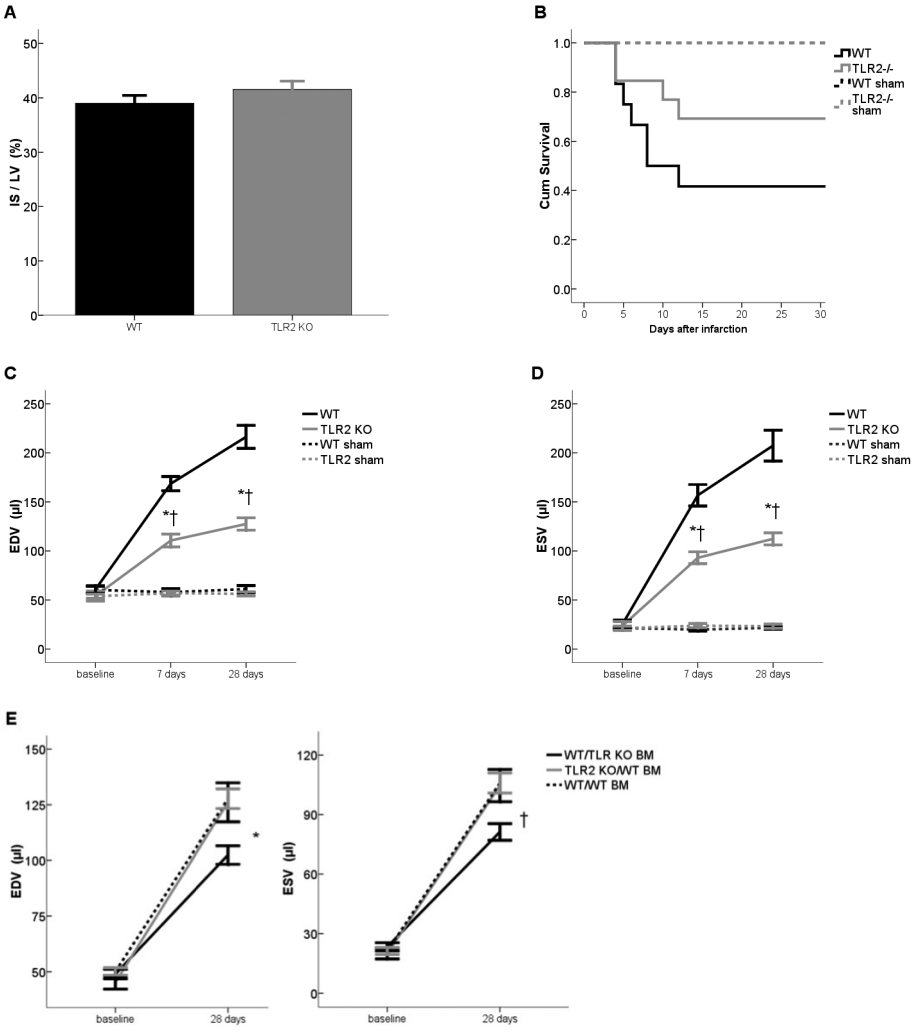

Figure 1. Circulating TLR2 mediates adverse remodeling after myocardial infarction. *(**A**) Infarct size (IS) as a percentage of the left ventricle (LV) 2 days after infarction. (**B**) Kaplan-Meier survival curve. (**C**) and (**D**), End-diastolic and end-systolic volume, respectively (EDV, ESV); p-values see Table 1. (**E**) EDV and ESV in chimeric mice 28 days after infarction; *p=0.005 †p=0.007 compared to TLR2 KO/WT BM. Each bar represents Mean±SEM, n=5/group for infarct size assessment, n=12 in WT and n=13 in TLR2$^{-/-}$ group for survival analysis. TLR2 KO/WT BM=irradiated TLR2$^{-/-}$ mice with WT bone marrow, WT/TLR2 KO BM= irradiated WT mice with TLR2$^{-/-}$ bone marrow, WT/WT BM=irradiated WT with WT bone marrow.*

Table 1.

	C57BL6/J WT			TLR2-/-				
	Baseline	7 days MI	28 days MI	Baseline	7 days MI	†p	28 days MI	†p
EDV, µl	60.9±3.7	168.6±7.2*	216.3±11.8**	54.1±5.1	110.7±6.6*†	<0.001	127.5±6.3**†	<0.001
ESV, µl	25.4±4.1	156.7±10.9*	207.4±15.7**	23.7±4.3	93.1±6.0*†	<0.001	112.4±6.2**†	<0.001
EF, %	59.1±4.1	7.2±2.8*	4.3±2.3**	57.9±4.3	16.0±1.1*	NS	11.9±1.0**	NS
WT septum (remote, mm)	0.90±0.01	0.67±0.06*	0.75±0.02**	0.85±0.02	0.72±0.01*	NS	0.71±0.03**	NS
WT free wall (infarct, mm)	0.90±0.02	0.60±0.08*	0.45±0.04**	0.89±0.01	0.55±0.03*	NS	0.45±0.07**	NS
SWT septum (remote, %)	47.1±1.9	20.6±5.0*	16.1±4.7**	47.1±2.1	36.9±3.1*†	0.009	35.8±3.2**†	0.012
SWT free wall (infarct, %)	52.0±1.9	-34.0±5.7*	-56.6±3.6**	54.2±1.8	-18.6±4.2*	NS	-26.2±4.0**†	0.027

*One-way ANOVA post hoc Dunnett t-test (2-sided), *p<0.05 compared to baseline, †p compared to WT mice. EDV=end-diastolic volume, ESV=end-systolic volume, EF=ejection fraction, WT=wall thickness, SWT=systolic wall thickening*

TLR2 Deficiency Reduces Inflammation After Infarction

Myocardial infarction is characterized by cytokine and chemokine induction and leukocytosis. In our experiments, TLR2 deficiency resulted in a significant reduction of TNFα, IL-1α, IL-10 and GM-CSF 3 days after infarction (Figure 2A – D). White blood cell counts revealed that $TLR2^{-/-}$ animals exhibited reduced leukocytosis compared to WT mice after infarction (Figure 2E).

TLR2 Mediates Integrin-α4 Expression On Circulating Monocytes After Infarction

Monocyte migration to the heart is an integrin-dependent process[15]. The expression of CD11b did not differ between the groups after infarction (Figure 3A). However, compared to WT animals, circulating monocytes of $TLR2^{-/-}$ mice expressed decreased levels of CD49d after infarction (Figure 3B).

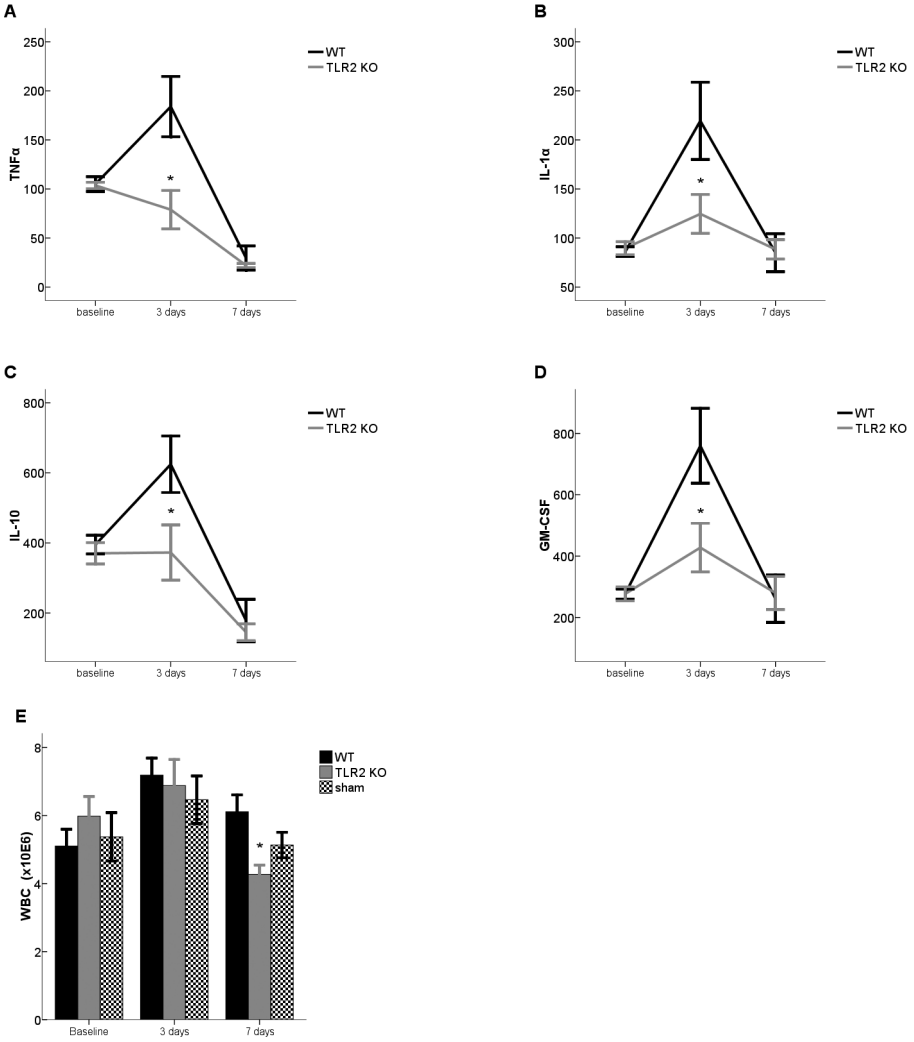

Figure 2. Lack of TLR2 reduces tissue cytokine levels and leukocytosis after infarction. *Tissue levels of (**A**) TNFα; *p=0.032 B, (**B**) IL-1α; *p=0.032 C, (**C**) IL-10; *p=0.063 and (**D**) GM-CSF; *p=0.046 compared to WT animals. (**E**) White blood cell counts (WBC) after infarction; *p=0.05 compared to WT animals. Each bar represents Mean±SEM, n=6/group/time point.*

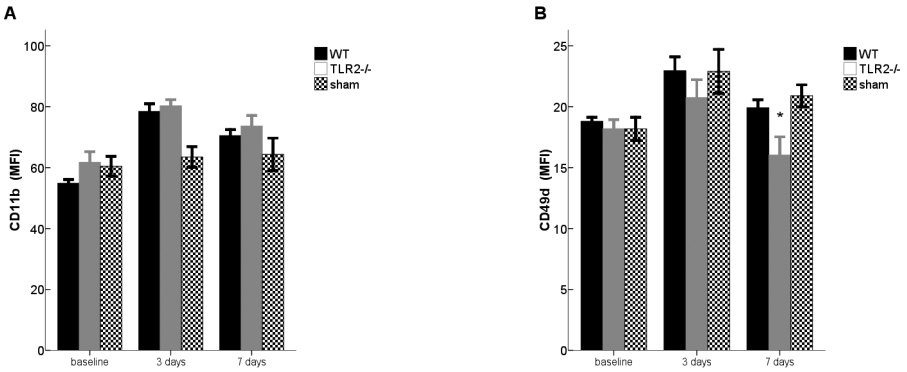

Figure 3. Lack of TLR2 reduces integrin-α4, but not CD11b expression on monocytes after myocardial infarction. *(**A**) CD11b and (**B**) CD49d on circulating monocytes; *p=0.023 compared to WT animals. Each bar represents Mean±SEM, n=6/group/time point. MFI=mean fluorescent intensity*

DISCUSSION

Toll-like receptors as therapeutic targets may hold great therapeutic value in the near future. We have shown in both murine and porcine (unpublished data) models that TLR2 inhibition is a good candidate for infarct size reduction after ischemia/reperfusion[13]. The question remains whether TLR2 inhibition has adverse effects on remodeling of the scar and remote myocardium in the long-term. There are tragic examples in which inflammatory interventions with beneficial effects in the acute phase turned out to be devastating in the long-term. Corticosteroid administration reduced infarct size in animal experiments, but appeared to result in aneurysm formation and cardiac ruptures in patients after infarction[6, 7]. The main issue of down toning inflammation is impaired healing resulting in reduced collagen deposition in the scar and ventricular dilatation. Severe suppression of the immune response is associated with a so-called "mummified myocardium", characterized by delayed debris removal and decrease infarct collagen content[16]. In addition, reduced infarct collagen is associated with more pronounced LV dilatation and dysfunction[17]. A report by Mersmann J *et al*. suggests that TLR2 deficiency results in adverse remodeling after infarction, despite smaller infarct size compared to WT animals[18]. Unfortunately, in their study the background of the TLR2$^{-/-}$ and WT mice were different: C57Bl6 vs. C3HeN, respectively. For this reason, it is difficult to draw firm conclusion from these experiments.

In the present study, we investigated the healing process after infarction in TLR2$^{-/-}$ and WT mice, both on a C57Bl6/J background. Despite similar infarct size, cardiac MRI assessments revealed that LV dilatation and functional deterioration is relatively prevented in TLR2$^{-/-}$ mice. The improved cardiac function and geometry is likely the reason for improved survival in TLR2$^{-/-}$ animals. Moreover, in our experiments lack of TLR2 was relatively protective against bulging of the infarcted myocardium. It is known that bulging of the infarct (i.e. aneurysm formation) is associated with reduced collagen density in the scar[17].

We have previously shown that circulating TLR2 expression mediates ischemia/reperfusion injury of the heart[13]. In addition, it is well-established that leukocytes migrate to the heart to initiate the process of myocardial healing[2, 5]. Hence, we hypothesized that TLR2 expression on circulating blood cells is also the main determinant for adverse remodeling. WT mice with TLR2 knock-out bone marrow were indeed

relatively protected against adverse remodeling compared to TLR2$^{-/-}$ mice with WT bone marrow. Findings by Shishido *et al*.[14] and the present study are in strong contrast to the study by Mersmann *et al*. in which TLR2 deficiency was associated with impaired cardiac function and geometry. We believe that the different strains used in their experiments (C3HeN background was compared to C57Bl6 background) are the main reason for the conclusions drawn by Mersmann *et al*. rather than the TLR2 knock-out. It is known that mouse strains strongly differ in myocardial healing after infarction[19]. Since improvement in cardiac function is a relative measure, it is of utmost importance that the intervention (e.g. knock-out) is the only differing variable and that confounding factors like background strain are absent.

Furthermore, we demonstrated that TLR2$^{-/-}$ mice exhibit reduced cytokine levels and leukocytosis compared to WT animal after infarction. These findings are in line with the pro-inflammatory actions of TLR2 upon activation. CD49d is an important integrin for leukocyte migration and myofibroblast transdifferentiation[15, 20]. Whether leukocyte infiltration and myofibroblast transdifferentiation is altered in TLR2$^{-/-}$ mice remains to be addressed. However, the reduced CD49d expression on circulating TLR2$^{-/-}$ monocytes after infarction suggests that leukocyte migration and myofibroblast transdifferentiation may be altered in TLR2$^{-/-}$ mice.

In conclusion, we have shown that circulating TLR2 mediates maladaptive remodeling after myocardial infarction. Lack of TLR2 improves survival and prevents post-infarct heart function deterioration via decreased inflammation and reduced migration capacity of monocytes. The exact mechanisms by which TLR2 mediates leukocyte migration and myofibroblast transdifferentiation in the healing heart remains to be addressed. Our study demonstrates that chronic absence of TLR2 is beneficial after myocardial infarction and is a good candidate as a therapeutic target in patients after myocardial infarction.

Acknowledgements

We would like to thank the following persons for their assistance: Ben J. van Middelaar, Cees van der Kolk and Arjan Schoneveld (all from the UMC Utrecht, The Netherlands).

Funding Sources

This work is supported by research grants from Netherlands Organisation for Scientific Research (NWO) Mozaïek grant (contract 017.004.004 to F.A.), Netherlands Heart Foundation (contract 2010.T001 to F.A.) and Bekales Foundation (P.A.D.)

METHODS

Animals and Experimental Design

TLR2$^{-/-}$ animals were backcrossed for 6 generations into a C57Bl6 background. Male C57Bl6/J and C57Bl6-TLR2$^{-/-}$ mice (10-12 wks, 25-30 g) received standard diet and water *ad libitum*. Myocardial infarction was induced by permanent left coronary artery ligation, just below the left atrial appendage as described previously. Digital images of the infarcts were encrypted before being analyzed by the researcher. Heart function and geometry assessments were done by a technician blinded to treatment. All animal experiments were performed in accordance with the national guidelines on animal care and with prior approval by the Animal Experimentation Committee of Utrecht University.

Myocardial Infarction In Vivo

Mice were anesthetized with a mixture of Fentanyl (Jansen-Cilag) 0.05 mg/kg, Dormicum (Roche) 5 mg/kg and medetomidine 0.5 mg/kg through an intraperitoneal injection. Core body temperature was maintained around 37°C during surgery by continuous monitoring with a rectal thermometer connected to an automatic heating blanket. Mice were intubated and ventilated (Harvard Apparatus Inc.) with 100% oxygen. The left coronary artery (LCA) was permanently ligated using an 8-0 vicryl suture. Ischemia was confirmed by bleaching of the myocardium and ventricular tachyarrhythmia. In sham operated animals the suture was placed beneath the LCA without ligating. The chest wall was closed and the animals received subcutaneously Antisedan (Pfizer) 2.5 mg/kg, Anexate (Roche) 0.5 mg/kg and Temgesic (Schering-Plough) 0.1 mg/kg.

Infarct Size

Infarct size (IS) as a percentage of the left ventricle (LV) was determined using Evans' blue dye injection and TTC staining, 2 days after infarction (n=5/group). By assessing infarct size in the acute phase (at 2 days), one can determine whether differences are present between WT and TLR2$^{-/-}$ mice in myocardial perfusion. Hence, 4% Evans blue dye was injected via the thoracic aorta in a retrograde fashion. By doing so, one can demarcate the area-at-risk (AAR), the extent of myocardial tissue that underwent ischemia (i.e. endangered myocardium). Hearts were rapidly explanted, rinsed in 0.9% saline and put in -20ºC freezer for 1 hour. Hereafter, hearts were mechanically sliced into four 1-mm cross sections. Heart sections were incubated in 1% triphenyltetrazolium-chloride (Sigma-Aldrich) at 37ºC for 15 minutes before placing them in formaldehyde for another 15 minutes. Viable tissue stains red and infarcted tissue appears white. Heart sections were digitally photographed (Canon EOS 400D) under a microscope (Carl Zeiss®). IS, AAR and total LV area were measured using ImageJ software (version 1.34). Infarct size was corrected for the weight of the corresponding heart slice.

Generation of Chimeric Mice

We generated chimeric mice to study the relative contribution of TLR2 expression in blood and parenchymal cells to cardiac remodeling. Donor bone marrow (BM) cells were collected from wild-type (WT) C57Bl6 and TLR2 knock-out (TLR2$^{-/-}$) mice by flushing humerus, femurs and tibiae with RPMI-1640 medium. Recipient mice received 5x10^{6} BM cells after receiving a single dose of 7 Gy. Mice recovered for 6 weeks to ensure stable engraftment of the donor bone marrow cells. Hereafter, chimerization was confirmed by phenotyping TLR2 expression on peripheral blood samples with Cytomics FC500 (Beckman Coulter) analysis. Successful chimerization (>95% circulating donor cells) was achieved in all mice (data not shown). Irradiated WT mice with TLR2$^{-/-}$ bone marrow are referred as WT/TLR2 KO BM, and TLR2$^{-/-}$ mice with WT bone marrow as TLR2 KO/WT BM.

Magnetic Resonance Imaging

Twenty-three mice (*n*=5 in WT, *n*=6 in TLR2$^{-/-}$ and *n*=6 in sham operated mice) underwent serial assessment of cardiac dimensions and function by high resolution magnetic resonance imaging (MRI, 9.4T, Bruker, Rheinstetten, Germany) under isoflurane anesthesia before, 7 and 28 days after MI. Long axis and short axis images with 1.0 mm interval between the slices were obtained and used to compute end-diastolic volume (EDV, largest volume) and end-systolic volume (ESV, smallest volume). The ejection fraction (EF) was calculated as 100*(EDV-ESV)/EDV. Wall thickness (WT) and systolic wall thickening (SWT) were assessed from both the septum (remote myocardium) and free wall (infarct

area). All MRI data are analyzed using Qmass digital imaging software (Medis, Leiden, The Netherlands).

Protein Isolation

Total protein was isolated from snap frozen infarcted heart sections (infarct and remote area separated) using 40 mM Tris pH 7.4.

Flow Cytometry

Tumor necrosis factor (TNF)-α, IL-1α, IL-10, and granulocyte macrophage-colony stimulating factor (GM-CSF) levels in isolated tissue protein samples were measured by flow cytometry (Cytomics FC500, Beckman Coulter) using the Th1/Th2 customized multiplex kit (Bender MedSystems, Vienna, Austria). The protein samples were diluted 1:1 in assay buffer, and the protocol is further followed according to the manufacturer's instructions.

CD11b and CD49d expression was assessed on circulating monocytes of EDTA anticoagulated blood by flow cytometry. Whole blood was stained for CD11b (FITC, eBioscience, San Diego, Calif), and CD49d (Alexa Fluor 488, Serotec, Oxford, UK) and F4/80 for monocytes (Alexa Fluor 647, Serotec, Oxford, UK).

Statistical Analysis

Data are represented as Mean±SEM. One-way ANOVA with post-hoc LSD test was used for comparison >2 groups. Non-parametric t-test for 2 group comparisons. Kaplan-Meier survival analysis with log-rank test was used to evaluate mortality differences between groups. All statistical analyses were performed using SPSS 15.1.1. and $p<0.05$ was considered significant.

The authors had full access to and take full responsibility for the integrity of the data. All authors have read and agree to the manuscript as written.

REFERENCES

1 Juenger J, Schellberg D, Kraemer S, Haunstetter A, Zugck C, Herzog W, Haass M. Health related quality of life in patients with congestive heart failure: comparison with other chronic diseases and relation to functional variables. Heart. 2002;87:235-241.

2 Frangogiannis NG. The immune system and cardiac repair. Pharmacol Res. 2008;58:88-111.

3 Arroyo AG, Iruela-Arispe ML. Extracellular matrix, inflammation, and the angiogenic response. Cardiovasc Res. 2010;86:226-235.

4 Frantz S, Vincent KA, Feron O, Kelly RA. Innate immunity and angiogenesis. Circ Res. 2005;96:15-26.

5 Frangogiannis NG. Chemokines in the ischemic myocardium: from inflammation to fibrosis. Inflamm Res. 2004;53:585-595.

6 Libby P, Maroko PR, Bloor CM, Sobel BE, Braunwald E. Reduction of experimental myocardial infarct size by corticosteroid administration. J Clin Invest. 1973;52:599-607.

7 Roberts R, DeMello V, Sobel BE. Deleterious effects of methylprednisolone in patients with myocardial infarction. Circulation. 1976;53:I204-I206.

8 Ionita MG, Arslan F, de Kleijn DP, Pasterkamp G. Endogenous inflammatory molecules engage Toll-like receptors in cardiovascular disease. J Innate Immun. 2010;2:307-315.

9 Chao W. Toll-like receptor signaling: a critical modulator of cell survival and ischemic injury in the heart. Am J Physiol Heart Circ Physiol. 2009;296:H1-12.

10 Arslan F, Keogh B, McGuirk P, Parker AE. TLR2 and TLR4 in ischemia reperfusion injury. Mediators Inflamm. 2010;2010:704202.

11 Riad A, Jager S, Sobirey M, Escher F, Yaulema-Riss A, Westermann D, Karatas A, Heimesaat MM, Bereswill S, Dragun D, Pauschinger M, Schultheiss HP, Tschope C. Toll-like receptor-4 modulates survival by induction of left ventricular remodeling after myocardial infarction in mice. J Immunol. 2008;180:6954-6961.

12 Timmers L, Sluijter JP, van Keulen JK, Hoefer IE, Nederhoff MG, Goumans MJ, Doevendans PA, van Echteld CJ, Joles JA, Quax PH, Piek JJ, Pasterkamp G, de Kleijn DP. Toll-like receptor 4 mediates maladaptive left ventricular remodeling and impairs cardiac function after myocardial infarction. Circ Res. 2008;102:257-264.

13 Arslan F, Smeets MB, O'Neill LA, Keogh B, McGuirk P, Timmers L, Tersteeg C, Hoefer IE, Doevendans PA, Pasterkamp G, de Kleijn DP. Myocardial ischemia/reperfusion injury is mediated by leukocytic toll-like receptor-2 and reduced by systemic administration of a novel anti-toll-like receptor-2 antibody. Circulation. 2010;121:80-90.

14 Shishido T, Nozaki N, Yamaguchi S, Shibata Y, Nitobe J, Miyamoto T, Takahashi H, Arimoto T, Maeda K, Yamakawa M, Takeuchi O, Akira S, Takeishi Y, Kubota I. Toll-like receptor-2 modulates ventricular remodeling after myocardial infarction. Circulation. 2003;108:2905-2910.

15 Sopel M, Ma I, Gelinas L, Oxner A, Myers T, Legare JF. Integrins and monocyte migration to the ischemic myocardium. J Invest Surg. 2010;23:79-86.

16 Kloner RA, Fishbein MC, Lew H, Maroko PR, Braunwald E. Mummification of the infarcted myocardium by high dose corticosteroids. Circulation. 1978;57:56-63.

17 Jugdutt BI, Joljart MJ, Khan MI. Rate of collagen deposition during healing and ventricular remodeling after myocardial infarction in rat and dog models. Circulation. 1996;94:94-101.

18 Mersmann J, Habeck K, Latsch K, Zimmermann R, Jacoby C, Fischer JW, Hartmann C, Schrader J, Kirschning CJ, Zacharowski K. Left ventricular dilation in toll-like receptor 2 deficient mice after myocardial ischemia/reperfusion through defective scar formation. Basic Res Cardiol. 2010.

19 van den Borne SW, van dS, V, Strzelecka AE, Vervoort-Peters HT, Lijnen PM, Cleutjens JP, Smits JF, Daemen MJ, Janssen BJ, Blankesteijn WM. Mouse strain determines the outcome of wound healing after myocardial infarction. Cardiovasc Res. 2009;84:273-282.

20 Wang Q, Wang Y, Hyde DM, Gotwals PJ, Lobb RR, Ryan ST, Giri SN. Effect of antibody against integrin alpha4 on bleomycin-induced pulmonary fibrosis in mice. Biochem Pharmacol. 2000;60:1949-1958.

CHAPTER 9

This chapter demonstrates the pivotal role of fibronectin-EDA in adverse remodeling after myocardial infarction

Fatih Arslan, Mirjam B. Smeets, Paul W. Riem Vis, Jacco C. Karper, Paul H. Quax, Lennart G. Bongartz, John H. Peters, Imo E. Hoefer, Pieter A. Doevendans, Gerard Pasterkamp & Dominique P. de Kleijn

Lack of fibronectin-EDA promotes survival and prevents adverse remodeling and heart function deterioration after myocardial infarction

Background

The extracellular matrix (ECM) may induce detrimental inflammatory responses upon degradation, causing adverse cardiac remodeling and heart failure. The ECM protein fibronectin-EDA (EIIIA; EDA) is upregulated after tissue injury and may act as a 'danger signal' for leukocytes to cause adverse cardiac remodeling after infarction. In the present study, we evaluated the role of EDA in regulation of post-infarct inflammation and repair after myocardial infarction.

Methods and Results

Wild-type and $EDA^{-/-}$ mice underwent permanent ligation of the LCA. Despite equal infarct size between groups (38.2±4.6% vs. 38.2±2.9% of LV (p=.985)), $EDA^{-/-}$ mice exhibited less left ventricular dilatation and enhanced systolic performance compared to wild-type mice as assessed by serial cardiac MRI measurements. In addition, $EDA^{-/-}$ mice exhibited reduced fibrosis of the remote area without affecting collagen production, cross-linking and deposition in the infarct area. Subsequently, ventricular contractility and relaxation was preserved in $EDA^{-/-}$. At tissue level, $EDA^{-/-}$ mice showed reduced inflammation, metalloproteinase 2 and 9 activity and myofibroblast transdifferentiation. Bone marrow transplantation experiments revealed that myocardium-induced EDA and not EDA from circulating cells regulates post-infarct remodeling. Finally, the absence of EDA reduced monocyte recruitment as well as monocytic TLR2 and CD49d expression after infarction.

Conclusions

Our study demonstrated that parenchymal fn-EDA plays a critical role in adverse cardiac remodeling after infarction. Absence of fn-EDA enhances survival and cardiac performance by modulating matrix turn-over and inflammation via leukocytes and fibroblasts after infarction.

Circ Res. 2011;108(5):582-92

Heart failure (HF) is becoming a major socio-economic burden for Western societies, for both incidence and prevalence numbers are increasing.[1] Improved reperfusion strategies have caused a decline in death rates after acute myocardial infarction (MI). However, since more patients do survive the initial infarction, infarct-related morbidity increases. The extent of tissue loss in the acute phase after MI is a major determinant of the degree of adverse remodeling. However, chronic processes like extracellular matrix (ECM) turnover, fibrosis and inflammation are key mediators of post-MI cardiac repair and adverse remodeling.[2] Despite pharmacological advances (e.g. β-blockers, Renin-Angiotensin-Aldosterone system inhibitors),[3,4] incidence for HF is increasing and mortality remains very high (5-year mortality 30-70%).[5] Inflammation is the first critical step in tissue repair responses after myocardial infarction. Many interventions have been studied to modulate the inflammatory reaction in order to enhance heart function and attenuate structural changes leading to HF. However, interfering within the innate immune system is not without danger and necessitates understanding in temporal, spatial as well as the (patho) physiological role of the target.[2,6] Endogenous "danger" signals have gained much interest recently, since they are released upon tissue injury and do not play a biological role under normal conditions. Danger signals (e.g. cardiac myosin[7] and HMGB1[8]) are released upon ECM degradation or cardiomyocyte death and can activate leukocytes, thereby inducing the detrimental responses seen after myocardial infarction. Toll-like receptors are postulated as one of the main targets for endogenous ligands released after infarction.[9] Upon recognition of endogenous ligands, TLRs exert the same detrimental inflammatory processes via cytokine and chemokine expression. Cellular fibronectin is a multifunctional adhesive glycoprotein present in the ECM and is produced by cells (e.g. fibroblast, endothelial cells) in response to tissue injury. It contains an alternatively spliced exon encoding type III repeat extra domainA (EIIIA; EDA), that act as an endogenous ligand for both TLR2 and 4; *in vitro*, EDA induces pro-inflammatory gene expression and activates monocytes.[10] Furthermore, *in vivo* injection of EDA in murine joints results in enhanced inflammation via NF-κB activation.[11] In addition to its pro-inflammatory actions, EDA also acts as a ligand for several integrins (e.g. VLA-4/CD49d) regulating cell adhesion and proliferation.[12,13] The presence of EDA is also crucial for myofibroblast phenotype induction and function.[14]
In summary, EDA is able to activate leukocytes and cause an upregulation of cytokines and chemokines. One might hypothesize that upon degradation of the ECM and/or *de novo* synthesis after infarction, EDA could cause detrimental inflammatory responses. In the present study we show, *in vivo*, that the lack of EDA indeed prevents adverse cardiac remodeling and enhances cardiac function after acute MI.

RESULTS

Lack of EDA promotes survival and prevents heart function deterioration as well as maladaptive remodeling after myocardial infarction

EDA synthesis is stimulated after infarction in both infarct and remote myocardium, reaching a peak at 7 and 3 days, respectively (Online Figure I). Baseline MRI assessment of cardiac function and dimensions revealed no differences between $EDA^{-/-}$ and WT mice. Microscopic analyses did not show any alterations in cellularity and matrix composition in $EDA^{-/-}$ mice (Online Figure II).
The extent of endangered myocardium (AAR/LV) determined at 2 days post-MI was similar between the groups. Infarct size (IS) as percentage of LV was also similar between groups (IS/LV 38.2±1.2%, p=0.985; Figure 1A). Kaplan-Meier survival analysis showed a significant survival benefit in $EDA^{-/-}$ mice over WTs (Figure 1B). Most deaths occurred after day 6 and were not caused by cardiac rupture (only

2 ruptures in the WT and 1 rupture in EDA$^{-/-}$ mice were observed during 28 days follow-up). In line with increased mortality, WT mice had greater LV dimensions and reduced systolic performance compared to EDA$^{-/-}$ mice (Figure 1C; Table 1). These significant differences were already present 7 days after infarction, and continued to deteriorate till 28 days post-MI. EDA$^{-/-}$ mice were relatively protected against remodeling and exhibited better systolic function after MI (Figure 1C; Table 1). The protective effect seen in EDA$^{-/-}$ was not attributable to changes in the extent of viable tissue, because infarct size did not differ between WT and EDA$^{-/-}$ mice 28 days post-MI (33.7±2.3% vs. 34.3±3.5%, respectively; p=0.818). However, wall thickness of the infarct area did not decline in EDA$^{-/-}$ mice as much as in WTs. At day 28 post-infarction, the entire infarct area was replaced by a dense collagen network in both groups. At day 7, however, there was reduced granulation of the infarct as shown by delayed degradation of acellular matrix in EDA$^{-/-}$ mice (Figure 1D).

Lack of EDA decreases endogenous MMP-2, -9 and elastase activities

Enhanced MMP2 and -9 activities are detrimental for cardiac performance and geometry during the post-infarct healing process. We performed zymography to study whether the protection against adverse remodeling seen in EDA$^{-/-}$ mice is also attributable to changes in proteinase activity. In line with the reduced matrix degradation in the knock-out animals at day 7 observed in histology, both active forms of MMP-2 and -9 in infarct areas were reduced in EDA$^{-/-}$ mice, 7 days post-infarction (Figure 2). Analysis of the remote area after 7 days infarction was not possible due to very low signal intensity. Finally, we studied whether elastase activity was also affected by the absence of EDA. In line with reduced MMP2 and -9 activity, elastase activity was also reduced in EDA$^{-/-}$ mice 7 days after infarction (Online Figure III).

EDA$^{-/-}$ mice exhibit less post-infarct fibrosis

Collagen deposition occurs in the infarct area upon degradation of the matrix and in the remote myocardium upon changes in wall stress. Myofibroblasts are the primary source of *de novo* collagen synthesis.[2] In our study, collagen deposition in both the infarct and remote area was similar between the groups at day 7 post-MI (Online Figure IV). After 28 days, collagen content was again similar in the infarct area, suggesting that scar formation is not negatively affected in EDA$^{-/-}$ mice (Figure 3A). However, the remote myocardium now contained less collagen fibers in EDA$^{-/-}$ mice compared to WT animals (Figure 3B; lower pixel count in the small-size grey value spectrum). These findings were supported at the mRNA level. Both procollagen-1 and -3 are reduced in the remote myocardium of EDA$^{-/-}$ mice (Figure 3C). Within the infarct, collagen synthesis in EDA$^{-/-}$ mice was again comparable to WT animals. There was no difference in lysyl-oxidase and TIMP-2 production between the groups, suggesting no differences in collagen cross-linking and protease inhibition, respectively (Online Figure V and VI). The reduced fibrosis in the remote myocardium at 28 days post-MI is preceded by a significantly decreased myofibroblast transdifferentiation in EDA$^{-/-}$ mice, in both remote and infarct areas 7 days after infarction (Figure 3D and E). Periostin is described as a maturation factor of cardiac fibroblasts.[15] In our study, periostin-positive area was reduced as well in EDA$^{-/-}$ mice compared to WT animals (Figure 3F; Online Figure VII). To study whether WT and EDA$^{-/-}$ myofibroblasts differed in their matrix synthesis activity and MMP expression profile, we cultured post-infarct myofibroblasts and stained for myofibroblast markers and pro-collagen-III. *In vitro*, There were no differences between the two genotypes (Online Figure VIII). In addition, zymography was done using the supernatants of the cells and showed also no differences in MMP2 and -9 activity (Online Figure IX).

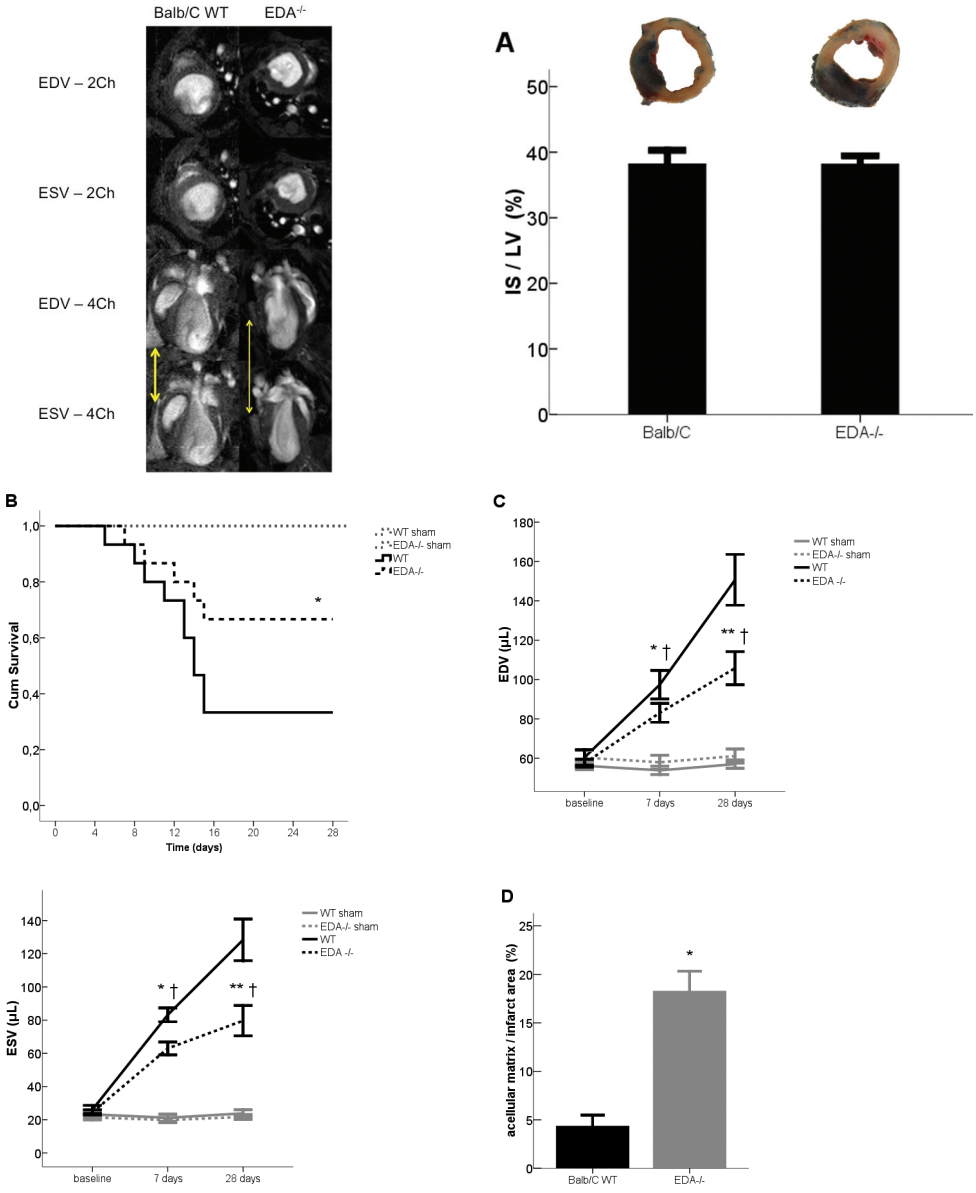

Figure 1. Lack of EDA preserves heart function and geometry after MI. (**A**) *Infarct size (IS) as a percentage of the left ventricle (LV) after day 2 ischemia. Representative cross-sections after TTC staining are shown below corresponding bars; n=5/group.* (**B**) *Kaplan-Meier survival curves; *p0.04 compared with WT ischemic mice; ischemic 15/group, sham 6/group.* (**C**), *Cardiac geometry in ischemic mice; *p<0.03 and **p<0.001 compared with baseline and sham-operated mice; †p-value (see Table 1) compared with WT ischemic mice. Representative short-axis and 4-chamber views of WT and EDA$^{-/-}$ mice 28 days post-MI. Note the massive pulmonary edema in WT mice (**yellow arrows**), which is almost absent in EDA$^{-/-}$ animals.* (**D**) *Reduced matrix degradation in EDA$^{-/-}$ mice 7 days post-MI. *p=0.004. Each bar represents mean±SEM, n=15/ischemic group; n=6/sham group. EDV indicates end-diastolic volume; ESV=end-systolic volume; Ch=chamber.*

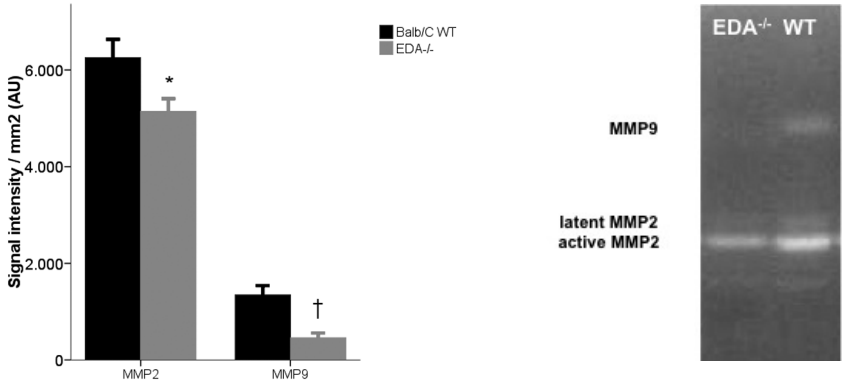

***Figure 2. Reduced MMP-2 and -9 activities in EDA$^{-/-}$ mice**. Isolated infarct samples of WT and EDA$^{-/-}$ mice, 7 days post-MI. The bars represent the signal intensity/mm^2 after background subtraction. Illustrative zymography results are shown next to the bars. *p=0.042, †p=0.001 compared to WT animals. Each bar represents Mean±SEM, n=6/group.*

Lack of EDA results in enhanced inotropy and lusitropy

Altered fibrotic processes in EDA$^{-/-}$ mice indicate that diastolic function could be affected as well. Table 2 shows the results from the invasive LV pressure assessments. Contractility, as indicated by dP/dT_{max}, was much higher in EDA$^{-/-}$ mice after 28 days infarction. This confirmed our previous MRI findings, that EDA$^{-/-}$ mice exhibit enhanced systolic performance (Table 1). Increase of LVEDP and tau is detrimental for heart function and is caused by increase of EDV and/or fibrosis; one of the hallmarks of heart failure. Compared to WT animals, diastolic performance was also significantly enhanced in EDA$^{-/-}$ mice after 28 days infarction. Both parameters were significantly lower in EDA$^{-/-}$ mice compared to WT animals, providing evidence that the improved survival in EDA$^{-/-}$ mice is a consequence of both systolic and diastolic functional improvements.

EDA regulates post-MI inflammation

Lack of EDA should result in a decreased inflammatory status, since EDA is considered as a ligand for TLR2 and 4. Neutrophils are the first leukocyte subset migrating upon tissue injury and are known to be associated with the extent of damage. Neutrophil count in the infarct area was not different between the groups (Figure 4A). Hereafter, macrophages clear cell debris (e.g. necrotic neutrophils and cardiomyocytes) and, more importantly, initiate the remodeling process after infarction.[2] In our study, the number of macrophages was highly reduced in EDA$^{-/-}$ mice 7 days post-infarction (Figure 4B). There were no cells detectable after 28 days infarction in both groups (data not shown). In concordance with the reduced macrophage influx, levels of TNFα, RANTES, GM-CSF (responsible for recruitment, differentiation and maturation of macrophages) and IL-10 were highly reduced in EDA$^{-/-}$ mice, 7 days after infarction (Figure 4C-F). In contrast, MCP-1 levels were increased in EDA$^{-/-}$ mice compared to WT animals at protein and mRNA level (Online Figure X).

Parenchymal EDA mediates post-infarct survival and maladaptive remodeling

We generated chimeric mice to differentiate between the contribution of the blood and parenchymal compartments to the observed effects after MI. Interestingly, WT/EDA KO BM had similar survival rates and cardiac performance compared to WT/WT BM animals. In contrast, EDA KO/WT BM were similar

Table 1. Cardiac function and geometry after infarction.

	Balb/C WT			$EDA^{-/-}$					WT/EDA KO BM			EDA KO/WT BM				
	Baseline	**7 days MI**	**28 days MI**	**Baseline**	**7 days Mi**	**†*p***	**28 days MI**	†*p*	**Baseline**	**7 days MI**	**28 days MI**	**Baseline**	**7 days MI**	**†*p***	**28 days MI**	†*p*
Heart rate, BPM	311±10	328±7	328±12	317±10	329±5	NS	324±15	NS	291±8	303±15	321±17	307±10	312±11	NS	329±11	NS
EDV, µL	60.4±3.9	97.4±7.3*	150.7±12.9**	57.5±2.1	83.1±4.8*†	0.043	105.8±8.4**†	0.001	62.5±2.9	98.8±3.5*	113.6±3.8**	60.9±1.9	81.9±2.7**†	<0.001	93.2±3.6**†	<0.001
ESV, µL	26.2±2.5	83.2±4.2*	128.4±12.5**	24.5±1.5	63.0±3.9*†	<0.001	79.7±9.1**†	0.001	35.6±2.9	78.8±3.1*	96.8±3.2**	31.7±1.6	62.2±2.4**†	<0.001	70.5±3.8**†	<0.001
EF, %	57.3±2.4	13.8±3.5*	15.4±2.2**	57.6±1.6	24.1±1.9*†	0.041	25.9±3.1**†	0.016	44.2±3.0	20.2±1.2*	14.6±2.5**	47.8±2.3	24.1±1.1**†	NS	24.5±2.1**†	0.017
WT septum (remote, mm)	0.89±0.02	0.72±0.03*	0.91±0.04	0.86±0.02	0.77±0.01*	NS	0.84±0.03	NS	0.89±0.01	0.77±0.01*	0.77±0.03**	0.91±0.01	0.83±0.02**†	0.019	0.86±0.02**	0.026
WT free wall (infarct, mm)	0.90±0.03	0.57±0.03*	0.57±0.03**	0.90±0.01	0.72±0.03*†	0.009	0.71±0.03**†	0.003	0.88±0.01	0.57±0.02*	0.49±0.03**	0.90±0.01	0.71±0.02**†	0.009	0.64±0.01**†	0.002
SWT septum (remote, %)	51.0±1.6	51.0±3.7	43.3±3.9	52.0±1.7	41.4±2.7*†	0.023	37.8±3.7**	NS	51.0±1.4	43.6±3.7	37.8±2.4**	52.0±1.8	43.7±3.7**	NS	40.1±4.0**	NS
SWT free wall (infarct, %)	54.6±2.4	-24.2±4.9*	-28.1±4.1**	54.8±2.6	2.8±1.8*†	<0.001	-14.7±2.4**†	0.019	50.5±1.5	-24.6±3.3*	-30.5±4.9**	48.9±1.8	1.9±2.4**†	<0.001	-13.4±2.2**†	0.009

*For the normal WT and $EDA^{-/-}$ mice experiments: One-way ANOVA post-hoc LSD: *p<0.03 and **p<0.001 compared to baseline and sham operated animals; †p value compared to Balb/C WT, n=15/group. For the chimeric mice experiments: One-way ANOVA post-hoc LSD with chimeras (WT/EDA KO BM; EDA KO/WT BM), WT in WT (WT/WT) and KO in KO (EDA KO/EDA KO) mice: *p<0.03 and **p<0.001 compared to baseline and sham operated animals; †p value compared to WT/$EDA^{-/-}$ BM animals. Data are represented as Mean±SEM, n=11/group. WT/EDA KO BM= WT animals with $EDA^{-/-}$ bone marrow, EDA KO/WT BM=$EDA^{-/-}$ mice with WT bone marrow, BPM=beats per minute, EDV=end-diastolic volume, ESV=end-systolic volume, EF=ejection fraction, WT=wall thickness, SWT=systolic wall thickening, NS=not significant.*

to EDA KO/EDA KO BM animals and showed higher survival rates and exhibited less adverse remodeling after MI, compared to WT/EDA KO BM (Figure 5A and B; Table 1). These data indicate that post-infarct parenchymal EDA expression drives maladaptive remodeling. From a danger model perspective, we may postulate that EDA expression as a danger signal can have profound effects on circulating cells which are responsible for post-infarct repair responses.

EDA mediates both integrin-α4 and Toll-like receptor signaling in circulating monocytes

EDA is a known ligand for integrin-α4β1 (VLA-4)[12] and TLR2 and 4.[10] Since parenchymal EDA mediates adverse remodeling, we hypothesized that EDA from the heart may serve as an endogenous activator of circulating cells after infarction. $EDA^{-/-}$ mice showed a significant reduction in peripheral monocytes 3 days after infarction, whereas after 7 days the numbers were similar between the groups (Figure 6A). TLR2 expression on monocytes was significantly altered in the absence of EDA, while TLR4 did not show any difference in expression levels after MI between the groups (Figure 6B and C). Integrin-α4 (CD49d) expression was also significantly reduced on monocytes of $EDA^{-/-}$ mice after infarction (Figure 6D). In addition, there was a subgroup of monocytes that showed a significant higher expression level of CD49d. $EDA^{-/-}$ mice showed again a reduced CD49d expression in this subgroup, 7 days post-infarction (Figure 6E).

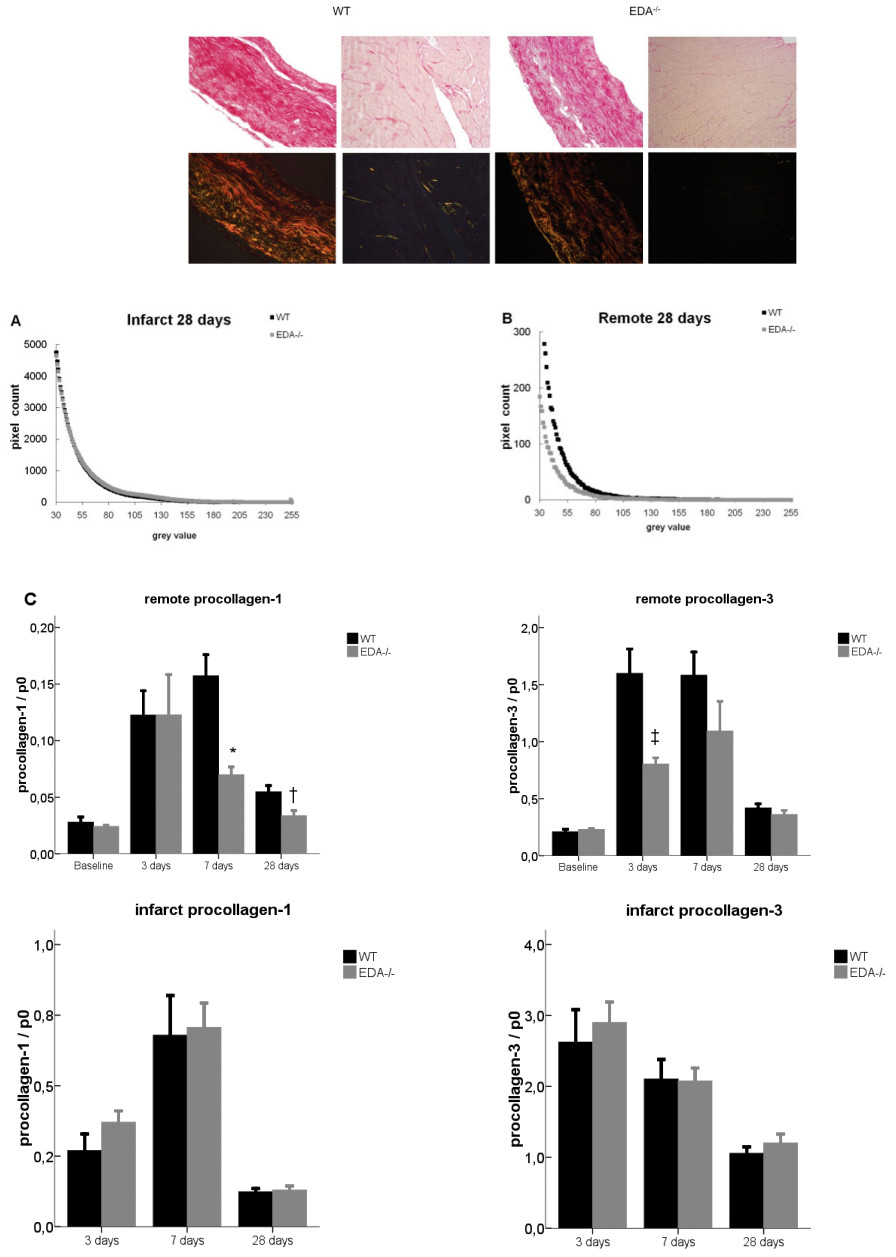
WT
EDA-/-
A
Infarct 28 days
WT
EDA-/-
pixel count
grey value
B
Remote 28 days
C
remote procollagen-1
procollagen-1 / p0
Baseline
3 days
7 days
28 days
remote procollagen-3
procollagen-3 / p0
infarct procollagen-1
infarct procollagen-3

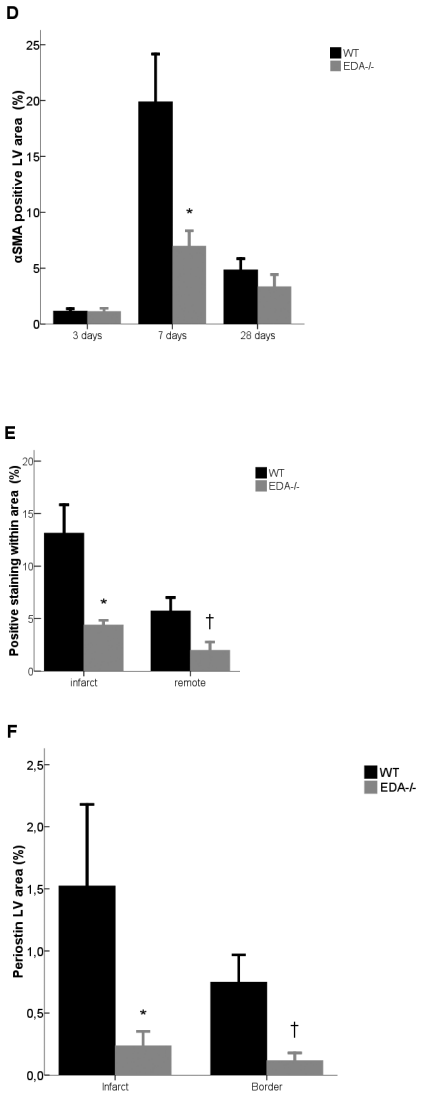

Figure 3. EDA-/- mice exhibit less fibrosis after MI. *Histograms give an overview of the entire spectrum of collagen intensity. The larger the grey value, the intenser the collagen staining. Grey values below 30 are considered as background signal of the intensity image acquired after polarized light microscopy. (**A**) Collagen intensity in the infarct area, 28 days post-MI. (**B**) Collagen intensity in the remote myocardium, 28 days post-MI. *p=0.042 area under the curve. (**C**) mRNA levels in infarct and remote areas during infarct development. Procollagen-1 and -3 mRNA levels in the remote area are significantly reduced in EDA$^{-/-}$ mice. *p=0.004, p=0.008, p=0.007 compared with WT animals. (**D**) Positive α-SMA fraction in LV wall during cardiac repair. Vessels are not taken in the positive area fraction calculation. *p=0.014. (**E**) Positive α-SMA fraction in infarct and remote area 7 days post-infarct. *P=0.009, P=0.047. (**F**) Periostin-positive area within infarct and border zone. *p=0.018, p=0.045. Representative images of collagen intensity using white and polarized light microscopy. Each bar represents mean±SEM, n=6/group/time point. LV indicates left ventricular*

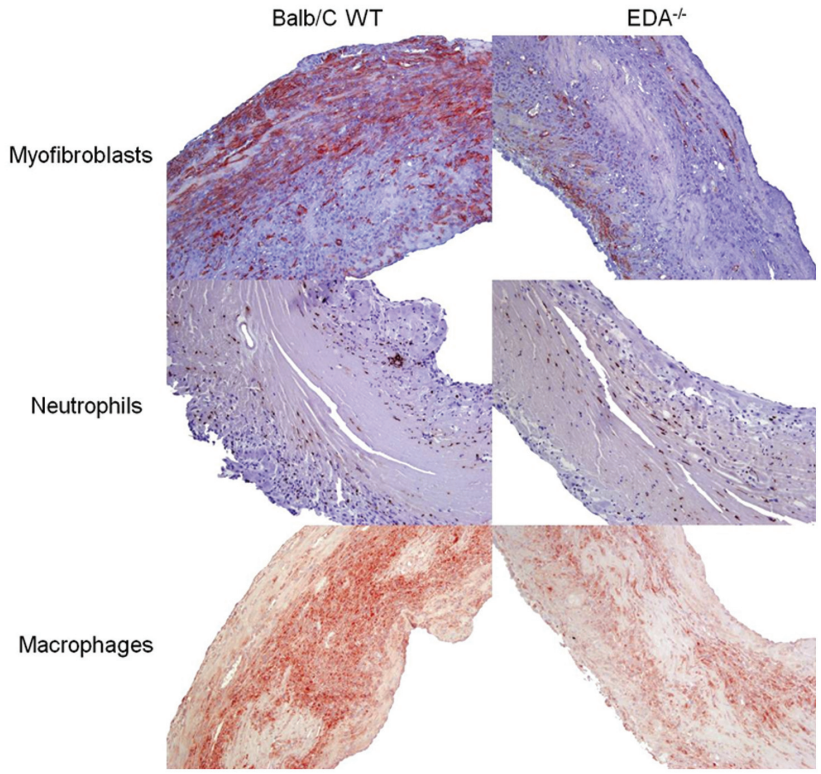
Balb/C WT
EDA-/-
Myofibroblasts
Neutrophils
Macrophages

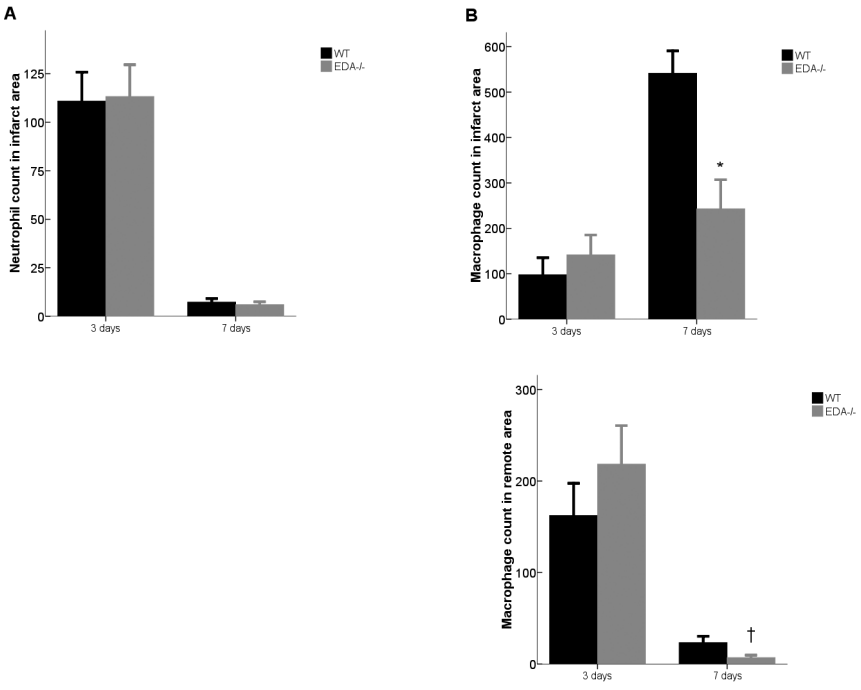
A
Neutrophil count in infarct area
125
100
75
50
25
0
3 days
7 days
WT
EDA-/-
B
Macrophage count in infarct area
600
500
400
300
200
100
0
*
3 days
7 days
WT
EDA-/-
Macrophage count in remote area
300
200
100
0
†
3 days
7 days
WT
EDA-/-

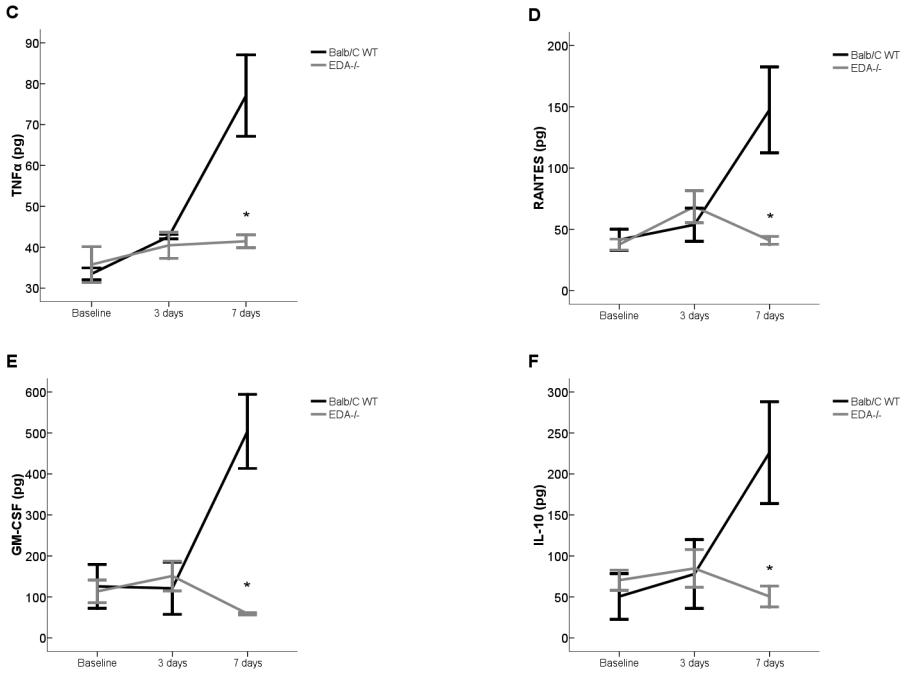

Figure 4. EDA mediates detrimental inflammatory responses after MI. *(**A**) Number of neutrophils in the infarct area. (**B**) Reduced macrophage influx in infarct and remote area in EDA$^{-/-}$ mice after infarction. *p=0.028, †p=0.047 compared to WT. (**C**) Reduced TNFα levels in heart tissue in EDA$^{-/-}$ mice after infarction. *p=0.011 compared to WT. (**D**) RANTES levels. *p=0.023 compared to WT. (**E**) GM-CSF levels. *p=0.002 compared to WT. (**F**) IL-10 levels. *p=0.033 compared to WT. Representative images of heart cross-sections stained for myofibroblasts (7 days post-MI), neutrophils (3 days post-MI) and macrophages (7 days post-MI). Each bar represents Mean±SEM, n=6/group/time point.*

Table 2. Left ventricular pressure development in WT and EDA-/- mice 28 days after infarction.

	Balb/C WT	EDA$^{-/-}$	*p*
Heart rate, BPM	407±17	455±18	NS
LVESP, mmHg	104±4	108±7	NS
LVEDP, mmHg	41±4	22±5	0.014
dP/dT$_{max}$, mmHg/s	3362±277	5315±720	0.024
Tau, ms	26±3	14±1	0.018

Npar-test, p-values are shown in table. Data are represented as Mean±SEM, n=5/group. BPM=beats per minute, LVESP=left ventricular end-systolic pressure, LVEDP=LV end-diastolic pressure, NS=not significant.

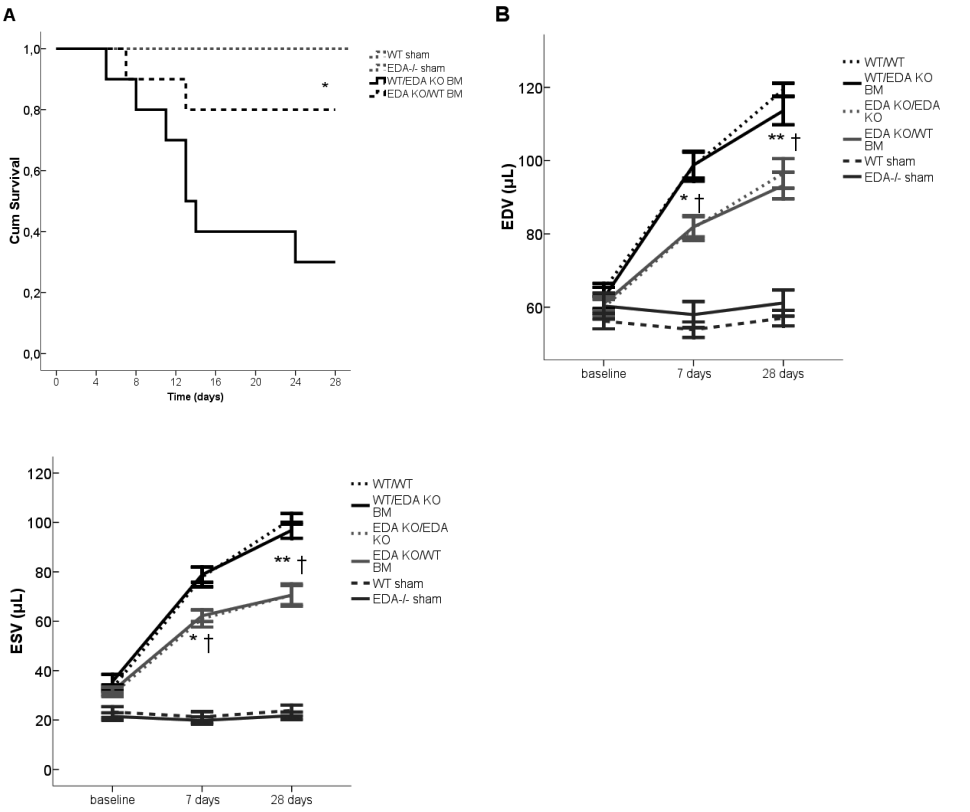

Figure 5. Myocardial EDA expression mediates survival and adverse cardiac remodeling after myocardial infarction. *(**A**) Kaplan-Meier survival curves; *p=0.037 compared to WT/EDA KO BM ischemic mice. (**B**) Cardiac geometry and ejection fraction in ischemic mice; *p<0.03 and **p<0.001 compared to baseline and sham operated mice; †p-value (see Table 1.) compared to WT/EDA$^{-/-}$ BM ischemic mice. Each bar represents Mean±SEM, n=11/group. WT/WT BM indicates WT with WT bone marrow, EDA KO/EDA KO BM=EDA$^{-/-}$ mice with EDA$^{-/-}$ bone marrow. WT/EDA KO BM=WT mice with EDA$^{-/-}$ bone marrow, EDA KO/WT BM=EDA$^{-/-}$ animals with WT bone marrow.*

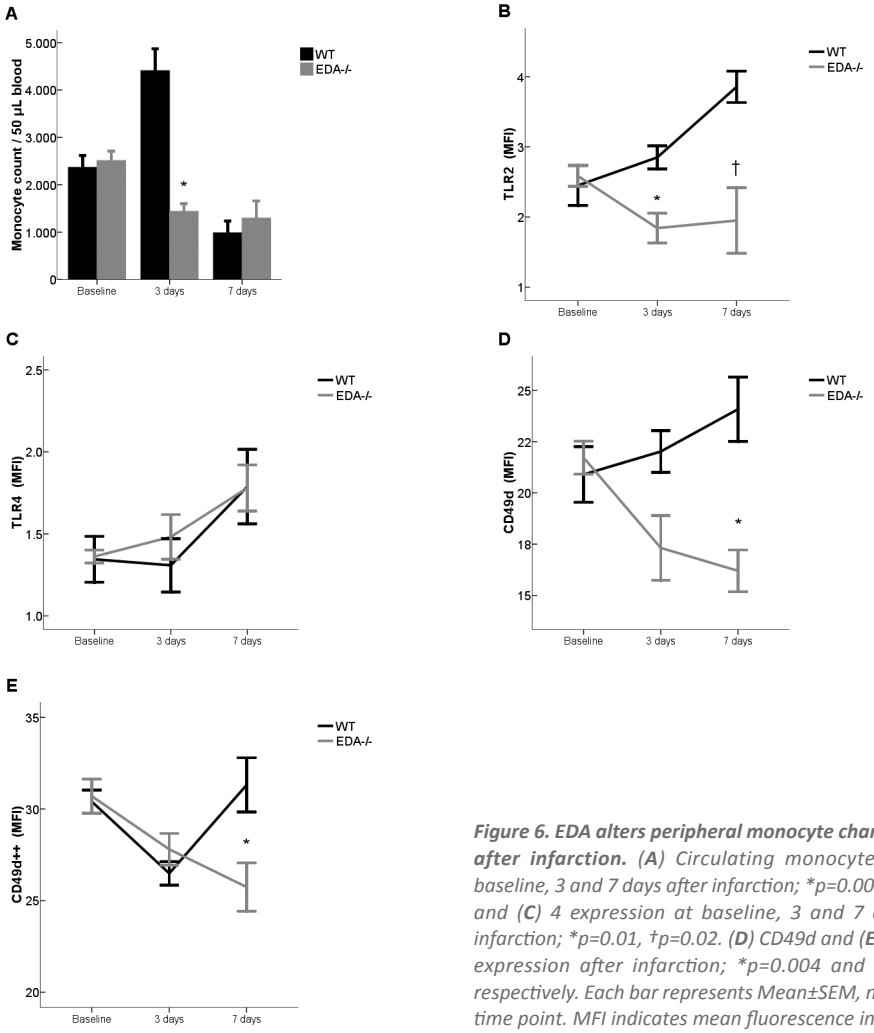

Figure 6. EDA alters peripheral monocyte characteristics after infarction. *(**A**) Circulating monocyte count at baseline, 3 and 7 days after infarction; *p=0.006. (**B**) TLR2 and (**C**) 4 expression at baseline, 3 and 7 days after infarction; *p=0.01, †p=0.02. (**D**) CD49d and (**E**) CD49d^{high} expression after infarction; *p=0.004 and *p=0.028, respectively. Each bar represents Mean±SEM, n=8/group/time point. MFI indicates mean fluorescence intensity.*

DISCUSSION

Heart failure (HF) is already considered as an epidemic of the 21st century and its socio-economic burden of HF is likely to increase.[16] Mortality after acute MI declines due to pharmacological and technical advances facilitating early reperfusion and survival. However, morbidity increases due to the excessive tissue loss and detrimental chronic processes during infarct healing. Inflammation is necessary for adequate wound healing and interfering with anti-inflammatory agents may be devastating.[17] However, post-infarct recovery is characterized by an auto-destructive inflammatory response causing a vicious circle. Hereby, the same inflammatory response influences cardiac performance and geometry in a detrimental way. This adverse healing process causes changes in ventricular structural design and dimension, referred as adverse cardiac remodeling. Despite the therapeutic advances for patients suffering from acute MI, there is a window of opportunity for adjunctive interventions. Especially therapeutic targets within our innate immune system hold great promise for future application for cardiomyocyte salvage after acute MI.[18, 19] Ideally, the optimal therapy for patients suffering from acute MI encompasses both cardiomyocyte salvage and attenuating adverse remodeling, without affecting a proper scar formation. The discovery of Toll-like receptors (TLRs) has not only provided us with great insight into pathophysiological mechanisms in HF, but may also hold therapeutic value. We and others have shown that deficient TLR2 and 4 activation has therapeutic effects in murine models of atherosclerosis[10, 20] and cardiac ischemia.[19, 21-23] The idea that pattern recognition receptors also induce detrimental inflammatory responses in non-infectious settings has resulted in the search for endogenous ligands, so called “danger” signals. These danger signals are thought to be released and/or produced during tissue injury and cell stress. From this ‘danger model’ perspective,[24] EDA may be a critical mediator of adverse remodeling after myocardial infarction.

We have shown that EDA is indeed upregulated after acute MI. This is in line with previous reports that EDA is produced in response to tissue injury (reviewed in Ref.[12]). EDA mRNA levels peaked at day 7 post-MI in the infarcted wall and returned to baseline levels after 28 days. Immunohistochemistry suggested similar if not greater expression of EDA in the remote myocardium. The discrepancy between mRNA and protein levels and EDA staining could potentially reflect sampling of EDA pools of differing solubility. Experiments with cultured cells have shown that, after synthesis and secretion, soluble fibronectin dimers first appear at the cell surface but, over time, incorporate into less soluble multimeric aggregates in the ECM.[25] Immunohistologic analysis has the capacity to detect such *insoluble* fibronectin aggregates in the ECM of tissues, whereas immunoblot analysis is apt to preferentially detect soluble extractable fibronectins.[25] Potentially, EDA that is produced after the modest increase in EDA transcription in remote myocardium could preferentially incorporate into an insoluble fibronectin pool, thereby becoming relatively more evident by immunohistologic than immunoblot analysis (Online Figure I). Despite similar infarct size, $EDA^{-/-}$ mice showed enhanced survival compared to WT animals. In addition, WT animals exhibited a severely affected cardiac function and profound expansive remodeling during 28 days of recovery. In contrast, $EDA^{-/-}$ mice showed preserved LV geometry, better systolic performance and less LV bulging during systole. Interestingly, this protective effect was already significant 7 days after infarction and continued to be apparent in the long-term follow-up. The detrimental changes were associated with the EDA mRNA peak seen at day 7.
We explored several cellular and molecular mechanisms to explain the protective effect of EDA absence after myocardial infarction.

First, we showed that EDA$^{-/-}$ mice have a normal scar formation (normal collagen content in infarct area) whereas remote fibrosis was decreased. This was also supported at the mRNA level for both procollagen-1 and -3, showing only decreased expression in the remote area. Furthermore, granulation of the infarct area was delayed and wall thickness did not decline in EDA$^{-/-}$ mice as much as in WT animals. In addition, myofibroblast transdifferentiation in the post-infarct ventricular wall was highly suppressed in EDA$^{-/-}$ mice. These observations suggest that EDA does not mediate fibrosis directly, since there is selective attenuation of fibrosis in the remote myocardium and not in the scar area in EDA$^{-/-}$ mice. We may hypothesize the following mechanisms: due to delayed matrix degradation in EDA$^{-/-}$ after infarction, infarct thinning is also delayed. The thicker wall of the infarct area in EDA$^{-/-}$ mice results in less wall stress and thus end-diastolic volume is limited. In addition, the decreased wall stress in EDA$^{-/-}$ mice may explain the decreased LV pressure-overload in these mice. Subsequently, reduced ventricular pressure may result in reduced fibrosis of the remote myocardium, as observed in our EDA$^{-/-}$ animals 28 days after infarction. Invasive pressure measurements indeed revealed that WT animals have nearly 90% increase of both LVEDP and LV relaxation time compared to EDA$^{-/-}$ mice. We studied whether apoptosis in the remote myocardium could explain the functional impairment in WT animals, but did not observe a difference in caspase 3 and 7 activity between the groups during follow-up (Online Figure XI).

Secondly, we studied the inflammatory status in the post-infarct hearts. The absence of EDA did not affect neutrophil count, suggesting that the extent of tissue injury was similar between the groups. This is supported by the observation that infarct size did not differ between the groups. In contrast, macrophages (known as key players in adverse cardiac remodeling) migrated less in both the infarct and remote myocardium of EDA$^{-/-}$ mice. In addition, lack of EDA protected the animals against the production of TNFα, RANTES and GM-CSF; all known detrimental (chemotactic) cytokines in acute MI and HF, affecting negatively cardiomyocyte survival and function, and ECM remodeling.[2, 18] In contrast, MCP-1 is increased in EDA$^{-/-}$ mice. There are several possible explanations for reduced migration of mononuclear cells in EDA$^{-/-}$ mice despite increased MCP-1 levels. First, decreased CD49d expression seen in our experiments results in reduced migration capacity of monocytes (Figure 6).[26] It is likely that MCP-1 fails to cause effective migration due to reduced CD49d expression on monocytes. The complexity of the role of MCP-1 in adverse remodeling is also shown by the fact that several studies have reported contradictory results. Both cardiac-specific MCP-1 overexpression and MCP-1 inhibition have shown to prevent adverse remodeling and fibrosis after infarction.[27-29]

Thirdly, we studied MMP and elastase secretion since MMP2, -9 and elastase have been described as mediators of adverse cardiac remodeling.[30] Both endogenous MMP2, -9 and elastase activities were decreased in EDA$^{-/-}$ mice compared to WT animals. These findings corroborate our MRI observations, in which wall thickness of the infarcted free wall is thicker in EDA$^{-/-}$ mice, already at 7 days post-MI (Table 1). Our observation of decreased endogenous MMP2 and -9 activities in the absence of EDA is supported by Okamura Y et al. They showed that EDA mediates MMP9 production via TLR4 activation.[31] Despite the fact that they did not see any effect on MMP2 production *in vitro*, we did show that MMP2 was affected as well *in vivo*. One possible explanation is that the *in vitro* setting used by Okamura Y *et al*. does not represent the spatial and temporal dependence of MMP production; infarct and remote myocardium have their own MMP signature during the post-MI period.[30] In addition, we examined whether EDA is a direct inhibitor of MMP2 and 9. Adding recombinant EDA to MMP2 and 9 did not

have an inhibitory effect (Online Figure XII) suggesting that the reduced MMP2 and 9 activity observed *in vivo* is likely via reduced secretion.

Finally, we found that EDA expression in resident myocardial cells mediate LV remodeling after infarction. Moreover, we have shown that circulating monocytes are significantly affected in the absence of EDA. Besides the fact that monocyte numbers are temporarily decreased after infarction, the absence of EDA also downregulates TLR2 and CD49d expression *in vivo*.
Taking these novel findings into account, we can hypothesize the following on the mode of action of EDA; 1) both leukocytes and cardiac fibroblasts, critically involved in cardiac remodeling, are activated by the "danger" signal EDA produced in the heart after MI; 2) leukocytic integrins (e.g. α4β1) have higher binding affinity to the ECM in the presence of EDA,[32] resulting in increased migration and/or differentiation of leukocytes after MI. It is very likely, that both fibroblast transdifferentiation and leukocytic activation and migration contribute equally to the observed effects in our study.

In summary, we have shown that EDA is upregulated in response to the infarction and returns to normal levels after long-term survival. In the absence of EDA, post-infarct adverse remodeling is highly attenuated with concomitant survival benefit. $EDA^{-/-}$ mice are relatively protected against the profound expansive remodeling. In addition, both systolic and diastolic performance is preserved in $EDA^{-/-}$ mice via decreased fibrosis and altered inflammation

Acknowledgements

We would like to thank the following persons for their assistance: Ben J. van Middelaar, Krista den Ouden, Chaylendra Strijder, Petra Homoet, Arjan Schoneveld, Wies Lommen, Lars Akeroyd (all from the UMC Utrecht, The Netherlands).

Funding Sources

This work is supported by research grants from the Netherlands Organisation for Scientific Research (NWO) & Utrecht University & NWO Mozaïek grant (contract 017.004.004 to F.A.), Netherlands Heart Foundation (contract 2010.T001 to F.A.), Bekales Foundation (P.A.D.), Merit Grant from US Dept. of Veterans Affairs and See Foundation (both to J.H.P.).

METHODS

Animals and experimental design

$EDA^{-/-}$ mice are kindly provided by dr. John H. Peters and backcrossed into a Balb/C background for 8 generations. Male Balb/C wild-type (WT), $EDA^{-/-}$ and chimeric mice (10-12 wks, 25-30 g) received standard diet and water *ad libitum*. Myocardial infarction was induced by left coronary artery ligation, just below the left atrial appendage. All animal experiments are performed in accordance with the national guidelines on animal care and with prior approval by the Animal Experimentation Committee of Utrecht University. The authors had full access to and take full responsibility for the integrity of the data. All authors have read and agree to the manuscript as written.

Data Supplement

An expanded Methods section is available in the Online Data Supplement at http://circres.ahajournals.org and contains detailed information regarding MI *in vivo*, protein and RNA isolation, flow cytometry, the generation of chimeric mice, infarct size calculation, MRI measurements, invasive left ventricular (LV) pressure measurements, immunohistochemistry, polymerase chain reaction, zymography, caspase 3/7 activity, elastase activity, myofibroblast culture, fibronectin-EDA Western blotting, and statistical analysis.

REFERENCES

1 International Cardiovascular Disease Statistics - 2009 Update. American Heart Association 2009;Available at: URL: http://www.americanheart.org/downloadable/heart/1236204012112INTL.pdf.

2 Frangogiannis NG. The immune system and cardiac repair. Pharmacol Res. 2008;58:88-111.

3 McMurray JJ, Pfeffer MA, Swedberg K, Dzau VJ. Which inhibitor of the renin-angiotensin system should be used in chronic heart failure and acute myocardial infarction? Circulation. 2004;110:3281-3288.

4 Wollert KC, Drexler H. The renin-angiotensin system and experimental heart failure. Cardiovasc Res. 1999;43:838-849.

5 Roger VL, Weston SA, Redfield MM, Hellermann-Homan JP, Killian J, Yawn BP, Jacobsen SJ. Trends in heart failure incidence and survival in a community-based population. JAMA. 2004;292:344-350.

6 Hamid T, Gu Y, Ortines RV, Bhattacharya C, Wang G, Xuan YT, Prabhu SD. Divergent tumor necrosis factor receptor-related remodeling responses in heart failure: role of nuclear factor-kappaB and inflammatory activation. Circulation. 2009;119:1386-1397.

7 Zhang P, Cox CJ, Alvarez KM, Cunningham MW. Cutting edge: cardiac myosin activates innate immune responses through TLRs. J Immunol. 2009;183:27-31.

8 Kitahara T, Takeishi Y, Harada M, Niizeki T, Suzuki S, Sasaki T, Ishino M, Bilim O, Nakajima O, Kubota I. High-mobility group box 1 restores cardiac function after myocardial infarction in transgenic mice. Cardiovasc Res. 2008;80:40-46.

9 Miyake K. Innate immune sensing of pathogens and danger signals by cell surface Toll-like receptors. Semin Immunol. 2007;19:3-10.

10 Schoneveld AH, Hoefer I, Sluijter JP, Laman JD, de Kleijn DP, Pasterkamp G. Atherosclerotic lesion development and Toll like receptor 2 and 4 responsiveness. Atherosclerosis. 2008;197:95-104.

11 Gondokaryono SP, Ushio H, Niyonsaba F, Hara M, Takenaka H, Jayawardana ST, Ikeda S, Okumura K, Ogawa H. The extra domain A of fibronectin stimulates murine mast cells via toll-like receptor 4. J Leukoc Biol. 2007;82:657-665.

12 Liao YF, Gotwals PJ, Koteliansky VE, Sheppard D, Van De WL. The EIIIA segment of fibronectin is a ligand for integrins alpha 9beta 1 and alpha 4beta 1 providing a novel mechanism for regulating cell adhesion by alternative splicing. J Biol Chem. 2002;277:14467-14474.

13 Manabe R, Oh-e N, Sekiguchi K. Alternatively spliced EDA segment regulates fibronectin-dependent cell cycle progression and mitogenic signal transduction. J Biol Chem. 1999;274:5919-5924.

14 Serini G, Bochaton-Piallat ML, Ropraz P, Geinoz A, Borsi L, Zardi L, Gabbiani G. The fibronectin domain ED-A is crucial for myofibroblastic phenotype induction by transforming growth factor-beta1. J Cell Biol. 1998;142:873-881.

15 Snider P, Standley KN, Wang J, Azhar M, Doetschman T, Conway SJ. Origin of cardiac fibroblasts and the role of periostin. Circ Res. 2009;105:934-947.

16 Schocken DD, Benjamin EJ, Fonarow GC, Krumholz HM, Levy D, Mensah GA, Narula J, Shor ES, Young JB, Hong Y. Prevention of heart failure: a scientific statement from the American Heart Association Councils on Epidemiology and Prevention, Clinical Cardiology, Cardiovascular Nursing, and High Blood Pressure Research; Quality of Care and Outcomes Research Interdisciplinary Working Group; and Functional Genomics and Translational Biology Interdisciplinary Working Group. Circulation. 2008;117:2544-2565.

17 Roberts R, DeMello V, Sobel BE. Deleterious effects of methylprednisolone in patients with myocardial infarction. Circulation. 1976;53:I204-I206.

18 Arslan F, de Kleijn DP, Timmers L, Doevendans PA, Pasterkamp G. Bridging innate immunity and myocardial ischemia/reperfusion injury: the search for therapeutic targets. Curr Pharm Des. 2008;14:1205-1216.

19 Arslan F, Smeets MB, O'Neill LA, Keogh B, McGuirk P, Timmers L, Tersteeg C, Hoefer IE, Doevendans PA, Pasterkamp G, de Kleijn DP. Myocardial ischemia/reperfusion injury is mediated by leukocytic toll-like receptor-2 and reduced by systemic administration of a novel anti-toll-like receptor-2 antibody. Circulation. 2010;121:80-90.

20 Schoneveld AH, Oude Nijhuis MM, van MB, Laman JD, de Kleijn DP, Pasterkamp G. Toll-like receptor 2 stimulation induces intimal hyperplasia and atherosclerotic lesion development. Cardiovasc Res. 2005;66:162-169.

21 Arslan F, Keogh B, McGuirk P, Parker AE. TLR2 and TLR4 in ischemia reperfusion injury. Mediators Inflamm. 2010;2010:704202.

22 Timmers L, Sluijter JP, van Keulen JK, Hoefer IE, Nederhoff MG, Goumans MJ, Doevendans PA, van Echteld CJ, Joles JA, Quax PH, Piek JJ, Pasterkamp G, de Kleijn DP. Toll-like receptor 4 mediates maladaptive left ventricular remodeling and impairs cardiac function after myocardial infarction. Circ Res. 2008;102:257-264.

23 Shimamoto A, Chong AJ, Yada M, Shomura S, Takayama H, Fleisig AJ, Agnew ML, Hampton CR, Rothnie CL, Spring DJ, Pohlman TH, Shimpo H, Verrier ED. Inhibition of Toll-like receptor 4 with eritoran attenuates myocardial ischemia-reperfusion injury. Circulation. 2006;114:I270-I274.

24 Matzinger P. The danger model: a renewed sense of self. Science. 2002;296:301-305.

25 Choi MG, Hynes RO. Biosynthesis and processing of fibronectin in NIL.8 hamster cells. J Biol Chem. 1979;254:12050-12055.

26 Rose DM, Alon R, Ginsberg MH. Integrin modulation and signaling in leukocyte adhesion and migration. Immunol Rev. 2007;218:126-134.

27 Dewald O, Zymek P, Winkelmann K, Koerting A, Ren G, bou-Khamis T, Michael LH, Rollins BJ, Entman ML, Frangogiannis NG. CCL2/Monocyte Chemoattractant Protein-1 regulates inflammatory responses critical to healing myocardial infarcts. Circ Res. 2005;96:881-889.

28 Hayashidani S, Tsutsui H, Shiomi T, Ikeuchi M, Matsusaka H, Suematsu N, Wen J, Egashira K, Takeshita A. Anti-monocyte chemoattractant protein-1 gene therapy attenuates left ventricular remodeling and failure after experimental myocardial infarction. Circulation. 2003;108:2134-2140.

29 Morimoto H, Takahashi M, Izawa A, Ise H, Hongo M, Kolattukudy PE, Ikeda U. Cardiac overexpression of monocyte chemoattractant protein-1 in transgenic mice prevents cardiac dysfunction and remodeling after myocardial infarction. Circ Res. 2006;99:891-899.

30 Spinale FG. Myocardial matrix remodeling and the matrix metalloproteinases: influence on cardiac form and function. Physiol Rev. 2007;87:1285-1342.

31 Okamura Y, Watari M, Jerud ES, Young DW, Ishizaka ST, Rose J, Chow JC, Strauss JF, III. The extra domain A of fibronectin activates Toll-like receptor 4. J Biol Chem. 2001;276:10229-10233.

32 Cantor JM, Ginsberg MH, Rose DM. Integrin-associated proteins as potential therapeutic targets. Immunol Rev. 2008;223:236-251.

CHAPTER

10

In this chapter we demonstrated that haptoglobin deficiency results in increased oxidative stress, impaired neovascularization and subsequent improper scar formation and maturation after myocardial infarction

Fatih Arslan, Mirjam B. Smeets, Lars Akeroyd, Ben van Middelaar, Leo Timmers, Krista den Ouden, Gerard Pasterkamp, Sai Kiang Lim & Dominique P. de Kleijn

Haptoglobin deficiency reduces PAI-1 activity, microvascular integrity and enhances adverse remodeling after myocardial infarction

Background

Decreased haptoglobin (Hp) functionality due to allelic variations is associated with worsened outcome in patients after myocardial infarction (MI) due to increased oxidative stress. However, other mechanisms may be involved in a complex process as post-infarct cardiac remodeling. In the present study, we identified for the first time PAI-1 activity and VEGFα signaling as novel Hp-mediated pathways involved in early and late cardiac repair responses after experimental MI.

Methods and Results

Left coronary artery ligation was performed in $Hp^{-/-}$ and wild-type (WT) mice. Death rate was significantly higher in Hp-/- mice (63% vs. 20% in WT mice), commonly caused by cardiac rupture in $Hp^{-/-}$ animals. Histological analysis of 3 and 7 days old non-ruptured infarcted hearts revealed more frequent and more severe intramural hemorrhage and disorganized granulation tissue in $Hp^{-/-}$ mice. Analyses of non-ruptured hearts revealed reduced PAI-1 activity and enhanced VEGFα transcription in $Hp^{-/-}$ mice. In line with these observations, we found an increased angiogenic response and increased microvascular permeability of newly formed vessels in $Hp^{-/-}$ hearts after infarction. During long-term follow-up of the surviving animals, we observed altered matrix turnover, impaired scar formation and worsened cardiac function and geometry in $Hp^{-/-}$ mice.

Conclusions

Haptoglobin deficiency severely deteriorates tissue repair and cardiac performance after experimental MI. Haptoglobin plays a crucial role in both short- and long-term cardiac repair responses by maintaining microvascular integrity, myocardial architecture, provisional matrix formation and proper scar formation.

Under revision

Genetic predispositions of individuals are related with the development of post-ischemic heart failure (HF)[1]. Haptoglobin (Hp) gene polymorphisms are determinants in the outcome of patients after myocardial infarction[2]. The haptoglobin gene has two polymorphic alleles, referred as 1 and 2, that results in three different phenotypes in man (Hp 1-1, 1-2, 2-2) that exhibit distinct properties. In contrast, mice only carry the Hp-1 allele. The Hp protein has several functions in the repair process following acute injury. Hp binds free hemoglobin to prevent hemoglobin-induced oxidative stress[3]. Anti-inflammatory and angiogenic functions have also been postulated for Hp[4]. Interestingly, there appears to be a gradual scale of functionality for the different Hp phenotypes: Compared to Hp 1-2 and especially to Hp 2-2, Hp 1-1 is superior in forming a complex with free hemoglobin and is associated with less adverse atherosclerotic manifestations[4, 5]. Previous studies showed that increased oxidative stress contributed to increased tissue damage in mice with reduced Hp functionality (Hp 2-2)[6]. However, healing and remodeling of the infarcted heart is a complex process involving multiple biological pathways and (resident and migrating) cells[7, 8]. Influx of circulating blood cells, neoangiogenesis, matrix turnover and scar maturation are well orchestrated processes determining the fate of both the infarcted and remote myocardium. Recent insight showed that non-traditional pathways are involved in infarct healing as well. Factors from the coagulation cascade (e.g. FXIII)[9], enzymes involved in fibrinolysis (e.g. PAI-1, u-PA)[10-15] are known to be critical for wound healing after infarction. Therefore, besides oxidative stress, other factors may be involved in the Hp-mediated healing processes during infarct remodeling.
In the present study, we studied the role of Hp in both immediate and chronic repair responses by thorough temporal characterization of the healing myocardium after infarction. We report for the first time that Hp mediates proper granulation of the injured myocardium and vascular permeability of newly formed vessels. Furthermore, Hp regulates PAI-1 activity, matrix turnover and scar maturation after infarction. Together, these observations show that Hp, in addition to its anti-oxidative stress properties, is critically involved in acute and chronic healing processes of the heart after infarction.

RESULTS

Haptoglobin deficiency causes cardiac rupture and worsens survival after myocardial infarction

Baseline MRI assessment of cardiac function and dimensions and histological examination of cellularity in HE stained hearts revealed no differences between $Hp^{-/-}$ and WT mice. Hp transcript level was increased in heart tissue after infarction and remained elevated within the infarct area during follow-up (Figure 1a). Infarct size was similar between the groups (37.1±0.9% vs. 37.9±1.3%, p=0.806; Figure 1b). Kaplan-Meier survival analysis showed a significant increase in mortality in $Hp^{-/-}$ mice around day 3 and 4 compared to WT animals (Figure 1c). All early deaths (<7 days) in $Hp^{-/-}$ mice were attributable to cardiac ruptures (Figure 1d).
Histological analysis of non-ruptured hearts revealed disorganized granulation of infarcted $Hp^{-/-}$ hearts (Figure 1e): 3 days post-infarct $Hp^{-/-}$ hearts showed loss of linear and/or striated architecture of enucleated cardiomyocytes, random infiltration of leukocytes and red blood cell (RBC) deposition; 7 days post-infarct $Hp^{-/-}$ hearts showed enhanced infiltration, presence of a medial layer of residual enucleated cardiomyocyte/matrix and again RBC deposition. These characteristics were not or significantly less evident in WT animals. Quantification of RBC deposition areas showed that the extent of intramural hemorrhage was higher in $Hp^{-/-}$ animals (Figure 1f).

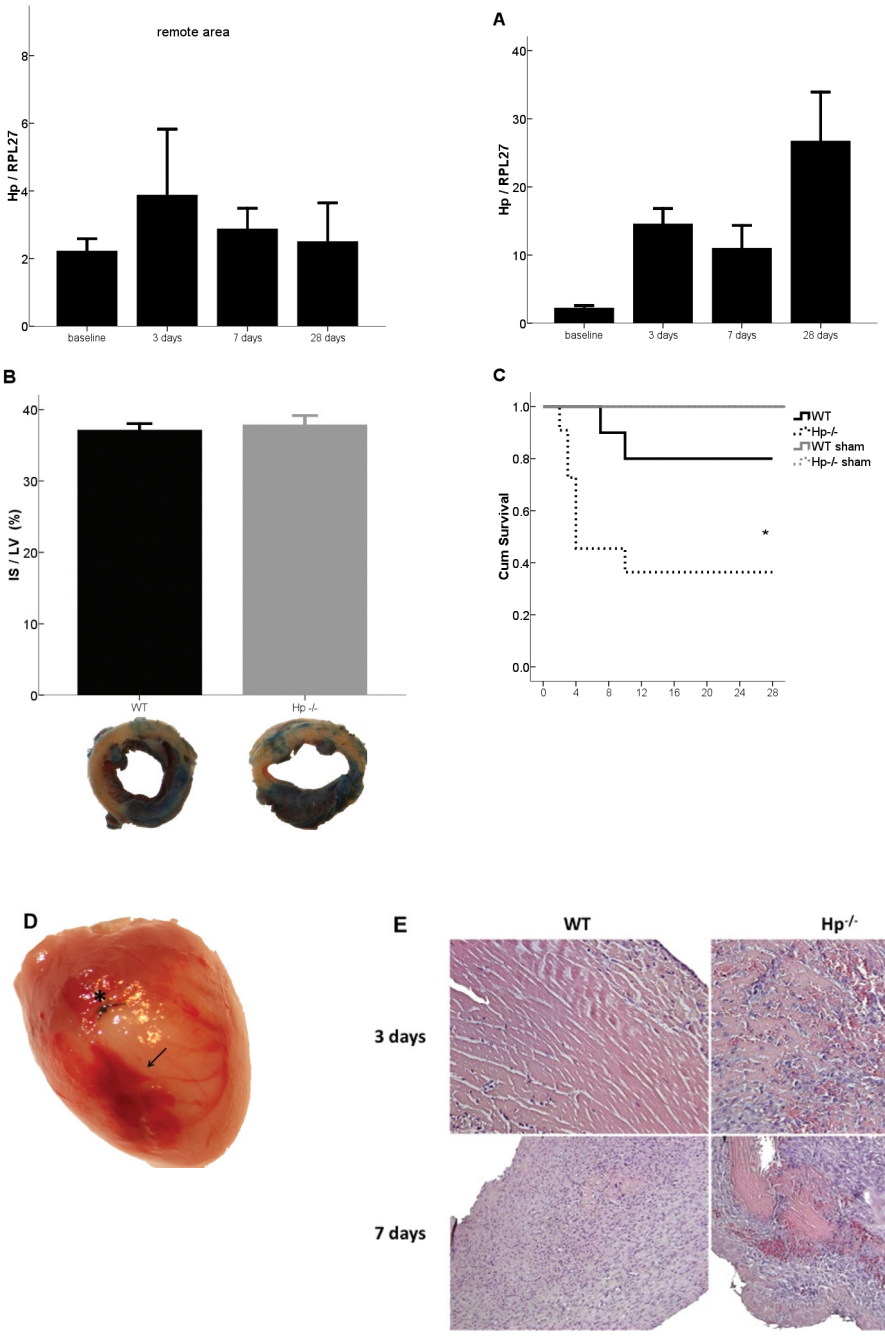

Figure 1. Haptoglobin deficiency worsens survival and causes intramural hemorrhage after MI. *(**A**) Haptoglobin mRNA levels in the heart during infarct development; *p<0.05 compared to baseline. (**B**) Infarct size (IS) as a percentage of the left ventricle (LV) 2 days after infarction. Representative cross-sections after TTC staining are shown below corresponding bars; n=5/group. (**C**) Kaplan-Meier survival curves; *p=0.03 compared to WT ischemic mice. (**D**) Cardiac rupture; arrow indicates site of rupture, note the massive hemorrhage area within the infarct (bleach area), asterix indicates the LCA ligation. (**E**) Representative images of hematoxyllin-eosin stained hearts. Note the excessive red blood cell deposition and disorganized granulation in the Hp$^{-/-}$ hearts.*

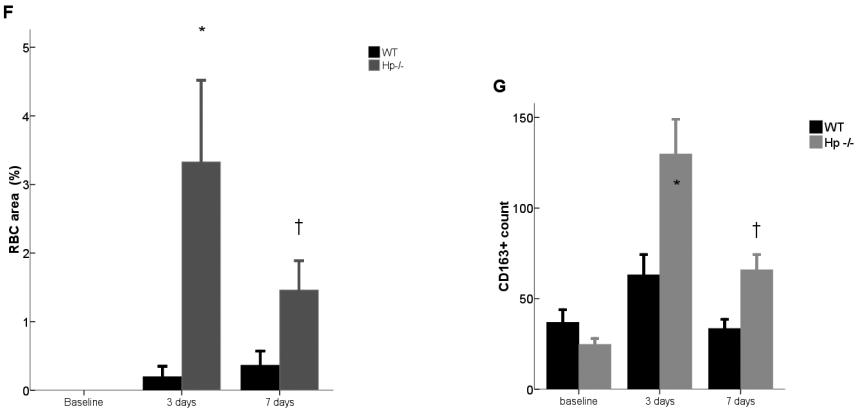

Figure 1. Haptoglobin deficiency worsens survival and causes intramural hemorrhage after MI. *(F) Quantification of total red blood cell positive area as a percentage of the field (10x magnification); *p=0.026 and †p=0.029 compared to WT animals. (G) CD163+ cell count in infarct and remote area. Representative images are shown; *p=0.03, †p=0.024 and ‡p=0.028 compared to WT animals. Each bar represents Mean±SEM, n=7/group.*

To study whether differences in intraventricular pressure development could contribute to the higher incidence of cardiac rupture in $Hp^{-/-}$ animals, we performed invasive pressure-volume loop recordings in a subgroup of mice 3 days after infarction. No differences were found in any of the hemodynamic parameters (Table 1).

Finally, we studied CD163 expression in response to the intramural hemorrhages, since haptoglobin forms a complex with free hemoglobin to facilitate hemoglobin removal by $CD163^{pos}$-macrophages[3]. In line with the increased amount of RBC deposition, we observed more $CD163^{pos}$ cells in both the infarct and remote area in $Hp^{-/-}$ mice, 3 and 7 days after infarction (Figure 1g).

Haptoglobin deficiency results in increased angiogenic response, vascular permeability and oxidative stress

Hp is known to be involved in angiogenesis[16]. Newly formed vessels may become leaky and lead to bleeding in the vascular wall. Therefore, we quantified capillary density at baseline and during follow-up. At baseline, the capillary density was lower in $Hp^{-/-}$ mice. However, the absolute number of newly formed capillaries did not differ between the groups after infarction (Figure 2a). Taking into account

Table 1. LV hemodynamics

	C57Bl6 WT	Haptoglobin$^{-/-}$	*p*
Heart rate, BPM	406±34	418±37	0.65
LVESP, mmHg	101±14	97±10	0.62
LVEDP, mmHg	8±4	9±1	0.60
dP/dTmax, mmHg/s	6579±654	5839±760	0.19
dP/dTmin, mmHg/s	-5266±763	-5047±768	0.70
Tau, ms	17±3	16±4	0.82

All values represent Mean±SEM. BPM=beats per minute, LVESP=left ventricular end-systolic pressure, LVEDP=LV end-diastolic pressure.

the lower capillary density at baseline, the percentage increase of newly formed capillaries (angiogenesis index) was higher in $Hp^{-/-}$ mice (Figure 2b).

Vascular endothelial growth factor (VEGF) and Angiopoietin-1 (Ang-1) are key players in vessel formation and maturation, respectively. It has been shown that newly developed vessels are more leaky when they are formed by accentuated VEGF induction without being maturated by Ang-1[17]. In $Hp^{-/-}$ mice, we observed significantly higher VEGFα transcription levels compared to WT animals, whereas Ang-1 did not differ between the groups during the first week of infarction. Additionally, the ratio VEGFα/Ang-1 was significantly increased in $Hp^{-/-}$ mice (Figure 2c). Since this finding may contribute to the formation of leaky vessels and subsequent RBC deposition, we performed a vascular permeability assay *in vivo*. As shown in Figure 2d, $Hp^{-/-}$ mice exhibited a significantly increased cardiac vascular leakage despite equal plasma Evans' blue dye concentrations after infarction (Figure 2e). We next determined the extent of oxidative stress, since it is mediated by haptoglobin and results in increased angiogenesis. In line with increased red blood cell deposition and free hemoglobin burden after infarction, we observed increased oxidative stress in haptoglobin deficient mice 3 days after infarction (Figure 2f). At baseline, the extent of vascular junctions, as demonstrated by retinal angiography, was also impaired in the absence of haptoglobin (Figure 2g).

Haptoglobin deficiency results in maladaptive remodeling and impaired scar formation

Having established the short term effects of Hp deficiency on cardiac repair, we studied its long term impact on post-infarct remodeling. Serial MRI measurements showed that surviving $Hp^{-/-}$ mice beyond day 7, exhibit increased LV dilatation during follow-up (Figure 3a). Systolic wall thickening as a measure for systolic performance was also worsened in the absence of Hp as well as cardiac output and LV mass (Table 2). Increased bulging of the free wall (i.e. infarct area) suggests impaired formation of a firm scar.

Table 2. Cardiac function and geometry after MI

	C57Bl6 WT			Haptoglobin$^{-/-}$				
	Baseline	**7 days**	**28 days**	**Baseline**	**7 days**	**†*p***	**28 days**	**†*p***
BPM	367±13	391±17	374±7	399±14	424±15	NS	374±19	NS
EDV, µL	51.6±4.9	103.6±9.3	132.8±6.7	53.0±4.9	131.9±9.5*†	0.018	201.9±24.1**†	0.001
ESV, µL	20.2±4.7	81.6±8.6	108.8±6.1	22.9±3.9	112.4±10.3*†	0.007	181.3±23.9**†	0.001
EF, %	63.7±5.3	22.0±1.6	18.0±2.2	57.7±4.1	15.1±2.0*	NS	11.0±1.3**†	0.06
CO, mL/min	11.6±0.8	8.6±0.6	7.6±0.8	12.0±1.0	8.2±0.6*	NS	5.7±0.3**	NS
LV mass, mg	84.4±4.3	99.2±4.1	99.3±5.3	82.6±3.8	104.6±2.6*	NS	113.0±4.4**†	0.07
WT septum (remote, mm)	0.95±0.02	0.80±0.02*	0.86±0.01	0.89±0.03	0.72±0.02*†	0.026	0.89±0.03	NS
WT free wall (infarct, mm)	0.97±0.02	0.67±0.04*	0.48±0.03**	0.93±0.02	0.48±0.05*†	0.027	0.40±0.03**	NS
SWT septum (remote, %)	53.8±1.5	37.6±3.1*	44.5±1.3	55.9±1.7	33.7±2.1*	NS	37.0±2.2**†	0.027
SWT free wall (infarct, %)	55.5±3.9	-17.4±1.2*	-30.8±1.8**	54.4±2.1	-30.6±1.7*†	0.007	-44.3±2.1**†	0.001

*One-way ANOVA post-hoc LSD: *p<0.03 and **p<0.001 compared to baseline and sham group; †p value compared to C57Bl6 WT and sham group. Data are represented as Mean±SEM, n=10 in WT, n=20 in $Hp^{-/-}$ and n=6 in sham group. EDV=end-diastolic volume, ESV=end-systolic volume, EF=ejection fraction, CO=cardiac output, LV-left ventricular, WT=wall thickness, SWT=systolic wall thickening, NS=not significant.*

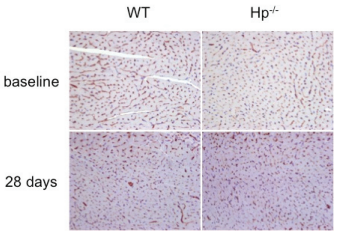
WT
Hp-/-
baseline
28 days

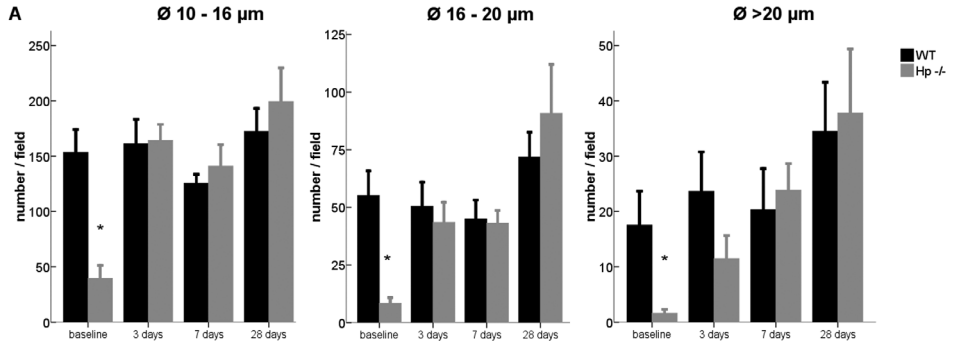
A
Ø 10 - 16 µm
Ø 16 - 20 µm
Ø >20 µm
number / field
baseline
3 days
7 days
28 days
WT
Hp -/-

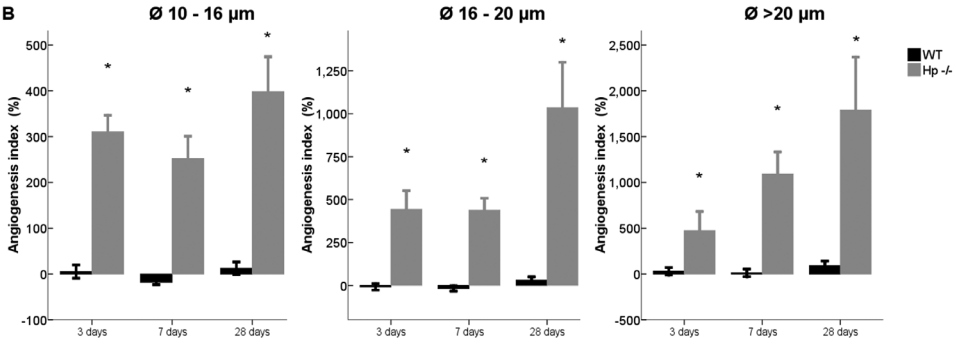
B
Ø 10 - 16 µm
Ø 16 - 20 µm
Ø >20 µm
Angiogenesis index (%)
3 days
7 days
28 days
WT
Hp -/-

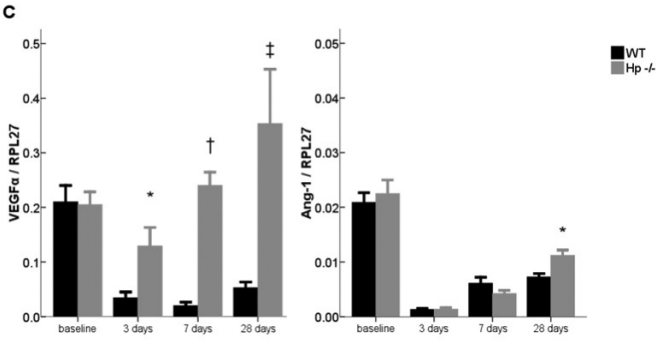
C
VEGFα / RPL27
Ang-1 / RPL27
baseline
3 days
7 days
28 days
WT
Hp -/-

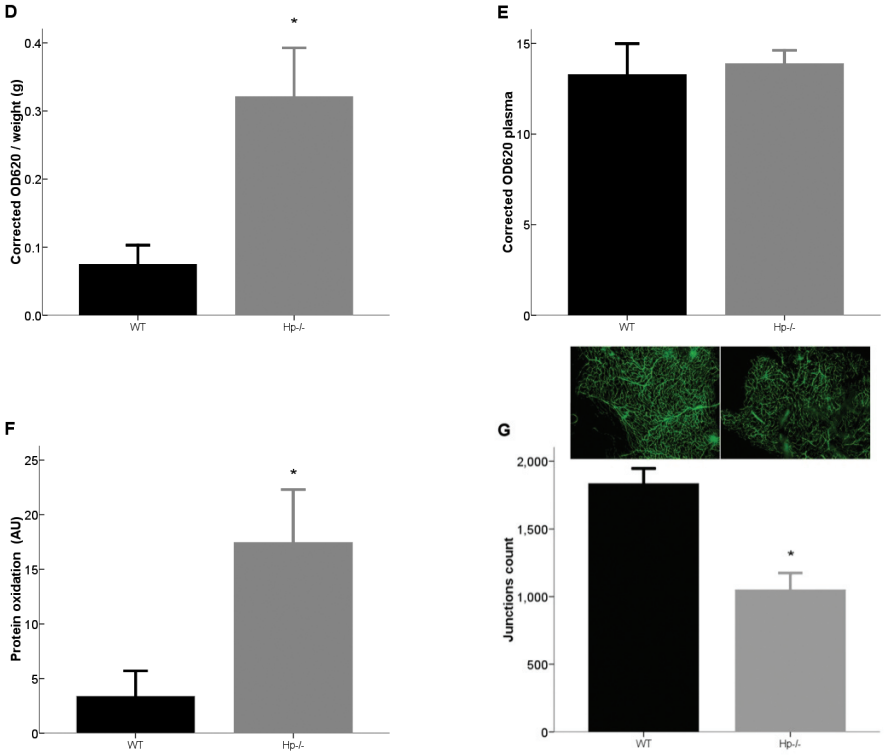

***Figure 2. Hp mediates angiogenic responses and vascular permeability after MI**. (**A**) Microvessel formation (lectin^{pos} vessels) after MI; *p<0.003 compared to WT animals. Representative images from baseline and 28 days post-infarct hearts are shown. (**B**) Relative increase from baseline in capillary density during follow up; *p<0.016 compared to WT animals. (**C**) Tissue levels of VEGFα and Ang-1 mRNA after infarction; for VEGFα *p=0.005, †p=0.002, ‡p=0.001; for Ang-1 *p=0.011; for VEGFα/Ang-1 ratio *p=0.021, †p=0.002, ‡p=0.028 compared to WT animals. (**D**) Cardiac vascular permeability; *p<0.014 compared to WT hearts. (**E**) Plasma Evans' blue dye concentration. (**F**) Oxidative stress in cardiac protein extracts 3 days after infarction; *p=0.043. (**G**) Retinal angiography and quantification of intervascular junctions; *p=0.021. Each bar represents Mean±SEM, n=7/group/time point, n=4/group for vascular permeability assay.*

Table 3. Procollagen-1, -3 and lysyl-oxidase mRNA levels after MI

	C57Bl6 WT				Haptoglobin$^{-/-}$				
Days after MI	0	3	7	28	0	3	7	28	†*p*
Procollagen-1	.01±.001	.21±.03*	.72±.06*	.14±.02*	.01±.002	.16±.01*	.83±.13*	.11±.02*	NS
Procollagen-3	.09±.01	1.55±.17*	5.63±.64*	1.87±.24*	.11±.01	1.39±.14*	5.93±.86*	1.20±.15*†	.02
TGF-β1	.01±.001	.02±.002	.03±.008*	.03±.005*	.01±.002	.02±.004	.03±.006*	.01±.003*†	.005
LOX	.01±.002	.10±.01*	.40±.02*	.15±.02*	.01±.001	.10±.01*	.40±.05*	.11±.01*†	.04

*All values represent Mean±SEM. mRNA levels are expressed as a ratio to RPL27 mRNA. LOX=lysyl-oxidase, NS=not significant. *p<0.05 compared to baseline and †p-value compared to WT*

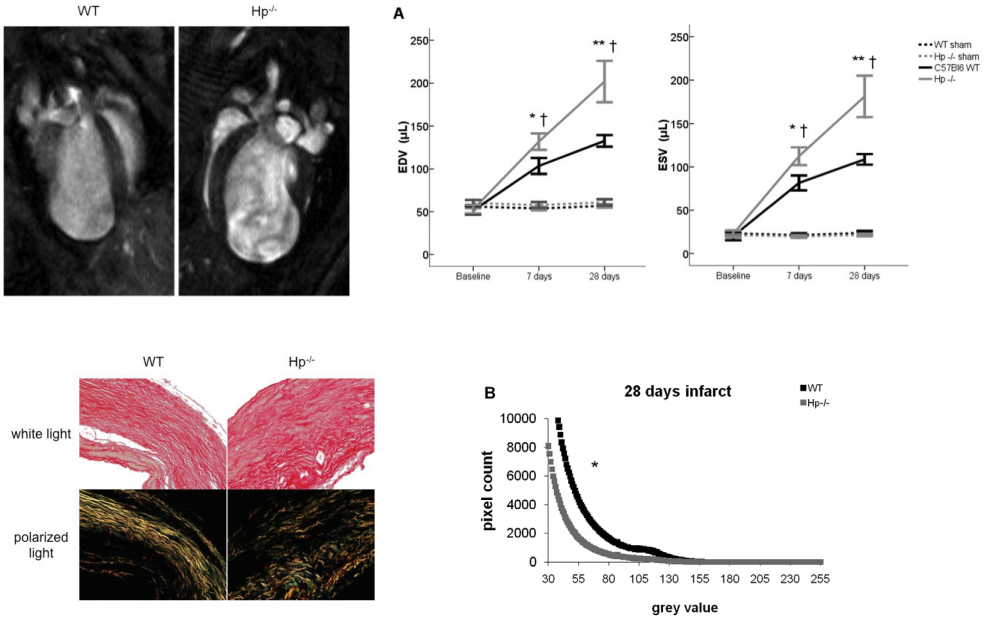

Figure 3. Hp$^{-/-}$ mice exhibit exaggerated ventricular dilatation after MI. *(**A**) cardiac geometry in ischemic and sham operated animals. Representative images in the end-diastolic phase are shown; *p<0.03 and **p<0.001 compared to baseline and sham operated mice; †p-value (see Table 2.) compared to WT ischemic mice. (**B**) Histograms give an overview of the entire spectrum of collagen density. The larger the grey value, the higher the collagen density. Grey values below 30 are considered as background signal of the intensity image acquired after polarized light microscopy. Representative images of 28 days post-infarct hearts are shown. Note the dense and organized collagen fiber structure in WT heart in contrast to Hp$^{-/-}$ heart; *p=0.039 difference in area under the curve. Each bar represents Mean±SEM, MRI study: n=10 in WT, n=20 in Hp$^{-/-}$, n=6/sham group; Histology n=7/group. EDV=end-diastolic volume, ESV=end-systolic volume.*

Indeed, collagen density staining analysis revealed reduced collagen deposition in Hp$^{-/-}$ mice (Figure 3b). Histological examination revealed, again, loss of structured striation of collagen fibers in the infarct zone. We measured mRNA levels of pro-collagen-1/3 and TGF-β1 to investigate whether collagen synthesis could explain the observed morphological observations. Both procollagen-3 and TGF-β1 mRNA were significantly reduced in Hp$^{-/-}$ mice 28 days after MI (Table 3). In addition, lysyl-oxidase levels were reduced as well, suggesting impaired collagen cross-linking in Hp$^{-/-}$ mice (Table 3).

Haptoglobin deficiency reduces endogenous activity of PAI-1 and MMP2, and fibronectin transcription.

Previous studies have shown that PAI-1 knock-out animals have impaired infarct healing and die mostly from cardiac ruptures[12, 13, 15]. We studied whether Hp regulated PAI-1 activity to explain high incidence of cardiac ruptures in Hp$^{-/-}$ mice. In mice with non-ruptured hearts 3 days after infarction, PAI-1 activity was highly reduced in both heart tissue and plasma of Hp$^{-/-}$ animals (tissue 3.5±0.8 vs. 1.5±0.2; plasma 0.12±0.01 vs. 0.08±0.009; Figure 4a).

Orchestrated matrix breakdown is essential for proper scar formation and collagen deposition[18, 19]. In order to quantify the pathological feature of delayed debris removal in Hp$^{-/-}$ animals (Figure 1e), we determined the area of enucleated cardiomyocytes within the infarct area in hearts 7 days post-

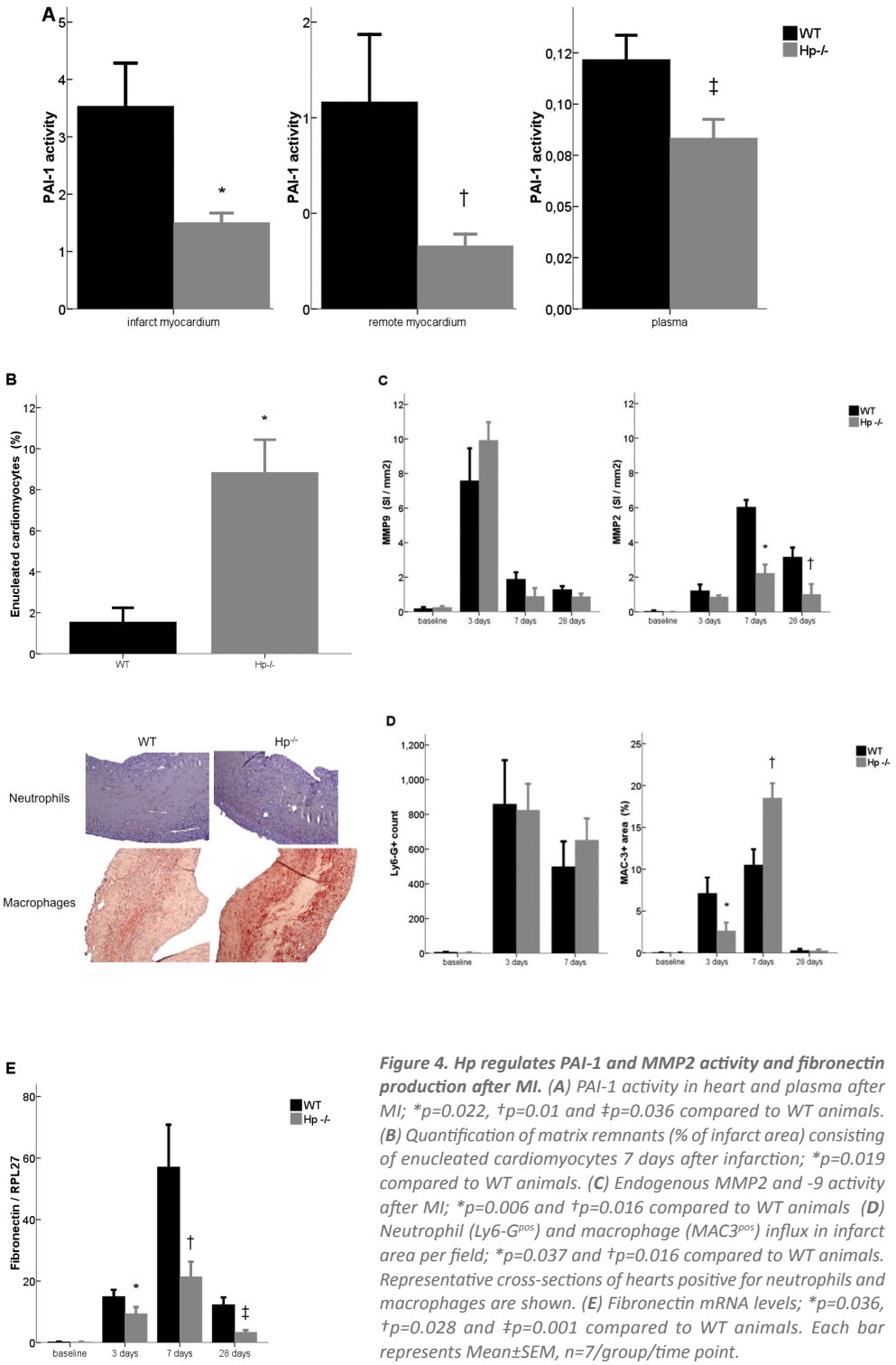

Figure 4. Hp regulates PAI-1 and MMP2 activity and fibronectin production after MI. *(**A**) PAI-1 activity in heart and plasma after MI; *p=0.022, †p=0.01 and ‡p=0.036 compared to WT animals. (**B**) Quantification of matrix remnants (% of infarct area) consisting of enucleated cardiomyocytes 7 days after infarction; *p=0.019 compared to WT animals. (**C**) Endogenous MMP2 and -9 activity after MI; *p=0.006 and †p=0.016 compared to WT animals (**D**) Neutrophil (Ly6-G^{pos}) and macrophage (MAC3^{pos}) influx in infarct area per field; *p=0.037 and †p=0.016 compared to WT animals. Representative cross-sections of hearts positive for neutrophils and macrophages are shown. (**E**) Fibronectin mRNA levels; *p=0.036, †p=0.028 and ‡p=0.001 compared to WT animals. Each bar represents Mean±SEM, n=7/group/time point.*

infarction. Hp deficiency resulted in impaired removal of enucleated cardiomyocytes (Figure 4b), which may be due to reduced MMP2 activity (Figure 4c).
Although neutrophil influx did not differ between the groups, influx of macrophages was increased in $Hp^{-/-}$ animals 7 days after MI (Figure 4d). Hereafter, we studied the involvement of fibronectin since it is critically involved in the formation of a provisional matrix to facilitate scar maturation. In line with the observed delayed matrix turnover, fibronectin production was also impaired in $Hp^{-/-}$ mice during cardiac remodeling (Figure 4e).

DISCUSSION

Patients differ in their response to ischemic injury and subsequent recovery. It is difficult to assess which factor(s) determine the fate of post-infarct repair responses. It is challenging to fully understand a complex process such as post-infarct remodeling in which inflammatory, angiogenic and genetic mediators play all an important role. Haptoglobin has been shown to be a critical genetic mediator of clinical outcome in patient after myocardial infarction[20, 21]. Further elucidation of haptoglobin-mediated pathways involved in cardiac repair after infarction may provide new therapeutic targets to optimize treatment for myocardial infarction.
In the present study we used $Hp^{-/-}$ mice in order to investigate its causal role and identify critical pathways mediated by haptoglobin in the response of the heart to myocardial infarction. The most evident role of haptoglobin appeared to be the maintenance of normal morphological features of wound healing after infarction. We observed that cardiac ruptures occurred more frequently in $Hp^{-/-}$ animals and that histological analysis revealed disorganized granulation of the healing myocardium. Analysis of hearts that did not rupture showed that in $Hp^{-/-}$ the incidence and size of intramural hemorrhages within the infarcted wall is higher compared to WT animals. One possible explanation may be the increased microvascular permeability in $Hp^{-/-}$ hearts after infarction. We found that neoangiogenesis in Hp deficient mice was accompanied with leakage-prone capillary formation via isolated VEGFα induction, resulting in unbalanced VEGFα/Ang-1 transcription. To our knowledge, this is the first time that Hp is associated with VEGFα signaling. Further exploration revealed that indeed vascular permeability was increased in $Hp^{-/-}$ animals after infarction. The mechanisms by which microvascular permeability is increased in newly formed vessels have been attributed to an unbalanced VEGF/Ang-1 transcription. VEGF overexpression without Ang-1 induction results in increased leakage-prone vessel formation[17]. Furthermore, our findings may explain previous observations in which reduced Hp functionality (Hp 2-2) is associated with intraplaque hemorrhage[22, 23]. We have previously shown that $Hp^{-/-}$ carotid arteries share similar morphological features during flow-mediated remodeling. The arterial wall was characterized by enhanced leukocyte infiltration and RBC deposition[24]. Furthermore, our findings indicate that therapeutics involving VEGF induction without induced Ang-1 may result in adverse hemorrhagic effects in the heart as well. Especially stent-based gene therapy to induce VEGF for myocardial ischemia necessitates careful evaluation[25].
Secondly, we have identified that PAI-1 activity is haptoglobin-dependent in the early angiogenic response after infarction. The detrimental post-infarct phenotype of $Hp^{-/-}$ animals associated with reduced PAI-1 activity corroborates previous studies involving PAI-$1^{-/-}$ mice. PAI-$1^{-/-}$ mice exhibit cardiac ruptures, ventricular dilatation and impaired cardiac function after infarction[12, 13, 15], comparable to our findings. Recently, it was shown that PAI-1 deficiency results in increased cardiac vascular permeability[26].

Our observation that reduced PAI-1 activity is associated with increased VEGF transcription and subsequent increased angiogenic response, is supported by earlier experiments. PAI-1 overexpression inhibited angiogenic properties of pancreatic cancer cells[27], while PAI-1 inhibition enhanced capillary formation by endothelial cells in a VEGF- and TGF-β1-dependent manner[28]. Additionally, the enhanced VEGFα transcription may be the result of increased oxidative stress, as illustrated by increased $CD163^{pos}$ cell count in $Hp^{-/-}$ mice. It has been shown that angiogenesis is enhanced in the presence of increased oxidative stress via enhanced VEGFα signaling[29].

One of the consequences of intramural hemorrhage may be increased free hemoglobin-induced oxidative stress. It was previously observed that free hemoglobin released during hemolysis was associated with severe renal oxidative stress in $Hp^{-/-}$ mice[30]. Excessive free hemoglobin is a source of ferrous ions for the Fenton reaction that results in the highly reactive hydroxyl free radical. Although we did not assess the amount of oxidative stress, we do have indirect evidence for increased oxidative burden in $Hp^{-/-}$ hearts. Previous studies have shown that haptoglobin binds hemoglobin and enables CD163-mediated clearance by macrophages, thereby preventing the release of ferrous ions from free hemoglobin and the subsequent formation of reactive free radicals[3, 31]. In our study, the extent of intramural hemorrhage observed in $Hp^{-/-}$ animals was associated with increased number of $CD163^{pos}$ cells. This may be due to a compensatory mechanism in which the absence of haptoglobin impairs hemoglobin uptake via CD163. As a consequence, the impaired uptake of free hemoglobin results in increased oxidative stress resulting in greater cellular damages and an increased need for scavenging activity. This postulated mechanism is supported by previous studies in which Hp 2-2 (less functional phenotype) is associated with increased intraplaque hemorrhage and redox-active iron[22, 23]. Furthermore, experimental studies have shown that Hp 2-2 mice have higher oxidative stress burden compared to Hp 1-1 mice[6].

Finally, in line with previous studies[32], we found that the absence of haptoglobin results in impaired healing and adverse remodeling after infarction. Haptoglobin appears to be critically involved in organizing wound structure and preventing expansive remodeling after infarction. Moreover, fibronectin production and collagen deposition were severely affected in $Hp^{-/-}$ mice. After MI, efficient matrix breakdown is necessary to form a provisional matrix that can be replaced by a firm collagen-based scar[18]. Our findings suggest that matrix breakdown occurs inefficiently in $Hp^{-/-}$ mice due to decreased MMP-2 activity, together with improper formation of a provisional matrix via decreased fibronectin production. Our study shows that $Hp^{-/-}$ mice exhibit reduced procollagen-3, TGF-β1 and lysyl-oxidase transcription and subsequent reduced collagen deposition 28 days after MI. These significant impairments in scar formation may be triggered by suboptimal MMP-2 activity and fibronectin production in the early phase after MI. Furthermore, previous clinical studies confirm the deleterious consequence of intramural hemorrhage after myocardial infarction. The presence of myocardial hemorrhage is an independent determinant of adverse remodeling in patients with acute MI.[33]

These new functions of haptoglobin may extent our knowledge about impaired tissue repair responses associated with the different haptoglobin genotypes. VEGFα signaling, PAI-1 activity and fibronectin production in Hp 1-1 compared to Hp 2-2 subjects after infarction is required to validate these mechanisms in humans.

In conclusion, our findings show that haptoglobin is involved in remodeling after infarction. We have identified PAI-1 activity, VEGFα/Ang-1 signaling and scar maturation as novel processes regulated by haptoglobin. The present study provides new insights in myocardial responses after infarction and thus may lead to novel therapeutic strategies for cardiac repair after MI.

Acknowledgements

We would like to thank Arjan Schoneveld (from the UMC Utrecht, The Netherlands) for his technical assistance.

Funding Sources

This work was supported by research grants from the European Community's 6th Framework Program (contract LSHMCT-2006-037400, IMMUNATH) and NWO Mozaïek grant (contract 017.004.004 to F.A.).

METHODS

Animals and experimental design

$Hp^{-/-}$ mice are generated by dr. Sai Kiang Lim[34] and backcrossed into a C57Bl6 background for 8 generations. Male C57Bl6 wild-type (WT), $Hp^{-/-}$ (10-12 wks, 25-30 g) received standard diet and water ad libitum. Myocardial infarction was induced by left coronary artery ligation, just below the left atrial appendage. Detailed information is available in the online Data Supplement. Digital photos of infarcts were encrypted before being analyzed by the researcher. Heart function and geometry assessment was done by a technician blinded to genotype. All animal experiments are performed in accordance with the national guidelines on animal care and with prior approval by the Animal Experimentation Committee of Utrecht University.

Myocardial infarction *in vivo*

Mice were anesthetized with a mixture of Fentanyl (Jansen-Cilag) 0.05 mg/kg, Dormicum (Roche) 5 mg/kg and medetomidine 0.5 mg/kg through an intraperitoneal injection. Core body temperature was maintained around 37°C during surgery by continuous monitoring with a rectal thermometer connected to an automatic heating blanket. Mice were intubated and ventilated (Harvard Apparatus Inc.) with 100% oxygen. The left coronary artery (LCA) was permanently ligated using an 8-0 vicryl suture. Ischemia was confirmed by bleaching of the myocardium and ventricular tachyarrhythmia. In sham operated animals the suture was placed beneath the LCA without ligating. The chest wall was closed and the animals received subcutaneously Antisedan (Pfizer) 2.5 mg/kg, Anexate (Roche) 0.5 mg/kg and Temgesic (Schering-Plough) 0.1 mg/kg.

Data Supplement

The online Data Supplement contains detailed information on infarct size calculation, protein and RNA isolation, MRI measurements, invasive LV pressure measurements, immunohistochemistry, polymerase chain reaction, zymography, oxidative stress, PAI-1 activity assay and vascular permeability assay

Statistics

Data are represented as Mean±SEM. One-way ANOVA with post-hoc LSD test was used for comparison >2 groups. Non-parametric t-test (abnormally distributed data) and independent-samples t-test (for normally distributed data) for 2 group comparisons. Kaplan-Meier survival analysis with log-rank test was used to evaluate mortality differences between groups. All statistical analyses were performed using SPSS 15.1.1. and $p<0.05$ was considered significant. The authors had full access to and take full responsibility for the integrity of the data. All authors have read and agree to the manuscript as written.

REFERENCES

1 Morita H, Seidman J, Seidman CE. Genetic causes of human heart failure. J Clin Invest. 2005;115:518-526.

2 Chapelle JP, Albert A, Smeets JP, Heusghem C, Kulbertus HE. Effect of the haptoglobin phenotype on the size of a myocardial infarct. N Engl J Med. 1982;307:457-463.

3 Buehler PW, Abraham B, Vallelian F, Linnemayr C, Pereira CP, Cipollo JF, Jia Y, Mikolajczyk M, Boretti FS, Schoedon G, Alayash AI, Schaer DJ. Haptoglobin preserves the CD163 hemoglobin scavenger pathway by shielding hemoglobin from peroxidative modification. Blood. 2009;113:2578-2586.

4 Levy AP, Asleh R, Blum S, Levy NS, Miller-Lotan R, Kalet-Litman S, Anbinder Y, Lache O, Nakhoul FM, Asaf R, Farbstein D, Pollak M, Soloveichik YZ, Strauss M, Alshiek J, Livshits A, Schwartz A, Awad H, Jad K, Goldenstein H. Haptoglobin: basic and clinical aspects. Antioxid Redox Signal. 2010;12:293-304.

5 Roguin A, Koch W, Kastrati A, Aronson D, Schomig A, Levy AP. Haptoglobin genotype is predictive of major adverse cardiac events in the 1-year period after percutaneous transluminal coronary angioplasty in individuals with diabetes. Diabetes Care. 2003;26:2628-2631.

6 Blum S, Asaf R, Guetta J, Miller-Lotan R, Asleh R, Kremer R, Levy NS, Berger FG, Aronson D, Fu X, Zhang R, Hazen SL, Levy AP. Haptoglobin genotype determines myocardial infarct size in diabetic mice. J Am Coll Cardiol. 2007;49:82-87.

7 Frangogiannis NG. The immune system and cardiac repair. Pharmacol Res. 2008;58:88-111.

8 Dobaczewski M, Gonzalez-Quesada C, Frangogiannis NG. The extracellular matrix as a modulator of the inflammatory and reparative response following myocardial infarction. J Mol Cell Cardiol. 2010;48:504-511.

9 Nahrendorf M, Hu K, Frantz S, Jaffer FA, Tung CH, Hiller KH, Voll S, Nordbeck P, Sosnovik D, Gattenlohner S, Novikov M, Dickneite G, Reed GL, Jakob P, Rosenzweig A, Bauer WR, Weissleder R, Ertl G. Factor XIII deficiency causes cardiac rupture, impairs wound healing, and aggravates cardiac remodeling in mice with myocardial infarction. Circulation. 2006;113:1196-1202.

10 Heymans S, Luttun A, Nuyens D, Theilmeier G, Creemers E, Moons L, Dyspersin GD, Cleutjens JP, Shipley M, Angellilo A, Levi M, Nube O, Baker A, Keshet E, Lupu F, Herbert JM, Smits JF, Shapiro SD, Baes M, Borgers M, Collen D, Daemen MJ, Carmeliet P. Inhibition of plasminogen activators or matrix metalloproteinases prevents cardiac rupture but impairs therapeutic angiogenesis and causes cardiac failure. Nat Med. 1999;5:1135-1142.

11 Creemers E, Cleutjens J, Smits J, Heymans S, Moons L, Collen D, Daemen M, Carmeliet P. Disruption of the plasminogen gene in mice abolishes wound healing after myocardial infarction. Am J Pathol. 2000;156:1865-1873.

12 Heymans S, Luttun A, Nuyens D, Theilmeier G, Creemers E, Moons L, Dyspersin GD, Cleutjens JP, Shipley M, Angellilo A, Levi M, Nube O, Baker A, Keshet E, Lupu F, Herbert JM, Smits JF, Shapiro SD, Baes M, Borgers M, Collen D, Daemen MJ, Carmeliet P. Inhibition of plasminogen activators or matrix metalloproteinases prevents cardiac rupture but impairs therapeutic angiogenesis and causes cardiac failure. Nat Med. 1999;5:1135-1142.

13 Zaman AK, Fujii S, Schneider DJ, Taatjes DJ, Lijnen HR, Sobel BE. Deleterious effects of lack of cardiac PAI-1 after coronary occlusion in mice and their pathophysiologic determinants. Histochem Cell Biol. 2007;128:135-145.

14 Zaman AK, French CJ, Schneider DJ, Sobel BE. A profibrotic effect of plasminogen activator inhibitor type-1 (PAI-1) in the heart. Exp Biol Med (Maywood). 2009;234:246-254.

15 Askari AT, Brennan ML, Zhou X, Drinko J, Morehead A, Thomas JD, Topol EJ, Hazen SL, Penn MS. Myeloperoxidase and plasminogen activator inhibitor 1 play a central role in ventricular remodeling after myocardial infarction. J Exp Med. 2003;197:615-624.

16 Cid MC, Grant DS, Hoffman GS, Auerbach R, Fauci AS, Kleinman HK. Identification of haptoglobin as an angiogenic factor in sera from patients with systemic vasculitis. J Clin Invest. 1993;91:977-985.

17 Thurston G, Suri C, Smith K, McClain J, Sato TN, Yancopoulos GD, McDonald DM. Leakage-resistant blood vessels in mice transgenically overexpressing angiopoietin-1. Science. 1999;286:2511-2514.

18 Sluijter JP, de Kleijn DP, Pasterkamp G. Vascular remodeling and protease inhibition--bench to bedside. Cardiovasc Res. 2006;69:595-603.

19 Sierevogel MJ, Velema E, van der Meer FJ, Nijhuis MO, Smeets M, de Kleijn DP, Borst C, Pasterkamp G. Matrix metalloproteinase inhibition reduces adventitial thickening and collagen accumulation following balloon dilation. Cardiovasc Res. 2002;55:864-869.

20 Blum S, Vardi M, Brown JB, Russell A, Milman U, Shapira C, Levy NS, Miller-Lotan R, Asleh R, Levy AP. Vitamin E reduces cardiovascular disease in individuals with diabetes mellitus and the haptoglobin 2-2 genotype. Pharmacogenomics. 2010;11:675-684.

21 Suleiman M, Aronson D, Asleh R, Kapeliovich MR, Roguin A, Meisel SR, Shochat M, Sulieman A, Reisner SA, Markiewicz W, Hammerman H, Lotan R, Levy NS, Levy AP. Haptoglobin polymorphism predicts 30-day mortality and heart failure in patients with diabetes and acute myocardial infarction. Diabetes. 2005;54:2802-2806.

22 Moreno PR, Purushothaman KR, Purushothaman M, Muntner P, Levy NS, Fuster V, Fallon JT, Lento PA, Winterstern A, Levy AP. Haptoglobin genotype is a major determinant of the amount of iron in the human atherosclerotic plaque. J Am Coll Cardiol. 2008;52:1049-1051.

23 Kalet-Litman S, Moreno PR, Levy AP. The haptoglobin 2-2 genotype is associated with increased redox active hemoglobin derived iron in the atherosclerotic plaque. Atherosclerosis. 2010;209:28-31.

24 de Kleijn DP, Smeets MB, Kemmeren PP, Lim SK, Van Middelaar BJ, Velema E, Schoneveld A, Pasterkamp G, Borst C. Acute-phase protein haptoglobin is a cell migration factor involved in arterial restructuring. FASEB J. 2002;16:1123-1125.

25 Gaffney MM, Hynes SO, Barry F, O'Brien T. Cardiovascular gene therapy: current status and therapeutic potential. Br J Pharmacol. 2007;152:175-188.

26 Xu Z, Castellino FJ, Ploplis VA. Plasminogen activator inhibitor-1 (PAI-1) is cardioprotective in mice by maintaining microvascular integrity and cardiac architecture. Blood. 2010;115:2038-2047.

27 Inoue M, Sawada T, Uchima Y, Kimura K, Nishihara T, Tanaka H, Yashiro M, Yamada N, Ohira M, Hirakawa K. Plasminogen activator inhibitor-1 (PAI-1) gene transfection inhibits the liver metastasis of pancreatic cancer by preventing angiogenesis. Oncol Rep. 2005;14:1445-1451.

28 Kellouche S, Mourah S, Bonnefoy A, Schoevaert D, Podgorniak MP, Calvo F, Hoylaerts MF, Legrand C, Dosquet C. Platelets, thrombospondin-1 and human dermal fibroblasts cooperate for stimulation of endothelial cell tubulogenesis through VEGF and PAI-1 regulation. Exp Cell Res. 2007;313:486-499.

29 Ushio-Fukai M, Alexander RW. Reactive oxygen species as mediators of angiogenesis signaling: role of NAD(P)H oxidase. Mol Cell Biochem. 2004;264:85-97.

30 Lim YK, Jenner A, Ali AB, Wang Y, Hsu SI, Chong SM, Baumman H, Halliwell B, Lim SK. Haptoglobin reduces renal oxidative DNA and tissue damage during phenylhydrazine-induced hemolysis. Kidney Int. 2000;58:1033-1044.

31 Asleh R, Guetta J, Kalet-Litman S, Miller-Lotan R, Levy AP. Haptoglobin genotype- and diabetes-dependent differences in iron-mediated oxidative stress in vitro and in vivo. Circ Res. 2005;96:435-441.

32 Asaf R, Blum S, Roguin A, Kalet-Litman S, Kheir J, Frisch A, Miller-Lotan R, Levy AP. Haptoglobin genotype is a determinant of survival and cardiac remodeling after myocardial infarction in diabetic mice. Cardiovasc Diabetol. 2009;8:29.

33 Ganame J, Messalli G, Dymarkowski S, Rademakers FE, Desmet W, Van de WF, Bogaert J. Impact of myocardial haemorrhage on left ventricular function and remodelling in patients with reperfused acute myocardial infarction. Eur Heart J. 2009;30:1440-1449.

34 Lim SK, Kim H, Lim SK, bin AA, Lim YK, Wang Y, Chong SM, Costantini F, Baumman H. Increased susceptibility in Hp knockout mice during acute hemolysis. Blood. 1998;92:1870-1877.

PART III

CHAPTER 11

Past, Present & Future

Fatih Arslan

Discussion

PAST

Acute myocardial infarction and related complications are an increasing burden to society and healthcare systems.[1, 2] Although the risk for cardiovascular disease has risen exponentially after the industrial revolution,[3] there is a great deal of evidence that ancient societies were well aware of the lethal consequences of myocardial infarction. The first clinical descriptions of myocardial infarction dates from at least 1550 BC. The ancient Egyptians described "pain in his arm, pain in his breast, on the side of his cardia" as symptoms related to a condition in which "death approaches him" (Ebers Papyrus, University of Leipzig).[4] Some argue that a tomb relief from the 6th Dynasty (2625-2475 BC) named "Sudden Death" is the earliest illustration of a lethal acute coronary event (Figure 1).[5] Hippocrates (460-377 BC) also acknowledged that "frequent recurrence of cardialgia, in an elderly person, announces sudden death".[6, 7] More interestingly, without having the possibility to examine post-mortem hearts, Hippocrates raised the idea that "with this alteration in the blood (hypercoagulability), air cannot pervade the natural passages (stasis)".[4] In this remarkable notion, Hippocrates stated 2 of the three factors influencing thrombosis as defined by Virchow 2200 years later. It was William Heberden to introduce "angina pectoris" for the first time as a medical term to describe the clinical symptoms related to coronary narrowing.[8, 9] However, his

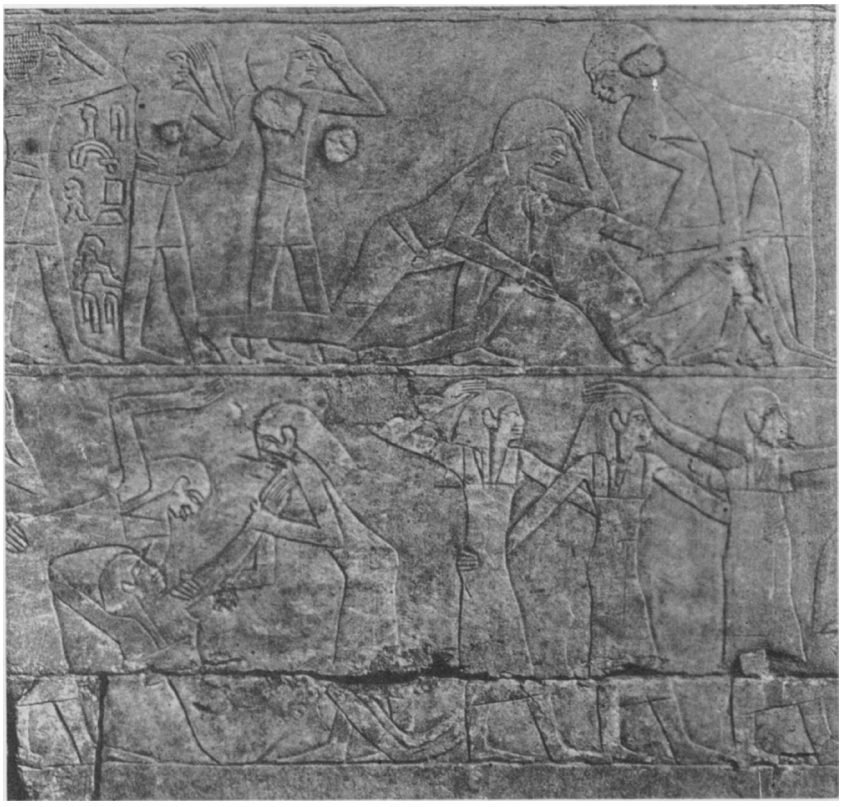

Figure 1. *Tomb relief illustrating the sudden death of an Egyptian nobleman (upper right), surrounded by his grieving family and two servants. His wife, (lower left) overcome by emotion, has fainted while two women try to revive her. The lower right shows the wife holding on to two servants while she is being led from the scene (interpretation adapted from Bruetsch WL[5]; Tomb of Sesi at Sakkara. 6th Dynasty 2625-2475 B.C.).*

contemporary John Fothergill and his close friend Edward Jenner were the first to associate coronary calcification and thrombosis to the ischemic origin of angina pectoris, respectively.[10, 11] At the time, it was already a major achievement if one could link the clinical symptoms of myocardial infarction to the post-mortem findings. It was not until the beginning of the 20th century, when Vasilii P. Obraztsov first described the clinical presentation and coronary thrombosis in the setting of a myocardial infarction.[12] Two years after the Russian publication, dr. James B. Herrick speculated that "the hope for the damaged myocardium lies in the direction of securing a supply of blood through friendly neighbouring vessels so as to restore as far as possible its functional integrity". Unfortunately, reperfusion therapy became only possible in the 70'ies due to limitations of medical practice at that time. First, Robert B. Jennings showed that there is a reversible character of cell death after ischemia in 1960.[13] Eugene Braunwald and co-workers pioneered with pharmacological interventions in animal experiments and human to further limit infarct size after successful reperfusion.[14-16] The GISSI study group was the first to prove that early reperfusion was associated with smaller infarct size and improved clinical outcome after myocardial infarction.[17] However, experimental data showed that there is an increase in cell death during reperfusion, and that adjunctive reperfusion strategies are able to further reduce final infarct size.[18, 19] Despite the extensive pre-clinical evidence for reduction of reperfusion-induced injury by adjunctive interventions, there is not a single example of successful translation from the pre-clinical setting into the clinical arena. Nevertheless, optimized blood flow restoration through the culprit coronary artery has resulted in increased survival of patients after myocardial infarction over the past decade. Together with an aging population, however, increased survival of post-infarct patients resulted in higher incidence of infarct-related complications in the long-term.[1] One of the most common and severe infarct-related complications is heart failure. The increasing incidence and prevalence of heart failure intensified research in etiology and therapy to decrease the socio-economic burden to society. It becomes more and more clear that successful reperfusion is not sufficient to enhance myocardial viability after infarction. Enhancing cardiac repair using cellular or biological therapeutic approaches has become a dynamic field of research. Intrinsic repair mechanisms initiated after myocardial infarction may result in maladaptive remodeling, also referred to as adverse remodeling, of both the infarcted and non-infarcted remote myocardium. Adverse remodeling is not a research area that emerged in the past decade. It was already acknowledged in the late 70'ies and early 80'ies that healing after infarction was a dynamic process, and that it could predispose congestive heart failure and cardiac dysfunction.[20-22] Despite a long-lasting understanding of post-infarct repair mechanisms and experimental success to reduce reperfusion-induced injury, the current status holds a painful truth: increase in infarct-related morbidity of which heart failure has reached epidemic proportions in Western societies.[1, 2, 23, 24]

PRESENT

In this thesis, we have investigated novel therapeutic targets to enhance cardiac repair and improve cardiac function after myocardial infarction. We have tried to approach this objective by targeting 3 major determinants of post-infarct adverse remodeling and subsequent heart function deterioration:

1. infarct size
2. detrimental activation of circulating cells
3. deleterious action of danger signals

Independent from each other, the above mentioned determinants may have direct influence on cardiac

repair and function. However, they may influence one another in great sense. In fact, each factors is able to trigger a positive feedback mechanism. The exaggeration of the one may result in an accentuation of the other and subsequently of the entire triangle (Figure 2). This suggested concept is not entirely hypothetical: infarction triggers the release of danger signals due to cell death and matrix turnover. In turn, danger signals can activate circulating cells involved in innate immunity.[25-27] Enhanced immune responses may induce cell death and increase infarct size via increased leukocyte extravasation and activation.[28-30] As one of the determinants becomes exaggerated or enhanced, it may initiate a vicious circle of progressive deterioration of cardiac function and geometry. The following studies demonstrate that the same determinants can be used as therapeutic targets to stop the vicious circle and thus enhance myocardial viability and cardiac performance.

First, we have shown in Chapter 2 that final infarct size is determined by TLR2 expression on circulating cells. Lack of TLR2 on circulating cells reduced infarct size after myocardial ischemia/reperfusion (I/R) injury. In line with this observation, systemic inhibition of TLR2 reduced infarct size and deactivated circulating monocytes. The therapeutic effect of TLR2 inhibition was established mainly via reduction of innate immune activation. Although we have not addressed this point, we suggest that danger signals (i.e. DAMPs) released after I/R injury engage with TLR2 on circulating cells in order to activate them (Chapter 1). In addition, in Chapter 3, we showed that TLR2 inhibition exerts a therapeutic effect in a large animal model. In Chapter 7 we showed that, despite similar infarct size, mice with TLR2 deficient bone marrow cells were protected against cardiac function deterioration and adverse remodeling compared to mice with wild-type bone marrow. Together, these data show that absent TLR2 signaling in circulating cells is able to reduce innate immune activation, reduce infarct size and enhances cardiac repair after myocardial infarction.

Secondly, we established infarct size reduction by mesenchymal stem cell (MSC)-derived exosome administration (Chapter 4-6). We showed that MSC-derived exosome administration just prior to reperfusion improves cardiac function and preserves left ventricular dimensions after myocardial I/R injury (Chapter 6). Serial analysis of ischemic/reperfused heart samples revealed that pro-survival pathways were activated and pro-apoptotic signaling was reduced, while initial inflammatory responses did not differ upon MSC-derived exosome treatment. However, we did observe a reduction in secondary leukocytosis during follow-up, when infarct size was finalized (Chapter 6). These data confirm previous

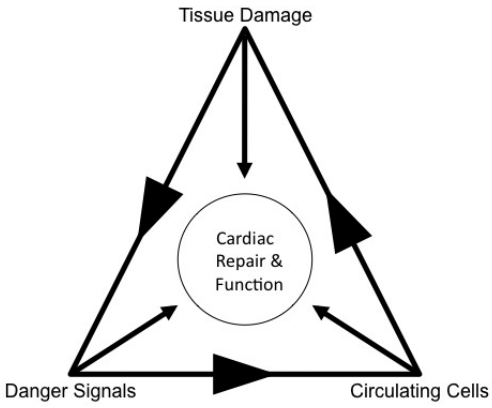

Figure 2. *Schematic overview of determinants of cardiac repair and function*

clinical studies in which infarct size is shown to be directly proportional to white blood cell counts and/or inflammation after myocardial infarction.[31-33] In addition, increased number of circulating white blood cells or monocytes are associated with adverse remodeling.[34-37] Langendorff-perfused heart experiments revealed that exosomes exert their therapeutic action by direct engagement with cardiac cells. Unlike TLR2 inhibition, exosomes directly inhibit apoptosis of the myocardium without interplay of circulating cells. Together with our findings (Chapter 6), these data confirm that infarct size and peripheral blood composition are independent mediators of cardiac repair and function.

Thirdly, we studied the effect of danger signal modification on adverse remodeling. We used fibronectin-EDA as a target to alter cardiac repair responses after myocardial infarction. Despite similar infarct size, mice lacking fibronectin-EDA exhibited less expansive remodeling and improved cardiac performance and survival compared to wild-type animals (Chapter 8). Immunohistochemical analysis of post-infarct hearts revealed that leukocyte influx was reduced in fibronectin-EDA$^{-/-}$ mice. Biochemical assessment of tissue cytokine levels confirmed the reduction of inflammation: TNFα, RANTES, IL-10 and GM-CSF were all significantly reduced in the absence of fibronectin-EDA. Analysis of peripheral blood cells showed that both the number and activation of monocytes were reduced in fibronectin-EDA$^{-/-}$ mice, compared to wild-type animals. These data indicate that fibronectin-EDA has a direct effect on innate immune responses and circulating cells, subsequently altering cardiac repair and performance. Ischemia/reperfusion experiments revealed that the lack of fibronectin-EDA does not affect infarct size, suggesting that fibronectin-EDA does not mediate myocardial viability after I/R injury (unpublished data). In line with the proposed notion (Figure 2), the fibronectin-EDA experiments show that danger signal modification alters behavior of circulating cells involved in innate immunity and subsequently affect cardiac repair.

Finally, we studied whether exaggeration of one of the elements in Figure 2 could worsen cardiac repair and enhance adverse remodeling. As shown in chapter 9, haptoglobin deficiency resulted in a dramatic phenotype after myocardial infarction. Mice lacking haptoglobin exhibited intramural hemorrhage, delayed wound repair and subsequent deteriorated scar maturation. All these morphological changes resulted in increased cardiac ruptures, increased dilatation of the left ventricle and reduced cardiac performance and survival. We hypothesized that the detrimental changes in the heart were initiated at a very early stage after the ischemic injury, since immunohistochemical analysis revealed dramatic tissue alterations 3 days after infarction. Compared to wild-type animals, haptoglobin deficient mice exhibited reduced PAI-1 activity 3 days after infarction. Previous studies with PAI-1 deficient mice documented a similar phenotype after infarction.[38-40] Furthermore, evaluation of the angiogenic response revealed that haptoglobin deficiency was associated with enhanced VEGFα transcription without upregulation of Angiopoietin-1. These findings suggested increased vessel formation without maturation, thus predisposing leaky vessels. Indeed, the angiogenic response was increased in post-infarct hearts of haptoglobin deficient mice. In vivo assessment of vascular permeability confirmed that haptoglobin deficient mice exhibited increased vessel permeability after infarction, compared to wild-type animals. The question remained what the trigger was for these detrimental biochemical modifications in haptoglobin deficient mice. The main function of haptoglobin is the binding of free hemoglobin in order to facilitate its clearance by CD163^{pos} macrophages. Excessive free hemoglobin is a source of ferrous ions that cause oxidative stress. In concordance with the observation of increased intramural hemorrhage in haptoglobin deficient mice, we found increased expression of CD163^{pos} cells and increased oxidative stress in the absence of haptoglobin. It is likely that in our study oxidative stress due to excessive red blood cell deposition is the main trigger for all deleterious consequences in haptoglobin deficient animals after myocardial infarction. Oxidative stress has also been proposed as a danger signal.[27, 41] However,

there seems to be a different mechanism underlying the reduced PAI-1 activity in the absence of haptoglobin. Earlier reports show that oxidative stress actually increases PAI-1 transcription and activity.[42, 43] Future studies are needed to further explore the link between haptoglobin and PAI-1 activity. Nevertheless, as proposed in Figure 2, exaggeration of oxidative stress (i.e. danger signal) triggered a positive feedback loop that resulted in deterioration of cardiac repair and function in haptoglobin deficient mice after myocardial infarction.

FUTURE

So far, successful pre-clinical interventions to enhance myocardial viability or repair have failed in the clinical practice.[44, 45] There are many reasons, but several major drawbacks from earlier studies have resulted in this failure to translate. First, many drugs have been administered before the ischemic insult to test their efficacy. Administration prior to the occurrence of acute myocardial infarction is not possible in the clinical setting, since acute myocardial infarction is not an elective event and prophylactic administration to high-risk patients is not likely. More importantly, reperfusion after ischemia triggers different signaling cascades compared to those that are activated during ischemia alone. For this reason, compounds that target ischemia-related processes, may not be effective to alter reperfusion-induced mechanisms. For example, p38-MAPK inhibitor SB239063 has shown to reduce infarct size when administered before the ischemic injury. However, we have demonstrated that SB239063 fails to do so when it is given just prior to reperfusion (Chapter 2). The lack of large animal testing is another reason for failure to translate pre-clinical success. It is of utmost importance to reproduce murine results in an animal model that shares the same cardiac physiology and anatomy with human (e.g. pigs, sheep). We have undertaken the first step to translate TLR2 inhibition into the clinical setting. Using a humanized anti-TLR2 antibody OPN-305, we demonstrated that TLR2 inhibition significantly reduces infarct size and improves systolic performance in pigs (Chapter 3). In the near future, OPN-305 will enter phase-I/II clinical trials. Mesenchymal stem cell (MSC)-derived exosomes are the second potential candidates for therapeutic applications. MSCs have shown to elicit a therapeutic effect in human.[46] However, it is widely accepted that paracrine factors secreted by stem cells are responsible for the observed cardioprotective effect.[47] MSC-derived exosomes provide an “off-the-shelf” therapeutic option, whereas current stem cell therapy needs autologous enrichment and local delivery. Furthermore, MSC-derived exosomes are non-viable thus potentially safer and cheaper to manufacture and store compared to current stem cell-based solutions. Currently, MSC-derived exosomes are being tested in porcine models for myocardial I/R injury, skin wounds and human models for alopecia (i.e. hair loss). It is unquestionable that the near future will hold either great breakthroughs or major disappointments in the effort to enhance myocardial viability and repair after myocardial infarction. Designing theoretical frameworks based on experimental or empirical data is not always helpful to understand pathophysiological processes. The ancient Egyptians postulated that angina was the result of noxious substances that could be eliminated via the anus with faeces (Ebers Papyrus).[4] We know now that atherosclerotic plaques may cause cardiac ischemia. In both eras, people tried to understand a pathological event by putting an observation in a theoretical framework. However, we still do not know why suddenly a plaque ruptures; how in turn our innate immune system becomes activated after myocardial infarction and why it may cause more damage than it actually repairs the cardiac wound. In essence, scientific progress is merely changing glasses to optimize one’s vision: still, we are hampered by our limited ability to ‘see’ and ‘understand’ the divine nature of the human body.

REFERENCES

1 International Cardiovascular Disease Statistics - 2009 Update. American Heart Association 2009;Available at: URL: http://www.americanheart.org/downloadable/heart/1236204012112INTL.pdf.

2 European cardiovascular disease statistics. European Heart Network 2008.

3 Martin W. The beriberi analogy to myocardial infarction. Med Hypotheses. 1983;10:185-198.

4 Leibowitz J.O. The history of coronary heart disease. Berkeley: University of California press; 1970.

5 BRUETSCH WL. The earliest record of sudden death possibly due to atherosclerotic coronary occlusion. Circulation. 1959;20:438-441.

6 Cheng TO. Hippocrates and cardiology. Am Heart J. 2001;141:173-183.

7 KATZ AM, KATZ PB. Diseases of the heart in the works of Hippocrates. Br Heart J. 1962;24:257-264.

8 Michaels L. The eighteenth-century origins of angina pectoris: predisposing causes, recognition and aftermath. Med Hist Suppl. 2001:1-219.

9 Aisner M. Angina pectoris 1768-1970. N Engl J Med. 1970;282:746-748.

10 Proudfit WL. John Fothergill and angina pectoris. Br Heart J. 1991;66:322-324.

11 Proudfit WL. Origin of concept of ischaemic heart disease. Br Heart J. 1983;50:209-212.

12 Muller JE. Diagnosis of myocardial infarction: historical notes from the Soviet Union and the United States. Am J Cardiol. 1977;40:269-271.

13 JENNINGS RB, SOMMERS HM, SMYTH GA, FLACK HA, LINN H. Myocardial necrosis induced by temporary occlusion of a coronary artery in the dog. Arch Pathol. 1960;70:68-78.

14 Braunwald E, Maroko PR, Libby P. Reduction of infarct size following coronary occlusion. Circ Res. 1974;35 Suppl 3:192-201.

15 Maroko PR, Braunwald E. Effects of metabolic and pharmacologic interventions on myocardial infarct size following coronary occlusion. Circulation. 1976;53:I162-I168.

16 Markis JE, Malagold M, Parker JA, Silverman KJ, Barry WH, Als AV, Paulin S, Grossman W, Braunwald E. Myocardial salvage after intracoronary thrombolysis with streptokinase in acute myocardial infarction. N Engl J Med. 1981;305:777-782.

17 Effectiveness of intravenous thrombolytic treatment in acute myocardial infarction. Gruppo Italiano per lo Studio della Streptochinasi nell'Infarto Miocardico (GISSI). Lancet. 1986;1:397-402.

18 Braunwald E, Kloner RA. Myocardial reperfusion: a double-edged sword? J Clin Invest. 1985;76:1713-1719.

19 Murry CE, JENNINGS RB, Reimer KA. Preconditioning with ischemia: a delay of lethal cell injury in ischemic myocardium. Circulation. 1986;74:1124-1136.

20 Hutchins GM, Bulkley BH. Infarct expansion versus extension: two different complications of acute myocardial infarction. Am J Cardiol. 1978;41:1127-1132.

21 Roberts CS, Maclean D, Braunwald E, Maroko PR, Kloner RA. Topographic changes in the left ventricle after experimentally induced myocardial infarction in the rat. Am J Cardiol. 1983;51:872-876.

22 Roberts CS, Maclean D, Maroko P, Kloner RA. Early and late remodeling of the left ventricle after acute myocardial infarction. Am J Cardiol. 1984;54:407-410.

23 Weir RA, McMurray JJ, Velazquez EJ. Epidemiology of heart failure and left ventricular systolic dysfunction after acute myocardial infarction: prevalence, clinical characteristics, and prognostic importance. Am J Cardiol. 2006;97:13F-25F.

24 McMurray JJ, Pfeffer MA. Heart failure. Lancet. 2005;365:1877-1889.

25 Arslan F, de Kleijn DP, Pasterkamp G. Innate immune signaling in cardiac ischemia. Nat Rev Cardiol. 2011.

26 Seong SY, Matzinger P. Hydrophobicity: an ancient damage-associated molecular pattern that initiates innate immune responses. Nat Rev Immunol. 2004;4:469-478.

27 Matzinger P. The danger model: a renewed sense of self. Science. 2002;296:301-305.

28 Frangogiannis NG, Youker KA, Rossen RD, Gwechenberger M, Lindsey MH, Mendoza LH, Michael LH, Ballantyne CM, Smith CW, Entman ML. Cytokines and the microcirculation in ischemia and reperfusion. J Mol Cell Cardiol. 1998;30:2567-2576.

29 Jordan JE, Zhao ZQ, Vinten-Johansen J. The role of neutrophils in myocardial ischemia-reperfusion injury. Cardiovasc Res. 1999;43:860-878.

30 Vinten-Johansen J. Involvement of neutrophils in the pathogenesis of lethal myocardial reperfusion injury. Cardiovasc Res. 2004;61:481-497.

31 Prasad A, Stone GW, Stuckey TD, Costantini CO, Mehran R, Garcia E, Tcheng JE, Cox DA, Grines CL, Lansky AJ, Gersh BJ. Relation between leucocyte count, myonecrosis, myocardial perfusion, and outcomes following primary angioplasty. Am J Cardiol. 2007;99:1067-1071.

32 Smit JJ, Ottervanger JP, Slingerland RJ, Kolkman JJ, Suryapranata H, Hoorntje JC, Dambrink JH, Gosselink AT, de Boer MJ, Zijlstra F, van 't Hof AW. Comparison of usefulness of C-reactive protein versus white blood cell count to predict outcome after primary percutaneous coronary intervention for ST elevation myocardial infarction. Am J Cardiol. 2008;101:446-451.

33 Chia S, Nagurney JT, Brown DF, Raffel OC, Bamberg F, Senatore F, Wackers FJ, Jang IK. Association of leukocyte and neutrophil counts with infarct size, left ventricular function and outcomes after percutaneous coronary intervention for ST-elevation myocardial infarction. Am J Cardiol. 2009;103:333-337.

34 Barron HV, Harr SD, Radford MJ, Wang Y, Krumholz HM. The association between white blood cell count and acute myocardial infarction mortality in patients > or =65 years of age: findings from the cooperative cardiovascular project. J Am Coll Cardiol. 2001;38:1654-1661.

35 Maekawa Y, Anzai T, Yoshikawa T, Asakura Y, Takahashi T, Ishikawa S, Mitamura H, Ogawa S. Prognostic significance of peripheral monocytosis after reperfused acute myocardial infarction:a possible role for left ventricular remodeling. J Am Coll Cardiol. 2002;39:241-246.

36 Jugdutt BI. Monocytosis and adverse left ventricular remodeling after reperfused myocardial infarction. J Am Coll Cardiol. 2002;39:247-250.

37 Bauters A, Ennezat PV, Tricot O, Lallemant R, Aumegeat V, Segrestin B, Quandalle P, Lamblin N, Bauters C. Relation of admission white blood cell count to left ventricular remodeling after anterior wall acute myocardial infarction. Am J Cardiol. 2007;100:182-184.

38 Askari AT, Brennan ML, Zhou X, Drinko J, Morehead A, Thomas JD, Topol EJ, Hazen SL, Penn MS. Myeloperoxidase and plasminogen activator inhibitor 1 play a central role in ventricular remodeling after myocardial infarction. J Exp Med. 2003;197:615-624.

39 Zaman AK, Fujii S, Schneider DJ, Taatjes DJ, Lijnen HR, Sobel BE. Deleterious effects of lack of cardiac PAI-1 after coronary occlusion in mice and their pathophysiologic determinants. Histochem Cell Biol. 2007;128:135-145.

40 Zaman AK, French CJ, Schneider DJ, Sobel BE. A profibrotic effect of plasminogen activator inhibitor type-1 (PAI-1) in the heart. Exp Biol Med (Maywood). 2009;234:246-254.

41 Yan SF, Ramasamy R, Schmidt AM. The RAGE axis: a fundamental mechanism signaling danger to the vulnerable vasculature. Circ Res. 2010;106:842-853.

42 Hasan RN, Schafer AI. Hemin upregulates Egr-1 expression in vascular smooth muscle cells via reactive oxygen species ERK-1/2-Elk-1 and NF-kappaB. Circ Res. 2008;102:42-50.

43 Vulin AI, Stanley FM. Oxidative stress activates the plasminogen activator inhibitor type 1 (PAI-1) promoter through an AP-1 response element and cooperates with insulin for additive effects on PAI-1 transcription. J Biol Chem. 2004;279:25172-25178.

44 Arslan F, de Kleijn DP, Timmers L, Doevendans PA, Pasterkamp G. Bridging innate immunity and myocardial ischemia/reperfusion injury: the search for therapeutic targets. Curr Pharm Des. 2008;14:1205-1216.

45 Bolli R, Becker L, Gross G, Mentzer R, Jr., Balshaw D, Lathrop DA. Myocardial protection at a crossroads: the need for translation into clinical therapy. Circ Res. 2004;95:125-134.

46 Martin-Rendon E, Brunskill S, Doree C, Hyde C, Watt S, Mathur A, Stanworth S. Stem cell treatment for acute myocardial infarction. Cochrane Database Syst Rev. 2008:CD006536.

47 Gnecchi M, Zhang Z, Ni A, Dzau VJ. Paracrine mechanisms in adult stem cell signaling and therapy. Circ Res. 2008;103:1204-1219.

CHAPTER 12

Summary

More patients survive the initial myocardial infarction, thanks to pharmacological advances (e.g. anti-thrombotics) and technical breakthroughs (e.g. stent technology). Unfortunately, the surviving patients do suffer from progressive deterioration of cardiac function. For this reason, the incidence of heart failure and other MI-related morbidity is increasing. Hence, novel adjunctive therapeutics are necessary to further reduce cardiac injury and/or prevent the development of infarct-related complications. In this thesis, we studied two major determinants for progressive deterioration of heart function after myocardial infarction: 1. **myocardial ischemia/reperfusion (I/R) injury** and 2. **adverse ventricular remodeling.**

Myocardial I/R injury is a very complex process involving divergent intracellular pathways as well as extracellular mediators causing additional post-ischemic injury. Mediators responsible for cell death during ischemia are different from those during the reperfusion phase. Some of the reperfusion-induced characteristic molecular alterations have been used as therapeutic targets in both pre-clinical and clinical studies, with little success. In **Part I** of this thesis, we have used the inflammatory response and signaling pathways within cardiomyocytes to enhance myocardial viability after I/R injury. In **Part II**, we used certain targets within innate immunity that are crucial for post-infarct repair responses. The reparative processes in the infarcted heart, referred to as remodeling, are characterized by inflammation, matrix turnover and subsequently scar formation and maturation. The remodeling process may result in the preservation of cardiac function after MI. However, when the initial immune response is enhanced and detrimentally activated, the heart may dilate and the function will deteriorate. This process of **adverse remodeling** may result in heart failure after MI.

In **Chapter 1**, we introduced several basic principles of the post-ischemic repair response mediated by innate immunity. Recent basic scientific research has provided exciting insights into the pathogenesis of deleterious immune responses after MI. One major radical shift in scientific thinking was the postulation of the 'danger model' as described first by Polly Matzinger. It provides a theoretical framework to understand and explain innate immune activation after cardiac injury. Briefly, molecules associated with cell death and matrix degradation (danger associated molecular patterns; DAMPs) may trigger immune responses in the absence of pathogens. DAMPs can activate receptors that are known as pathogen recognition receptors (PRRs), which are traditionally used by white blood cells to clear pathogens like bacteria or virus. But what defines a DAMP? And how do DAMPs activate receptors that are designed for pathogen removal? Are PRRs designed for pathogen at all? Despite the fact that these questions still remain to be addressed, the 'danger model' did trigger the scientific community to search for DAMPs that were upregulated after cardiac injury and activated innate immunity. From a 'danger model' perspective, one could downregulate detrimental immune responses by either preventing DAMP-PRR interaction or decreasing DAMP release after cardiac injury. In this thesis we used the 'danger model' as a theoretical framework to study the molecular and physiological consequences of interventions that affected DAMP-PRR interactions using animal models of myocardial infarction. The conclusions of the studies are described in Table 1.

Table 1. Conclusions of the thesis

Conclusions	Chapter
Every single molecule released after tissue injury is a potential danger signal	1
Circulating TLR2 mediates TLR2-induced I/R injury	2
TLR2 inhibition reduces infarct size and improves cardiac performance after I/R injury	2 & 3
Exosomes are the mediators of paracrine actions in MSC secretion	4 - 7
MSCs originating from embryonic and fetal tissue secrete similar cardioprotective exosomes	5
Immortalization of MSCs may overcome production and scaling hurdles of exosomes	6
Exosomes interact directly with cardiac cells to reduce injury	7
Intact exosomes are a prerequisite to establish infarct size reduction after I/R injury	7
Exosome treatment reduces infarct-related inflammation	7
Circulating TLR2 mediates TLR2-induced adverse remodeling	8
Lack of TLR2 in circulating cells improves cardiac function and geometry after infarction	8
Fibronectin-EDA activates circulating cells and subsequently mediates adverse remodeling after infarction	9
Haptoglobin is crucial for scavenging oxidative stress in the infarcted heart	10
Haptoglobin mediates vascular permeability of newly formed vessels and scar maturation after infarction	10

PART I

In **Chapter 2**, we described the use of Toll-like receptor (TLR)-2, a known PRR, as a therapeutic target to reduce infarct size in mice. The most interesting finding of the study was the fact that TLR2-associated myocardial I/R injury was mediated by bone marrow derived blood cells that express TLR2 on their cell surface. For this reason, we successfully used an anti-TLR2 antibody for systemic administration. As demonstrated, we observed a 45% reduction in myocardial injury and subsequent improvement in heart function via reduced inflammation. The therapeutic effect of TLR2 inhibition was also tested in pigs, which is a critical step in clinical translation of pre-clinical success. In **Chapter 3**, we showed that a single intravenous bolus injection of a humanized anti-TLR2 antibody just prior to reperfusion resulted in significant reduction of infarct size and improvement in systolic performance of the infarcted area in pigs. Together, these data show that TLR2 inhibition is a potential candidate as an adjunctive therapeutic for patients suffering from acute MI.

In the above mentioned studies, we prevented the deleterious interaction of DAMPs and a PRR (i.e. TLR2) in myocardial I/R injury. Enhancement of myocardial viability and function may also be established by activating pro-survival signaling pathways and/or reducing pro-apoptotic signaling in cardiomyocytes. Previous studies have shown that stem cell secretion is able to enhance viability of cardiomyocytes, reduce infarct size and improve cardiac performance. This phenomenon is known as the 'paracrine action' of stem cells. In **Chapter 4**, we described the purification of microparticles, referred to as exosomes, mediating the therapeutic effect of mesenchymal stem cell (MSC) secretion. We demonstrated that a single intravenous bolus injection of exosomes, derived from either embryonic (**Chapter 4**), fetal (**Chapter 5**) or immortalized sources (**Chapter 6**), reduce infarct size and improve cardiac performance via downregulated apoptotic signaling and enhanced survival pathway activation.

Furthermore, exosomes appeared to have a direct therapeutic effect on cardiac cells, in contrast to anti-TLR2 treatment (which exerts its action via blood cells). Not surprisingly, the inflammatory response was downregulated in exosome treated animals, supporting the notion that the extent of tissue damage, and thus DAMP release, determines the severity of the inflammatory response (**Chapter 7**).

PART II

It is well documented that final infarct size is strongly associated with cardiac function and clinical outcome. In addition, repair of both the infarct and remote myocardium during the sub-acute and chronic phase after MI, may also have profound effects on function and outcome. Enhanced inflammation and suboptimal scarring and scar maturation may result in ventricular dilatation and dysfunction, referred to as adverse remodeling. In the second part of the thesis, we focused on targets that mediate adverse remodeling after infarction.

In line with the infarct size reduction after TLR2 inhibition, we demonstrated that the lack of TLR2 in bone marrow derived cells is also beneficial in the long-term. Despite equal infarct size, mice lacking TLR2 (compared to mice with functional TLR2) in circulating cells have improved cardiac function and preserved ventricular geometry after MI (**Chapter 8**). In this study, we inhibited DAMP-PRR interaction at the side of the target receptor (TLR2), while interference at DAMP-level may exert same protective effects. In **Chapter 9**, we studied the role of fibronectin-EDA in post-infarct remodeling. Fibronectin-EDA is upregulated after tissue injury and mediates inflammation via leukocyte activation. We showed that, in comparison to wild-type mice, the absence of fibronectin-EDA was associated with improved survival and enhanced cardiac performance after MI. Both studies (**Chapter 8 & 9**) demonstrate the crucial role of DAMP-PRR interaction in inflammation during cardiac repair mechanisms after infarction. In the final study, we approached the 'danger model' from a different perspective. Instead of using it for enhancement of cardiac function and repair, we tried to deteriorate cardiac repair and subsequent performance. In **Chapter 10**, we increased the DAMP burden in the heart by increasing oxidative stress after infarction. By using mice genetically deleted for the anti-oxidative protein haptoglobin, we showed that increased oxidative stress results in a series of detrimental processes in the heart; increased intramural hemorrhage and cardiac ruptures, increased macrophage influx and defective scarring and scar maturation. Subsequently, mice lacking haptoglobin exhibited decreased cardiac performance and lower survival rates compared to wild-type animals after MI.

In conclusion, the 'danger model' is a useful theoretic framework to understand and explore immune responses and repair processes after MI. So far, TLR2 inhibition and exosome treatment are potential candidates as adjunctive therapeutics to enhance cardiac repair and function in patients suffering from acute MI. Future studies are required to confirm the efficacy of exosome treatment in large animals and to further explore the role of fibronectin-EDA in infarct-related inflammation.

CHAPTER 13

Samenvatting

Dankzij de ontwikkelingen in zowel farmacologische (e.g. antitrombotica) als technologische interventies (e.g. stentplaatsing), overleven steeds meer patiënten een hartinfarct. Een keerzijde van een hogere overleving is dat er steeds meer patiënten zijn die chronisch ziek zijn. Doordat er steeds meer patiënten een hartinfarct overleven zien we een stijging van het aantal patiënten die lijden aan infarct-gerelateerde complicaties, zoals hartfalen. Vandaar dat er een grote behoefte bestaat om nieuwe therapieën te ontwikkelen die de schade na een hartinfarct nog verder beperkt en het herstel erna bevordert, zodat de kans op complicaties kleiner wordt. In dit proefschrift hebben we tweetal processen bestudeerd die van grote invloed zijn op de achteruitgang van de hartfunctie na een hartinfarct: 1. **ischemie/reperfusie (I/R) schade van het hart** en 2. **averechts remodelleren van de hartkamer.**

Ischemie/reperfusie schade is de celdood die ontstaat ten gevolge van het herstel van de bloedstroom (=reperfusie) in het gebied dat door een vernauwing of afsluiting van een slagader niet van voldoende zuurstof (**=ischemie**) werd voorzien. Dit is een nogal tegenstrijdig proces: het herstel van de bloedstroom is juist bedoeld om celdood te beperken. Het openen van een afgesloten vat is een voorwaarde voor het bevorderen van de levensvatbaarheid van bedreigd weefsel. De verantwoordelijke processen voor reperfusie schade verschillen sterk van de processen die celdood geven ten tijde van ischemie. Hierdoor kunnen therapieën ontwikkelt worden die reperfusie schade voorkomen. Experimenteel onderzoek heeft aangetoond dat schade ten gevolge van reperfusie voorkomen kan worden, zodat er min of meer alleen schade overblijft ten gevolge van ischemie. In **Deel I** van dit proefschrift beschrijven we het gebruik van ontstekingsprocessen en intracellulaire signaalwegen in hartspiercellen als aangrijpingspunten om de levensvatbaarheid van de hartspier te bevorderen. In **Deel II** maken we gebruik van aangrijpingspunten in ons immuunsysteem die bepalend zijn voor het herstel na een hartinfarct. De reparatieprocessen in het hart, ook wel remodelleren genoemd, worden gekenmerkt door ontstekingsreacties, gevolgd door weefselafbraak en opbouw. Uiteindelijk wordt er een stevig litteken gevormd in het afgestorven gebied en nemen de naburige gebieden een deel van de verloren functie over. Het remodelleren kan dusdanig geschieden dat de noodzakelijke ontstekingsreacties kwaadaardig worden en dus meer schade richten dan dat ze herstellen. Dit proces van kwaadaardige immuunreacties, die tot vergroting van de hartkamers leidt en uiteindelijk resulteert in hartfalen, wordt **averechts remodelleren** genoemd.

In **Hoofdstuk 1** zijn er een aantal basisprincipes geïntroduceerd van reparatie processen in het hart na een infarct, die gereguleerd worden door het aangeboren immuun systeem. Recent experimenteel onderzoek heeft tot nieuwe inzichten geleid omtrent het ontstaan van schadelijke immuunreacties na een hartinfarct. Een grote verandering in het wetenschappelijk denken over dit onderwerp was de introductie van het zogenaamde “danger model” (“gevaren model”) door Polly Matzinger. Het “gevaren model” is deels een theoretisch kader waarin men de immuunreacties na een hartinfarct kan begrijpen en verklaren. Daarnaast kan het dienen als een hypothese (i.e. ideeën) vergaarbak om nieuwe inzichten te toetsen. In het kort, beschrijft het “gevaren model” dat elk molecuul dat geassocieerd is met celdood of weefselafbraak kan dienen als een *gevaren signaal* (“**d**anger **a**ssociated **m**olecular **p**atterns; DAMPs). Deze gevaren signalen (i.e. DAMPs) kunnen een immuunreactie teweeg kan brengen, zonder dat daar een bacterie of virus bij betrokken is. DAMPs kunnen zogenaamde pathogeen herkennende receptoren (pathogen recognition receptors; PRRs) activeren. Deze PRRs bevinden zich op witte bloedcellen, zodat deze cellen infecties veroorzaakt door pathogenen (e.g. bacteriën, virussen) kunnen bestrijden. Maar wat maakt een DAMP tot een DAMP? Hoe activeren DAMPs de receptoren (i.e. PRRs) die eigenlijk

bedoeld zijn om bacteriën op te ruimen en infecties te bestrijden? Zijn PRRs eigenlijk wel bedoeld om bacteriën te bestrijden? Deze, en nog andere vragen blijven nog altijd een raadsel. Desondanks heeft het "gevaren model" wel de wetenschappelijke gemeenschap geprikkeld om naar moleculen te zoeken die vrijkomen na een hartinfarct en een immuunreactie ontketenen. Vanuit een "gevaren model" perspectief, kan men kwaadaardige immuunreacties temperen door de interactie DAMP-PRR te voorkomen of door de mate van DAMP productie c.q. afgifte te verminderen na hartschade. In dit proefschrift hebben we het "gevaren model" als een theoretisch kader gebruikt om moleculaire en fysiologische gevolgen te bestuderen van interventies die de het herstel na een hartinfarct positief dan wel negatief beïnvloedden. De conclusies van de dierexperimenten staan beschreven in Tabel 1.

Tabel 1. Conclusies van het proefschrift

Conclusies	Hoofdstuk
Elk molecuul dat vrijkomt na weefschade is een potentieel gevaren signaal	1
TLR2 op bloedcellen bepaald TLR2-gemedieerde I/R schade	2
Remmen van TLR2 verkleint de infarctgrootte en verbetert de hartfunctie na I/R schade	2 & 3
Exosomen zijn de actieve componenten in de secretie van mesenchymale stamcellen die het hart beschermen tegen ischemische schade	4 - 7
Mesenchymale stamcellen van embryonale en foetale origine scheiden vergelijkbare exosomen uit	5
Onsterfelijke mesenchymale stamcellen kunnen belemmeringen ten aanzien van productie en schaalvergroting van exosomen uit de weg helpen	6
Het beschermend effect van exosomen wordt bepaald door de directe interactie van exosomen met hartcellen	7
Exosomen dienen intact te zijn voor een beschermend effect	7
Exosomen reduceren infarct-gerelateerde ontsteking	7
TLR2 op bloedcellen bepaald TLR2-gemedieerde averechts remodelleren	8
Het ontbreken van TLR2 op bloedcellen verbetert de hartfunctie na een infarct	8
Fibronectin-EDA activeert bloedcellen en resulteert vervolgens in het averechts remodelleren van het hart na een infarct	9
Haptoglobine is cruciaal voor het wegvangen van oxidatieve stress in het geïnfarceerde hart	10
Haptoglobine is betrokken bij de vasculaire permeabiliteit van nieuwgevormde vaten en litteken vorming na een hartinfarct	10

DEEL I

In **Hoofdstuk 2** beschrijven we het gebruik van Toll-like receptor (TLR)-2, een bekende PRR, als aangrijpingspunt voor de behandeling om infarctgrootte te verminderen in muizen. De meest interessante bevinding van de studie was de ontdekking dat TLR2 op bloedcellen verantwoordelijk was voor de TLR2-gemedieerde I/R schade van het hart. Door een antistof tegen TLR2 in de bloedbaan te spuiten hebben we de infarctgrootte met 45% weten te beperken. We hebben gezien dat middels deze behandeling de hartfunctie aanzienlijk verbeterde door een afname van de kwaadaardige ontstekingsreacties in het hart. We hebben hierna de TLR2 antistof in een groot proefdiermodel getest, om een betere vertaalslag te kunnen maken naar de mens. In **Hoofdstuk 3** laten we in varkens zien dat

een eenmalige intraveneuze toediening van de antistof tot een significante vermindering van hartschade leidt. De behandeling resulteert in een verbeterde pompfunctie na I/R schade. Deze studies laten zien dat een antistof behandeling tegen TLR2 een optie kan zijn in de toekomst voor patiënten die een hartinfarct doormaken.

In de bovengenoemde studies hebben we de interactie tussen DAMPs en PRRs voorkomen door TLR2 te blokkeren middels een antistof. De levensvatbaarheid en functie van het hart kan ook bevorderd worden door bepaalde signaalwegen in hartspiercellen te activeren dan wel te remmen. Eerdere studies hebben aangetoond dat stamcel secretie de levensvatbaarheid van hartspiercellen bevorderd, de infarctgrootte verminderd en de hartfunctie verbeterd. Dit fenomeen wordt ook wel het “paracriene effect” van stamcellen genoemd: het zijn niet de stamcellen zelf die het werk doen, maar hetgeen wat ze uitscheiden is verantwoordelijk voor het beschermend effect. In **Hoofdstuk 4** beschrijven we minuscule deeltjes, zogenaamde exosomen, die verantwoordelijk zijn voor de beschermende effecten van mesenchymale stamcel (MSC) secretie. We tonen aan dat een eenmalige intraveneuze toediening van exosomen verkregen uit embryonale (**Hoofdstuk 4**), foetale (**Hoofdstuk 5**) en onsterfelijke MSC bronnen (**Hoofdstuk 6**), hartschade vermindert. In **Hoofdstuk 7** laten we zien dat de hartfunctie aanzienlijk verbetert door de activatie van zogenaamde “survival”-signaalwegen en de remming van “celdood”-signaalwegen in hartcellen. Daarnaast demonstreren we dat exosomen een direct effect hebben op hartcellen om de schade te beperken, in tegenstelling tot de TLR2 antistof behandeling die de schade beperkt via de remming van bloedcellen. Niet geheel onverwacht, zien we dat de ontstekingsreactie ook minder is in muizen die behandeld zijn met exosomen. Deze bevinding steunt de opvatting dat de mate van weefselschade, en dus de mate van DAMP afgifte, de ernst van de ontstekingsreactie bepaald (**Hoofdstuk 7**).

DEEL II

Het is reeds bekend dat de infarctgrootte een van de belangrijkste bepalende factoren is voor de hartfunctie en overleving na een hartinfarct. Het proces van remodelleren in het hart na een infarct kan ook verregaande gevolgen hebben op de functie en overleving. Versterkte ontstekingsreacties en matige littekenvorming kan resulteren in vergroting van de hartkamers en verminderde functie. In het tweede gedeelte van dit proefschrift hebben we ons gericht op aangrijpingspunten die een bepalende rol spelen in averechts remodelleren van het hart na een infarct.
Allereerst late we zien dat wederom in de afwezigheid van TLR2 op bloedcellen averechts remodelleren wordt voorkomen en hartfalen wordt beperkt in muizen na een hartinfarct (**Hoofdstuk 8**). In deze studie hebben we de interactie tussen DAMP en PRR voorkomen door TLR2 (een PRR) uit te schakelen op bloedcellen. Hierdoor kan het immuunsysteem niet geactiveerd raken door bepaalde DAMPs die vrijkomen na een hartinfarct. Men zou dus ook hetzelfde effect kunnen bereiken door een DAMP uit te schakelen zodat deze geen PRR kan activeren. In **Hoofdstuk 9** hebben we de rol van fibronectin-EDA bestudeerd in het remodelleren van het hart na een infarct. Fibronectin-EDA komt vrij na weefselschade en -afbraak en stuurt ontstekingsreacties aan via de activatie van (witte) bloedcellen. We laten zien dat muizen die geen fibronectin-EDA kunnen aanmaken een betere hartfunctie en overleving hebben na een infarct vergeleken met muizen die wel fibronectin-EDA aanmaken. Beide studies (**Hoofdstuk 8** & **9**) demonstreren de cruciale rol van DAMP-PRR interactie in ontstekingsreacties gedurende de

reparatieprocessen na een hartinfarct. In **Hoofdstuk 10** benaderen we het “gevaren model” van de andere kant: in plaats van het zoeken naar manieren om de hartfunctie en overleving te verbeteren, hebben we getracht deze te verslechteren door de DAMP-PRR interactie te versterken. Haptoglobine is een eiwit wat vrij komt bij weefselschade en ervoor zorgt dat bepaalde schadelijke stoffen weggevangen worden, zoals moleculen die oxidatieve stress veroorzaken. We laten zien dat door het verhogen van oxidatieve stress bij muizen die geen haptoglobine kunnen aanmaken er een keten van negatieve uitkomsten teweeg wordt gebracht. Muizen zonder haptoglobine hebben te maken met bloedingen en scheuren in de hartspierwand, verhoogde toestroom van ontstekingscellen en verslechterde littekenvorming. Hierdoor hebben muizen zonder haptoglobine een zeer matige hartfunctie en een lagere overlevingskans na een infarct in vergelijking met muizen die wel haptoglobine kunnen aanmaken.

We mogen concluderen dat het “gevaren model” een nuttig theoretisch kader is om immuunreacties en reparatieprocessen na een hartinfarct te begrijpen en te verkennen. Toekomstige studies zullen moeten uitwijzen of TLR2 antistof behandeling ook daadwerkelijk effectief zal zijn in de mens. Daarnaast zal uitgezocht moeten worden of behandeling met exosomen ook in een groot proefdiermodel werkt, alvorens de exosomen te testen in de mens. Tot slot dient de rol van fibronectin-EDA in de immuunreacties na een hartinfarct verder uitgezocht te worden om zodoende het werkingsmechanisme te begrijpen.

CHAPTER 14

Özet

Günümüzde daha fazla hasta, farmakolojik gelişmeler (örn. antitrombotikler) ve teknolojik atılımlar (örn. stent teknolojisi) sayesinde, miyokart enfarktüsün (kalp krizinin) başlangıcından sağ olarak çıkıyor. Ne yazık ki, kurtulan hastalarda kalp fonksiyon giderek kötüleşiyor ve sonuçta kalp yetmezliği ve diğer kalp krizi-ilişkili hastalıklar yükseliyor. Bu yüzden kriz sonrası zararı azaltan ve/veya kalp krizi ile ilgili gelişen komplikasyonların oluşumunu engelleyen yeni birleşik tedaviler geliştirilmesi gerekmektedir. Bu tezde, miyokart enfarktüs sonrasında kalp fonksiyonunun gittikçe kötüleşmesine yol açan iki büyük belirleyici etken üzerinde çalıştık: 1. **miyokardial iskemi/reperfüzyon (İ/R) hasarı ve** 2. **kalbin tersine yeniden biçimlenmesi**.

Miyokardiyal İ/R hasarı, iskemi sonrası ek hasara yol açan birbirinden farklı hücre içi mekanizmaların ve bir o kadar da hücre dışı aracıların dahil olduğu karmaşık bir işlemdir. İskemi sırasında, yani dokuda kan dolaşımı yetersiz olduğu anda, hücre ölümünden sorumlu olan aracılar reperfüzyon (kan dolaşımının tekrardan sağlanması) evresindekilerden farklıdır. Reperfüzyonun yol açtığı bazı moleküler değişimler klinik ve deneysel çalışmalarda tedaviye yönelik hedef alınsa da başarı çok azdır. Bu tezin 1. **bölümünde**, İ/R hasarı sonrası miyokardiyal, yani kalp kası, canlılığın geliştirilmesi amacıyla kardiyomiyositlerdeki sinyal yolları ve reperfüzyon uyarımı sonucu oluşan karakteristik moleküler değişimleri araştırdık. **İkinci Bölümde**, enfarktüse karşılık gelişen tamir mekanizmaları için son derece kritik olan, kalıtımsal (doğal) bağışıklık sistemindeki belirli hedefleri ele aldık. Kalp krizindeki birbirini izleyen, yeniden biçimlenme olarak adlandırılan, süreçler enflamasyon (yani iltihaplanma), doku dönüşümü ve arkasından yara oluşumu ve olgunlaşmasıyla tanımlanır. Yeniden biçimlenme süreci enfarktüs sonrası kalp fonksiyonların korunmasıyla sonuçlanabilir. Ancak, başlangıçtaki bağışıklık tepkisi büyük ve tahrip edici olduğunda, kalp genişleyebilir ve işlev kötüleşir. Kalpteki bu yeniden yapılaşma süreci enfarktüs sonrasında kalp yetmezliğiyle sonuçlanabilir

Birinci başlıkta, kalıtımsal bağışıklık sistemi tarafından aracılık edilen bazı iskemi-sonrası tamir cevabının temel ilkelerini sunduk. Güncel temel bilimsel araştırmalar kalp krizi sonrasındaki yıkıcı bağışıklık cevabının patolojik mekanizmalarının iç yüzünü anlamamızda heyecan verici bilgiler sağladı. Bilimsel düşüncedeki radikal değişimlerden biri, ilk olarak Polly Matzinger tarafından tanımlanan 'tehlike modeli' hipotezi oldu. Bu hipotez bize, hasar sonrasında kalıtımsal bağışıklığın etkinleşmesini anlamak ve açıklamak için teorik bir taslak sağladı. Kısaca açıklamak gerekirse, hücre ölümü ve doku yıkımı ile ilgili olan moleküller (İngilizce: danger associated molecular patterns; **DAMPs**) patojenler olmadan da bağışıklık sistemini tetikleyebilir. DAMPs patojen tanıma reseptörleri (İngilizce: pathogen recognition receptors; **PRRs**) olarak bilinen reseptörleri uyarabilir, ki bu reseptörler geleneksel olarak mikrop ve virüslerin temizlenmesi için ak yuvarlar tarafından kullanılır. Ancak, bir DAMP ne olarak tanımlanabilir? Ve patojenlere karşı oluşturulmuş bir reseptörü nasıl etkinleştirebilir? PRR'ler sadece patojenlere karşı mı oluşturulmuştur? Bu soruların hala cevaplandırılmayı beklediği gerçeğine karşın, 'tehlike modeli' hasar sonrası üretimleri artan ve etkin hale gelen DAMP'ların bilimsel camia tarafından araştırılmasını tetiklemiştir. 'Tehlike modeli' bakış açısına göre, DAMP-PRR etkileşiminin engellenmesi ya da kalbin hasar sonrasında DAMP salgılanmasının azaltılması, yıkıcı bağışıklık cevabının baskılanmasını sağlayabilir. Bu tezde, hayvan miyokardiyal enfarktüs modellerinde DAMP-PRR ilişkilerini etkileyen müdahalelerin moleküler ve fizyolojik sonuçlarını çalışmak için 'tehlike modelini' teorik bir çerçeve olarak kullandık. Çalışmaların sonuçları Tablo 1 de açıklanmıştır.

Tablo 1. Tezin sonuçları

Sonuçlar	Başlık
Doku hasarından sonra serbestleşen bütün moleküller potansiyel bir tehlike sinyalidir.	1
Dolaşımdaki TLR2, TLR2 tarafından tetiklenen İ/R hasarına aracılık eder.	2
İ/R hasarı sonrası TLR2 baskılanması enfarktüs büyüklüğünü azaltır ve kalp performansını arttırır	2 & 3
Ekzozomlar MSC salgılarındaki parakrin etkiyi yapan aracılardır	4 - 7
Fetal ve embriyonik dokulardan kaynaklanan MSC'ler benzer kalp koruyucu ekzozomlar salgılar.	5
MSC'lerin ölümsüzleştirilmesiyle ekzozomların üretimi ve ölçeklendirilmesi engeli aşılabilir.	6
Ekzozomlar kalp hücrelerle direk etkileşime girerek hasarı azaltırlar.	7
Sağlam ekzozomlar İ/R hasarından sonra enfarkt büyüklüğünü düşürmede önkoşuldur.	7
Ekzozom tedavisi enfarktüse bağlı enflammasyonu düşürür	7
Dolaşımdaki TLR2, TLR2 tarafından indüklenen tersine yeniden biçimlenmeye aracılık eder.	8
Dolaşımdaki hücrelerde TLR2 eksikliği enfarktüs sonrasında kalp fonksiyonun ve geometrinin iyileşmesine sebep olur	8
Fibronectin-EDA enfarktüs sonrasında dolaşım hücrelerini etkinleştirir ve sonrasında tersine yeniden biçimlenmeye aracılık eder.	9
Haptoglobin enfarktüs bölgesinde oksidatif stresin ortadan kaldırılmasında kritik öneme sahiptir.	10
Haptoglobin enfarktüs sonrasında yara ve yeni oluşan damarların olgunlaşmasına aracılık eder.	10

BÖLÜM I

İkinci başlıkta, iyi bilinen bir PRR olan *Toll-like receptor*-2 (TLR2) enfarktüs büyüklüğünü düşürecek bir tedavi hedefi olarak kullanımını açıkladık. Çalışmanın en ilginç bulgusu, TLR2 bağımlı miyokardiyal İ/R hasarının, hücre yüzeylerinde TLR2 bulunan kemik iliği kaynaklı hücreler tarafından aracılık edilmesidir. Bu sayede, anti-TLR2 antikorunu sistemik olarak başarıyla uyguladık. Çalışmada gösterildiği gibi, miyokardiyal hasar %45 azaldı ve enflamasyonun azalışına bağlı olarak kalp fonksiyonunda ilerleme kaydedildi. TLR2 baskılanmasının tedaviye yönelik etkileri klinik öncesi çalışmaların kliniğe taşınmasında kritik bir basamak olan domuzlarda da denedik. **Üçüncü başlıkta**, domuzlarda insan için hazırlanan anti-TLR2 antikorunun reperfüzyondan hemen önce damar içi enjekte edilmesinin enfarktüs alanını önemli derecede azalttığını ve enfarktüs bölgesindeki kalbin performansını arttırdığını gösterdik. Bu verilerin hepsi birlikte, TLR2 baskılanmasının kalp krizi geçiren hastalarda potansiyel ek tedavi adayı olduğunu göstermektedir.

Yukarıda bahsedilen çalışmalarda, miyokardiyal İ/R hasarında DAMP ve PRR arasındaki zararlı etkileşimleri önlemeye çalıştık. Kalp kasının canlılığı ve fonksiyonu arttırılması, kardiyomyositlerde sağ kalım sinyal mekanizmalarının etkinleştirilmesi ve/veya pro-apoptotik sinyallerin baskılanmasıyla da başarılabilir. Diğer araştırmacılar tarafından gösterildiği gibi, kök hücre salgıları kardiyomiyositlerde canlılığı arttırıyor, enfarktüs büyüklüğünü azaltıyor ve kalp performansını geliştirir. Bu fenomen kök hücrelerin 'parakrin etkisi' olarak bilinir. **Dördüncü başlıkta**, mezenşimal kök hücrelerin (MSC) tedavi edici etkilerine aracılık eden ve ekzozom olarak adlandırılan mikro parçacıkların saflaştırılmasını tarif ettik. Embriyonik kaynaklı (**Başlık 4**), fetal (**Başlık 5**) ya da ölümsüzleştirilen kaynaklardan (**Başlık 6**) elde edilen ekzozomların tek bir dozu damar içine verildiğinde, apoptotik sinyallerin baskılanması ve sağkalım yollarının aktive olmasıyla enfarktüs büyüklüğünün azaldığını ve kardiyak performansının arttığını gösterdik. Bunlara ek

olarak, anti-TLR2 tedavisinin tersine (etkisi kan hücreleri üzerinedir) ekzozomlar kalp hücreleri üzerinde direk tedavi edici etki gösteriyorlar. Bağışıklık cevabı ekzozom uygulanan hayvanlarda azalıyor, bu da doku hasarının artması ve DAMP salınımının bağışıklık cevabının şiddetini belirlediğine dair görüşü destekler niteliktedir (**Başlık 7**).

BÖLÜM II

Enfarktüs alanı büyüklüğünün, kalp fonksiyonu ve klinik sonuçlarla çok güçlü olarak ilişkili olduğu oldukça iyi belgelenmiştir. Ek olarak, hem enfarktüs alanı hem de canlı dokunun enfarktüs sonrası tamiri, kalbin fonksiyon ve klinik sonuçları üzerine derin etkileri olabilir. Şiddetli enflamasyon, optimum düzeyin altında kalan yara olgunlaşması, *tersine yeniden biçimlenme* olarak belirtilen kalp genişlemesi ve performans düşmesi ile sonuçlanabilir.

TLR2 baskılanması sonrası enfarktüs büyüklüğünde azalışla paralel olarak, kemik iliği kaynaklı hücrelerde TLR2 eksikliğinin uzun dönemde yararlı olduğunu gösterdik. Eşit enfarktüs büyüklüğüne karşın, dolaşımdaki hücrelerde TLR2 eksikliği olan fareler (fonksiyonel TLR2'ye sahip farelerle karşılaştırıldı) enfarktüs sonrasında daha iyi kalp fonksiyonu ve korunmuş kalp geometrisine sahiptirler (**Başlık 8**). Bu çalışmada, DAMP düzeyinde engelleme de aynı etkiyi gösterirken, DAMP-PRR etkileşimini hedef reseptör bölgesinde (TLR2) baskıladık. **Dokuzuncu başlıkta**, fibronectin-EDA'nın enfarktüs sonrası yeniden biçimlenmedeki rolünü araştırdık. Fibronectin-EDA doku hasarından sonra üretimi artıyor ve lökosit (akyuvarlar) aktivasyonu üzerinden enflamasyona yol açıyor. Normal farelerle karşılaştırıldığında, enfarktüs sonrasında fibronectin-EDA eksikliğinin yüksek kalp performansıyla ilişkili olduğunu gösterdik. Her iki çalışmada (**Başlık 8 & 9**) enfarktüsten sonra kalbin tamiri sırasında DAMP-PRR etkileşiminin ne kadar önemli bir rolü olduğunu gösteriyor. Son çalışmada, "tehlike modeline" farklı bir açıdan yaklaştık. Kalbin fonksiyon ve tamir mekanizmalarının iyileştirilmesinde kullanımı yerine, kalbin tamir mekanizmalarını bozmaya ve sonucunda performansı kötüleştirmeye çalıştık. **Onuncu başlıkta**, kalpte oksidatif stresi artırarak DAMP yükünü arttırdık. Bir anti-oksidan protein olan haptoglobin geninin eksik olduğu farelerde, oksidatif stresin artışı kalp kasının içinde kanamalara, kalp duvarının yırtılmasına, artmış lökosit göçüne, hatalı yara oluşumu ve olgunlaşması gibi bir dizi yıkıcı olaya neden olduğunu gösterdik. Bunlara bağlı olarak, normal farelerle kıyaslandığında haptoglobinin olmadığı farelerde düşük kalp performans ve yüksek ölüm oranı görülmektedir.

Sonuç olarak, "tehlike modeli" kalp krizi sonrasında bağışıklık cevabı ve tamir mekanizmalarını keşfetmek için uygun bir teorik kalıptır. Şu ana kadar yaptığımız çalışmalar göstermektedir ki, TLR2 baskılanması ve ekzozom tedavisi kalp krizi geçiren hastalarda kalbin tamir ve fonksiyon mekanizmalarının iyileştirilmesi için potansiyel ek tedavi edici adaylardır. Bir sonraki adımda, ekzozom tedavisinin yararlılığının büyük hayvanlarda teyit edilmesi ve fibronectin-EDA'nın enfarktüs ilişkili enflamasyonda rolünün daha ileri düzeyde açıklanması için başka çalışmaların yapılması gerekmektedir.

CHAPTER 15

Waarschijnlijk is het schrijven van een dankwoord een van de lastigste (stiekem ook de leukste) taken voor een promovendus. Manuscripten zijn technisch en zakelijk, en op persoonlijk vlak kan er eigenlijk niet veel mis gaan (zelfs de grootste rivalen kunnen coauteur van elkaar zijn). Maar in een dankwoord moet je toch wel even opletten dat je mensen niet tekort doet. Of erger, vergeet! Negatieve emoties die vrij komen wanneer de een meer regels aan dankwoord krijgt dan de ander, of wie er als eerste vermeld wordt. We zijn maar simpele wezens, van vlees en bloed, van altruïstisch tot hoogmoed. Mensen zijn menselijk, gelukkig maar. Vandaar dat ik ervoor gekozen heb om mijn dankwoord chronologisch te verwoorden: van de eerste persoon die mij in de wereld die "Wetenschap en Onderzoek" heet heeft geduwd, tot aan mijn liefste die mij tot het laatste moment van dit proefschrift heeft gesteund. En iedereen daartussen die ook maar 1 letter heeft bijgedragen bij de totstandkoming van dit proefschrift, ontzettend bedankt!

Prof. dr. M.A. Vos, beste **Marc**, je vroeg ooit als tutor in jaar 3 van mijn studie Geneeskunde: "Fatih, hoe ga jij je onderscheiden tussen al die 250 studenten?", waarop ik antwoordde,"door hoge cijfers te halen." Jij gaf aan dat er nog steeds 100 studenten overbleven. Onderzoek! Dat was waarin je mij graag wilde zien. Ik hoop dat dit proefschrift enigszins een antwoord op je vraag is. Dank voor het wegwijs maken en de stimulerende woorden!

Prof. dr. P.A.F.M. Doevendans, beste **Pieter**, uit de kamer van prof. Vos naar jouw kamer gehold om te vragen of je mijn begeleider wilde zijn voor mijn onderzoek aan de Gazi University te Ankara. Eenmaal terug met 2 artikelen, vroeg je wat het werkingsmechanisme was achter het probleem van een van de artikelen ("reduced myocardial blush grade" na een hartinfarct). Na wat literatuur onderzoek stuitte ik op de fenomenen ischemie/reperfusie schade en no-reflow. Dat was het begin van mijn huidige interesse in de moleculaire biologie achter (patho)fysiologische fenomenen van het hart. Het volgende wat je zei was: "schrijf maar een onderzoeksvoorstel en daarna het lab in, hier beneden om de hoek." Ik wil je bedanken voor de manier waarop je mij hebt weten te prikkelen, met kritische vragen en uitdagende uitspraken. Je hebt een eigen stijl, die niet berust op handje vasthouden, maar meer een die de weg wijst en bij uiterste noodzaak bijstuurt. Jij was er altijd, bij die eerste (ontgroenings)momenten: mijn eerste orale voordrachten als student op de NVVC, daarna de ESC. Ik waardeer je eerlijkheid en openheid. Je misgunt geen succes, integendeel je stimuleert. Ik hoop dat je dat altijd zal blijven doen en kijk uit naar ons volgende etentje.

Prof. dr. G. Pasterkamp, beste **Gerard**, ik kan mijn glimlach niet verbergen tijdens mijn dankwoord gericht aan jou. Ik herinner me nog dat ik per ongeluk jouw kamer binnenliep en jij me aankeek met een blik van: "wat moet die jongen hier met dat ingewikkeld moleculair-biologisch verhaal." Vanaf dat moment heb ik je zowel op professioneel en persoonlijk vlak mogen leren kennen. Het met "U" aangesproken worden heb je er met veel moeite eruit gekregen bij mij. Ik heb ontzettend veel van je geleerd en leer nog steeds van je. Ondanks dat je je eigen inbreng bagatelliseert, heb je ontzettend veel bijgedragen aan de opzet en uitvoering van de experimenten. Daarnaast zijn je kritische revisies van wezenlijk belang geweest voor de duidelijkheid van en de klinische twist aan de manuscripten. Ik ben vooral dankbaar voor de vrijheid de je me hebt gegund om de dingen te doen die ik leuk vond, zonder dat je me wilde vastpinnen aan voorgeschreven projecten. Ook op persoonlijk vlak heb ik veel van je geleerd; je benadering ten opzichte van dilemma's (onze gesprekken in de taxi van en naar contractresearch vergaderingen) en mensen (wetenschappelijk belang vs. industrie belang), of zoals

hoe je met bepaalde zaken in een huwelijk omgaat ;). Ik heb veel bewondering voor je; je bevlogenheid en inzet voor de Athero-Express, de manier waarop je de tijd managet, hoe je de groep leidt, maar vooral je eerlijkheid en integriteit. Ik hoop de komende jaren nog veel met je te kunnen samenwerken en zie de toekomst positief en met veel plezier tegemoet.

Prof. dr. D.P.V. de Kleijn, beste **Dominique**, ook bij jou krijg ik flashbacks van plezierige en grappige momenten. Door Gerard bij jou gestationeerd om op moleculair niveau een sparringpartner te hebben. Ik realiseer me dat ik geen makkelijke promovendus voor je was. Ik ben eigenwijs en weet maar al te graag wat en hoe ik dingen wil. Desondanks, heb je op een hele plezierige manier tijdens werkbesprekingen mij op nieuwe gedachten weten te brengen of zaken verder te helpen verhelderen. Dat is een kwaliteit waar ik veel bewondering voor heb en hoop dat ik me dat eigen kan maken. Bedankt dat ik altijd onaangekondigd bij je binnen kon lopen. Je kennis op moleculair-biologisch vlak hebben mij de verdieping gegeven waarnaar ik zocht. Je bent groepsleider en professor, maar je bent niet vies om je mouwen op te stropen en zelf aan de slag te gaan in het lab. Zoals toen met de kinetiek experimenten voor de TLR2 studie in varkens. In de groene OK pakken, op klompen, dag in en dag uit in die stinkende stallen bloed afnemen. Zij aan zij. Ook jij misgunt succes niet, maar stimuleert tot meer. Je hebt een hartverwarmende persoonlijkheid, die de 'ander' met open armen ontvangt en niet veroordeelt op basis van uiterlijk, achtergrond of wat dan ook. Het gaat je om de mens inside en zijn/haar kwaliteiten. Daarnaast hebben we eigenlijk vooral veel plezier met elkaar beleefd; Singapore (sleepy sleepy boulevard, Chilli Crab on the beach), congressen en bij jou thuis (Fatma heeft het nog steeds over de bbq!). Ik prijs me gelukkig met jou als promotor en ben ervan overtuigd dat de toekomst nog veel leuke en succesvolle momenten zal brengen.

Mw. I. Houwelingen, beste **Ineke**, *Moeders*, ik geloof dat er maar weinig stafsecretarissen zijn die de passie en betrokkenheid tonen zoals jij die hebt voor het lab. Ik heb altijd je inzet gewaardeerd om allerlei zaken op een juiste manier af te handelen. Door je enorme verantwoordelijkheidsgevoel weet jij ons lab financieel te monitoren en excessen direct aan te pakken. Niet onbelangrijk voor een organisatie waarvan de levensvatbaarheid vooral van financiën afhangt. Ik heb genoten van onze gesprekken omtrent de films van de Coen brothers of van Robert Downey Jr. Je optredens in je koor, met name de smartlappen waren hilarisch en geweldig om te zien. Ik kijk nog altijd uit naar het volgende diner, waarbij je weer alles uit de kast haalt om overheerlijk te koken. Op sommige dagen konden we maar beter uit je buurt blijven, want dan was er weer eens iemand die je even moest aanpakken in het belang van het lab. Maar veelal kon ik bij je binnenlopen, voor de gezelligheid een praatje maken. Ook van jou heb ik veel geleerd, of beter gezegd je hebt me redelijk goed weten op te voeden. Mijn bonnetjes kan ik nu beter bewaren en laat ik niet alles rondslingeren. Behalve mijn sleutels…tja. Je bent een sterke vrouw met karakter, met wie ik hoop zo lang mogelijk mee samen te werken in mijn carrière. Tot snel!

Mw. M. de Rooij, beste **Marjolein**, *Mar*, ik zal je lachende groet in de vroege ochtend missen. Meestal voor 8 uur nog, wanneer je onze AIO-kamer binnenliep en vroeg: "Heb je al koffie gezet, of moet ik het weer doen?". Stiekem wachtte ik totdat jij de koffie ging zetten, want ik vond het leuk om je lachend onze kamer binnen te zien lopen en even bij te praten. Je bent een druk baasje, die ook nog eens haar eigen onderneming probeert op te zetten. Ik heb ontzettend veel bewondering voor je energie en doorzettingsvermogen, want het is niet makkelijk om secretarieel werk (lab én CTMM!) te combineren

met het opzetten van een eigen bedrijf. Je blijft altijd lachen, ook al zit het even niet mee. Ik hoop dat je ondernemerschap snel tot successen zal leiden, die je van harte zijn gegund. Als lab waarderen we enorm je inzet en vrolijkheid. Ook jij hebt veel bijgedragen aan mijn opvoeding. Als het mijn sleutels niet waren, dan was het wel een afspraak die ik vergeten was. We hebben veel gelachen, met elkaar en om elkaar. Ik hoop je zo lang mogelijk mee te maken in het lab, en kijk uit naar je volgende kop koffie!

Dr. M.B. Smeets, beste **Mirjam**, jij bent de belangrijkste factor geweest in de snelheid waarmee de experimenten werden afgerond. Je in vitro vaardigheden zijn van ongekende waarde geweest voor dit proefschrift. In elk opzicht was onze samenwerking een groot succes en zal de komende tijd nog zijn. Qua werkmentaliteit lijken we veel op elkaar, waardoor de samenwerking des te plezieriger verloopt. We hebben veel frustraties gedeeld, met name het haptoglobine stuk. Desondanks laat je je niet gek maken en ga je door tot dat ene succesvolle moment, en het resultaat mag er zijn! Er breekt een nieuwe fase aan in onze samenwerking, waarin we het EDA-project een niveau hoger zullen tillen. Je bent onlangs moeder geworden van je derde kind en wens ook hierin jou veel geluk en plezier toe. Ik hoop nog lang met je te kunnen samenwerken. Ontzettend bedankt en tot onze volgende werkbespreking!

Beste **Imo**, mijn voorliefde voor de Duitse taal is niet het enige waarom ik je enorm waardeer als collega en vriend. Je eerlijkheid, je gevoel voor humor en interesse in auto's, voetbal en alle andere mooie dingen maken dat ik je een geweldige collega en persoon vind. Je wetenschappelijke input en kritische blik zijn van groot belang geweest voor mijn experimenten (e.g. TLR2 chimeren weddenschap). Daarnaast hoop ik dat we ooit die eerste prijs binnenhalen tijdens het UMCU voetbaltoernooi, altijd maar 2e of 3e is mooi geweest (bij de laatste kon je helaas niet bij zijn en zie daar het resultaat!). Ik kijk uit naar onze samenwerking in het lab en hoop dat we weer snel de BBQ kunnen aansteken.

Ing. B.J. van Middelaar, beste **Ben**, *Meester Ben*, ook aan jou heb ik veel te danken op het gebied van de microchirurgie. Ik weet nog heel goed toen ik als student het lab binnenkwam en het opereren moest leren. Wat ben jij een geweldige leermeester! Geduldig en accuraat! We hebben heel wat tijd doorgebracht in het GDL. Eenmaal de basisprincipes te hebben geleerd, was de volgende uitdaging het opzetten van een muis ischemie/reperfusie model. Wat een drama was dat in het begin. Na 4 maanden van tegenslag hebben we het roer omgegooid. Verfijnde operatie technieken, nieuwe anesthesie methode, nieuw apparatuur. Vanaf dat moment ging het alsmaar beter. Jouw inzet is van ongekende waarde geweest voor het model. Iedereen die nu I/R schade toepast in de muis hoort zich dat realiseren. Je bent er om 7:30 en gaat pas weg als het werk af is. Als promovendus kun je je geen betere biotechnicus wensen. Maar het allerbelangrijkste is je zachtaardigheid en je vriendelijkheid. Je bent een goede vriend in goede en slechte tijden. Een luisterend oor. We hebben zo veel lol gehad tijdens onze "Evans' blue & TTC sessies" en daarbuiten. Je humor was aanstekelijk; na 8 uur lang opereren kun je niet veel anders dan om jezelf lachen! Je hebt onlangs voor een carrière gekozen als basisschool docent. Een moedige keuze, omdat het niet makkelijk is om op latere leeftijd jezelf om te laten scholen. Dit bewijst andermaal je doorzettingsvermogen. Ik wens je heel veel sterkte en plezier toe. Ben, ontzettend bedankt voor je immense bijdrage aan dit proefschrift en je vriendschap!

Ing. A. Schoneveld, beste **Arjan**, *Koning*, ontzettend bedankt voor je bijdrage aan de experimenten.

Ondanks je strenge blik, ben je de vriendelijkheid zelve. Daarnaast vond ik onze discussies omtrent immunologische fenomenen zeer leerzaam, met name de Treg cel responsen (we moeten dat idee concreet gaan aanpakken!). Het feit dat een van je stukken een van de meest geciteerde studies zijn van ons lab bewijst je gevoel voor doelgericht experimenteren en vernieuwing. Bij dezen wil ik je nogmaals uitnodigen om te promoveren, al was het alleen voor het feestje ;). Met plezier kijk ik terug aan ons Singapore tripje, en wie weet kunnen we dat nog eens over doen. Bedankt en kijk uit naar onze volgende proef.

Ing. C. Strijder, beste **Chaylendra**, *Dushi*, bedankt voor het bijbrengen van methodes om mijn Excel-sheets te ordenen, mijn samples te nummeren en op te bergen. Daarnaast was je de eerste die mij leerde eiwit te isoleren, een ELISA te doen en een kleuring toe te passen op mijn allereerste studie samples. Bedankt voor je gezelligheid, de koffiepauze-momenten en de roti-tips. Heel veel succes met je nieuwe carrière en hoop je snel weer te zien!

Mijn bachelor- en masterstudenten **Gert-Jan**, **Wies**, **Judith**, **Lena** en **Lars**. Jullie inzet is onmiskenbaar geweest voor het eindresultaat. Al die coupes, eiwit en RNA samples bewerken en analyseren is werkelijk monnikenwerk. Maar ik heb jullie nooit horen klagen (waarschijnlijk wel tegen anderen). Ik hoop dat ik jullie enigszins heb kunnen enthousiasmeren voor onderzoek en wetenschap. Zo niet, we hebben in ieder geval ontzettend veel lol gehad. Sommigen van jullie zie ik zeker nog terug, anderen hopelijk tot ziens!

Mw. E. Velema, beste **Evelyn**, ontzettend bedankt voor je inzet om de experimenten dusdanig in te plannen dat ze toch in een kort tijdsbestek zijn afgerond. Met name in een periode waarin we wel 3 operaties per dag hadden en biotechnici zich figuurlijk in tweeën moesten delen om de proeven te doen. Je hebt ons, onderzoekers, altijd gestimuleerd om kritischer te zijn naar de uitvoerbaarheid van de experimenten. Bedankt voor het meedenken, je collegialiteit en energie die je in de projecten hebt gestoken. Tot de volgende planning en groot proefdieroverleg!

Dhr. C. Verlaan, beste **Cees**, *Opa*, ik ga je ontzettend missen! Je ervaring en kundigheid zijn van groot belang geweest voor het direct slagen van de proeven. Je was altijd in voor een grapje of een mop. Samen met Hans (Statler & Waldorf), was het elke ochtend weer lachen tijdens de ochtendkoffie sessies op het GDL. De hilarische momenten aan de operatietafel die we hebben gedeeld zodra we alleen waren zullen mij altijd bijblijven. Ook dat je een dag hebt meegevast tijdens de Ramadan vond ik hartstikke leuk om mee te maken. Ontzettend bedankt voor alles en wellicht tot ziens bij het volgende experiment, of aan wal ergens in het noorden van het land.

Mw. M. Emons, beste **Maringa**, bedankt voor je inzet tijdens de varkenexperimenten. Je betrokkenheid bij de proeven hebben er zeker bijgedragen dat de experimenten zorgvuldig werden uitgevoerd. Ook jij bent een doorzetter en wil graag jezelf verder ontwikkelen. De MRI experimenten in muizen had je snel genoeg in de vingers, waardoor je vrij snel zelfstandig inzetbaar werd. Daarnaast ben je een gezellige collega, waarmee ik graag in de toekomst mee samenwerk. Bedankt voor alles en tot snel!

Mw. M. Schurink, beste **Merel**, ook met jou was het heerlijk ontspannen werken. Je ervaring en vrolijke verschijning waren welkome eigenschappen tijdens de varkenexperimenten. Bedankt voor je collegialiteit

en gezelligheid, en we bestellen snel een broodje bij Tricolore!

Mw. J. Visser, beste **Joyce**, niets dan lof voor de kundigheid die je hebt ontwikkeld in een zeer kort tijdsbestek. Je was een gangmaker en een gezellige collega, waarmee ik graag samenwerkte. Veel geluk gewenst met je nieuwgeboren kind en het zoeken naar een groter huis. Bedankt en tot snel!

Mw. M. Jansen, beste **Marlijn**, je was to-the-point en heel netjes. Bedank dat je zelfs een paar varkens heb willen doen zonder dat ik erbij was. Veel succes in je nieuwe huis en zie je snel op OK of anders bij een borrel!

Collega's van het GDL; beste **Harry** en **Fred**, *geachte heren proefdierdeskundigen*, afgelopen 3 jaar heb ik met veel plezier met jullie mogen samenwerken. Jullie waren er altijd wanneer ik met een dilemma zat of een dringende vraag had. Met alle oprechtheid kan ik zeggen dat Utrecht boft met zulke proefdierdeskundigen. Jullie zijn niet alleen kritisch, maar reiken ook oplossingen aan wanneer het minder goed is. Jullie kritische blik draagt bij aan een betere opzet van de experimenten en tegelijkertijd bevordert die het welzijn van de dieren. Ontzettend bedankt voor jullie samenwerking en waarschijnlijk tot snel! **Hans**, ontzettend bedankt voor je tips en verhalen! Je bent altijd in voor een grapje, en kunt ook incasseren zoals toen met de pizzakoerier ;). Bedankt voor al die hilarische en gezellige momenten! **Jan**, Jantje, de grote vriendelijke reus. Bedankt voor het verzorgen van mijn muizen. Jouw betrokkenheid bij de zorg van de dieren is van groot belang geweest voor het welzijn van de muizen voor en na een experiment. Bedankt voor je collegialiteit en gezelligheid! **Hester**, **Jannie**, **Nico**, **Romy** (medewerker "*meegaandheidsoffice*"), **Anja**, **Helma**, **Jeroen**, **Tamara**, **Wendy**, **Toon**, **Jannico**, **Cees** en koffiemaatje **Peter**, allen bedankt voor de gezelligheid en collegialiteit. Jullie inzet voor de administratie en dierenverzorging heeft het mij stukken makkelijker gemaakt, maar vooral plezieriger!

Heel veel dank en waardering gaat uit naar mijn kamergenoten, mede promovendi en wetenschappers. Beste **Daphne**, inderdaad collega van het eerste uur, samen gestart en samen klaar. Bedankt voor je collegialiteit en de gezelligheid die je altijd en overal meebracht. Heel veel succes in de kliniek. Zoals Imo het al had verwoord, bij jou durf ik me zeker te laten behandelen mocht het ooit zover komen. **René**, altijd in voor een goede moleculair-biologische discussie, maar vooral een top vent met een vriendelijk en sociaal karakter. Altijd op zoek naar een promotiefilm-moment! Met jou erbij was het nooit saai. Bedankt voor alle kritische input, de gezellige momenten en de heerlijke koffie. Ik wens je veel succes met het afronden van je proefschrift en ben ervan overtuigd dat je het ver gaat schoppen in je nieuwe carrière! **Mihaela**, inmiddels volop aan de slag als patholoog in opleiding. Het was altijd lachen als jouw telefoon afging! Bedankt voor de gezellige momenten en heel veel succes in je carrière. **Marish**, met jouw komst waren de mannen weer in de meerderheid in onze kamer. Discussies gingen eindelijk weer vaker over mooie auto's en alles wat mannen nog meer interesseert, zoals voetbal ;). Succes met het afronden van je experimenten en klinische studie. Ik kijk uit naar onze samenwerking in de kliniek! **Ellen**, ik weet nog goed hoe jij je ambities uitsprak toen je in het lab begon. Hoge impact publicaties was een van je doelstellingen. Je talenten en doorzettingsvermogen heb je in ieder geval mee, en ik hoop van harte dat je erin slaagt om je ambities waar te maken. Bedankt voor de gezelligheid en heel veel succes met het afronden van je promotie! **Pleunie**, door jou komst waren we weer in de minderheid met de mannen, maar desondanks werd het er niet minder gezellig om. Heel veel succes met je promotie! **Sander vd L**, *sahbi!*, ik heb genoten van je enthousiasme en gedrevenheid, en hoop

dat de energie die je in je promotie steekt zich dubbel en dwars terugbetaalt. Ik kijk met plezier terug naar onze metafysische discussies, filmgesprekken en voetbalpraatjes. Veel succes met je promotie en tot snel! **Karlijn**, *Karlijneke*, je bent een aimabele collega waarmee ik niet alleen vakinhoudelijk leerzame gesprekken had, maar waarmee het ook heel erg gezellig was. Bedankt voor alles en veel succes met de voorbereidingen voor je huwelijk! **Eissa**, my dear friend, you have experienced many challenges and drawbacks during your PhD. For this reason, it is even more pleasing to see you succeed at the end. Thank you so much for your cooperation, in especially the MRI experiments. Good luck with preparing your thesis! Vince, mis je de kliniek al? Succes met je promotie! **Emrah**, it's not easy to leave your homeland behind to start a challenging research project. You are doing a great job so far, good luck with your PhD! **Willem**, **Wouter P**, **Wouter D**, **Rob**, **Guus**, **Vincent** en **Dave**, de chirurgen in spe. Ik heb veel van jullie onderzoek geleerd, met name de relatie tussen processen op moleculair en weefselniveau, en klinische uitkomst. Jullie waren altijd in voor een borrel, zonder moeite werden daar de kratten (ook frisdrank) en hapjes tevoorschijn gehaald. Bedankt voor alles en heel veel succes met jullie carrières!. Joost S, bedankt dat je zo nu en dan als sparringpartner optrad, **Joost F**, bedankt voor het kraken van mijn rug, **Alain**, **Krijn**, **Roberto**, **Loes**, **Esther**, **Marcel**, **Sandra**, **Cees**, **Sander vd W, Corina**, **Pradeep**, **Sridevi**, **Louise**, en oud collega's **Marie-José**, **Anke**, **Piet**, **Pieter**, **Kim**, **Simone**, **Linda**, **Angélique**, **Martha**, **Sebastian**, en **Willy**, jullie waren allen geweldige collega's. Bedankt!

De *Rotterdam-crew*, **Jaco**, **Renate** en **Kushan**, keiharde werkers en enorme doorzetters. Bedankt voor jullie hulp bij mijn varkenstudie en voor alle gezellige momenten!

Dear **Brian**, **Peter**, **Mary**, **Mark**, **Loretta**, **René**, **Andy**, **Leon** and **Christopher**, thank you all for the fruitful collaboration. Your input and support has played an important role in our Toll-like receptor 2 studies. I hope that we can continue our collaboration and that we may celebrate together our first successful treatment in patients suffering from myocardial infarction.

Dear **Sai Kiang**, it started with the mouse experiments finding the active component in MSC-conditioned medium, but it evolved in a great friendship. Thanks to you, I have gained much experience with mouse I/R experiments ;). Thank you very much for all the enjoyable moments here and in Singapore. Your friendship has opened doors in many ways for many of us. If you think you can convince me once again for extensive mouse experiments with chilli crab, than you are right! **Ruenn Chai**, *brother* and partner in crime, I truly enjoyed the many hours and days spent together in the lab during your visits to Europe. I say Europe, because you were more frequently outside Utrecht than inside. Nevertheless, you were able to get the job done at high quality and quantity! Together with **Kelvyn**, **Soon Sim**, **Ronne**, **Tiang Shen**, **Bin** and **Yijun**, we had so much fun! I will never forget the haute cuisine at the Hocker place, or our times smoking waterpipe! Thank you for being a great colleague and a friend!

Beste **Leo**, in veel opzichten lijken we op elkaar: onze interesse in ischemie-gerelateerd onderzoek, de verstrooidheid en interesse in mooie auto's (alhoewel ik toch een Porsche 911 turbo boven een Maserati GranTurismo prefereer). Jij vervulde een voorbeeldfunctie voor mij. Jouw proefschrift heb ik vaak genoeg opengeslagen om te zien hoe het moest. We zitten allebei nog in het lab met gezamenlijke projecten (Singapore, here we come!) en kijk uit naar de vele fantastische momenten die we zullen beleven. Ik waardeer enorm je collegialiteit en vriendschap, en ben blij dat je mijn paranimf bent.

Beste **Niek**, ik voel me gezegend met een maat als jij. We hebben veel met elkaar gedeeld; lief en leed, en meer (M.H. Trompstraat!). Ondanks het feit dat we allebei druk zijn (geweest) met onderzoek, heeft onze vriendschap er nooit onder geleden. Bedankt voor je steun wanneer ik dat nodig had. Ik ben ervan overtuigd dat je je promotie met succes zult afronden. Je stage aan de Johns Hopkins Hospital is daar een voorbode van. Ik kijk uit naar ons campingavontuur!

Sevgili **Ferhat**, *combam*, hedeflerime ulaşmaya çalışırken, zor anlarımda bana çok destek oldun. Senin de hedeflerine ulaşmanı ve hayallerini gerçekleştirmeni canı gönülden temenni ediyorum ve başaracağına eminim.

Sevgili **Babaannem**, **Anneannem** ve **Dedelerim**, bu doktora araştırmasının yoğunluğundan dolayı sizleri istediğim kadar ziyaret edemedim, arayamadım. Umarım bu tezi elinize aldığınızda beni anlayıp bağışlarsınız. Maddi ve manevi desteğinizi eksik etmediğiniz için teşekkür ederim.

Sevgili **Annem** ve **Babam**, **Serdar**, **Said** ve **Ömer**, sizlerin sonsuz sevginizi ve desteğinizi arkama alarak bu yola çıktım. Bu mutlu anı sizlerle paylaşmadan geçirmeyi düşünemiyorum. Sizleri çok seviyorum.

Lieve Fatma, *Sultanım*, zonder jouw steun en geduld zou ik dit resultaat niet hebben gehaald. Dankzij jouw overheerlijke boterhammen begin ik elke ochtend met volle overgave (collega's geloven het nog steeds niet). Je bent een geweldige echtgenote, mijn steun en toeverlaat. Je brengt rust, je remt en stimuleert, mijn tegenwicht, ik hou ontzettend veel van je!

CURRICULUM VITAE

Fatih Arslan was born on February 5, 1982 in Arnhem (the Netherlands). After graduating from the Thomas a Kempis College in 2000 (currently Arentheem College, Arnhem), he finished his propaedeutic psychology at the Radboud University Nijmegen in 2001. Hereafter, he studied medicine at the Utrecht University from 2001 to 2007. During this period, he visited Gazi University Hospital in Ankara for a clinical research project and Harvard University, Massachusetts General Hospital in Boston for a cardiac surgery clerkship. After graduating from medical school in 2007, he started as a PhD fellow in the Laboratory of Experimental Cardiology at the University Medical Center Utrecht. In December 2010, he finished his PhD fellowship, which led to this thesis. He has been awarded two times for the best abstract presentation from the Netherlands Society of Cardiology (NVVC) and second price for best Dutch publication in the field of vascular biology in 2010. Recently, he received the dr. E. Dekker grant "arts in opleiding tot specialist" from the Dutch Heart Foundation in order to fund a dedicated technician to support him with his research. Currently, he started his residency in Cardiology and is appointed as a post-doctoral fellow at the Laboratory of Experimental Cardiology (both University Medical Center Utrecht).

PUBLICATIONS

1. **Arslan F**, Kaya MG, van der Heijden G, Timurkaynak T, Cengel A. Hypertension as a predictor of adverse cardiac events in patients with borderline fractional flow reserve. *Acta Cardiol. 2007;62(4):367-72*

2. Timmers L, Lim SK, **Arslan F**, Armstrong JS, Hoefer IE, Doevendans PA, Piek JJ, El Oakley RM, Choo A, Lee CN, Pasterkamp G, de Kleijn DP. Reduction of myocardial infarct size by human mesenchymal stem cell conditioned medium. *Stem Cell Res. 2007;1(2):129-37*

3. Kaya MG, **Arslan F**, Abaci A, van der Heijden G, Timurkaynak T, Cengel A. Myocardial blush grade: a predictor for major adverse cardiac events after primary PTCA with stent implantation for acute myocardial infarction. *Acta Cardiol. 2007;62(5):445-51*

4. **Arslan F**, de Kleijn DP, Timmers L, Doevendans PA, Pasterkamp G. Bridging innate immunity and myocardial ischemia/reperfusion injury: the search for therapeutic targets. *Curr Pharm Des. 2008;14(12):1205-16*

5. **Arslan F**, Pasterkamp G, de Kleijn DP. Unraveling pleiotropic effects of statins: bit by bit, a slow case with perspective. *Circ Res. 2008;103(4):334-6*

6. **Arslan F**, Smeets MB, O'Neill LA, Keogh B, McGuirk P, Timmers L, Tersteeg C, Hoefer IE, Doevendans PA, Pasterkamp G, de Kleijn DP. Myocardial ischemia/reperfusion injury is mediated by leukocytic toll-like receptor-2 and reduced by systemic administration of a novel anti-toll-like receptor-2 antibody. *Circulation. 2010;121(1):80-90*

7. Lai RC, **Arslan F**, Tan SS, Tan B, Choo A, Lee MM, Chen TS, Teh BJ, Eng JK, Sidik H, Tanavde V, Hwang WS, Lee CN, El Oakley RM, Pasterkamp G, de Kleijn DP, Tan KH, Lim SK. Derivation and characterization of human fetal MSCs: an alternative cell source for large-scale production of cardioprotective microparticles. *J Mol Cell Cardiol. 2010;48(6):1215-24*

8. **Arslan F***, Lai RC*, Lee MM, Sze NS, Choo A, Chen TS, Salto-Tellez M, Timmers L, Lee CN, El Oakley RM, Pasterkamp G, de Kleijn DP, Lim SK. Exosome secreted by MSC reduces myocardial ischemia/reperfusion injury. *Stem Cell Res. 2010;4(3):214-22*

9. Ionita MG, **Arslan F**, de Kleijn DP, Pasterkamp G. Endogenous inflammatory molecules engage Toll-like receptors in cardiovascular disease. *J Innate Immun. 2010;2(4):307-15*

10. **Arslan F**, Keogh B, McGuirk P, Parker AE. TLR2 and TLR4 in ischemia reperfusion injury. *Mediators Inflamm. 2010;2010:704202*

11. **Arslan F**, Smeets MB, Riem Vis PW, Karper JC, Quax PH, Bongartz LG, Peters JH, Hoefer IE, Doevendans PA, Pasterkamp G, de Kleijn DP. Lack of fibronectin-EDA promotes survival and prevents adverse remodeling and heart function deterioration after myocardial infarction. *Circ Res. 2011;108(5):582-92*

12. Timmers L, Lim SK, Hoefer IE, **Arslan F**, Lai RC, van Oorschot AA, Goumans MJ, Strijder C, Sze SK, Choo A, Piek JJ, Doevendans PA, Pasterkamp G, de Kleijn DP. Human mesenchymal stem cell-conditioned medium improves cardiac function following myocardial infarction. *Stem Cell Res. 2011;6(3):206-14*

13. **Arslan F**, de Kleijn DP, Pasterkamp G. Innate immune signaling in cardiac ischemia. *Nat Rev Cardiol. 2011;8(5):292-300*

14. Chen TS, **Arslan F**, Yin Y, Tan SS, Lai RC, Choo AB, Padmanabhan J, Lee CN, de Kleijn DP, Lim SK. Enabling a robust scalable manufacturing process for therapeutic exosomes through oncogenic immortalization of human ESC-derived MSCs. *J Transl Med. 2011;9:47*

15. **Arslan F**, Smeets MB, Akeroyd L, Buttari B, van Middelaar B, Timmers L, den Ouden K, Pasterkamp G, Lim SK, de Kleijn DP. Haptoglobin deficiency reduces PAI-1 activity, microvascular integrity and enhances adverse remodeling after myocardial infarction. *Under Revision*

16. **Arslan F**, Lai RC, Choo A, Aguor ENE, Smeets MB, Akeroyd L, van Rijen HV, Timmers L, Doevendans PA, Pasterkamp G, Lim SK, de Kleijn DP. Exosomes target multiple mediators to reduce cardiac injury. *Submitted*

17. **Arslan F**, Houtgraaf JH, Keogh B, Kazemi K, McCormack WJ, O'Neill LAJ, de Jong R, Timmers L, Smeets MB, Akeroyd L, Reilly M, Pasterkamp G, de Kleijn DP. Treatment with OPN-305, a humanized anti-TLR2 antibody, reduces myocardial ischemia/reperfusion injury in pigs. *Under Revision*